Water Quality Studies in Support of Salton Sea Restoration

Final Report
December, 2007

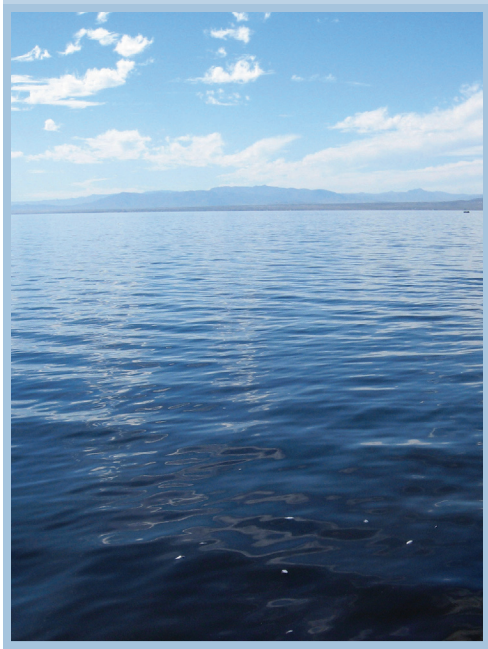

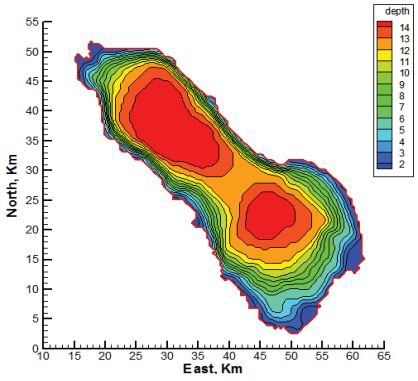

Prepared for:
Salton Sea Authority

Prepared by:

TETRA TECH

Tetra Tech, Inc.
3746 Mount Diablo Blvd # 300
Lafayette, CA 94549

Overview

P4435
BAKER
TANKS

depth
14
13
12
11
10
9
8
7
6
5
4
3
2
North, Km
East, Km
0
5
10
15
20
25
30
35
40
45
50
55
60
65

Overview of Water Quality Studies Performed in Support of Salton Sea Restoration

The Salton Sea, a terminal, 350-square mile water body in Southern California, is largely fed by nutrient-rich agricultural drainwater discharge, and has suffered from problems of eutrophication for many years. It is also impacted by increasing salinity which is a result of evaporative losses exceeding water inflows. Over the next decade and beyond, the Salton Sea will receive less inflow drainwater due to the out-of-basin transfer of 200,000 acre feet/year of irrigation water from the Imperial Valley. As a result of this water transfer, the salinity level of the Salton Sea is expected to continue to increase. Influent phosphorus levels are also expected to increase further, promoting increased eutrophication. A higher eutrophication state will, in turn, further degrade water quality by causing lower dissolved oxygen (DO) levels, increased sediment phosphorus release (i.e., internal loading) and increased ammonia and hydrogen sulfide concentrations. Even if salinity is stabilized, the continued degradation of these water quality parameters will make the Sea unsafe for fish and wildlife, even more unsuitable than present for recreational use, and an even greater public nuisance than present due to persistent noxious odors.

In an attempt to alleviate these problems, the Salton Sea Authority (SSA) has developed a combined Salton Sea Revitalization and Restoration Plan (the "SSA Plan") that focuses on balancing inflows and evaporative losses and improving water quality for multiple project purposes. The plan includes separating the sea into two basins (deep north and shallow south), canals for water exchange between basins, treatment of water at key inflow and outflow locations in the system, removal and treatment of hypolimnetic water, and a brine pool for final disposal of hypersaline water (Figure ES-1). The goal of this combined natural and treatment-plant approach for improving water quality is to return the smaller restored Salton Sea in the SSA Plan into a water body that supports regional recreational and local economic development activities, and to provide safe habitat for wildlife, as was the case during the Salton Sea's heydays in the 1950s and 1960s.

The focus of the studies described in this document was to understand how this overall system will work, and whether responses, especially as related to the water quality in the Sea, will be as anticipated in the SSA plan. Toward this end, this study consisted of four distinct tasks:

Task 1: Detailed field measurements of hydrogen sulfide and other water quality parameters at selected locations in the Salton Sea, including measurements of hydrogen sulfide volatilization from the surface of the Sea

Task 2: Three-dimensional hydrodynamic and water quality modeling to understand how the restored Sea would behave if divided with a mid-Sea barrier.

Task 3: Pilot testing of ozonation of the hypolimnetic waters of the Sea, to determine whether this is a feasible technology to address the key odor causing constituent, hydrogen sulfide.

Task 4: Engineering cost estimation of an ozonation treatment plant associated with the SSA plan.

This summary presents the key findings of the individual tasks. Detailed reports, prepared by the lead investigators for each task, are appended in the following sections. These studies were performed through a contract between the SSA and Tetra Tech, and was funded by the

Bureau of Reclamation. The period of performance was August 1, 2006 to December 31, 2007.

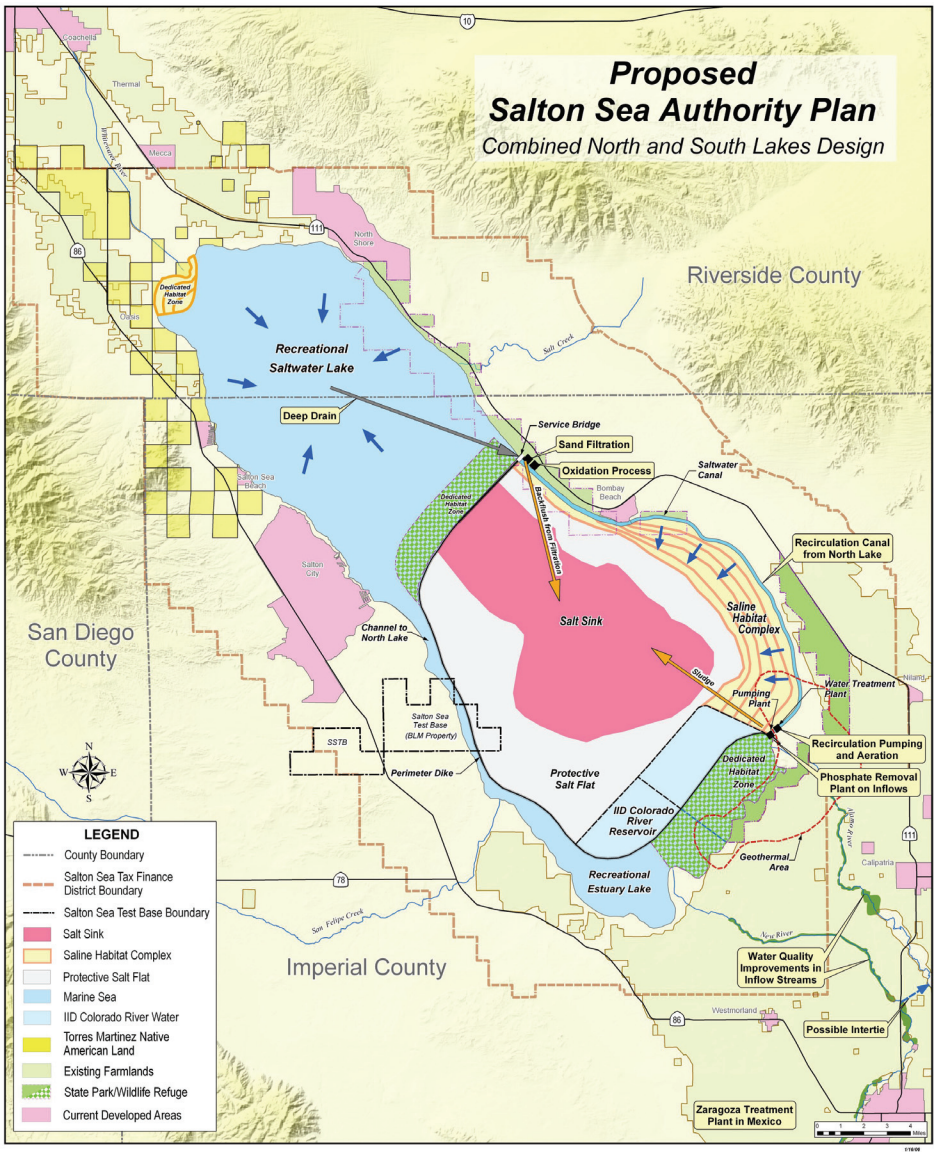

Figure ES-1. Proposed Salton Sea Revitalization Plan

1. Task 1. Field Measurements of Hydrogen Sulfide Production and Volatilization in the Salton Sea

The high temperatures, algal productivity and sulfate concentrations in the Salton Sea have been recognized for some time as conditions well-suited for hydrogen sulfide production, although no studies have been conducted to understand the sulfur biogeochemistry in the Sea. Field and laboratory measurements were thus conducted to better understand the cycling of this important element. Hydrolab casts, water column samples and sediment samples were collected at 12 locations around the Sea (Figure ES-2). Dissolved oxygen levels showed strong seasonal patterns, with values near zero during the warmest summer months in the bottom waters (Figure ES-3). Hydrogen sulfide concentrations were generally below

detection (<4 μM) in the water column during the cool, well-mixed conditions present between November and April. Sulfide levels increased strongly in bottom waters following onset of stratification, reaching concentrations of 1 mM in bottom water in the north basin in early June 2006. Somewhat lower levels were found at mid-lake and south basin sites (0.2-0.3 mM). Mixing events redistributed dissolved oxygen and hydrogen sulfide within the water column, with three primary events identified based upon measured temperature differences between near surface and bottom water temperatures (ΔT), as well as redox potential, sulfide and ammonium concentrations, and other properties. These mixing events lowered bottom water sulfide concentrations and increased concentrations in the upper portions of the water column. Representative sulfide data in the water column and in the porewater are shown in Figure ES-4. A major mixing event occurred at the end of July 2006 that brought hydrogen sulfide to the surface waters, depleted available dissolved oxygen throughout the water column (Figure ES-3), and triggered a massive fish kill. Very poor water quality conditions persisted for over a month following this event. A mixing event in September 2006 broke down the residual thermal stratification and helped reaerate the water column down to the bottom sediments.

Hydrogen sulfide flux from the bottom sediments was estimated to range from approximately 2-3 mmol m^{-2} d^{-1} during the winter and up to 8 mmol m^{-2} d^{-1} during the summer. The sulfide released from the sediments during the winter was reoxidized within the water column, although atmospheric H_2S measurements suggest that some is lost to volatilization. Atmospheric H_2S concentrations increased dramatically following the mixing event in late July 2006, and reached 1.0 μmol m^{-3} (34 μg m^{-3}). Application of the 2-layer model for volatilization indicates that >1.2 mmol m^{-2} d^{-1} volatilized from the surface of the Salton Sea during this event. While it is estimated that >95% of the hydrogen sulfide that is produced in the Sea is simply reoxidized by molecular oxygen, hydroxyl radicals and other oxidants, the total annual export of sulfide due to volatilization is about 335 Mg y^{-1}. This compares with the total annual California statewide industrial emissions of 2,600 Mg y^{-1}

The reducing conditions present during summer stratification also influenced the concentrations of other chemical species in the Sea. Ammonium-N and soluble-reactive phosphorus concentrations in the bottom waters both increased quite markedly in the summer, reaching levels that were 2-5 times higher than found during the winter. Sulfate reduction combined with microbial respiration also increased alkalinity and lowered pH near the sediments. Concentrations of sulfide and ammonium-N were dramatically higher in the sediment pore water and the concentration gradients between the pore water and the overlying lake water were used to determine the flux of sulfide and NH_4-N to the water column.

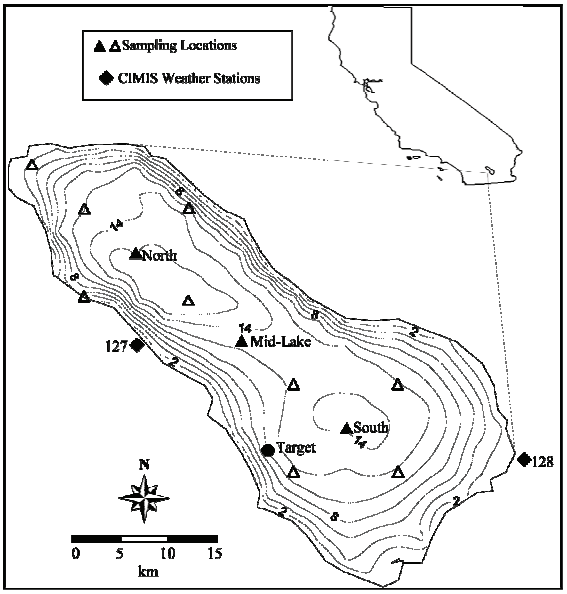

Figure ES-2. Locations of sampling sites.

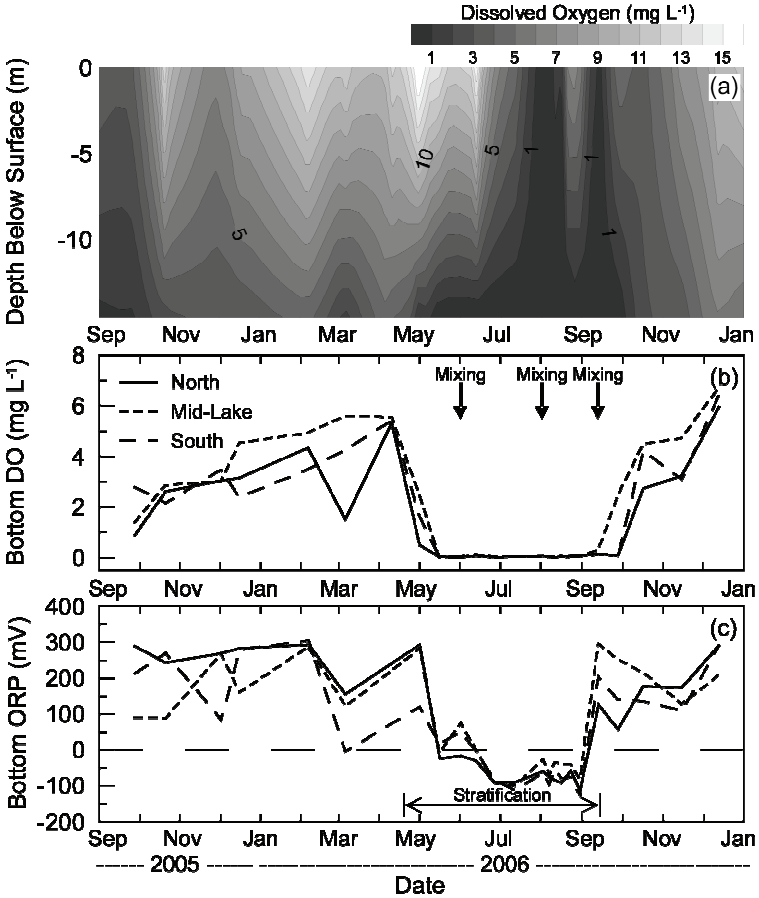

Figure ES-3. a) Contour plot of dissolved oxygen at the north basin locations, b) dissolved oxygen concentration of the bottom water, and c) oxidation-reduction potential of the bottom waters.

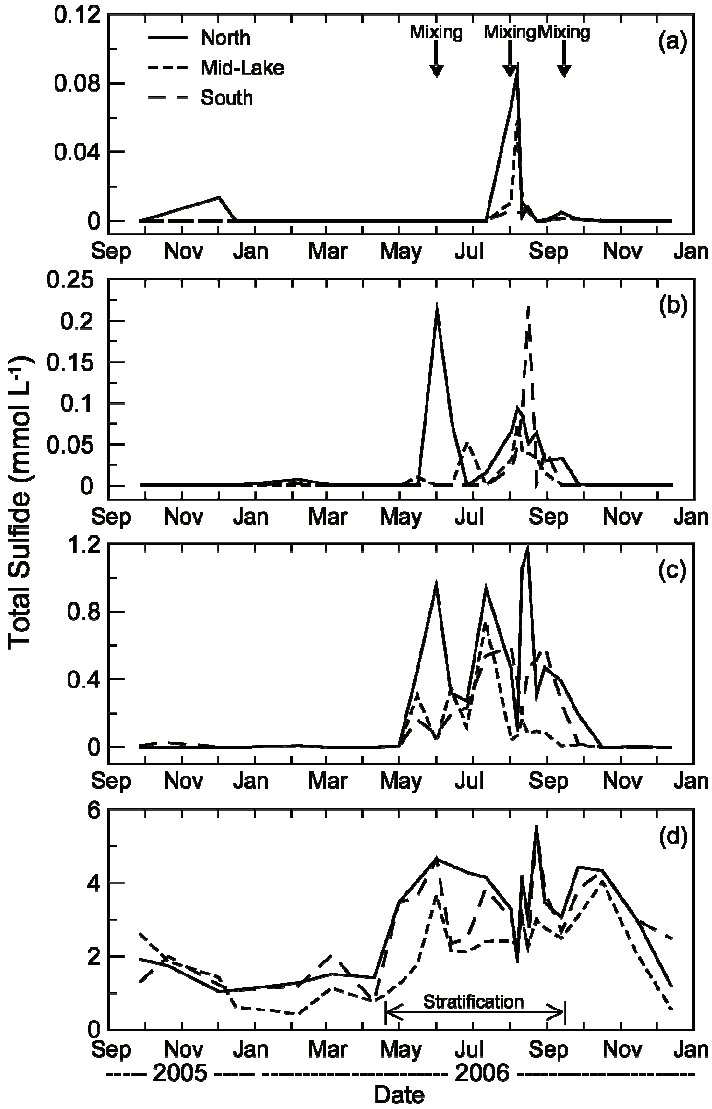

Figure ES-4. Total sulfide concentrations in a) the surface waters (approx 10 cm below surface), b) mid-depth (approx 6-7 m below surface), c) bottom waters, and d) pore water.

2. Task 2. Implementation of EFDC Model to Predict Hydrodynamics and Water Quality in the Salton Sea

This task was focused on the development of a hydrodynamic and water quality model of the Salton Sea for use in assessing recent hydrodynamic and water quality conditions and evaluating changes resulting from various restoration plans including the Salton Sea Authority Plan. It is widely accepted that physical and biogeochemical processes in the Salton Sea are fundamentally three-dimensional in space and highly variable in time. Similarly, biogeochemical processes exhibit a range of time scale with nutrient dynamics responding to both continued loads to the system and large scale internal nutrient recycling between the water column and sediment bed. Surface water modeling systems capable of representing the relevant hydrodynamic and water quality processes determined to be significant in the Salton Sea are rather limited. The Environmental Fluid Dynamics Code (EFDC) model was selected for this study primarily on the basis that it incorporates all of the relevant hydrodynamic and water quality processes. Other advantages of the EFDC model

include its open source-public domain status, track record of applications, including regulatory applications in the NPDES, TMDL and Superfund programs, and extensive scientific peer review.

The EFDC model was configured to simulate the 1997 through 1999 historical period coinciding with extensive physical and biogeochemical observational data sets obtained during 1997 and 1999, respectively. Model spatial resolution is approximately 0.61 meters vertically and either 1200 or 600 meters horizontally, with the coarser horizontal resolution used for preliminary calibration and the finer resolution used for final calibration and verification and restoration alternatives evaluation. Various spatially altered marine sea and salinity habitat alternatives can be readily incorporated into either of the two horizontal resolution configurations. The model historical simulation period can be readily extended past 1999 subject to the availability of atmospheric and hydrologic data.

Calibration results, presented herein, indicate that both the hydrodynamic and water quality components of the model perform well in representing spatial variations and seasonal and event time scale variations in circulation, thermal structure and water quality processes. Hydrodynamic and thermal calibration utilized the 1997 observational data set, with the 1999 data set being used for thermal validation. Hydrodynamic and thermal responses are most sensitive to the wind field over the Sea, which must be estimated by height adjustment and spatial interpolation of wind data from five to seven nearby meteorological stations. Sensitivity studies indicate that the diurnal vertical temperature structure is sensitive to atmospheric heat exchange and wind stress induced mixing, but relatively insensitive to details of the horizontal current response to wind stress. For the water quality component of the model, the 1999 observational data was used for calibration. Another water quality data set as complete as the 1999 set was not available for validation and instead, a less formal validation was conducted using sparse data spanning 2000 to 2007. Vertical thermal structure and its influence on vertical mixing and reaction rates is the most sensitive physical process with respect to water quality response. Water quality reaction parameter values in both the water column and sediment diagenesis or flux sub-model were adjusted and optimized through sensitivity analysis. The robustness of the 1999 calibration was demonstrated by conducting a 15 year simulation based on repetition of 1999 hydrodynamics and nutrient loads.

The calibrated and verified hydrodynamic and water quality model was used to evaluated various aspects of the Salton Sea Authority preferred restoration plan involving a northern marine sea connected to a southern estuarine zone. Hydrodynamic simulations of the SSA plan indicated that thermal stratification and vertical mixing in the northern marine sea changed little form existing conditions. The water quality response of the northern marine sea was evaluated by conducting 15 year scenario simulations based on continued repetition of 1999 historical atmospheric, hydrologic, and nutrient loadings. Three scenarios and a baseline were simulated. The baseline corresponded to existing full sea conditions. The three scenarios included the mid-sea dike and a southeastern dike forming the estuarine zone. Two of these three scenarios involved various reductions in phosphorous loading, 0 percent and 90 per cent, from the inflowing rivers. The third scenario had no phosphorous loading reduction, but included withdrawal of hypolimnetic and surface water from the northern marine sea and its return into the southern estuarine region. The oxygen demand associated with hydrogen sulfide in the hypolimnetic withdrawal was reduced by 50 per cent before being returned to evaluate the effectiveness of a proposed ozone treatment plant to control sulfide. The spatial extent and duration of low dissolved oxygen water was used a metric to evaluate the effectiveness of the three scenarios relative to the baseline. All of the scenarios resulted in

reduction of per cent anoxic volume days relative to the base line. The hypolimnetic withdrawal and treatment showed no effect relative to the corresponding no phosphorous load reduction scenario. Response to phosphorous load reduction appears to be most sensitive to complete load reduction.

3. Task 3. Pilot Testing of Sand Filter and Ozonation System at the Salton Sea

This task involved the operation of a pilot treatment system (shown in Figure ES-5) to oxidize the hydrogen sulfide present in the waters of the hypolimnion in the Salton Sea. The pilot system used ozone and hydrogen peroxide to oxidize the hydrogen sulfide. Hydrogen sulfide is produced as a result of organic matter decay and oxygen depletion, and is a particular problem in the Salton Sea. Although the advanced ozonation system tested here is commonly used in water treatment, there are no data on its use under hypersaline conditions that occur in the Salton Sea. The high dissolved organic carbon and oxygen demand of the Salton Sea waters also make it different from most previous reports of ozonation treatment. The goal of the pilot test was to obtain performance data on oxidation of hydrogen sulfide under conditions that would apply were the treatment to be employed as part of the Salton Sea Authority's Revitalization and Restoration Plan.

Based on the results of analysis of water samples collected during pilot plant operation, the following general observations were made:

1. The sand filter was able to remove most of the TSS reported in water samples and in many cases demonstrated higher COD removal efficiencies when compared to the advanced oxidation system.

2. The oxidation of dissolved sulfide and total sulfide was demonstrated with the addition of ozone and ozone/peroxide. A residual concentration of 1.5 mg/L of ozone at the effluent was required to fully oxidize all sulfide in the water samples. The results indicated that about 3.76 mg/L of ozone were required to oxidize 1 mg/L of total sulfide. The ozone demand was expected to be associated mainly with the ozone required to oxidize total sulfide. However, other non-targeted inorganic and organic compounds in the hypolimnetic water were also expected to be oxidized by ozone, thus increasing ozone demand.

3. A reduction of COD in treated water samples was not consistently observed at increased ozone doses. This may have resulted from the interference of inorganic compounds in the matrix of the water samples.

4. Generally speaking, the high concentration of dissolved solids in the water samples caused problems during chemical analysis. However, the data demonstrated that the advanced oxidation system was effective in oxidizing dissolved sulfide and total sulfide.

Figure ES-5. Pilot plant for evaluation of ozonation of hypolimnetic Salton Sea water

4. Task 4. Develop Cost Estimates for Treatment and Other Elements of the Proposed Design

This task included preparation of preliminary engineering cost estimates for pipelines and a plant to extract and treat and large volume of hypolimnetic water (450 mgd). Conceptual site design plans were prepared for the treatment facilities along with process flow diagrams and hydraulic profile of the treatment facilities (Figures ES-6 and ES-7).

Conceptual planning level construction cost estimates were prepared from cost curves where possible that identified the major categories such as site work, mechanical, structural, electrical and instrumentation. Annual operations and maintenance costs were also estimated for the full scale treatment facilities, and included estimates for labor, power, maintenance, materials, and chemicals based on the results obtained in the sampling, pilot studies and modeling.

The total capital investment is estimated to be $1.28 billion, of which about 40% is associated with the construction of the system of pipes for hypolimnetic extraction. The total annual cost for operation and maintenance including labor, materials and utilities for the hypolimnetic water extraction, treatment and discharge system is estimated to be approximately $33 million. Amortized over a thirty-year period at an interest rate of 3.5%, the annualized capital cost is $69.5 million. The total annual costs are $102.3 million. In contrast to the hypolimnetic extraction and ozonation, a plant for the treatment of inflows is somewhat less expensive. Capital costs range from $208 million to $620 million, depending on the volumes of flow treated and whether filtration is used. The annualized capital and O&M costs range from $28 million to $50 million.

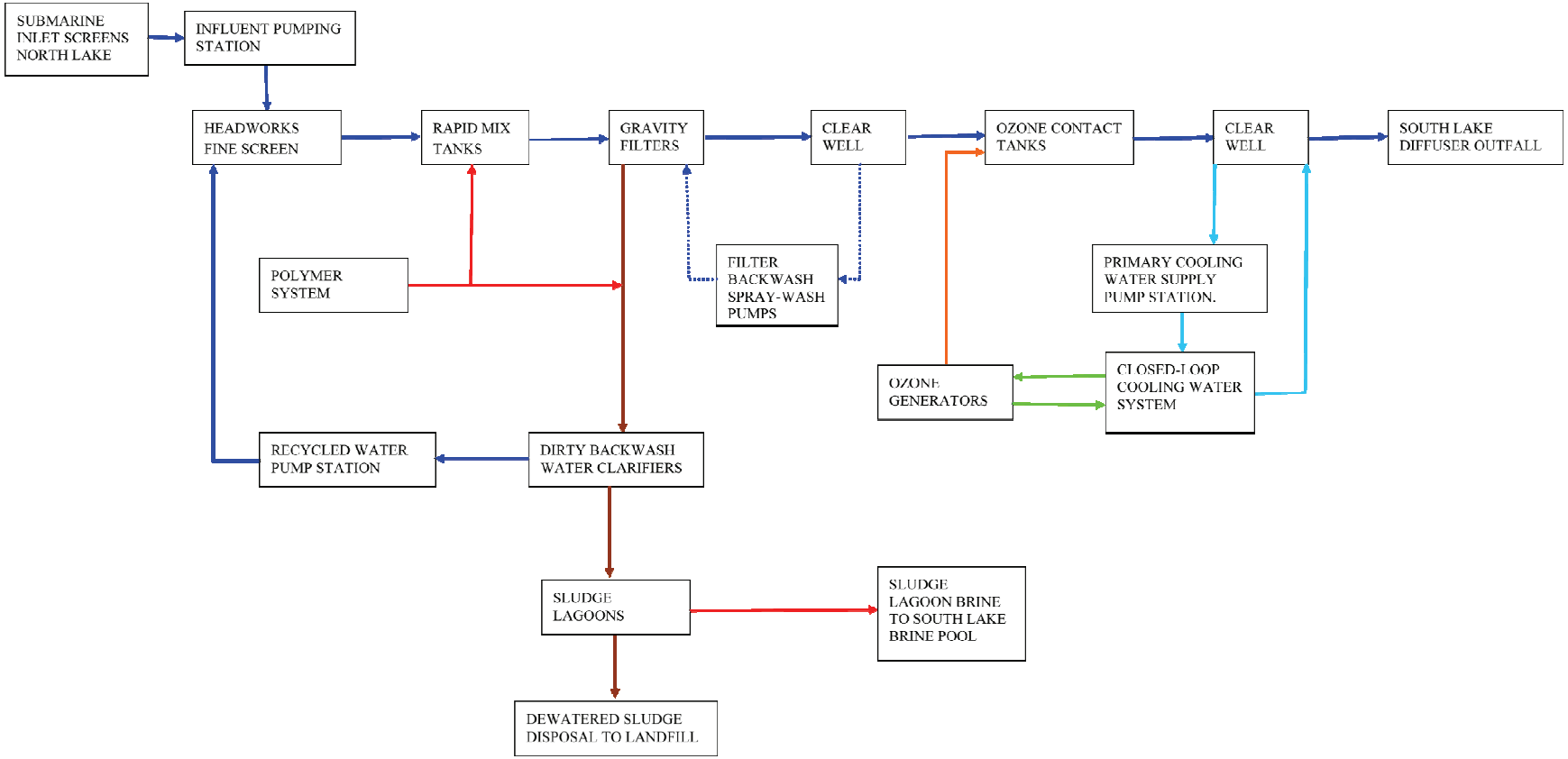

Figure ES-6. Schematic Process Flow Diagram for Salton Sea Hypolimnetic Water Treatment System

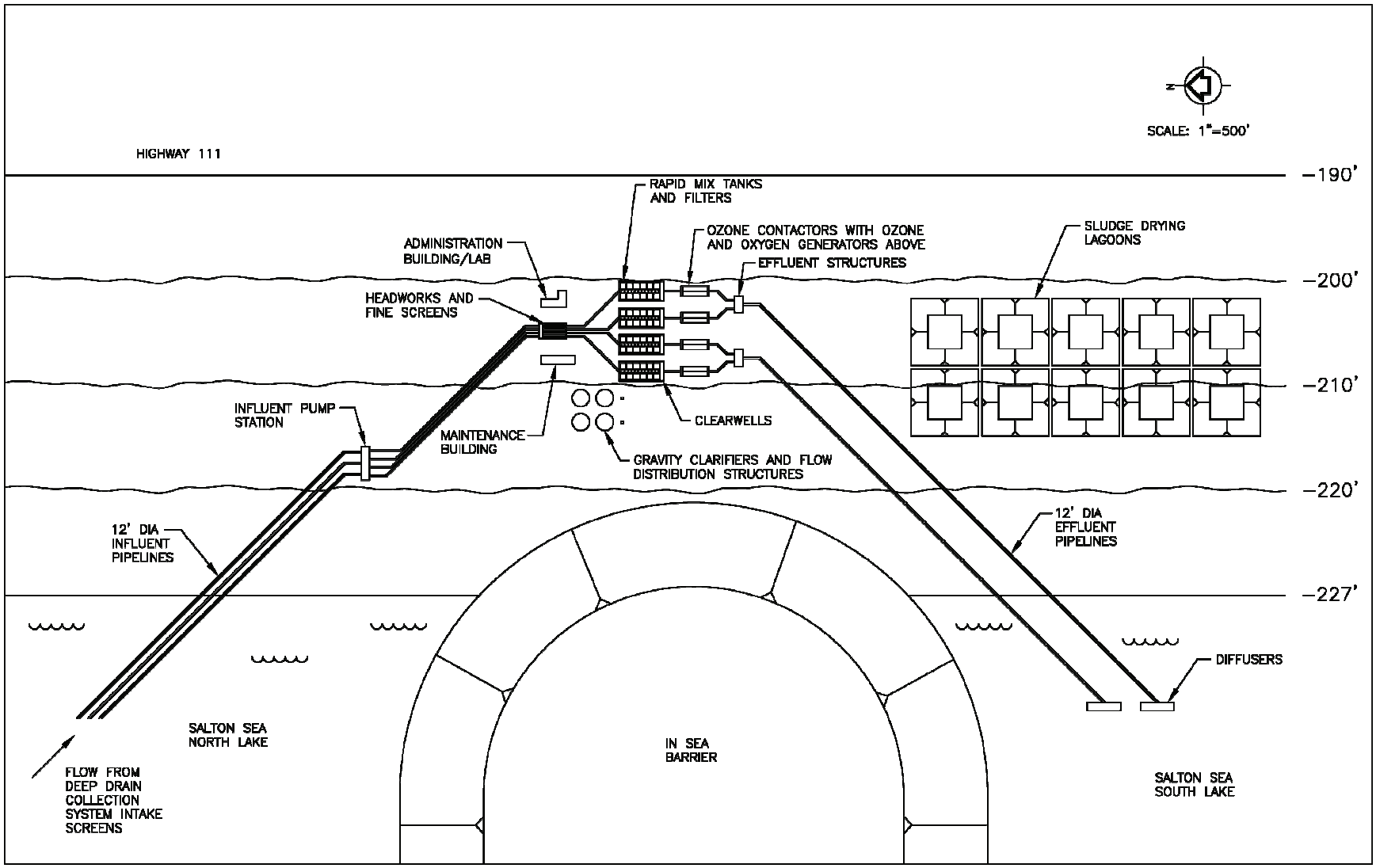

Figure ES-7. Salton Sea Hypolimnetic Treatment Plant – Conceptual Plant Layout

Table of Contents

Task 1: Hydrogen Sulfide Production and Volatilizationin the Salton Sea 1-1

1. Executive Summary 1-1
2. Introduction 2-1

2.1. Study Site 2-1

3. Methods 3-1

3.1. Field 3-1

3.1.1 Sediment 3-2
3.1.2 Water Column 3-2

3.1.3 Atmosphere 3-2

3.2. Laboratory Analysis 3-3

3.2.1 Sediment 3-3
3.2.2 Water Column and Pore Water 3-3

4. Results and Discussion 4-1

4.1. General Chemistry 4-1
4.2. Temperature 4-2

4.3. Dissolved Oxygen and Oxidation-Reduction Potential 4-3

4.4. Sulfide Chemistry 4-5

4.5. Sulfide Oxidation 4-9

4.6. Alkalinity and pH 4-10

4.7. Other Chemistry 4-11

4.8. Sulfide Flux at the Sediment-Water Interface 4-12

4.9. Sediment Oxygen Demand 4-14

4.10. Volatilization at the Air-Water Interface 4-16

5. Implications and Conclusions 5-1
6. References 6-1

7. Appendix 7-1

Task 2: Hydrodynamic and Water Quality Modeling to Support Restoration of the Salton Sea, California 1-1

1. Introduction 1-1
2. Conceptual Model 2-1

   2.1. Hydrodynamics 2-1
   2.2. Water Quality and Eutrophication 2-19

3. Model Selection 3-1
4. Model Configuration 4-1
5. Hydrodynamic and Thermal Calibration and Validation 5-1

   5.1. Hydrodynamic and Thermal Calibration 5-1
   5.2. Sensitivity of Temperature Prediction to Velocity Prediction 5-3
   5.3. Thermal Validation 5-4

6. Water Quality Calibration and Validation 6-1
7. Evaluation of the Salton Sea Authority Restoration Plan 7-1

   7.1. The Salton Sea Authority Plan 7-1
   7.2. Hydrodynamic and Thermal Response Evaluation 7-2
   7.3. Water Quality Response Evaluation 7-2

8. Summary 8-1
9. References 9-1
10. Appendix A. Excitation-Response Analysis of Circulation 10-1
11. Appendix B. Complete Results for Fifteen Year Water Quality Model Scenarios 11-1

Task 3: Pilot Testing of an Advanced Oxidation Water Treatment System for Sulfide Control at the Salton Sea, California 1-1

1. Project Site Description and Background 1-1
   - 1.1. Summertime Water Quality Concerns 1-1
   - 1.2. Advanced Oxidation System 1-1
2. The Pilot Plant System 2-1
   - 2.1. Purpose of the Pilot Plant Testing 2-1
   - 2.2. Collection of Hypolimnetic Water 2-1
   - 2.3. Sulfide Destruction with Ozone and Ozone/Peroxide 2-1
   - 2.4. Pilot Plant System Components 2-1
   - 2.5. Functionality of the Advanced Oxidation System 2-2
3. Pilot Plant Mobilization and Operation 3-1
   - 3.1. Bench Scale Testing 3-1
   - 3.2. Mobilization of Process Equipment 3-1
   - 3.3. Pilot Plant Operation with Clean Water 3-1
   - 3.4. Hypolimnetic Water Sample Collection by ERS 3-2
   - 3.5. Sample Spiking with Sodium Sulfide 3-2
   - 3.6. Selection of Operating Parameters During Pilot Plant Testing 3-3
   - 3.7. Sample Collection and Transportation 3-3
     - 3.7.1 Sample Labeling 3-4
     - 3.7.2 Calscience Environmental Laboratory 3-4
     - 3.7.3 University of California at Riverside Laboratory 3-4
4. Pilot Plant Results & Discussion 4-1
   - 4.1. Total Suspended Solids 4-1
   - 4.2. Dissolved and Total Sulfide 4-1
   - 4.3. Oxidation-Reduction Potential 4-2
   - 4.4. Total Organic Carbon 4-2
   - 4.5. Ammonia and Phosphate 4-3
   - 4.6. Chemical Oxygen Demand, Ultimate Biological Oxygen Demand, and Ultimate Nitrogenous Biological Oxygen Demand 4-3
   - 4.7. Nitrites, Nitrates, Total Kjeldahl Nitrogen, and Total and Dissolved Organic Nitrogen 4-4
   - 4.8. Foaming 4-5

5. Pilot Plant Demobilization 5-1
5.1. Physical Condition of the Pilot Plant 5-1
6. Summary of Results 6-1
Attachment A: Pilot Plant System Photos 6-1
Attachment B: Operations Logs 6-1
Attachment C: Summary of Pilot Plant Data Tables and Charts 6-1
Attachment D: Results of Analysis on Water Samples Laboratory Reports 6-1

Task 4: Ozonation Treatment Plant–Planning Level Cost Estimate...1-1

1. Background 1-1
2. Pilot Test 2-1
3. Design Criteria 3-1
4. Treatment System Processes 4-1
   4.1. Deep Drain Collection System 4-8
   4.2. Influent Pump Station 4-8
5. Treatment Plant 5-1
   5.1. Plant Headworks and Fine Screening System 5-1
   5.2. Filtration System 5-1
   5.3. Ozone Treatment System 5-2
   5.4. Treated Effluent Recycle 5-3
6. Operation and Maintenance cost 6-1
7. Comparison with Cost Estimates of Phosphorus Removal Plant for Inflows 7-1
   7.1. Capital Costs for Treating Inflows 7-1
   7.2. Operations and Maintenance Costs for Plant Treating Inflows 7-2
8. Summary 8-2
9. Supporting Documentation 9-1
10. References 10-1

Appendix A 10-3

Appendix B 10-5

Appendix C 10-7

Task 1:
Hydrogen Sulfide Production and Volatilization

Prepared by:
B.K. Reese, M.A. Anderson and C. Amrhein
Dept. of Environmental Sciences
Univ. of California
Riverside, CA 92521

1. Executive Summary

The high temperatures, algal productivity and sulfate concentrations in the Salton Sea have been recognized for some time as conditions well-suited for hydrogen sulfide production, although no studies have been conducted to understand the sulfur biogeochemistry there. Field and laboratory measurements were thus conducted to better understand the cycling of this important element in the Sea. Hydrogen sulfide concentrations were generally below detection (<4 μM) in the water column during the cool, well-mixed conditions present between November and April. Sulfide levels increased strongly in bottom waters following onset of stratification, reaching concentrations of 1 mM in bottom water in the north basin in early June 2006. Somewhat lower levels were found at mid-lake and south basin sites (0.2-0.3 mM). Mixing events redistributed dissolved oxygen and hydrogen sulfide within the water column, with three primary events identified based upon measured temperature differences between near surface and bottom water temperatures (ΔT), as well as redox potential, sulfide and ammonium concentrations, and other properties. These mixing events lowered bottom water sulfide concentrations and increased concentrations in the upper portions of the water column. A major mixing event occurred at the end of July 2006 that brought hydrogen sulfide to the surface waters, depleted available dissolved oxygen throughout the water column, and triggered a massive fish kill. Very poor water quality conditions persisted for over a month following this event. A mixing event in September 2006 broke down the residual thermal stratification and helped reaerate the water column down to the bottom sediments.

Hydrogen sulfide flux from the bottom sediments was estimated to range from approximately 2-3 mmol m^{-2} d^{-1} during the winter and up to 8 mmol m^{-2} d^{-1} during the summer. The sulfide released from the sediments during the winter was reoxidized within the water column, although atmospheric H_2S measurements suggest that some is lost to volatilization. Atmospheric H_2S concentrations increased dramatically following the mixing event in late July 2006, and reached 1.0 μmol m^{-3} (34 μg m^{-3}). Application of the 2-layer model for volatilization indicates that >1.2 mmol m^{-2} d^{-1} volatilized from the surface of the Salton Sea during this event. While we estimate that >95% of the hydrogen sulfide that is produced in the Sea is simply reoxidized by molecular oxygen, hydroxyl radicals and other oxidants, the total annual export of sulfide due to volatilization is about 335 Mg y^{-1}. This compares with the total annual California statewide industrial emissions of 2,600 Mg y^{-1}.

The reducing conditions present during summer stratification also influenced the concentrations of other chemical species in the Sea. Ammonium-N and soluble-reactive phosphorus concentrations in the bottom waters both increased quite markedly in the summer, reaching levels that were 2-5 times higher than found during the winter. Sulfate reduction combined with microbial respiration also increased alkalinity and lowered pH near the sediments. Concentrations of sulfide and ammonium-N were dramatically higher in the sediment pore water and the concentration gradients between the pore water and the overlying lake water were used to determine the flux of sulfide and NH_4-N to the water column.

2. Introduction

Saline lakes are often noted for their high productivity and their considerable ecological importance, particularly to endemic species and breeding migratory bird populations (Williams, 1972; Jellison et al., 2004). They are most common in arid or subarid regions where evaporation exceeds precipitation (Hammer, 1986). Salinisation can be natural (primary) due to the leaching or accumulation of salts in a closed basin, or anthropogenic (secondary), caused by irrigation runoff or inflow diversions. Increasing demand of freshwater for agricultural irrigation is proving to be devastating to the future of saline lakes, such as the Aral Sea, and in the western United States where the conflict between regional water demands and ecosystem viability exist (e.g. Mono Lake, Walker Lake, as well as the Salton Sea) (Kaiser, 1999; Williams, 2002).

The Salton Sea was legally designated as an agricultural drainage reservoir by the federal government in 1924; run-off from the irrigation of farmlands in the Imperial and Coachella Valleys (that provide a considerable portion of the nation's winter vegetables and alfalfa) is thus designated to end up in the Salton Sea. With this runoff come nutrients, such as nitrogen and phosphorus, as well as pesticide residues and other contaminants. High nutrient loading invariably leads to high biomass production and ultimately eutrophication. Eutrophication can generate anaerobic conditions, which is also associated with the production and accumulation of hydrogen sulfide and other chemically reduced species that can negatively impact the food web.

Combined with this, a water transfer from the agriculturally-dominated region of the Salton Sea to San Diego is also threatening to further reduce freshwater inflows. With decreased inflows, the hydrological balance becomes disturbed and lake volume will decrease; consequently, since the mass of salt remains more or less constant, the salinity will increase (Williams, 2001). In order to forecast the responses of the Salton Sea to human perturbations, a better understanding of its biogeochemistry is required.

While several studies have been conducted on the chemistry and mixing at the Salton Sea, including that of Carpelan (1958), Arnal (1961), Watts et al. (2001), and Holdren and Montaño (2002), comparatively little is known about the biogeochemistry of sulfur. A 15-month study was thus undertaken to quantify the water column and pore water sulfide concentrations and related chemical conditions in the Sea, atmospheric H_2S concentrations, oxygen demand, and the resulting sulfur fluxes across the sediment-water and the air-water interfaces.

2.1. Study Site

The Salton Sea is a warm, discontinuous polymictic lake located in an arid desert region of Southern California, approximately 50 miles southeast of Palm Springs. The lake currently has a surface elevation of 69.5 m below sea level, is relatively shallow with a maximum depth of 15 m, and has a long fetch (56 km). The Sea's surface area of 975 km^2 make it the largest lake in California.

It was formed, most recently, from 1905-1907 as a result of an attempt to cut a new irrigation channel into the bank of the Colorado River; a series of subsequent floods allowed it to flow westward, unrestricted, into a terminal basin known as the Salton Trough (Arnal, 1961). The breach was filled and the Sea is currently maintained by agricultural drainage inputs from the Whitewater River, New River, and Alamo River, that total approximately 1.3 maf annually. The only output is from evaporation. Although initially a freshwater lake when formed, saline riverine inputs combined with salts leaching from underlying soils and a high rate of

evaporation (1.8 m yr^{-1}), have contributed to the increasing salinity of the Sea (Wardlaw and Valentine, 2005).

The Salton Sea is a vital resource to migrating birds whose wetland habitats have been reduced by over 90% (Environmental Protection Agency). High levels of nutrients from agricultural drainage and municipal wastewater along with warm weather conditions have lead to a highly productive system with frequent algal blooms and massive summer fish and migratory bird die-offs (Kaiser, 1999; Schroeder, 2002).

Several studies have been conducted on mixing processes at the Salton Sea. Strong winds from the autumn to the spring allow for turbulent mixing of the water column during the cool winter months. This was observed not only in the current study, but also by Carpelan (1958), Arnal (1961), Watts et al. (2001), and Holdren and Montaño (2002). Arnal (1961) observed prevailing winds from the northwest in the north basin and from the east in the south basin, thus setting up a counter-clockwise circulation pattern around the Sea. Arnal also suggested that the south basin mixed more frequently than the north basin. Watts et al. (2001) further noted that the shallower southern basin has a greater surface area making it subject to more complete mixing during the spring and summer with lower wind speeds. During periods of high wind, however, the differences in the north and south basin would weaken due to horizontal advection.

3. Methods

3.1. Field

Samples were collected from three main sampling stations located in the north basin, mid-lake, and the south basin (Figure 3-1 and Table 3-1). These sites closely correspond to sampling sites used by Holdren and Montaño (2002). The sampling program commenced in September 2005 and continued until February 2007. Field and lab measurements were made on a monthly basis from September 2005 through March 2006, on a biweekly basis from April 2006 through October 2006, and again monthly from November to February 2007. Nine additional sites along three transects (Figure 3-1, open symbols) were sampled quarterly beginning in September 2005 until November 2006. Air samples were collected at a stationary pier in the southern portion of the lake known as the "Target" (Figure 3-1). Sampling sites were located using a Garmin eTrex global positioning system (GPS) and the WGS84 datum.

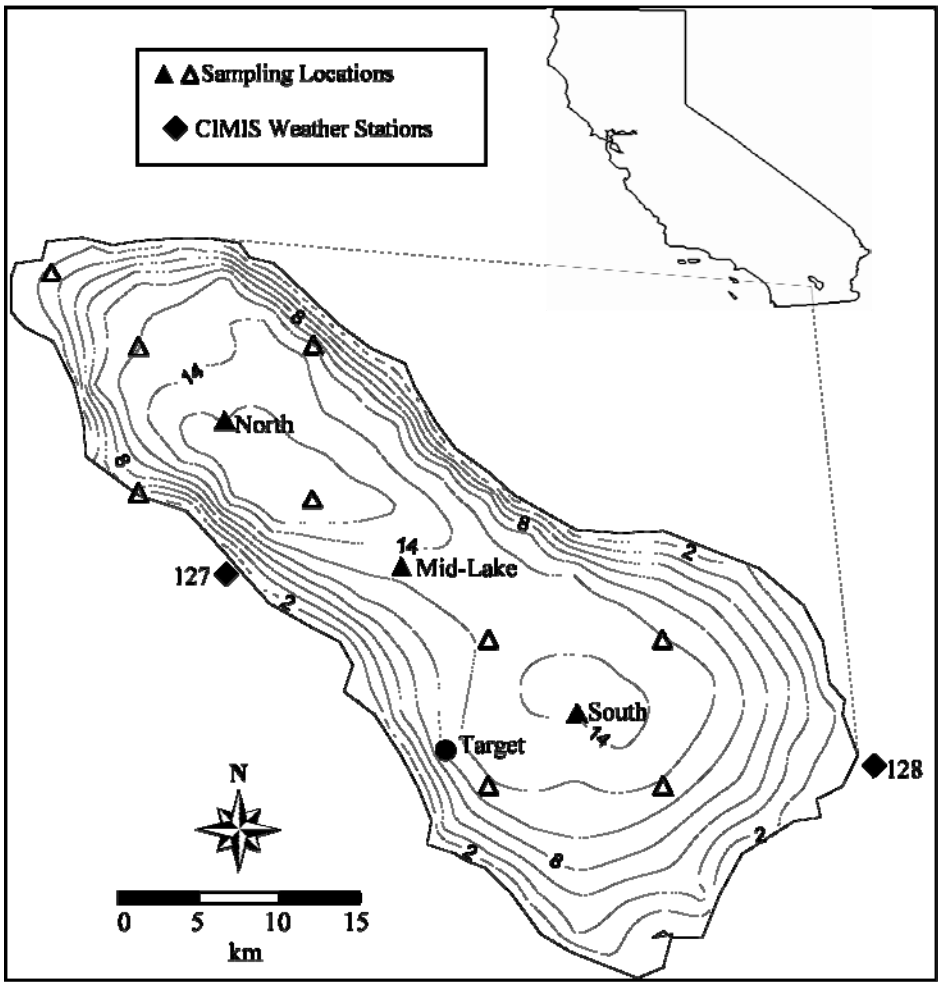

Figure 3-1. Locations of sampling sites.

Table 3-1
Location and depth of the three main sampling stations.

Site ID	Depth (m)	Latitude (deg)	Longitude (deg)
North Basin	15	33.4167	-115.952
Mid-Lake	12	33.33352	-115.85
South Basin	15	33.25	-115.7501

3.1.1 Sediment

Grab samples of the upper 10 cm of sediment were collected using a Petite Ponar dredge from each site sampled. The samples were briefly homogenized and then immediately placed in 500 mL wide-mouth glass jars with a lined screw-cap lid and 250 mL Nalgene® high density polyethylene centrifuge bottles. All samples were capped with minimal headspace that was flushed with N_2 gas and stored on ice for transport to the lab. Separately, triplicate intact cores were collected from the north, mid and south basin sites on February 21st, April 24th, and June 5th, 2007 and returned to the lab for determination of sediment oxygen demand (SOD).

3.1.2 Water Column

In situ water column measurements were made using a Hydrolab Sonde 4a calibrated following manufacturer's instructions. Hydrolab casts provided dissolved oxygen (mg L^{-1}), temperature (°C), electrical conductance (mS cm^{-1}), oxidation-reduction potential (mV), and pH as a function of depth. Measurements were made every 0.5 meter for the first 2 meters, then every meter thereafter. Transparency was also measured in the field using a 20 cm Secchi disk. Water samples were collected from the surface (approximately 10 cm depth), mid-depth, and just above the sediment from the three main sampling sites using a 2 L Van Dorn sampler bottle. During quarterly sampling at the remaining nine sites, only water samples just above the sediments were collected. Three sets of water samples were collected for each sampling site and depth and transported on ice to the lab for analysis. One set of water samples was collected in 125-ml bottles, which were completely filled with water, leaving no head space. One set of water samples was filtered and acidified in the field with concentrated HNO_3 to pH<2 for total metals analysis and one set was preserved upon collection with 50% antioxidant buffer (APHA, 1998) and capped with N_2 gas for sulfide analysis. The antioxidant buffer protects the sulfide from oxidation and the high pH converts all of the H_2S_{aq} and HS^- into S^{2-}. Analysis for H_2S was also performed in the field using a methylene blue method (APHA, 1998) with a set of pre-prepared comparators.

3.1.3 Atmosphere

Passive air diffusion sampling tubes, supplied by Gradko International Ltd (http://www.gradko.co.uk), were deployed at 137 cm, 175 cm, 213 cm, and 251 cm above the surface of the water at the Target. The tubes are designed to collect H_2S on an absorbent by passive diffusion. This absorbent is contained within an inert acrylic tube with a Teflon membrane and cap at one end and a mesh opening at the other end. The tubes were sent to the manufacturer for analysis. Measurements for wind speed and air temperature were obtained from two California Irrigation Management Information System (CIMIS) meteorological stations located on the east and west sides of the Sea (Figure 3-1, Nos. 127 and 128).

3.2. Laboratory Analysis

3.2.1 Sediment

Upon return to the lab, the sediment in the glass jars were promptly analyzed for oxidation-reduction potential (ORP) and pH in the lab using a platinum electrode and a combination electrode, respectively. Subsequently, the pore water was extracted from the sediments stored in 250 mL polypropylene bottles via centrifugation (6,000-7,000 rpm, 20 min) under N_2 gas and the resulting supernatant was filtered through a 0.45-micron polycarbonate filter and promptly analyzed as described below. The cores were sealed with zero headspace between measurements and covered with parafilm during sampling to minimize oxygen exchange.

3.2.2 Water Column and Pore Water

Unfiltered pore water and water column samples were analyzed for total alkalinity by titrating to an endpoint of pH 4.5 using a Beckman Autotitrator. Concentrations of total sulfide were determined on the unfiltered pore water and the field-preserved water column samples using an Orion IonPlus silver-sulfide ion-selective electrode on a Fisher Accumet mV meter. Standards were prepared using $Na_2S{\cdot}9H_2O$ in de-aerated water as outlined in standard methods (APHA, 1998). For comparison, we prepared a set of standards using 18.2 mΩ deionized water as well as a set using a saline water solution, similar to the composition of the Salton Sea, and found no difference in the electrode response to the two sets of standards. Other laboratory studies agreed with our finding (Frevert, 1980), therefore, we continued using deionized water in the preparation of the sulfide standards.

For major dissolved cation (Ca^{2+}, Cu^{2+}, Mg^{2+}, Mn^{2+}, Na^{+}, Si^{4+}, Sr^{2+}, K^{+} and total Fe) analysis, the extracted pore water samples and water column samples were filtered with a 30 mL syringe through a 0.45-micron polycarbonate filter. The samples were then preserved by acidifying with concentrated HNO_3 to pH<2. Due to the salinity interference, the samples were diluted 20:1 before being analyzed using the inductively coupled plasma (ICP) method on a Perkin-Elmer Optima 3000 DV ICP-OES.

Major anions (SO_4^{2-} and Cl^{-}) were analyzed using filtered (described above), unacidified pore water and water column samples, which were diluted 200:1, on a Dionex ion chromatograph with an IonPac ASII high capacity column. Dissolved Fe^{2+} was determined using the colorimetric *o*-phenanthroline method in the presence of an acetate buffer on a Milton Roy Spectronic 601 spectrophotometer at a 510 nm wavelength (APHA, 1998). Nutrients, including NO_3^{-}, PO_4^{3+}, and NH_4^{+}, were analyzed using a spectrophotometric method on a Technicon Autoanalyzer following standard methods (APHA, 1998). We performed statistical analysis using Student's t-test in Microsoft Excel.

4. Results and Discussion

4.1. General Chemistry

The Salton Sea is borderline hypersaline with a salinity of 46 - 48 ppt, currently, and has similar Mg^{2+}, Na^{+}, K^{+}, and Cl^{-} concentrations as seawater, but much higher concentrations of SO_4^{-} and HCO_3^{-} (Table 4-1). Sulfate increased from 13.7 percent of the total ion composition in 1907 to over 24 percent in 1999 (Holdren and Montaño, 2002); in the current study, sulfate has increased to approximately 26.5 percent of the total ion composition. The Cl^{-} concentration dominates the total ion composition at 40 to 42 percent currently, whereas in 1955 it comprised over 48 percent (Carpelan, 1958; Holdren and Montaño, 2002).

Table 4-1
Chemistry of the Salton Sea (this study).

Parameter	Units	Water Column	Pore Water
Salinity	g L^{-1}	46 - 48	NA
SO_4^{2-}	g L^{-1}	10 - 13	9 - 12
Cl^{-}	g L^{-1}	18 - 19	18 - 19
HCO_3^{-}	mg L^{-1}	200 - 300	800 - 1,200
Na^{+}	g L^{-1}	13 - 15	13 - 15
Ca^{2+}	mg L^{-1}	800 - 1,100	600 - 900
Fe^{2+}	mg L^{-1}	<0.005	<0.005
NH_4-N	mg L^{-1}	1.5 - 2.5	12 - 17
NO_3-N	mg L^{-1}	<0.005 - 0.2	<0.005 - 0.5
PO_4-P	mg L^{-1}	<0.005	1.0 - 2.5

Nitrate concentrations are high in the riverine inputs, which can be attributed to the agricultural and municipal waste loads; however, the concentrations in the lake are very low and often below the laboratory detection limits, perhaps due to high rates of denitrification. Ammonium concentrations clearly dominate the total nitrogen budget and exceed water quality standards set by the Environmental Protection Agency for aquatic species. Furthermore, the ammonium concentrations have increased over the past 50 years from maximally 0.04 mg L^{-1} in the bottom waters (Carpelan, 1958; Arnal, 1961) to as much as 2.5 mg L^{-1} currently (Table 4-1).

Although the loading of phosphorus into the Salton Sea has doubled over the past 30 years, the concentrations of phosphate have decreased, and based on N:P ratios, it is considered to be a phosphorus-limited system. This has been attributed to uptake by the biota as well as sedimentation and conceivably the precipitation of apatite minerals (Anderson and Amrhein, 2002). Seasonally, the ammonium and phosphate concentrations experience an increase during summer stratification, whereas nitrate increases in the winter months.

In spite of low redox potential in the sediments (discussed below), Fe^{2+} was not present in any significant concentration in pore water from the upper 10 cm of sediment (<0.05 mg^{-1} L) (Table 4-1). The high levels of sulfide would result in precipitation of Fe^{2+} as insoluble iron monosulfides (FeS) and pyrite (FeS_2), thus limiting Fe^{2+} accumulation in the sediment pore water and lower water column and imparting a characteristic dark color as observed in the sediments of the Salton Sea (de Koff et al., in press).

4.2. Temperature

The temperature of the water column is an important parameter due to its effect on chemical and biological processes as well as oxygen solubility and thermal stratification (Stumm and Morgan, 1981). Elevated temperatures typically increase the rate of chemical and biological processes and decrease the solubility of oxygen and other volatile compounds. The vertical temperature distribution for the north basin of the Salton Sea for 2005-2006 is shown in Figure 4-1a. The temperature at the Sea reached a maximum of more than 33°C on 7 August 2006 in the surface waters and a minimum of 14.3°C on 2 February 2006 in the bottom waters, consistent with the findings in previous years (Holdren and Montaño, 2002).

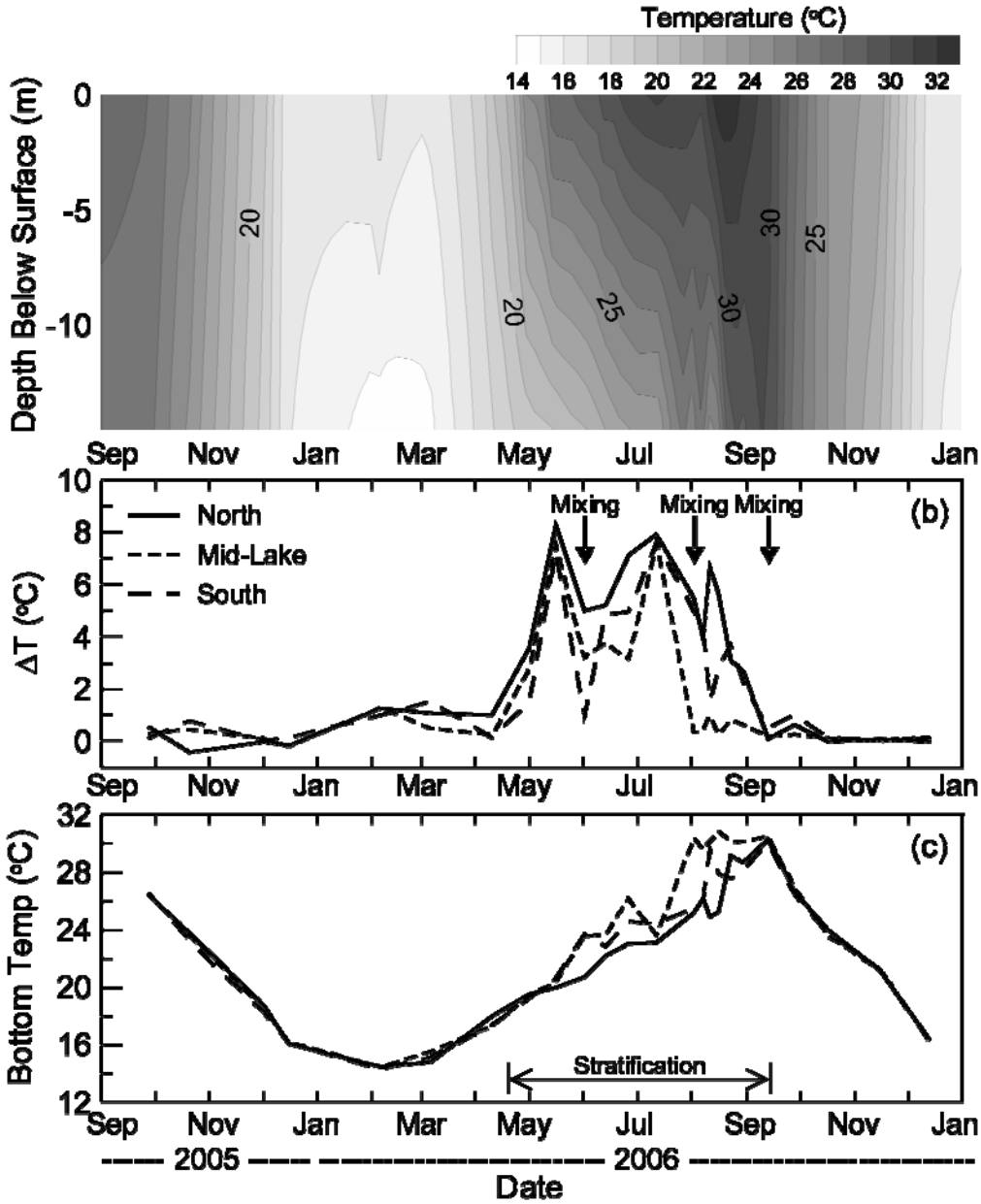

Figure 4-1. a) Contour plot of temperature at the north basin locations, b) temperature difference of the surface and bottom water, and c) bottom water temperatures.

Temperature profiles indicate that the Sea remained relatively well mixed from fall 2005 through the early spring 2006, after which rapid heating began from increased solar radiation. The temperature gradient from the surface to the bottom during the winter months was commonly less than 1°C (Figure 4-1b).

Increased daytime heating during the spring resulted in the warming of the surface water, thus making the density of the surface water less (i.e. more buoyant) than that of the cooler water below. Stratification begins when buoyant forces exceed wind-driven turbulent kinetic energy (TKE) inputs. Although the Salton Sea does not stably stratify for long periods of time (Arnal, 1961; Weiss, 1970; Holdren and Montaño, 2002), thermal stratification began in April 2006, and the difference in temperature (ΔT) between the surface and the bottom water rapidly exceeded 8°C (Figure 4-1b). Periodic, incomplete mixing was observed on several occasions, however, as indicated by the decreases in ΔT (Figure 4-1b) as well as the increase in the temperature of the bottom water, e.g., in late May (Figure 4-1c). A more severe mixing event (discussed in more detail below) occurred in late July-early August in which the temperature in the bottom waters reached more than 31°C. Stratification continued through the summer (approximately 4 months), until September when the ΔT again declined to < 1°C.

The temperature profiles for the south basin and mid-lake locations showed similar seasonal heating and cooling patterns; however, the south basin appeared to have mixed more frequently, e.g., the bottom water at this site was found to be 1-3°C warmer and ΔT was 3-4 °C lower than the north basin on 2 June and 11 August 2006 Figure 4-1c).

4.3. Dissolved Oxygen and Oxidation-Reduction Potential

The Sea was well aerated through winter 2005 and into the spring 2006, while some oxygen depletion was observed in the bottom waters in March (Figure 4-2a). Wind stirring combined with convective mixing and limited daytime heating prevented the development of thermal stratification in the late winter and early spring Figure 4-1a), thus delaying the onset of anoxia until summer. The daytime dissolved oxygen (DO) concentration in the epilimnion remained elevated, often reaching supersaturation (> 10 mg L^{-1}), throughout the summer stratification period because of photosynthesis.

The hypolimnetic DO concentration declined rapidly in April to less than 0.5 mg L^{-1} (Figure 4-2b), following onset of stratification (Figure 4-1b). Anoxic conditions can develop more easily in environments of elevated salinity, such as the Salton Sea, because the oxygen solubility decreases as salinity increases (Drever, 1988). Development of anoxia in the bottom layer did not begin until late April-early May, which was almost a month later than the previous study of Holdren and Montano (2002), indicating the sensitivity of stratification-mixing to meteorological forcing. The zone of anoxia spanned from approximately 7 m below the surface to a terminal depth of 15 m in the north and south basins and to a terminal depth of 12 m at the mid-lake location.

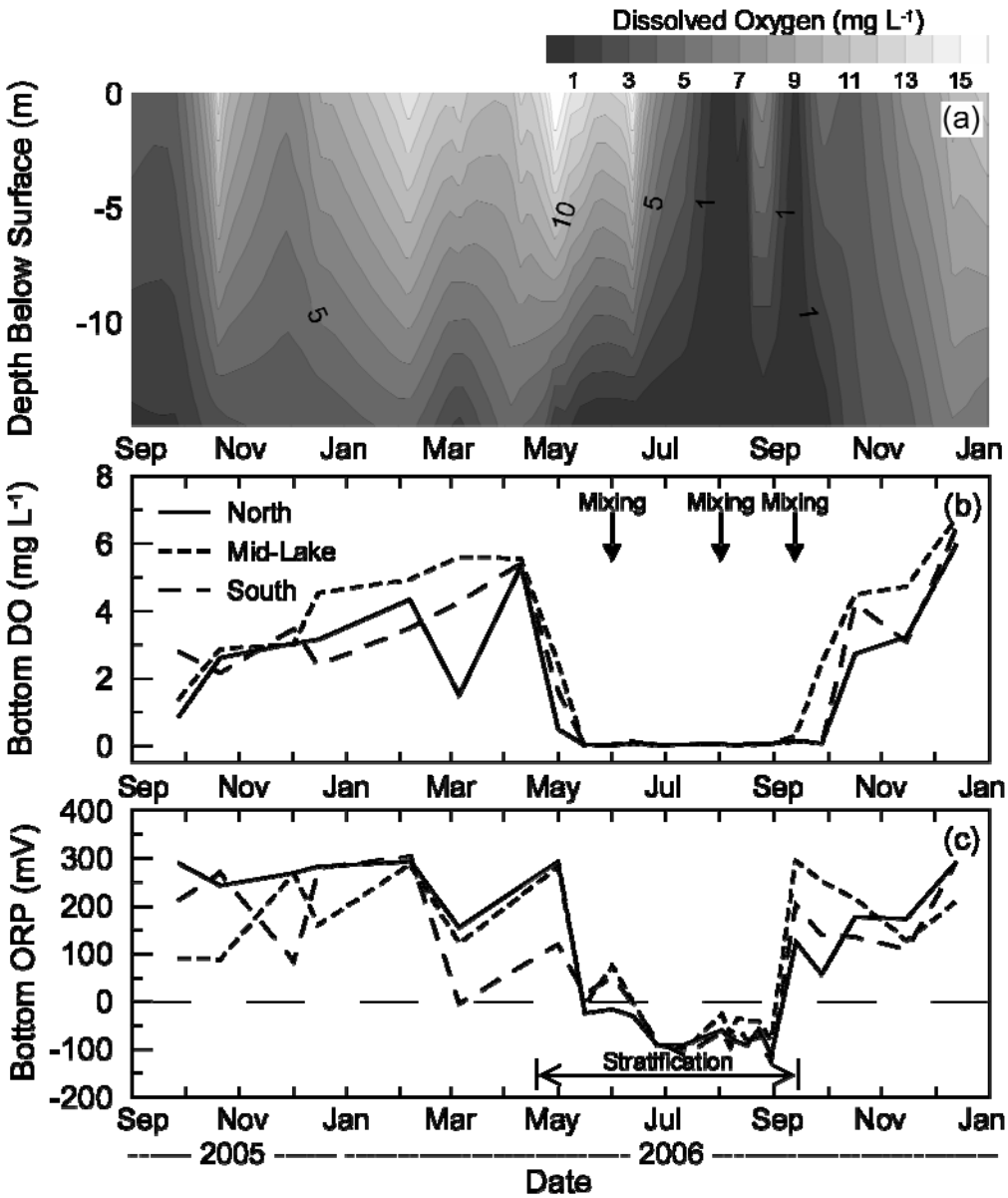

Figure 4-2. a) Contour plot of dissolved oxygen at the north basin locations, b) dissolved oxygen concentration of the bottom water, and c) oxidation-reduction potential of the bottom waters.

The volume of the anoxic hypolimnion was often greater than 65% of the total lake volume during stratification. Hypoxic or anoxic conditions in the hypolimnion persisted for over 4 months (Figure 4-2b). In contrast, Arnal (1961) noted that the bottom waters were usually oxic, with periods of anoxia developing for only a few days during the summer in 1954-1956.

During the mixing event in late July-early August (Figure 4-1), the zone of anoxia reached to the surface of the lake (Figure 4-2a), which (combined with other factors discussed in more detail below) resulted in a massive fish kill. Unfortunately, summer fish kills and whole-lake anoxia are not presently uncommon at the Salton Sea (e.g., Watts et al., 1998). More than 1 month was required to reoxygenate the water column (Figure 4-2b).

The oxidation-reduction potential (ORP) followed the DO concentrations, and the ORP was positive (generally >100 mV) when the water column was aerated and negative when the DO was less than 1 mg L^{-1} (Figure 4-2c). A large negative ORP is consistent with sulfate reduction near the sediments. Increases in bottom water ORP were observed during the summer mixing events in late May and late July, as well as the final mixing event in September that reduced ΔT (Figure 4-1b) and increased bottom water DO and ORP (Figure 4-2). During the mixing period in which the entire water column was anoxic, the ORP was negative (< -20 mV) from the surface to the bottom waters, signifying strongly reduced conditions throughout the water column. By late September 2006, ORP values returned to >200 mV and the DO concentration again approached or exceeded 7 mg L^{-1}.

4.4. Sulfide Chemistry

While the water column experienced wide swings in DO concentrations and redox potential, the sediment of the Salton Sea remained anoxic and highly reduced throughout the entire year (ORP < -100 mV). It is the combination of warm temperatures, high organic matter content, and limited availability of DO that favor sulfate reduction in the sediment. Under anoxic and strongly reducing conditions (<100 mV), such as that found in the sediments of the Salton Sea, sulfate is reduced to sulfide by dissimilatory sulfate reduction (Tobolsky, 1968).

We found sulfate concentrations to average around 12,000 mg L^{-1} (125 mM) in the pore water; inarguably the Salton Sea is not lacking in this important microbial substrate. During sulfate reduction, microbes use sulfate as the terminal electron acceptor during organic matter mineralization:

$$SO_4^{2-} + 2(CH_2O) \rightarrow 2HCO_3^- + H_2S \quad (1)$$

where organic matter (CH_2O) is oxidized and bicarbonate alkalinity and hydrogen sulfide are produced. Once sulfide diffuses out of the sediments and into an aerobic water column, sulfide oxidation occurs, as represented by the following reaction:

$$HS^- + 2O_2 \rightarrow SO_4^{2-} + H^+ \quad (2)$$

The sulfide produced in the sediments (eq 1) is readily oxidized and consumes oxygen (i.e., is a significant source of chemical oxygen demand, COD) when transported into aerobic regions, simultaneously producing sulfate and acidity (eq 2).

Consistent with this, we found that the sediment pore water was significantly elevated with respect sulfide concentrations when compared to the overlying water column (Figure 4-3). We observed a marked difference in SO_4^{2-} concentrations between the sediment pore water and overlying water column in the mid-lake and south basin locations, in which the sediments contained a lower concentration of sulfate than the water column, indicative of sulfate reduction (Table 4-1). This was observed in previous studies at the Salton Sea as well (Anderson and Amrhein, 2002; Wardlaw and Valentine, 2005).

Under aerobic conditions, like that present in the water column of the Salton Sea from late fall into early spring, sulfide averaged 1.6 – 1.8 mM in the pore water and no detectable sulfide concentrations (<0.004 mM) were present in the bottom and surface water (Figure 4-3), with the exception of 2 December 2006, in which low concentrations of sulfide in the north basin surface and bottom water (0.01 mM) (Figure 4-3). This may have coincided with a small mixing of bottom waters being brought to the surface on that day.

As stratification began in late spring and the hypolimnion became increasingly anaerobic, sulfide produced in the sediments continued to diffuse into an increasingly anaerobic bottom layer, and accumulate substantially in the hypolimnion when the bottom water temperature increased to >20 ^{o}C and the DO declined to <1 mg L^{-1} (Figure 4-1c and Figure 4-2b). Sulfide concentrations in the pore water and bottom water increased strongly following the onset of stratification. The pore water concentration increased from a mean concentration of 1 mM at the three main sampling locations to more than 3.5 mM; likewise, the sulfide concentrations in the north and south basin bottom water quickly increased from 0.05 mM on 1 May 2006 to 0.46 mM on 16 May 2006 (Figure 4-3c). Concentrations at the mid-lake location also showed a rapid accumulation of sulfide, but not quite as great as the north and south basin locations.

Even as thermal stratification began in late spring, the upper few meters of the water column continued to mix and, as noted earlier, maintained high concentrations of DO. Thus, any sulfide mixed into the upper portion of the water column would be reoxidized. After a month following the onset of stratification (interrupted with periodic mixing by upwelling and convective mixing), sulfide was consistently being observed at mid-depth (Figure 4-3b) as well as in the hypolimnion (Figure 4-3c). On 1 June 2006, the sulfide concentration in the north basin at 7 m was 0.2 mM, while the south basin contained much lower sulfide concentrations (0.01 mM). The lower concentrations observed in the south basin were possibly due to more frequent mixing (Watts et al., 2001).

After a few months of limited mixing and the accumulation of sulfide, bottom water sulfide concentrations reached the highest levels in late July: 0.95 mM in the north basin, 0.60 mM in the south basin, and 0.74 mM in the mid-lake location (Figure 4-3c). Pore water sulfide concentrations reached a maximum of 5.6 mM in the north and south basin and 3.1 mM in the mid-lake location (Figure 4-3d). The mean summertime sediment pore water concentration was greater than 3.3 mM in the north and south basins and 2.4 mM at the mid-lake location.

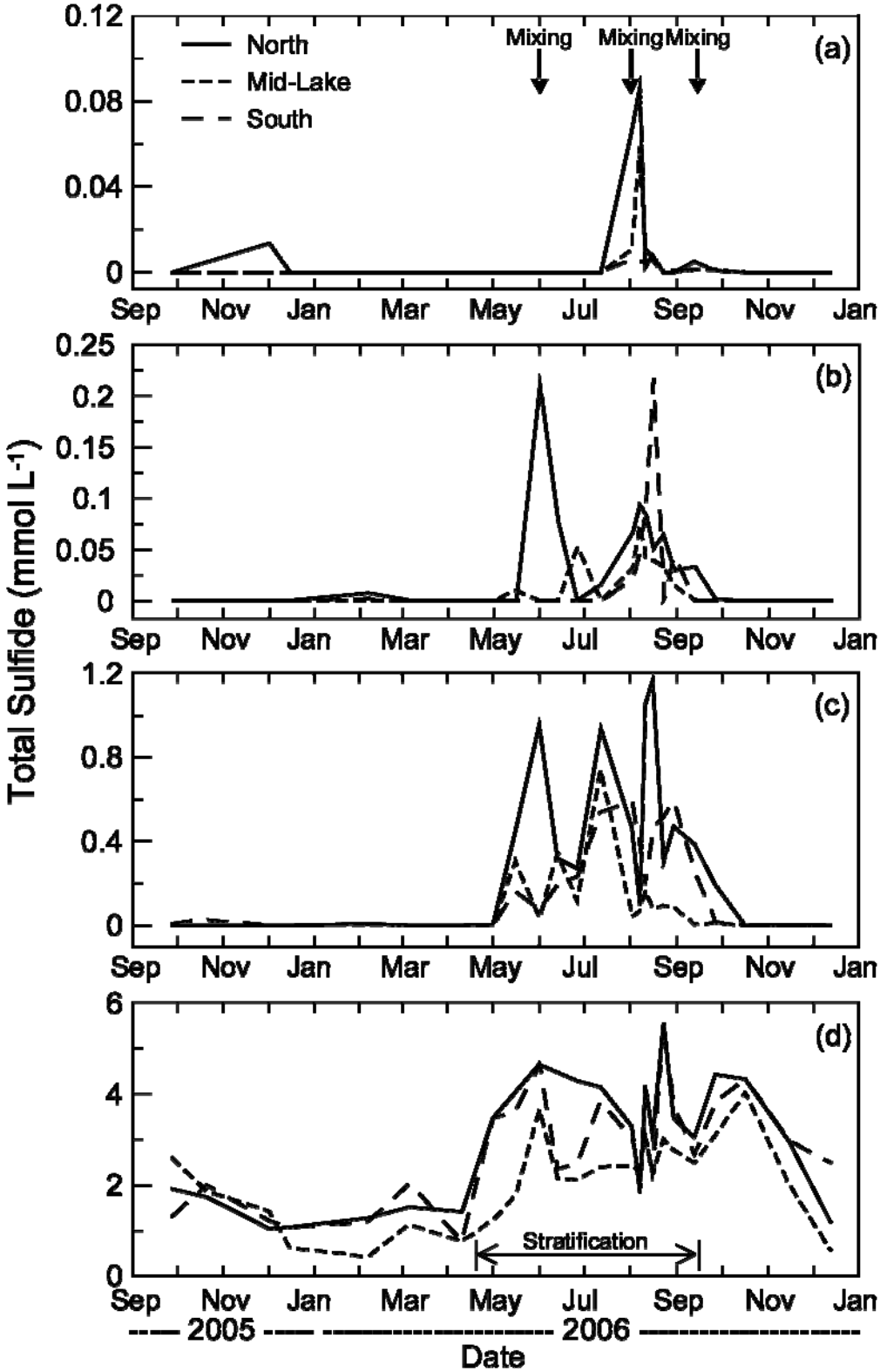

Figure 4-3. Total sulfide concentrations in a) the surface waters (approx 10 cm below surface), b) mid-depth (approx 6-7 m below surface), c) bottom waters, and d) pore water.

Sulfide concentrations in the bottom waters have increased at the Sea over the past five decades. In 1955, sulfide at the Sea was measured to be maximally 0.003 mM during the summer, in which stratification lasted only a couple of days (Carpelan, 1958). In 1998-1999, sulfide concentrations were reported to be 0.09 - 0.2 mM in the bottom (Watts et al., 2001), following a longer period of stratification and hypolimnetic anoxia than found in this study.

The sulfide concentrations in the north and south basin hypolimnia appear to be quite high based on the relatively short length of time of accumulation. Mono Lake, a much deeper (48 m) hypersaline, eutrophic lake with a smaller fetch, has prolonged periods of stratification with a pronounced chemocline. Reported sulfide concentrations maximally reached 1.82 mM in the mixolimnion of Mono Lake during a 4-year period of meromixis from 1984 to 1988 (Miller et al., 1993), a concentration only twice that of the Salton Sea that developed during only four months of stratification. Walker Lake in Nevada, a deeper (29 m) saline lake with smaller surface area than the Sea, had reported concentrations of only 0.3 mM sulfide in the hypolimnion with a 6 to 7 month stratification period (Beutel et al., 2001).

The areal rate of sulfide accumulation in the hypolimnetic bottom water of the Salton Sea can, with some assumptions, be estimated from the change in sulfide concentrations. The two main assumptions are the thickness of the bottom layer (assumed to be 1 m, representing the approximate sampling layer thickness), and the assumption that the sulfide produced was not entrained upward or oxidized. During the period of partial stratification from 1 May 2006 until a few weeks before mixing on 12 July 2006, the average daily accumulation rate was estimated to be 13 mmol m^{-2} day^{-1} in the north basin and 7.5 mmol m^{-2} day^{-1} in the south basin. For comparison, the rate of sulfide accumulation below the chemocline of Solar Lake, a shallow saline lake (6 m) on the east coast of Sinai, was estimated to be 36 mmol H_2S m^{-2} day^{-1} during a 3 month period from February to April (Jorgensen et al., 1979). High concentrations of sulfide are not uncommon in the anoxic monimolimnia of meromictic lakes (Wetzel, 2001); however, the accumulation of sulfide in polymictic systems is extremely rare and limited to hypereutrophic systems with high sulfate (Effler et al., 1988).

When dissolved oxygen concentrations are limited, such as the case of hypolimnetic water during summer stratification, sulfide can quickly consume all of the available oxygen (Cline and Richards, 1969). While most minor mixing events resulted in the oxidation of upwelled hypolimnetic H_2S into the epilimnion, this was not the case during the mixing in early August 2006. During this mixing, sulfide from the lower water column (e.g., the bottom and middle sampling depths) mixed upward and reacted with available dissolved oxygen. Sulfide transported to the upper water column was rapidly oxidized and O_2 was consumed; simultaneously, O_2 transported to the bottom layer was quickly consumed by sulfide oxidation.

The oxidation of 1 mol of sulfide requires 2 mol of oxygen, according to the stoichiometry of the reaction (eq 2). The total calculated volume of sulfide in the Sea on 12 July 2006, a couple of weeks prior to mixing, was estimated to be 55.4×10^7 mol. Based on the stoichiometry, 111×10^7 mol of oxygen would be required for complete oxidation of the sulfide. Using a volume-weighted average, the total calculated quantity of oxygen in the Sea on 12 July 2006 was estimated to be 63×10^7 mol. These results indicate that the oxygen demand exerted by H_2S exceeded the available oxygen supply; consistent with these calculations, sulfide was present throughout the upper water column at elevated concentrations following mixing in late July (Figure 4-1a and Figure 4-3).

On 2 August 2006, the first sampling date following this mixing event, a slight decrease in pore water and bottom water sulfide was initially observed and attributed to dilution and oxidation, but concentrations recovered to elevated levels again within a couple of weeks (Figure 4-3c and Figure 4-3d). Also on this date, the total sulfide measured in the surface water was 0.07 mM in the north basin, 0.02 mM in the south basin, and 0.01 mM at the mid-lake location (Figure 4-3a). Strong winds, at times exceeding 7 m s^{-1}, directed along the long axis of the Sea were present on July 26-28th and are thought to have set up the upwelling in the north basin that brought sulfide-rich bottom waters to the surface there (CIMIS, 2007). Five days later, total sulfide was measured in the surface water at 0.09 mM in the north basin and 0.06 at the mid-lake location. Sulfide concentrations in the surface waters remained elevated for over two weeks following mixing, indicative of the relatively slow rate of oxidation of hydrogen sulfide in the Salton Sea.

4.5. Sulfide Oxidation

Major sinks for dissolved and colloidal sulfide include oxidation, both biologically and chemically, escape to the atmosphere, or precipitation (e.g. FeS). Chemical oxidation by molecular oxygen appears to be the most significant sink for sulfide at the Salton Sea.

A sulfide oxidation rate for the Salton Sea was determined experimentally in the laboratory by simultaneously measuring the rate of sulfide and oxygen disappearance in freshly-collected, unfiltered water from the Salton Sea (Amrhein, unpublished data). The rate law was determined using the method of initial rates and the rate constant was determined by multiple linear regression. The sulfide oxidation rate for the Salton Sea is given by the following second-order rate expression:

$$\frac{d[S^{2-}]}{dt} = k[S^{2-}][O_2] \tag{3}$$

where time (t) is in seconds, the rate constant (k), and the concentrations of total sulfide and DO are in mM. When the sulfide concentrations were low, the laboratory-determined rate constant ($10^{-1.7}$ mM s^{-1}) resulted in a 20% overestimation of the sulfide oxidation rate, which was taken into account during our calculations (Amrhein, unpublished data). The half-life was calculated to be 131 hours, which is much longer than reported for ocean water by Cline and Richards (1969) or Almgren and Hagstrom (1973) (maximally 14 and 9.5 hours, respectively), likely due to the low oxygen solubility and high ionic strength of the Salton Sea as compared to ocean water. The estimated half-life for sulfide in the Black Sea, a more productive system than the Salton Sea, was 166 hours (Sorokin, 1971; Almgren and Hagstrom, 1973).

Using the concentrations of sulfide and oxygen measured on 7 August 2006 (0.09 mM and 0.003 mM, respectively) as the initial concentrations, we calculated approximately 13 days for complete sulfide oxidation to occur, assuming that the only sink for dissolved oxygen is sulfide oxidation. This estimate is in reasonable accord with our field measurements where we observed sulfide in the surface water for about 16 days following mixing. We attribute the small difference between predicted and observed values to the Salton Sea being an open system in which a continuous input of sulfide from the bottom waters into the surface waters prolonging the length of time for complete oxidation. The entire lake volume remained anoxic for over four weeks until the rate of reaeration exceeded the rate H_2S production, upward mixing, and sulfide oxidation. The Salton Sea recovered to its normal conditions

following holomixis in September 2006, and sulfide was no longer detectable in the surface water.

4.6. Alkalinity and pH

Sulfate reduction has long been linked with the generation of alkalinity (eq 1) and carbonate precipitation (Javor, 1989). At the same time, the oxidation of HS^- reduces the pH and alkalinity through the formation of stronger sulfoxy acids (eq 2) (Cline and Richards, 1969). Microbial respiration also lowers pH through hydration of respired CO_2 to form carbonic acid, followed by proton dissociation reactions.

Student t-tests using paired sample means were performed to compare pore water, surface water, and bottom water concentrations as well as seasonal variability. The two sets of data were considered to be significantly different with a p-value less than 0.05. Aligning with the above arguments, the sediment pore water was shown to be significantly elevated overall in comparison the overlying water column with respect to bicarbonate alkalinity and lower in pH (Figure 4-4).

Seasonal variations in the sediment pore water chemistry showed that the winter months had a slightly higher average pH (7.55-7.62) than did the summer stratified months (7.43-7.52) (Figure 4-4f). The bottom water pH was also slightly higher during the well-mixed months with an average 8.25-8.35, but during stratification, the pH dropped to its minimum in late July to 7.6 and 7.7 in the north and south basins, respectively. There was no significant seasonal difference in the surface water pH.

Alkalinity concentrations were statistically higher in the pore water and bottom water during the winter and early spring months than during the summer months at the three main sampling locations. The alkalinity levels in the pore water increased from 15 meq L^{-1} during the winter to 20-25 meq L^{-1} during summer stratification (Figure 4-4c), consistent with eq 1 and increased sulfide production and accumulation during summer stratification (Figure 4-3d). Likewise, alkalinity was relatively constant in the bottom water at 4.5-5 meq L^{-1} in the bottom water through the winter and increased slightly in the north and south basins during summer stratification (to 7.2 and 5.2 meq L^{-1}, respectively). Conversely, the surface water alkalinity concentrations were lower during summer stratification than during well-mixed months, due presumably in part to $CaCO_3$ precipitation, although no clear trends in dissolved Ca^{2+} were present (data not shown).

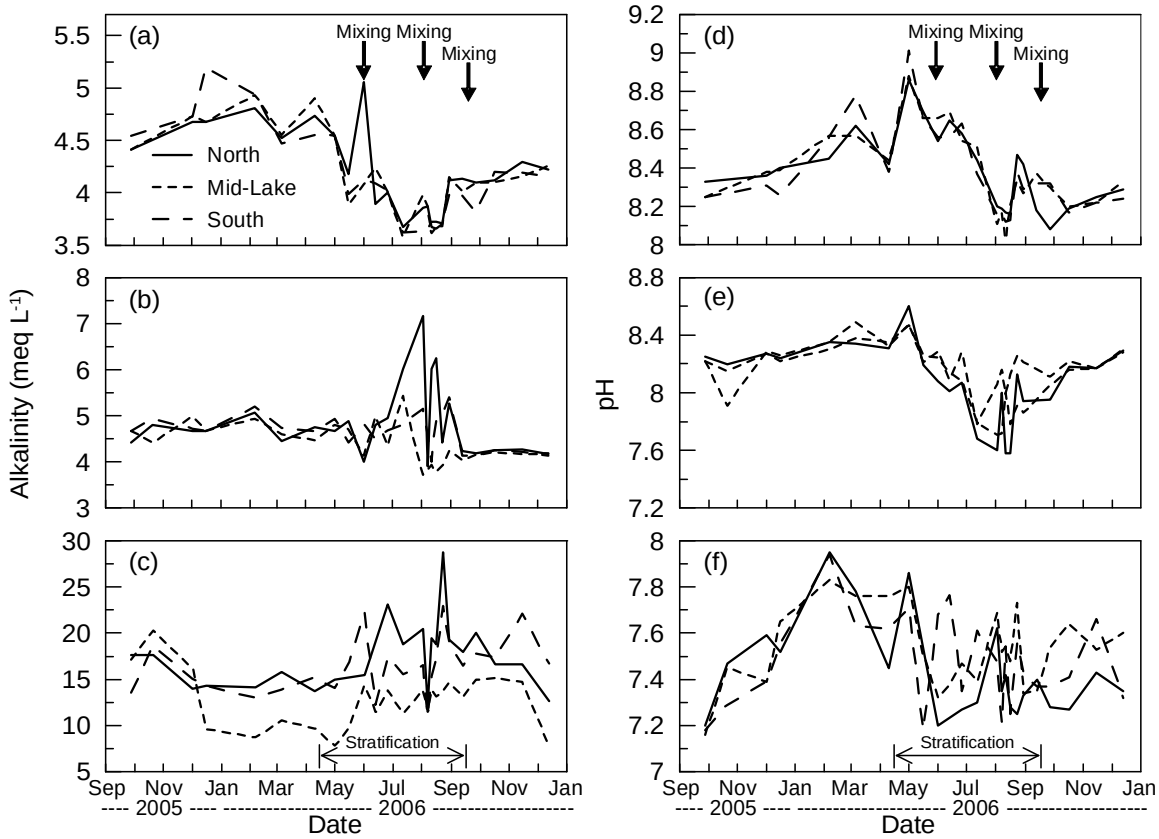

Figure 4-4. Time series of alkalinity in the: a) surface water, b) bottom water, c) pore water, and pH in the d) surface water, e) bottom water, and f) pore water.

The pH near the surface was often one pH unit greater than the pH of the bottom water as a result of CO_2 removal by photosynthesis in the surface and CO_2 formation during respiration and decomposition in the bottom layer (Wetzel, 2001; Stumm and Morgan, 1981). The pH in the surface water was statistically greater ($p<0.05$) than the bottom water and was greater in the winter months than the summer stratified months. This was also observed by Holdren and Montaño (2002). No statistically significant variation in the alkalinity concentration was observed during the fall-spring between the surface water and bottom water; the alkalinity in the surface water was 2-3 meq L^{-1} less than that of the bottom waters during the summer however.

Mixing events resulted in significant decreases in the pH of the surface water and bottom water (Figure 4-4) due in part to proton production resulting from sulfide oxidation (eq 2). The pH during mixing in late July averaged 8.12 - 8.18 and was relatively uniform from the surface into the bottom layer (Figure 4-4d and Figure 4-4e).

4.7. Other Chemistry

Chemical oxygen demand (COD) was also routinely determined on water samples beginning in the summer of 2006. COD was measured on surface and bottom water samples at the 3 main sites on 9 dates. COD values were high, averaging 198.0±60.7 mg L^{-1} (n=54). No clear seasonal trends were in place. Moreover, parametric and non-parametric statistical analyses (t-tests and sign tests) indicated no significant difference between surface waters and bottom waters. Assuming complete oxidation of HS^- to sulfate (eq 2), we estimate that, on average,

10.3% of the COD of the bottom water during the summer can be attributed to sulfide oxidation.

Dissolved nutrient concentrations in the bottom waters exhibited seasonal variation similar to that observed for sulfide. That is, during the winter and spring when the water column was cool and well-mixed, comparatively low concentrations of SRP and NH_4-N were measured above the sediments (Figure 4-5). Concentrations of SRP increased from values near 0.03 mg L^{-1} to 0.2 – 0.3 mg L^{-1} at the north basin site, although mixing events lowered SRP levels considerably (Figure 4-5a). Somewhat lower SRP concentrations were found during summer stratification at the mid-lake and south basin sites, but values remained above those found earlier in the year.

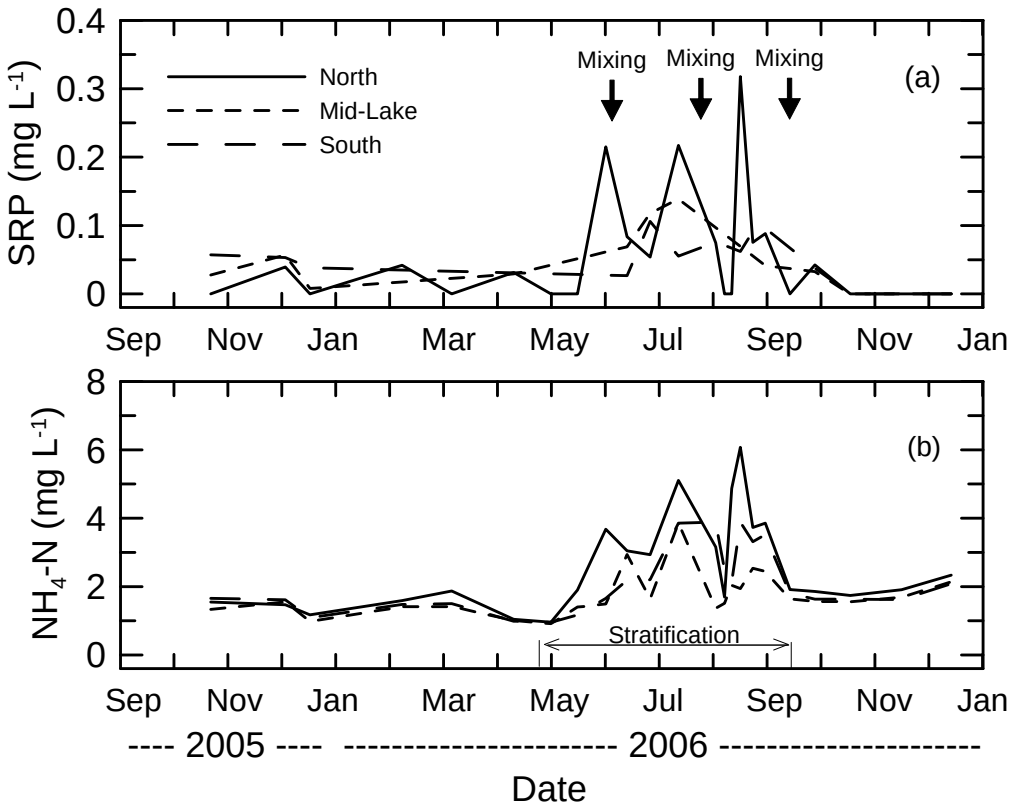

Figure 4-5. Concentrations of (a) SRP and (b) NH_4-N above the sediments at the main sampling sites.

Ammonium-N concentrations followed similar trends, with relatively stable concentrations (~1.3 mg L^{-1}) from October-April, and much higher concentrations observed from May-August (Figure 4-5b). As observed with sulfide (Figure 4-3c) and SRP (Figure 4-5a), concentrations were higher at the north basin site relative to the mid-lake or south basin sites (Figure 4-5b). Ammonium-N concentrations were, in fact, linearly correlated with sulfide levels (r^2=0.81). The observed accumulation of sulfide, NH_4-N, and SRP in the bottom waters reflects the microbial transformations and mineralization reactions in the sediments, modulated by the local mixing regime.

4.8. Sulfide Flux at the Sediment-Water Interface

In natural systems, transfer across the sediment-water interface is driven by two primary processes: advection resulting from bulk flow (including flows induced by sedimentation, compaction, or burrowing), as well as diffusion (molecular, ionic, or bioturbation) (Boudreau,

1996; Wardlaw and Valentine, 2005). The driving force of diffusion is a concentration gradient and the movement of material downgradient to achieve equilibrium. A key transport mechanism in the sediments of the Salton Sea appears to be diffusion, as supported by linear depth distributions of Wardlaw and Valentine (2005). The ionic diffusive flux of sulfide (HS^-) from the sediment to the overlying water column was estimated in our study using Fick's first law:

$$J = -\phi D_i \frac{dC}{dz} \tag{5}$$

where ϕ is the sediment porosity (m^3 pore water m^{-3} bulk sediment), D_i is the sediment diffusion coefficient of the ion in the porous medium (cm^2 sec^{-1}), and dC/dz is the change in concentration (in mM) with respect to a linear distance, z (cm). The flux due to molecular diffusion (J) is given as positive in the upward direction. The sediment diffusion coefficient was corrected for the absolute temperature of the water, dynamic viscosity in centipoise (Boudreau, 1996), tortuosity (Ullman and Aller, 1982), and the limiting ionic conductivity (Li and Gregory, 1974; Lasaga, 1979). The uncertainty of D_i has been estimated to be 0.5×10^{-6} cm^2 s^{-1} (Li and Gregory, 1974) and is accounted for in our flux calculations. The *in situ* water temperature, a salinity of 46 g kg^{-1}, and a hydrostatic pressure at the sediment-water interface of 2.4 atm were used to calculate the dynamic viscosity for each sampling date and location. A porosity of 0.85 was used for the north basin and the mid-lake location and a porosity of 0.87 was used for the south basin (Anderson et al., in review; Wardlaw and Valentine, 2005). The concentration gradient was estimated from the measured porewater concentration assuming a linear gradient over the approximately 10 cm sampling depth of the Ponar sampler. Based on the pH of the sediment and overlying bottom water (7.6-7.8 and 7.8-8.0, respectively), our flux estimates are based on the assumption that the dominant sulfide species was as HS^- (greater than 90%).

The calculated sulfide flux across the sediment-water interface at the Salton Sea ranged from 1.7 mmol m^{-2} day^{-1} in December 2005 in the north basin to a peak of 9.2 mmol m^{-2} day^{-1} in August 2006 before decreasing again to 2.3 mmol m^{-2} day^{-1} in December 2005 (Figure 4-6). Generally, the estimated flux was relatively steady through the winter and early spring at approximately 3 mmol m^{-2} day^{-1} in both the north and south basins. Assuming that sulfide is completely oxidized to sulfate (eq 2), this would result in an O_2 consumption rate of approximately 6 mmol m^{-2} day^{-1} during this time period. This approximated consumption rate was less than the available oxygen supply, which prevented the build-up of sulfide in the lowermost water column during the winter and early spring.

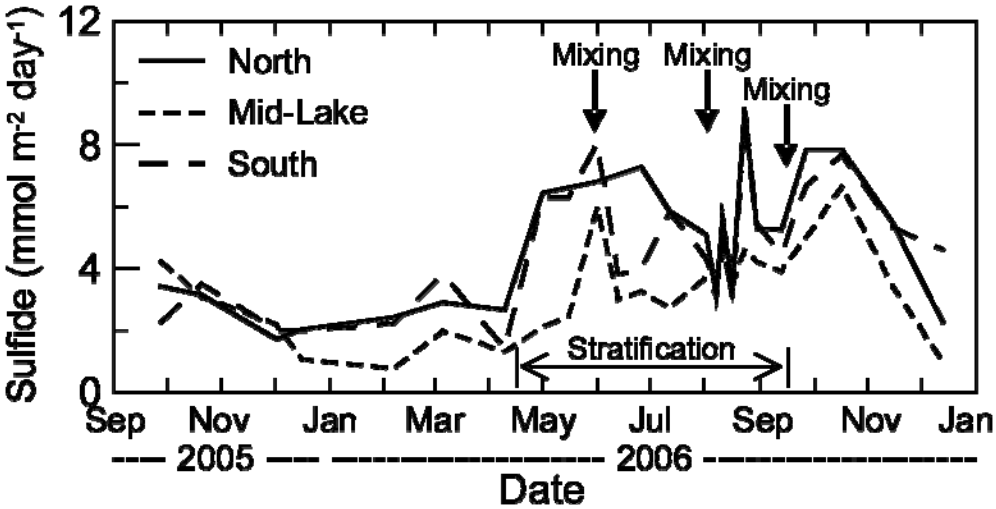

Figure 4-6. Sulfide flux from sediment to overlying water column.

The shallower mid-lake location (not shown) had a slightly lower flux, overall, than the deeper north and south basins. The highest estimated flux occurred during the summer months when the concentration gradient was greatest. A sharp decrease in the flux was observed following the mixing event in late July-early August due to the reduced concentration gradient (Figure 4-6).

The estimated daily flux at the Salton Sea during the 2005-2006 hydrologic year is comparable to the computed flux of Mono Lake in which a diffusive flux of sulfide (HS^-) of was calculated to be 6.3 mmol m^{-2} day^{-1} from the sediment to the monimolimnion during the 1982-1988 meromictic episode (Miller et al., 1993). Additionally, the flux of sulfide from Cape Lookout Bight in North Carolina, a coastal area known for its high organic sediments and nutrients, was estimated to be 9 mmol m^{-2} day^{-1} from July-September (Chanton, 1987). The flux of sulfide from the Salton Sea is comparatively very high given that it is a shallow, polymictic body of water. It is also an order of magnitude higher than the calculated and measured sulfide flux in the Santa Barbara Basin, a coastal zone also noted for its relatively high productivity and seasonal anoxia (Kuwabara et al., 1999).

4.9. Sediment Oxygen Demand

The flux of sulfide from the sediments exerts a strong oxygen demand; laboratory measurements were also conducted to determine sediment oxygen demand in the Salton Sea. Cores were collected in February, April and June 2007 and incubated at the approximate temperatures in place at the time of sampling. Results from the February sampling are shown in Figure 4-7. The DO levels declined rapidly in cores collected from all 3 sites, with very good reproducibility between triplicate cores at the north basin and mid-lake sites, although one replicate at the south basin site showed greater DO declines than the other two replicate cores from this site (Figure 4-7). The DO concentrations declined approximately linearly down to about 2 mg L^{-1}, although the kinetic response over the full time course of the measurements was better described with exponential curves (r^2~0.9). Nonetheless, these findings are consistent with other studies that indicate that the uptake rate of DO is independent of DO concentration in the overlying water in the concentration range of 2-5 mg/L (Thomann and Mueller, 1987). Dissolved oxygen concentrations in separate water samples incubated in the dark at this temperature declined only about 1 mg L^{-1} over 2.5 days.

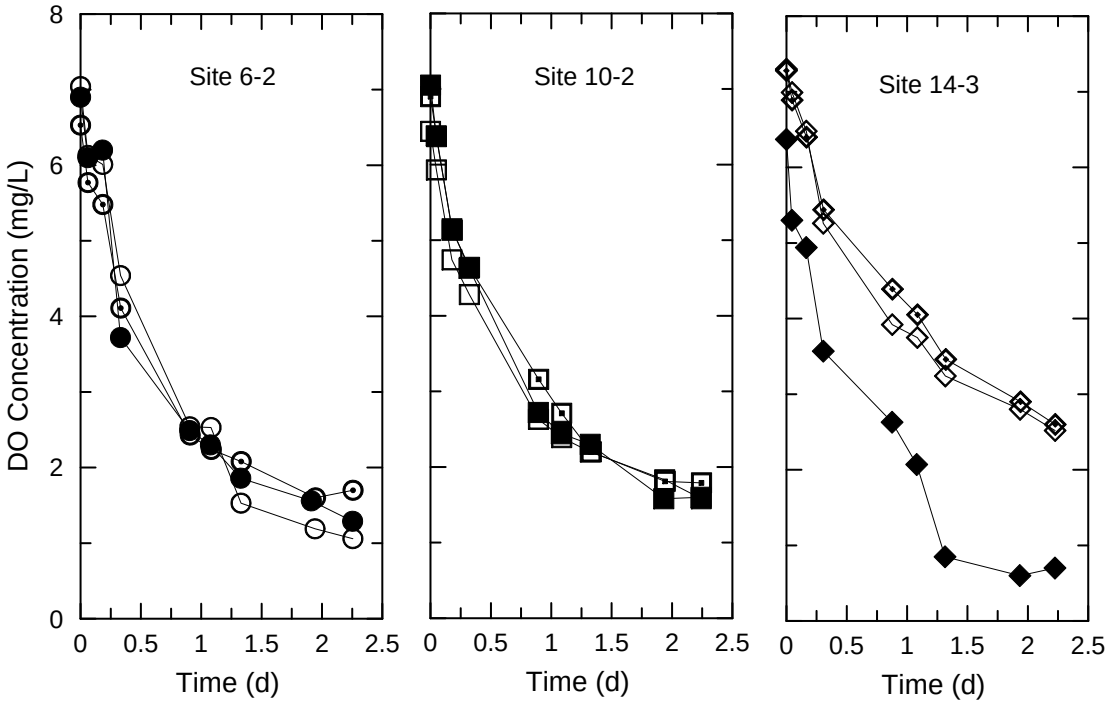

Figure 4-7. Dissolved oxygen concentrations in water overlying intact Salton Sea sediments collected from the 3 main sampling sites on February 21st, 2007.

Assuming a linear decrease in DO concentrations to approximately 2 mg L^{-1}, and using the volume of the overlying water of the cores (~0.5 L), and the cross-sectional area of the sediments (31.7 cm^2), we calculate average SOD values that decreased across the Sea, from 0.5 ± 0.0 g m^{-2} d^{-1} at the north basin site to 0.4 ± 0.1 g m^{-2} d^{-1} at south basin site (Table 4-2).

Table 4-2
SOD values at the main sampling sites on the Salton Sea.

	SOD (g m^{-2} d^{-1})		
Site	**February (15 ºC)**	**April (19 ºC)**	**June (23 ºC)**
North Basin	0.5 ± 0.0	2.4 ± 1.4	1.9 ±0.4
Mid-Lake	0.4 ± 0.0	2.3 ± 0.7	1.6 ± 0.1
South Basin	0.4 ± 0.1	2.1 ± 0.6	1.7 ± 0.1

SOD values were found to increase dramatically in April, exceeding 2 g m^{-2} d^{-1} at all 3 sites (Table 4-2). The observed increase is attributed to the higher temperatures and higher concentrations of free sulfide in the porewater and bottom waters at that time. SOD values remained high in June 2007, when cores were incubated at the ambient bottom water temperature of approximately 23 ºC (1.6 - 1.9 g m^{-2} d^{-1}), but were somewhat lower than observed in April (Table 4-2). The values are in general agreement with the average value of 1.8 g m^{-2} d^{-1} found previously (Amrhein and Anderson, 2005), The findings demonstrate that SOD rates are substantial in deeper regions of the Sea, especially during the spring and summer months when bottom water temperatures increase and hasten rates of chemical and biological processes there.

It is also instructive to compare measured SOD values with hydrogen sulfide flux estimates made over the past year. Hydrogen sulfide flux at the 3 main sampling sites averages about 3

mmol m^{-2} d^{-1} in the cool winter months (December-February) (Figure 4-5). Assuming oxidation of hydrogen sulfide to sulfate following eq 2, we estimate that 0.19 g m^{-2} d^{-1}, or 37 – 54% of the measured SOD in February, is due to oxidation of hydrogen sulfide. Sulfide oxidation appears to account for approximately 8 - 14 % of the SOD based upon April measurements and 21 - 32 % of SOD in June. High sulfide levels are known to inhibit both nitrification and denitrification reactions, so significant oxygen demand due to oxidation of ammonium is unlikely (and hence thought to account for the high NH_4^+ levels in the Sea). Moreover, porewater Fe^{2+} and Mn^{2+} levels are very low, such that negligible fluxes exist for these reduced species. Thus labile organic matter likely represents the balance of the oxygen demand in the sediments of the Sea.

4.10. Volatilization at the Air-Water Interface

The exchange of gases across the air-water interface plays an important role in biogeochemical cycling and the regulation of water quality pollutants, as well as maintaining adequate dissolved oxygen levels to support aquatic biota. Based on chemical considerations, the primary loss mechanism for sulfide in the Salton Sea is through sulfide oxidation; however, significant losses of H_2S also occur at the air-water interface. Similar to the exchange across the sediment-water interface, this exchange is also driven by a concentration gradient in which the aqueous phase concentration and the atmospheric concentration seek to reach equilibrium.

The average concentration of H_2S in the air approximately 1-2 m above the surface of the Salton Sea at the target was consistently elevated compared to that of the background location approximately 6.5 kilometers north of the lake. The concentration of the H_2S in the air phase above the Sea averaged 0.05 μmol m^{-3} (1.7 μg m^{-3}) through the winter and spring, while background levels averaged 0.009 μmol m^{-3} (0.3 μg m^{-3}) (Figure 4-8). The World Health Organization estimated the average ambient air hydrogen sulfide concentration as a result of natural sources to be 0.14 - 0.4 μg m^{-3} (WHO, 1981) and the average ambient air level of hydrogen sulfide in urban areas is estimated to be 0.3 μg m^{-3} (Robinson and Robbins, 1970). Increases in measured H_2S concentration in the atmosphere (exceeding 1.0 μmol m^{-3} or 34 μg m^{-3}) in late July and early August (Figure 4-8) coincided with dramatic increases in the surface water concentration of sulfide (Figure 4-3).

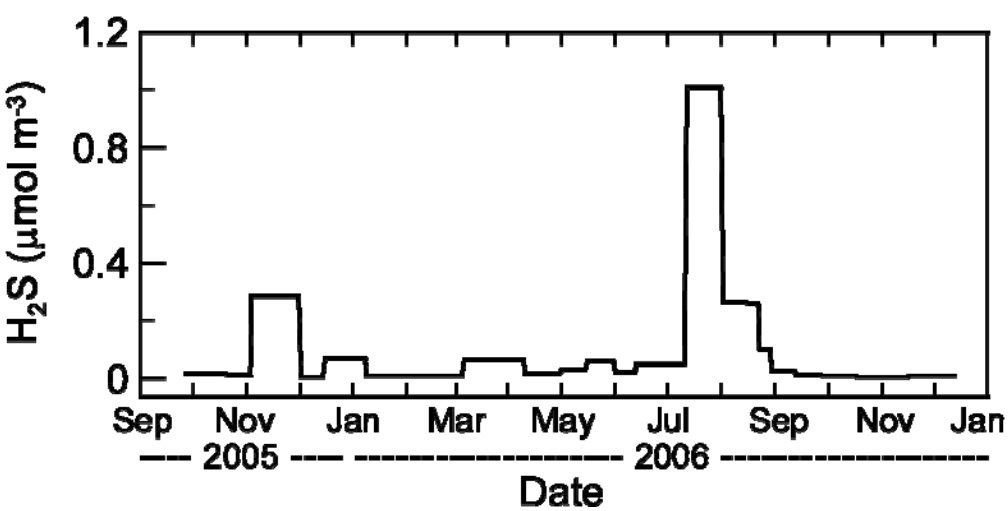

Figure 4-8. Atmospheric concentration of hydrogen sulfide at the "target".

The flux of gas across the air-water interface is described by the two-layer model that uses a modified Fickian formulation (Liss and Slater, 1974; Swarzenbach et al., 2003):

$$F = k(C_w - \frac{C_a}{H}) \tag{8}$$

where the flux (F) is defined as positive in the upward direction, k is the overall film transfer coefficient and has units of velocity (m s^{-1}), C_w and C_a are the concentrations in the water and the atmosphere (mmol m^{-3}), respectively, and H is the dimensionless Henry's Law constant for the gas of interest, which is corrected for temperature and pressure and is defined as the ratio of the concentration in the atmosphere to the concentration in the liquid. The transfer of gases such as molecular oxygen (O_2) is controlled by resistance in the liquid phase, while the flux of soluble gases such as H_2S is controlled by resistance in the gas layer (Liss and Slater, 1974; Balls and Liss, 1983). The magnitude of H decreases with increasing temperature and salinity, and is typically 16-19% lower in ocean water (Weiss, 1970; Gat and Shatkay, 1991).

The concentration of the volatile form of sulfide (H_2S) was determined through speciation using activity coefficients and ionic strength calculated by the Pitzer equation found in the geochemical speciation model "PHREEQC" (Parkhurst and Appello, 1999). Generally, in the pH range of the Salton Sea surface waters, aqueous sulfide is approximately 90% as HS^-, 10% as H_2S, and less than 0.1% is S^{2-} (Stumm and Morgan, 1981).

The film transfer coefficient (also referred to as the transfer or piston velocity) is a function of environmental factors such as wind speed, water temperature, and water turbulence and is described by the following equation (Liss and Slater, 1974):

$$\frac{1}{k} = \frac{1}{k_w} + \frac{1}{k_a H} \tag{9}$$

where k_w and k_a are the transfer velocities (m s^{-1}) in the water phase and air phase, respectively. The transfer velocity in the water is scaled by the ratio of the diffusivity (cm s^{-1}) of the compound of interest in the water (D_{i,H_2O}) and the diffusivity of molecular oxygen in water (D_{O_2,H_2O}) and is corrected for wind speed at 10 m above the interface (u_{10}) (Kanwisher, 1963; Swarzenbach et al., 2003):

$$k_w = 4 \times 10^{-4} + 4 \times 10^{-5} u_{10}{}^2 \left[\frac{D_{i,H_2O}}{D_{O_2,H_2O}} \right] \tag{10}$$

The diffusivity of H_2S and O_2 (cm^2 s^{-1}) in the water are determined using Hayduk and Laudie (1974) and are corrected for the solution dynamic viscosity (centipoise) and molar volume (cm^3 mol^{-1}).

Likewise, the transfer velocity in the air phase is scaled by the ratio of the atmospheric diffusivity of the compound ($D_{i,atm}$) and molecular oxygen ($D_{O_2,atm}$) and is also corrected for wind speed (Mackay and Yeun, 1983; Swarzenbach et al., 2003):

$$k_a = (0.3 + 0.2u_{10})\left[\frac{D_{i,atm}}{D_{O_2,atm}}\right]^{0.67} \tag{11}$$

The diffusivity of H_2S and O_2 in the atmosphere were determined using the relationship of Fuller (1966) and is corrected for air temperature (K), atmospheric pressure (atm), and molar volume. The exponent of 0.67 reflects the estimated boundary-layer thickness, which was estimated using an empirical relationship from the daily mean windspeeds measured at the CIMIS stations (Figure 3-1) (Wanninkhof, 1986). According to previous studies, the relationship between windspeed and boundary-layer thickness is not affected by salinities up to 75 ppt (Wanninkhof, 1986).

The estimated flux of hydrogen sulfide from the water column to the atmosphere was very low through the majority of the year (Figure 4-9a), although atmospheric H_2S concentrations above the background levels measured offsite suggest that there is some modest flux even during cool well-mixed conditions. The predicted volatilization flux of H_2S was greatest during the summer months when the concentration gradient was high. The peak volatilization rate occurred following mixing when sulfide was measurable in the surface waters of the Sea. The highest efflux in the north basin was estimated on 7 August 2006 at 1.3 mmol m^{-2} day^{-1} and 0.1 mmol m^{-2} day^{-1} in the south basin. A total estimated 245 tons of H_2S volatilized off the surface of the Salton Sea from 2 August until 27 September of 2006.

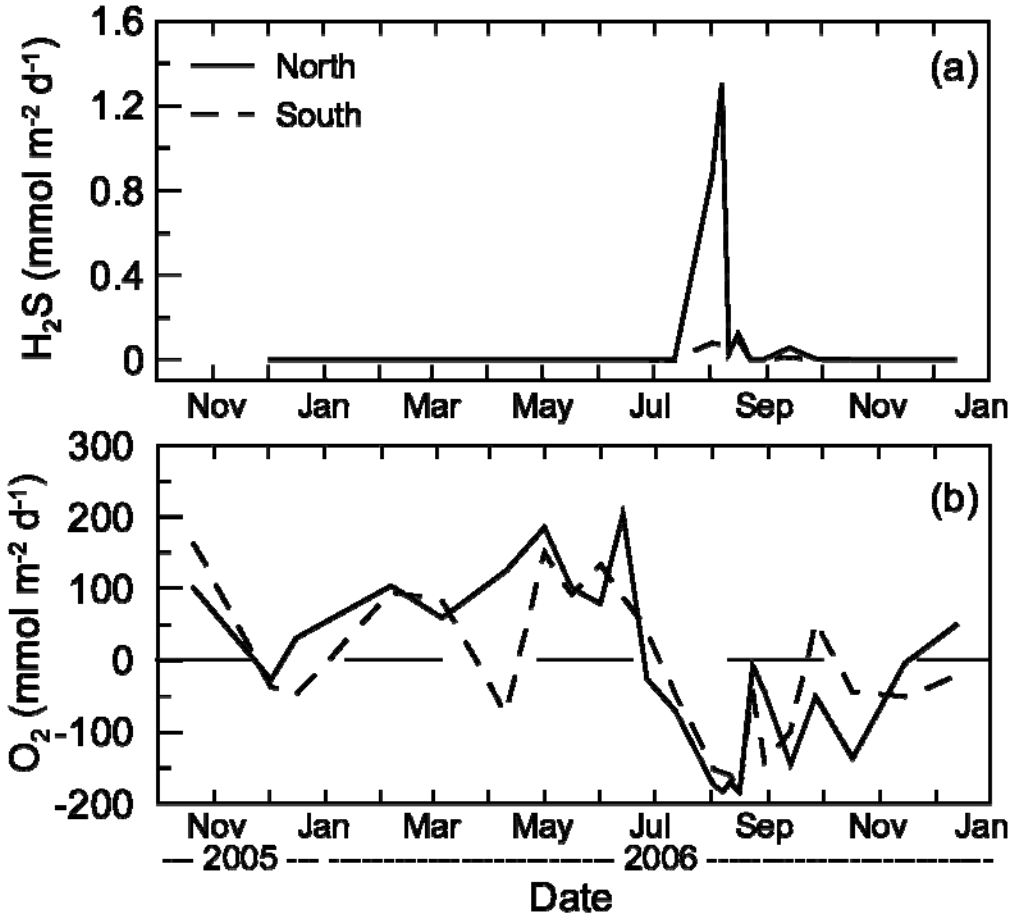

Figure 4-9. Flux from water column to the atmosphere: a) hydrogen sulfide and b) oxygen.

The flux of molecular oxygen was estimated to be positive (flux out of the water column) during the fall through spring months when the surface water was often super-saturated (Figure 4-1a and Figure 4-9b). However, beginning 26 June 2006 and coinciding with the first mixing event (Figure 4-1b), a negative flux (i.e., oxygen diffusion *into* the water column) persisted through the remainder of the summer (Figure 4-9b). The average O_2 flux during the summer at the Salton Sea was estimated to be approximately 60 mmol O_2 m^{-2} day^{-1} into the water column, and during the month of August 2006, during the H_2S event, the average was 172 O_2 mmol m^{-2} day^{-1}. These flux rates are comparable to the reported O_2 flux into hypereutrophic Onondaga Lake in New York that averaged 82 mmol O_2 m^{-2} day^{-1} during turnover that brought sulfide to the surface (Gelda and Effler, 2002). The predicted O_2 flux in August also exceeded the summer oxygen flux of 37.5 mmol O_2 m^{-2} day^{-1} into the Chesapeake Bay, a eutrophic estuary that experiences summer hypoxia (Kemp et al., 1992).

Following mixing in late July-early August, molecular oxygen diffused into the water column in conjunction with sulfide oxidation in order to reestablish oxic conditions in the surface waters. The first measured day of mixing, 2 August 2006, a flux of 170 mmol O_2 m^{-2} day^{-1} was estimated to potentially dissolve into the north basin water column. Based on the stoichiometry of eq 3 and assuming that the only sink for O_2 is sulfide oxidation, 85 mmol H_2S m^{-2} day^{-1} could potentially be oxidized by the influx of molecular oxygen on this date, indicating enough available oxygen to adequately oxidize the available sulfide. However, a flux of 0.88 mmol H_2S m^{-2} day^{-1} was estimated to have volatilized out of the north basin on this date. We can therefore assume that other significant sinks for the oxygen influx were present. Furthermore, sulfide oxidation in the Salton Sea is not instantaneous, as previously described, and although the oxygen input was sufficient, the oxidation reaction took several weeks to complete allowing for volatilization of hydrogen sulfide to occur in the meantime.

5. Implications and Conclusions

Polymixis is not an uncommon condition of many saline lakes, like the Salton Sea, as most are shallow and tend to mix more frequently because they are often found in regions with strong winds that tend to mix the water column and prevent stratification (Hammer, 1986). A substantial accumulation of hydrogen sulfide is not common in polymictic lakes, however, because anoxia must persist for a sufficient period of time to cause redox conditions that favor the formation of reduced sulfur species (Wetzel, 2001). Meromictic lake systems are most favorable to hydrogen sulfide production because of their depth and density-driven stratification (Hammer, 1986). The physical processes that control density and stratification also control the distribution of reduced chemical species; therefore most discussions relating to sulfur cycling in hypersaline systems are limited to the isolated area below the chemocline (Hammer, 1986; Miller et al., 1993).

Although the Salton Sea is a polymictic lake, it is the favorable combination of the conditions at the Salton Sea which allow for a significant flux of sulfide out of the sediments and subsequent build-up in the water column. The Salton Sea experiences high rates of sulfate reduction due to the combination of very high sulfate concentrations, high productivity and very warm summer temperatures. The flux of sulfide from the sediments to the water column is substantial, even as compared to meromictic systems with an evident chemocline.

Using our total flux estimates, we calculated over 13,000 tons of total sulfide diffused out of the sediments from the deepest locations of the north and south basins (representing approximately 20% of the total area) over the course of the study. Only after stratification began sulfide could accumulate below the oxycline. This persists until wind and convective mixing is able to overcome this partial stratification. Aside from the well-documented toxicity of hydrogen sulfide alone (Bagarinao, 1992), sulfide also reduces available oxygen, redox potential, as well as the pH, which leads to an inhospitable environment for fish and other aerobic organisms. Mixing events during the summer have been shown to have dire consequences to the fish and invertebrates in the Sea, as well as migrating birds that feed on them.

As has been noted, the dominant aquatic vertebrate species in the Salton Sea, tilapia (*Oreochromis mossambicus*), is subject to massive die-offs periodically. Laboratory studies conducted in seawater with a pH of 8, have suggested that 37 ± 12 μM (0.037 mM) of total sulfide was lethal to 50% of a test population of tilapia (5.7 g body weight) after just 59 ± 10 hours and 100% mortality was noted after 79 ± 12 hours at the same concentration. (Bagarinao and Lantin-Olaguer, 1999). The results showed slightly higher tolerance for larger tilapia (7.2 g) of 42 ± 5 μM total sulfide. Sulfide toxicity also increases with high temperature, low oxygen concentration, and low pH because H_2S, the toxic form of sulfide, is prevalent at lower pH (Smith and Oseid, 1974). The total sulfide measured at the Salton Sea on 2 August 2006 was 50% higher than the toxicity threshold reported by Bagarinao and Lantin-Olaguer (1999). The sulfide concentrations remained above the toxicity threshold in the north basin and mid-lake location for five or more days. The Department of Fish and Game estimated that three to four million tilapia (only 4-5 percent of the total population) perished in the late July-early August 2006 mixing event. The tilapia populations that were not killed in the initial upwelling of bottom waters had to survive in an anoxic, sulfide-rich environment for multiple days. The tilapia located on the lake perimeter and shallower locations were most likely the survivors. Algal productivity also diminished considerably following mixing, a phenomenon previously observed as well (Watts et al., 2001).

During mixing, not only were there lethal effects to the aquatic biomass, but the aesthetic effects were also realized to the surrounding communities. The odor of the Salton Sea was unmistakably that of hydrogen sulfide, a smell of rotten eggs, as well as other organic sulfur compounds. The total annual volatilization of H_2S out of the Salton Sea, based upon air sampling at the "target" was calculated to be 335 Mg y^{-1}. The total annual California statewide industrial emissions of H_2S from facilities reporting under the Air Toxics Hot Spots Information and Assessment Act is 2,600 Mg y^{-1} (Collins and Lewis, 2000). Thus, the Salton Sea can be considered a significant source of H_2S and may be comparable to living next to a large industrial emitter.

6. References

Almgren, T. and I. Hagstrom. 1977. The oxidation rate of sulphide in sea water. *Water Research.* 8:395-400.

Anderson, M.A. and C. Amrhein. 2002. *Nutrient cycling in the Salton Sea.* Final Report to the Salton Sea Authority. La Quinta, Calif.

Anderson, M.A., L. Whiteaker, E. Wakefield, and C. Amrhein. 2007. Properties and distribution of sediment in the Salton Sea, California: An assessment of predictive models. *Hydrobiologia. (in press)*

APHA (American Public Health Association). 1985. *Standard Methods for the Examination of Water and Wastewater.* 16th ed. Washington, D.C.

Arnal, R. E. 1961. Limnology, sedimentation, and microorganisms of the Salton Sea, California. *Geologic Society of America Bulletin.* 72:427–478.

Bagarinao, T. 1992. Sulfide as an environmental factor and toxicant: tolerance and adaptations of aquatic organisms. *Aquatic Toxicology* 24:21-62.

Bagarinao, T. and I. Lantin-Olaguer. 1999. The sulfide tolerance of milkfish and tilapia in relation to fish kills in farms and natural waters in the Philippines. *Hydrobiologia*. 382:137-150.

Balls, P.W. and P.S. Liss. 1983. Exchange of H_2S between water and air. *Atmospheric Environment.* 17:735-742.

Beutel, M.W., A.J. Horne, J.C. Roth, and N.J. Barratt. 2001. Limnological effects of anthropogenic desiccation of a large, saline lake, Walker Lake, Nevada. *Hydrobiologia*. 466:91-105.

Carpelan, L.H. 1958. The Salton Sea: Physical and Chemical Characteristics. *Limnology and Oceanography* 3:373-386.

Chanton, J.P. and C.S. Martens. 1987. Biogeochemical cycling in an organic-rich coastal marine basin. 7. Sulfur mass balance, oxygen uptake and sulfide retention. *Geochimica Cosmochimica Acta* 51:1187-1199.

Cline, J.D., and F.A. Richards. 1969. Oxygenation of hydrogen sulfide in seawater at constant salinity, temperature, and pH. *Environmental Science and Technology*. 3:838-843.

Collins J., and D. Lewis, 2000. *Hydrogen sulfide: Evaluation of current California air quality standards with respect to protection of children.* California Air Resources Board, California Office of Environmental Health Hazard Assessment. Sacramento, CA.

de Koff, J., M.A. Anderson, and C. Amrhein. 2007. Geochemistry of Iron in the Salton Sea. *Hydrobiologia*. (in press)

Drever, J.I. 1988. *The Geochemistry of Natural Waters*, 2nd ed. Prentice Hall, New Jersey.

Effler, S.W., J.P. Hassett, M.T. Auer, and N. Johnson. 1988. Depletion of epilimnetic oxygen and accumulation of hydrogen sulfide in the hypolimnion of Onondaga Lake, NY, U.S.A. *Water, Air, and Soil Pollution*. 39:59-74.

Frevert, T. 1980. Determination of hydrogen sulfide in saline solutions. *Schweiz. Z. Hydrol.* 42:255-268.

Gat, J.R. and M. Shatkay. 1991. Gas exchange with saline waters. *Limnology and Oceanography* 36:988-997.

Gelda, R.K. and S.W. Effler. 2002. Estimating oxygen exchange across the air-water interface of a hypereutrophic lake. *Hydrobiologia.* 48:243-254.

Hammer, U.T. 1986. *Saline Lake Ecosystems of the World*. DR W. Junk Publishers, Dordrecht.

Hayduk, W. and H. Laudie. 1974. Prediction of diffusion coefficients for nonelectrolytes in dilute aqueous solutions. *AlChE Journal*. 20:611-615.

Holdren, G.C., and A. Montano. 2002. Chemical and physical characteristics of the Salton Sea, California. *Hydrobiologia*. 473:1-21.

Howarth R.W., and J.W.B. Stewart. 1992. The Interactions of Sulphur with other Element Cycles in Ecosystems. p. 67-84. *In* Howarth RW , Stewart JWB , Ivanov MU (eds) *Sulphur Cycling on the Continents: Wetlands, Terrestrial Ecosystems and Associated Water Bodies*. *SCOPE* 48. John Wiley & Sons, New York.

Javor, B. 1989. *Hypersaline environments: microbiology and biogeochemistry*. Springer-Verlag, Berlin. 328 pp.

Jellison, R., Y.S. Zadereev, P.A. DasSarma, J.M. Melack, M.R. Rosen, A.G. Degermendzhy, S. DasSarma, and G. Zambrana. 2004. Conservation and management challenges of saline lakes: A review of five experience briefs. ThematicReview.http://worldlakes.org/uploads/Salt%20Lakes%20Thematic%20Paper%2022Jun04.pdf

Jorgensen, B.B., J.G. Kuenen, and Y. Cohen. 1979. Microbial transformations of sulfur compounds in a stratified lake (Solar Lake, Sinai). *Limnology and Oceanography* 24:799-822.

Kaiser, J. 1999. Battle over a dying sea. *Science.* 284:28-30.

Kanwisher, J. 1963. Effect of wind on CO_2 exchange across the sea surface. *Journal of Geophysical Research* 68:3921-3927.

Kemp, W.M., P.A. Sampou, J. Garber, J. Tuttle, and W.R. Boynton. 1992. Seasonal depletion of oxygen from bottom waters of Chesapeake Bay: roles of benthic and planktonic respiration and physical exchange processes. *Marine Ecology Progress Series.* 85:137-152.

Kuwabara, J.S., A. Van Geen, D.C. McCorkle, and J.M. Bernhard. 1999. Dissolved sulfide distributions in the water column and sediment pore waters of the Santa Barbara Basin. *Geochimica Cosmochimica Acta* 63:2199-2209.

Lasaga, A.C. 1979. The treatment of multi-component diffusion and ion pairs in diagenetic fluxes. *Am. Journal of Science.* 279:324-346.

Li, Y.-H. and S. Gregory. 1974. Diffusion of ions in sea water and in deep-sea sediments. *Geochimica Cosmochimica Acta* 38:703-714.

Mackay, D. and A.T.K. Yeun. 1983. Mass transfer coefficients correlations for volatilization of organic solutes from water. *Environmental Science and Technology* 17:211-233.

Miller, L.G., R. Jellison, R.S. Oremland, C.W. Culbertson. 1993. Meromixis in Hypersaline Mono Lake, California. 3. Biogeochemical Response to Stratification and Overturn. *Limnology and Oceanography* 38:10410-1051.

Parkhurst, D. L. & C. A. J. Appelo, 1999. *User's Guide to PHREEQC (Version 2) – A Computer Program for Speciation, Batch-Reaction, One-Dimensional Transport, and Inverse Geochemical Calculations*. Water-Resources Investigations Report 99-4259. U.S. Department of the Interior, U.S. Geological Survey, Denver, CO.

Robinson, E. and Robbins, R. C. 1970. Gaseous sulfur pollutants from urban and natural sources. *Journal of the Air Pollution Control Association* 20: 233-235.

Schroeder, R.A., W.H. Orem, Y.K. Kharaka. 2002. Chemical evolution of the Salton Sea, California: nutrient and selenium dynamics. *Hydrobiologia*. 473: 23-45.

Sorokin, Y.I. 1971. Experimental Data on the oxidation rate of hydrogen sulphide in the Black Sea. *Oceanology*. 11:423-431.

Smith, L.L. and D.M. Oseid. 1974. Effects of hydrogen sulfide on development and survival of eight freshwater fish species. In J.H.S. Blaxter (ed.), *Early Life History of Fishes*. Springer-Verlag, New York.

Stumm, W. 1985. *Chemical Processes in Lakes*. John Wiley and Sons, New York.

Swarzenbach R.P., P.M. Gschwend, and D.M. Imboden. 2003. *Environmental Organic Chemistry*, 2nd ed. John Wiley and Sons, New Jersey.

Tobolsky, A.V. 1968. *The Chemistry of Sulfides*. John Wiley and Sons, New York.

Ullman, W.J. and R.C. Aller. 1982. Diffusion coefficients in nearshore marine sediments. *Limnology and Oceanography* 27: 552-556.

Wanninkhof, R.H. 1986. Gas exchange on Mono Lake and Crowley Lake, California. *Journal of Geophysical Research* 92(C13): 14567-14580.

Wardlaw, G.D. and D.L. Valentine. 2005. Evidence for Salt Diffusion from Sediments Contributing to Increasing Salinity in the Salton Sea, California. *Hydrobiologia*. 533:77-85.

Watts, J.M., B.K. Swan, M.A. Tiffany, S.H. Hurlbert. 2001. Thermal, mixing, and oxygen regimes of the Salton Sea, California, 19997-1999. *Hydrobiologia*. 466:159-176.

Weiss, R.F. 1970. The solubility of nitrogen, oxygen, and argon in water and seawater. *Deep-Sea Research*. 17:721-735.

Wetzel, R.G. 2001. *Limnology: Lake and River Ecosystems*, 3rd edition. Academic Press, New York.

Williams, W.D. 1972. The uniqueness of salt lake ecosystems. In: Z. Kajak and A. Hillbricht-Ilkowska (eds.) *Productivity Problems of Freshwaters*. Proceedings of IBP-UNESCO Symposium. Polish Scientific Publishers, Warsaw.

Williams, W.D. 2001. Anthropogenic salinisation of inland waters. *Hydrobiologia*. 466:329-337.

Williams, W.D. 2002. Environmental threats to salt lakes and the likely status of inland saline ecosystems in 2025. *Environmental Conservation*. 2:154-167.

World Health Organization (WHO) Document (1981) ISBN 92-4-154079-6. IPCS International Programme on Chemical Safety, Environmental Health Criteria 19, Hydrogen Sulfide. Available at: http://www.inchem.org/documents/ehc/ehc/ehc019.htm

7. Appendix

Overall, sulfide concentrations in the deeper north and south basin sediments were greater than the more shallow locations (Figure 7-1). The deepest locations (> 12m) typically had sulfide pore water concentrations greater than 2.5 mM, whereas the shallowest locations (< 8m) had concentrations less than 1 mM. The same can be said of the concentrations of HS^- in the bottom water, in which the south and north basins had an annual average concentration of 0.30 and 0.18 mM, respectively, while the mid-lake location consistently had the lowest average sulfide concentrations of the three main sampling locations (0.08 mM) (Figure 4-3). The mid-lake site, as noted earlier, is shallower than the north and south basins and as such had a thicker oxic stratum, which provided for less production and accumulation of sulfide in the sediment and bottom layer. Sampling locations closer to shore (thus shallower depths) also had lower sulfide concentrations (Figure 3-1 and Figure 4-7). Watts et al. (2001) hypothesized that the shallower locations are subject to convection driven by greater nocturnal cooling of shallow waters, which probably contributes to the greater oxygenation and mixing of the near-shore (and shallower) waters.

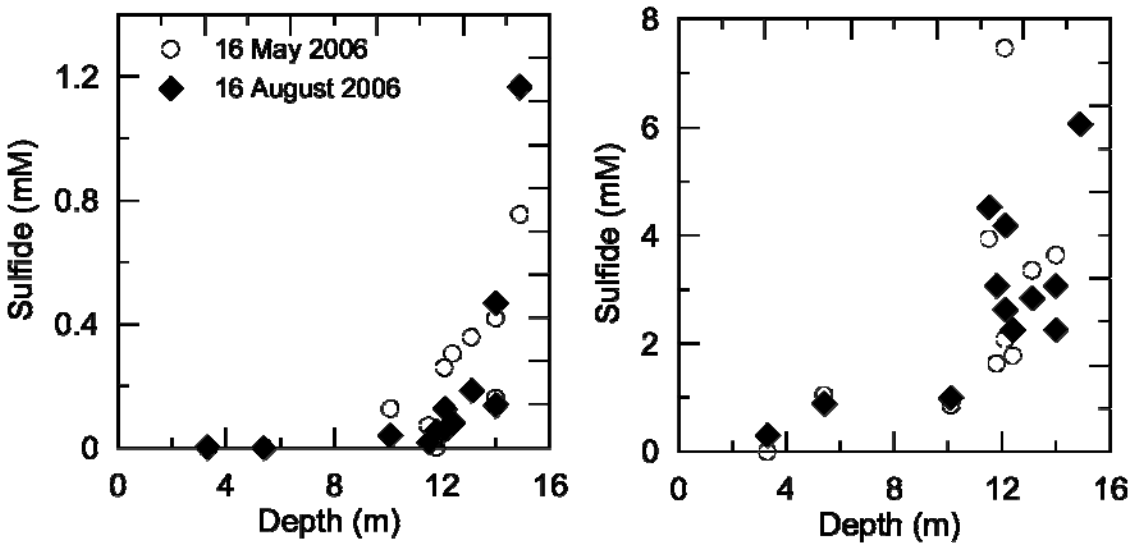

Figure 7-1. Sulfide concentrations (mM) as a function of water column depth: a) bottom (hypolimnetic) water and b) pore water.

The oxidation-reduction potential (ORP) was found to vary non-linearly with the strength of stratification (ΔT) (Figure 7-2). Weak stratification, as found during the winter, maintained aerobic conditions in the Sea and yielded high ORP values that served to keep redox sensitive elements in their oxidized forms. Conversely, strong stratification that yielded large ΔT values, as found during the late spring and summer, resulted in strongly reduced conditions (Figure 7-2).

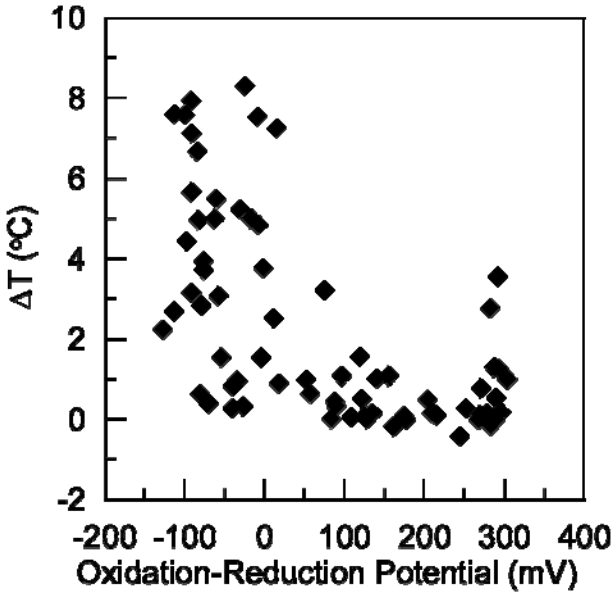

Figure 7-2. Measured ORP in bottom waters as a function of strength of stratification (ΔT).

The ORP was, in turn, a very useful index of sulfide concentrations in the Sea (Figure 7-3). Sulfide concentrations increased non-linearly with decreasing ORP, with concentrations increasing quite dramatically below approximately 100 mV (Figure 7-3). Ammonium-N concentrations exhibited very similar behavior, with NH4-N levels strongly and linearly correlated with sulfide (r^2=0.81). The slope of the regression line indicates that about 0.2 mols of NH_4-N is produced per mol of sulfide production (data not shown). This compares with a theoretical ratio of 0.3 mols NH4-N per mol sulfide assuming organic matter is at the Redfield ratio and that sulfate reduction follows eq 1.

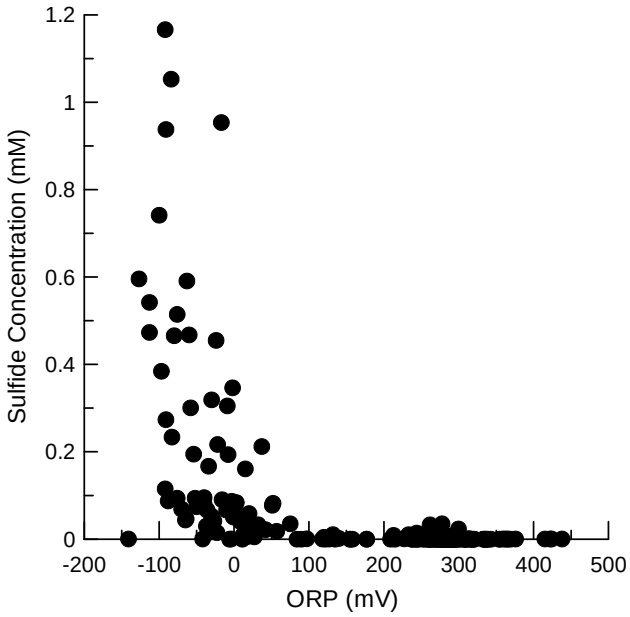

Figure 7-3. Sulfide concentration vs. ORP (all water column samples).

Task 2: Hydrodynamic and Water Quality Modeling to Support Restoration

Prepared by:

TETRA TECH

Executive Summary

This report documents the development of a hydrodynamic and water quality model of the Salton Sea for use in assessing recent hydrodynamic and water quality conditions and evaluating changes resulting from various restoration plans including the Salton Sea Authority Plan. It is widely accepted that physical and biogeochemical processes in the Salton Sea are fundamentally three-dimensional in space and highly variable in time. Similarly, biogeochemical processes exhibit a range of time scale with nutrient dynamics responding to both continued loads to the system and large scale internal nutrient recycling between the water column and sediment bed. Surface water modeling systems capable of representing the relevant hydrodynamic and water quality processes determined to be significant in the Salton Sea are rather limited. The Environmental Fluid Dynamics Code (EFDC) model was selected for this study primarily on the basis that it incorporates all of the relevant hydrodynamic and water quality processes. Other advantages of the EFDC model include its open source-public domain status, track record of applications, including regulatory applications in the NPDES, TMDL and Superfund programs, and extensive scientific peer review.

The EFDC model was configured to simulate the 1997 through 1999 historical period coinciding with extensive physical and biogeochemical observational data sets obtained during 1997 and 1999, respectively. Model spatial resolution is approximately 0.61 meters vertically and either 1200 or 600 meters horizontally, with the coarser horizontal resolution used for preliminary calibration and the finer resolution used for final calibration and verification and restoration alternatives evaluation. Various spatially altered marine sea and salinity habitat alternatives can be readily incorporated into either of the two horizontal resolution configurations. The model historical simulation period can be readily extended past 1999 subject to the availability of atmospheric and hydrologic data.

Calibration results, presented herein, indicate that both the hydrodynamic and water quality components of the model perform well in representing spatial variations and seasonal and event time scale variations in circulation, thermal structure and water quality processes. Hydrodynamic and thermal calibration utilized the 1997 observational data set, with the 1999 data set being used for thermal validation. Hydrodynamic and thermal responses are most sensitive to the wind field over the Sea, which must be estimated by height adjustment and spatial interpolation of wind data from five to seven nearby meteorological stations. Sensitivity studies indicate that the diurnal vertical temperature structure is sensitive to atmospheric heat exchange and wind stress induced mixing, but relatively insensitive to details of the horizontal current response to wind stress. For the water quality component of the model, the 1999 observational data was used for calibration. Another water quality data set as complete as the 1999 set was not available for validation and instead, a less formal validation was conducted using sparse data spanning 2000 to 2007. Vertical thermal structure and its influence on vertical mixing and reaction rates is the most sensitive physical process with respect to water quality response. Water quality reaction parameter values in both the water column and sediment diagenesis or flux sub-model were adjusted and optimized through sensitivity analysis. The robustness of the 1999 calibration was demonstrated by conducting a 15 year simulation based on repetition of 1999 hydrodynamics and nutrient loads.

The calibrated and verified hydrodynamic and water quality model was used to evaluated various aspects of the Salton Sea Authority preferred restoration plan involving a northern marine sea connected to a southern estuarine zone. Hydrodynamic simulations of the SSA plan indicated that thermal stratification and vertical mixing in the northern marine sea

changed little form existing conditions. The water quality response of the northern marine sea was evaluated by conducting 15 year scenario simulations based on continued repetition of 1999 historical atmospheric, hydrologic, and nutrient loadings. Three scenarios and a baseline were simulated. The baseline corresponded to existing full sea conditions. The three scenarios included the mid-sea dike and a southeastern dike forming the estuarine zone. Two of these three scenarios involved various reductions in phosphorous loading, 0 percent and 90 per cent, from the inflowing rivers. The third scenario had no phosphorous loading reduction, but included withdrawal of hypolimnetic and surface water from the northern marine sea and its return into the southern estuarine region. The oxygen demand associated with hydrogen sulfide in the hypolimnetic withdrawal was reduced by 50 per cent before being returned to evaluate the effectiveness of a proposed ozone treatment plant to control sulfide. The spatial extent and duration of low dissolved oxygen water was used a metric to evaluate the effectiveness of the three scenarios relative to the baseline. All of the scenarios resulted in reduction of per cent anoxic volume days relative to the base line. The hypolimnetic withdrawal and treatment showed no effect relative to the corresponding no phosphorous load reduction scenario. Response to phosphorous load reduction appears to be most sensitive to complete load reduction.

Table of Contents

1. Introduction 1-1
2. Conceptual Model 2-1
   2.1. Hydrodynamics 2-1
   2.2. Water Quality and Eutrophication 2-19
3. Model Selection 3-1
4. Model Configuration 4-1
5. Hydrodynamic and Thermal Calibration and Validation 5-1
   5.1. Hydrodynamic and Thermal Calibration 5-1
   5.2. Sensitivity of Temperature Prediction to Velocity Prediction 5-3
   5.3. Thermal Validation 5-4
6. Water Quality Calibration and Validation 6-1
7. Evaluation of the Salton Sea Authority Restoration Plan 7-1
   7.1. The Salton Sea Authority Plan 7-1
   7.2. Hydrodynamic and Thermal Response Evaluation 7-2
   7.3. Water Quality Response Evaluation 7-2
8. Summary 8-1
9. References 9-1
10. Appendix A. 10-1
11. Appendix B. 11-1

List of Tables

Table 3-1 Summary of 1997 Depth Average Current Components 2-3
Table 3-2. Water Column Algae Interactions 2-21
Table 3-3. Water Column Organic Carbon Interactions 2-21
Table 3-4. Water Column Organic Phosphorous Interactions 2-21
Table 3-5. Water Column Dissolved Orthophosphate Interactions 2-21
Table 3-6. Water Column Particulate Orthophosphate Interactions 2-22
Table 3-7. Water Column Organic Nitrogen Interactions 2-22
Table 3-8. Water Column Ammonium Interactions 2-22
Table 3-9. Water Column Nitrate Interactions 2-23
Table 3-10. Water Column Dissolve Oxygen Interactions 2-23
Table 3-11. Water Column Hydrogen Sulfide Interactions 2-23
Table 3-12. Water Column Sulfate Interactions 2-23
Table 4-1. EFDC Water Column State Variables 3-2
Table 7-1. Water Quality Parameters Related to Algae in the Water Column 6-3
Table 7-2 Parameters Related to Organic Carbon in the Water Column 6-4
Table 7-3. Parameters Related to Phosphorus in the Water Column 6-5
Table 7-4. Parameters Related to Nitrogen in the Water Column 6-6
Table 7-5 Parameters Related to Chemical Oxygen Demand and Dissolved Oxygen in the Water Column 6-7
Table 8-1 Per Cent Volume-Days with Dissolved Oxygen Lower than Threshold Value 7-4

List of Figures

Figure 2-1. Location of temperature and current profile sites in the Salton Sea during 1997. (Cook and Orlob, 2002) 2-4
Figure 2-2. Depth average velocity components at sites 1 and 3, May 8-20, 1997. 2-5
Figure 2-3. Wind velocity components, May 8-20, 1997. 2-6
Figure 2-4. Depth average velocity components at sites 1 and 3, May 15-16, 1997 2-7
Figure 2-5. Depth average velocity components at sites 1 and 5, May 20-31, 1997 2-8
Figure 2-6. Wind velocity components, May 20-31, 1997 2-9
Figure 2-7. Depth average velocity components at sites 1 and 5, May 24-25, 1997 2-10
Figure 2-8. Depth average velocity components at site 1, May 8-31, 1997 2-11
Figure 2-9. Temperature at site 1, May 8-31, 1997 2-11
Figure 2-10. Temperature at site 3, May 8-31, 1997 2-12
Figure 2-11. Temperature at site 5, May 8-31, 1997 2-12
Figure 2-12. Depth average velocity components at site 1, October 17-31, 1997 2-13
Figure 2-13. Wind velocity components, October 17-31, 1997. 2-14
Figure 2-14. Depth average velocity components at sites 1 and 5, October 26-27, 1997 2-15
Figure 2-15. Kinetic energy spectral density, site 1, May 8-20, 1997 2-16
Figure 2-16. Kinetic energy spectral density, site 3, May 8-20, 1997 2-16
Figure 2-17. Kinetic energy spectral density, site 1, May 20-31, 1997 2-17
Figure 2-18. Kinetic energy spectral density, site 5, May 20-31, 1997 2-17
Figure 2-19. Kinetic energy spectral density, site 1, October 20-31, 1997 2-18
Figure 2-20. Kinetic energy spectral density, site 5, October 20-31, 1997 2-18
Figure 2-21. Schematic of nutrient cycling in the water column 2-24
Figure 2-22. Schematic of sediment diagenesis processes (note chemical oxygen demand release, COD, represents chemical oxygen demand associated with sulfide flux from the bed into the water column) 2-25
Figure 2-23. Location of water quality monitoring sites in the Salton Sea during 1999. 2-26
Figure 4-1. Horizontal grid of the Salton Sea with 600 meter square cells. 4-2
Figure 4-2. Bathymetry of the Salton Sea on 600 meter horizontal grid. 4-3
Figure 4-3. Inflow to the Salton Sea, 1997-99. 4-3
Figure 4-4. Atmospheric temperature in vicinity of Salton Sea, 1997-99. 4-4
Figure 5-1. Depth average current velocity comparison at Sites 1 and 3 during early May. 5-5
Figure 5-2. Depth average current velocity comparison at Sites 1 and 5 during late May 5-6
Figure 5-3. Depth average current velocity comparison at Sites 1 and 5 during late October 5-7
Figure 5-4. Comparison of observed temperature (top panel) with model predicted temperature for the first eight months of 1997 at Site 1 5-8
Figure 5-5. Comparison of observed temperature (top panel) with model predicted temperature for the last seven months of 1997 at Site 1. 5-9
Figure 5-6. Comparison of observed temperature (top panel) with model predicted temperature for the first eight months of 1997 at Site 2 5-10
Figure 5-7. Comparison of observed temperature (top panel) with model predicted temperature for the last seven months of 1997 at Site 2. 5-11
Figure 5-8. Comparison of observed temperature (top panel) with model predicted temperature for the first eight months of 1997 at Site 3. 5-12

Figure 5-9. Comparison of observed temperature (top panel) with model predicted temperature for the last seven months of 1997 at Site 3. 5-13
Figure 5-10. Comparison of observed temperature (top panel) with model predicted temperature for the first eight months of 1997 at Site 4. 5-14
Figure 5-11. Comparison of observed temperature (top panel) with model predicted temperature for the last seven months of 1997 at Site 4. 5-15
Figure 5-12. Comparison of observed temperature (top panel) with model predicted temperature for the first eight months of 1997 at Site 5. 5-16
Figure 5-13. Comparison of observed temperature (top panel) with model predicted temperature for last 7 months of 1997 at Site 5. 5-17
Figure 5-14. Velocity at Site 5 in late May. Top panel without data assimilation. Bottom panel with data assimilation..... 5-18
Figure 5-15. Model predicted temperature at Site 5 in late May. Top panel without velocity data assimilation. Bottom panel with velocity data assimilation..... 5-19
Figure 5-16. Velocity at Site 5 in late October. Top panel without data assimilation. Bottom panel with data assimilation..... 5-20
Figure 5-17. Model predicted temperature at Site 5 in late October. Top panel without velocity data assimilation. Bottom panel with velocity data assimilation 5-21
Figure 5-18. Comparison of observed temperature (circles) with model predicted temperature for 1999 at BOR Stations SS1. 5-22
Figure 5-19. Comparison of observed temperature (circles) with model predicted temperature for 1999 at BOR Stations SS2. 5-23
Figure 5-20. Comparison of observed temperature (circles) with model predicted temperature for 1999 at BOR Stations SS2 5-24
Figure 6-1. Comparison of observed and predicted water quality constituent concentrations near the water surface at USBOR Site SS-1 during 1999..... 6-9
Figure 6-2. Comparison of observed and predicted water quality constituent concentrations near the water column bottom at USBOR Site SS-1 during 1999. 6-11
Figure 6-3. Comparison of observed and predicted water quality constituent concentrations near the water surface at USBOR Site SS-2 during 1999..... 6-13
Figure 6-4. Comparison of observed and predicted water quality constituent concentrations near the water column bottom at USBOR Site SS-2 during 1999. 6-15
Figure 6-5. Comparison of observed and predicted water quality constituent concentrations near the water surface at USBOR Site SS-3 during 1999..... 6-17
Figure 6-6. Comparison of observed and predicted water quality constituent concentrations near the water column bottom at USBOR Site SS-3 during 1999. 6-19
Figure 6-7. Comparison of observed and predicted dissolved oxygen at the water surface, quarter depth, mid-depth and bottom at USBOR Site SS-1 during 1999. 6-20
Figure 6-8. Comparison of observed and predicted dissolved oxygen at the water surface, quarter depth, mid-depth and bottom at USBOR Site SS-2 during 1999. 6-21
Figure 6-9. Comparison of observed and predicted dissolved oxygen at the water surface, quarter depth, mid-depth and bottom at USBOR Site SS-3 during 1999. 6-22
Figure 6-10. Comparison of calibration and 15 year base-line simulation predicted surface and bottom dissolved oxygen as USBOR Station SS-1..... 6-23

Figure 6-11. Near bottom dissolved oxygen, phosphate, sulfide component of chemical oxygen demand and sediment oxygen demand, for 15 year base-line simulation at USBOR Station SS-1. 6-24
Figure 7-1. Major components of the Salton Sea Authority's restoration plan. 7-4
Figure 7-2. Model predicted temperature at Site 5. Top panel is current conditions. 7-6
Figure 7-3. Model predicted temperature at Site 5. Top panel is current conditions. 7-7
Figure 7-4. Histogram of Temperature Stratification. Top panel is current conditions. 7-8
Figure 7-5. Model predicted velocities at Site 5 in late May. Top panel is current conditions. Bottom panel is SSA restoration alternative 7-9
Figure 7-6. Comparison surface dissolve oxygen at USBOR Station SS-1 for 15 year baseline and restoration scenario simulations. 7-10
Figure 7-7. Comparison bottom dissolve oxygen at USBOR Station SS-1 for 15 year baseline and restoration scenario simulations. 7-11
Figure 7-8. Comparison surface chlorophyll 'a' at USBOR Station SS-1 for 15 year baseline and restoration scenario simulations 7-13
Figure 7-9. Comparison bottom chemical oxygen demand due to hydrogen sulfide at USBOR Station SS-1 for 15 year baseline and restoration scenario simulations 7-14

1. Introduction

This report documents the development of a hydrodynamic and water quality model of the Salton Sea to support restoration planning efforts. Over the coming decades, brackish drainwater inflows to the Sea will decrease due to planned out of basin transfer of irrigation water from the Imperial Valley resulting in a higher rate of salinity increase in the Sea. At the same time, it is anticipated that phosphorous levels in the inflows and associated total load will increase worsening the existing highly eutrophic state of the sea. A higher eutrophication state will, in turn, further degrade water quality by causing lower dissolved oxygen (DO) levels, increased sediment phosphorus release (i.e., internal loading) and increased ammonia and hydrogen sulfide concentrations.

In an attempt to alleviate these problems, the Salton Sea Authority (SSA) has developed a combined Salton Sea Revitalization and Restoration Plan (the "SSA Plan") that focuses on balancing inflows and evaporative losses and improving water quality for multiple project purposes. The plan includes separating the sea into two basins (deep north and shallow south), canals for water exchange between basins, treatment of water at key inflow and outflow locations in the system, removal and treatment of hypolimnetic water, and a brine pool for final disposal of hypersaline water. By treating certain inflow streams for phosphorous removal and installing facilities to circulate and treat the lake-water it is expected that DO levels will increase and hydrogen sulfide and ammonia concentrations will decrease. The treatment plants in this overall water-quality improvement plan will be used to supplement the natural water purification processes and provide a positive control mechanism for reducing algal blooms, hydrogen sulfide gas build-up in the hypolimnetic water, toxic ammonia levels, organic sulfides, and other malodorous or harmful organic matter in the lake-water system, as well as improving the clarity of the two lakes. The goal of this combined natural and treatment-plant approach for improving water quality is to return the smaller restored Salton Sea in the SSA Plan into a water body that supports regional recreational and local economic development activities, and to provide safe habitat for wildlife, as was the case during the Salton Sea's heydays in the 1950s and 1960s.

By design, implementation of the SSA Plan is expected to bring about significant changes in the chemistry of the Sea's water. For example, withdrawal and treatment of hypolimnetic water is expected to reduce the extent and duration of anoxic conditions and associated sulfide and ammonia problems. However, increased oxygenation of sediments could solubilize selenium and phosphorus which, in turn, may increase the phosphorous concentration in the water column. Reduction in the size of the Sea in the SSA Plan has the potential modifying wind driven circulation and the frequency and magnitude of mixing events. The development of a hydrodynamic and water quality model of the Salton Sea is essential in evaluating the effectiveness of various components of the SSA Plan as well as other proposed restoration alternatives. Better understanding of current and future conditions gained through model application will contribute significantly to identifying the most cost effective technologies for providing the greatest improvement in water quality.

The organization of this document follows the generally accepted steps in model development and applications. Chapter 2 summarizes the current conceptual understanding of hydrodynamic and water quality processes in the Salton Sea and establishes model requirements to simulate these processes in a predictive manner. Chapter 3 describes the public domain Environmental Fluid Dynamics Code (EFDC) which was selected as the basis for model development, while Chapter 4 summarizes the configuration of the EFDC model for current conditions and modified conditions corresponding the Salton Sea Authority's proposed revitalization and restoration plan (SSA Plan). The credibility of the hydrodynamic

and water quality components of the modeling system is established by calibration and validation with respect to current conditions in Chapters 5 and 6, respectively. The effectiveness of the major components of the SSA Plan is evaluated in Chapter 7 using decadal time scale model simulations.

2. Conceptual Model

Conceptualization of hydrodynamic and water quality processes in the water body to be modeled is an essential first step in the modeling process which ensures that an appropriate modeling system is selected and applied in a manner such that modeling goals are met. The goal of the Salton Sea modeling effort is the development of a hydrodynamic and water quality model which accurately represents recent conditions in the Salton Sea and provides a modeling tool for predicting future condition in the Sea under alternate proposed restoration plans including the SSA Plan. Conceptualization takes into account both the analysis and interpretation of observational data and the results of previous modeling studies.

2.1. Hydrodynamics

Cook (2000) and Cook and Orlob (2002)reported an extensive set of hydrodynamic observations in the Salton Sea in 1997 and also conducted a three-dimensional hydrodynamic model study. The observational program included continuous measurements of temperature over depth at five stations, Figure 2-1, and shorter duration acoustic Doppler current profiler (ADCP) deployments at three of the same stations. Current meter observations focused on two periods, one during May when temperature stratification was pronounced and other during late October when the water column was completed mixed. Based on this work, the hydrodynamics of the Salton Sea are reasonably well understood.

Large scale circulation in the Salton Sea is wind driven and highly variable as illustrated by the current observations of Cook (2006), summarized in Table 2-1. Figure 2-2 shows the depth averaged currents at sites 1 and 3 in the southern basin, during mid-May 1997. Current vector components have be aligned toward the northeast, across the lake and toward the northwest, along the lakes major axis. Mean currents at site 1 are to the northwest while at site 3 the currents are to the southeast, suggesting a counterclockwise gyre in the southern basin. Current component magnitudes at both sites oscillate at a period on the order of one day while a slow modulation of the mean currents occurs over the 12 day observational period. Figure 2-3 shows wind velocity components at three wind stations during this same period. The wind components exhibit a pronounced diurnal or daily scale oscillation as well as significant spatial variability. Higher frequency oscillations are also present in the current records as shown in Figure 2-4, a two day interval during this period. Periods of approximately 1 hour, 3 to 4 hours, and 12 hours are visually evident. Depth average currents at site 1 and site 5 during late May 1997 are shown in Figure 2-5. The mid-May circulation pattern appears to persist at site 1. At site 5, in the northern basin, mean currents are to the southwest during the first 6 days, followed by a 3 day event response, with the currents tending back to a southwest mean on the last two days, but with a pronounced oscillation having a period of approximately one day. Wind components during this period are shown in Figure 2-6. Two-day internals from this period are shown in Figure 2-7, with oscillations at a period of approximately 3 to 4 hours being evident.

Figure 2-8 shows the full May depth averaged current record at site 1. Figure 2-9–Figure 2-11 show temperature records at the surface, quarter, middle and bottom of the water column at sites 1, 3, and 5 for May 8-31, 1997. At site 1, the water column is temperature stratified between days 130 and 142, with the stronger currents between days 142 and time 144 completely mixing the water column. The bottom temperature sensor at site 3 is not active during the corresponding current meter observation period, however the temperature record indicates stratified conditions between days 139 and 141 days with complete vertical mixing occurring by day 142 as is observed at site 1. Bottom temperatures remain constant and the water column strongly stratified at site 5 in the north basin with significant mid-depth

temperature oscillations occurring between days 135 and 144. The strong currents between days145 and 148 result in the upper half of the water column becoming completely mixed. The temperature records are all characterized by strong diurnal variability in the surface temperature with nocturnal mixing occurring over approximately the upper quarter of the water column due to thermal instability. Deeper mixing to mid-depth and over the entire water column occurs during periods of strong currents and associated higher surface wind stresses.

A second set of current observations were taken in late October at sites 1 and 5 when the water column was completely mixed thermally. Figure 2-12 shows the depth averaged current components with corresponding wind components shown in Figure 2-13. Mean currents at site 1 are to the northwest, as during the May period, with a pronounced nocturnal intensification at day 296. A modulation of the current magnitude at a period of approximately 3 days is also somewhat evident. Mean currents at site 5 are south to southeast. The event response at day 296 is evident as well as an event response at time 298, which has no corresponding signature at site 1. Zoomed plots of two day intervals during this period are shown in Figure 2-14. Oscillations with periods in the range of one to four hours are evident.

Depth-average kinetic energy density spectral distributions for the six current meter records are shown in Figure 2-15 through Figure 2-20. In all cases, the largest spectral peaks are associated with the observational period mean flow and the first few lowest frequencies. Large values at the first few lowest frequencies tend to represent variability over the record period rather than specific dynamic processes. At sites 1 and 3 in mid-May low energy activity is evident in the region between 0.02 and 0.03 cycles per hour and between 0.04 and 0.045 cycles per hour. Site 1, in mid-May shows low energy activity in the vicinity of 0.015 and 0.04 cycles per hours. Site 5, in mid-May shows a wider range of low frequency activity and a higher frequency spike at approximately 0.032 cycles per hour. It is noted however that kinetic energy density at site 5 is almost and order of magnitude low than the southern basin site 1 during this period, which is consistent with the persistent thermally stratification at site 5, Figure 2-11. Kinetic energy density distributions are quite similar between sites 1 and 5 during the October period, but again with significant lower density at site 5. It is noted that the kinetic energy spectral density plots are truncated at 0.06 cycles per hour, corresponding to a period of approximately 16 hours, since energy density at higher frequencies is essentially insignificant. Even thought high frequency oscillations are observed in the 3 to 4 hour period range in the velocity time series, their contribution to energetic of the currents and associated vertical mixing dynamics are negligible.

Some additional insight into the circulation can be gained from an excitation-response point of view which describes the response of the Sea in terms of its normal or natural mode spatial response patterns having associated natural frequencies. Spatial and temporal variations in the wind field, the excitation, having similar structures as the normal modes produce resonant circulation responses. Details of a preliminary analysis for the Salton Sea are presented in Appendix A. The longest period, first class or gravity-inertia modes of the Sea are identified to be approximately 3.3 and 1.4 hours corresponding to uni-nodal sieches along the Sea's longitudinal and transverse axes. The inertial period of the Sea is approximately is approximately 22 hours, and close to the diurnal period. Although no natural periods were identified near the diurnal period, the proximity will tend to amplify responses of the sea to daily scale wind variability. An analysis of second class normal modes corresponding to topographic Rossby waves indicates the possibility of their existence with periods ranging from approximately 30 hours to 200 hours, corresponding to the frequency range of approximately 0.005 to 0.03 cycles per hours. This range of periods was also identified for

internal first class modes under stratification conditions during the May observation period. The kinetic energy spectral shows activity in this frequency band, but the relative shortness of the observational records precludes a more definitive pronouncement as to associating this activity with first class internal modes or topographic Rossby waves.

In summary, observational data from the Salton Sea in combination with analysis indicates that circulation in the Sea is highly variable in the horizontal extent, and vertical temperature structure is likewise highly variable at time scales ranging from less than daily to seasonal. Vertical current structure, although not presented herein, also exhibits similar variability. This suggest that a three-dimensional hydrodynamic model with coupled temperature prediction, that includes turbulence closure model to predict vertical mixing processes under stratified conditions, is essential to quantify the transport and mixing fields necessary for water quality modeling.

Table 2-1
Summary of 1997 Depth Average Current Components

Site	Date	Number of Observations	Mean, East cm/s	Mean, North cm/s
1	May 8-20	837	-4.598	4.062
3	May 8-20	1095	5.882	-5.814
1	May 20-31	755	-6.712	6.716
5	May 20-31	1000	-0.219	-2.609
1	Oct 20-31	756	-3.694	4.131
5	Oct 20-31	984	0.871	-2.372

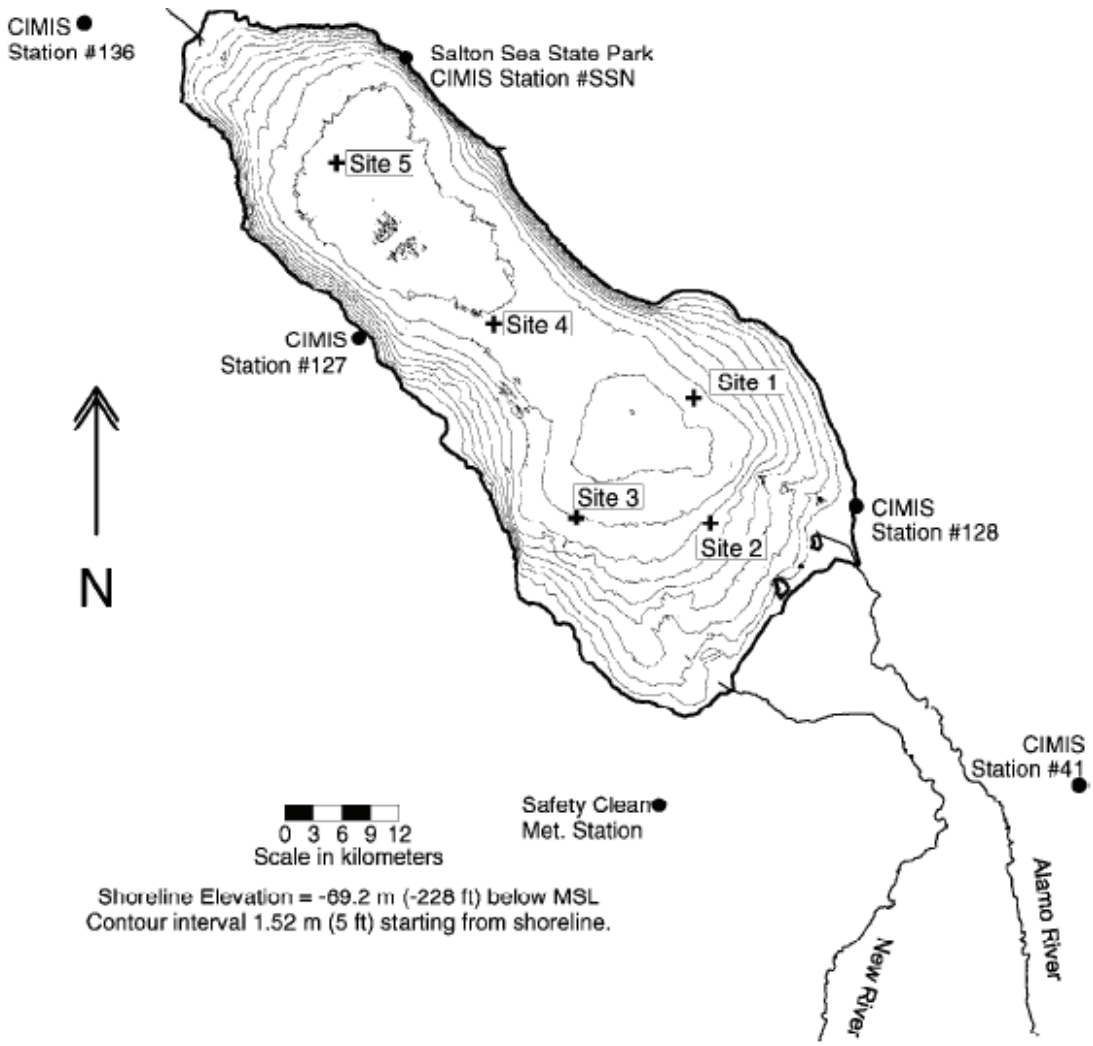

Figure 2-1. Location of temperature and current profile sites in the Salton Sea during 1997. (Cook and Orlob, 2002)

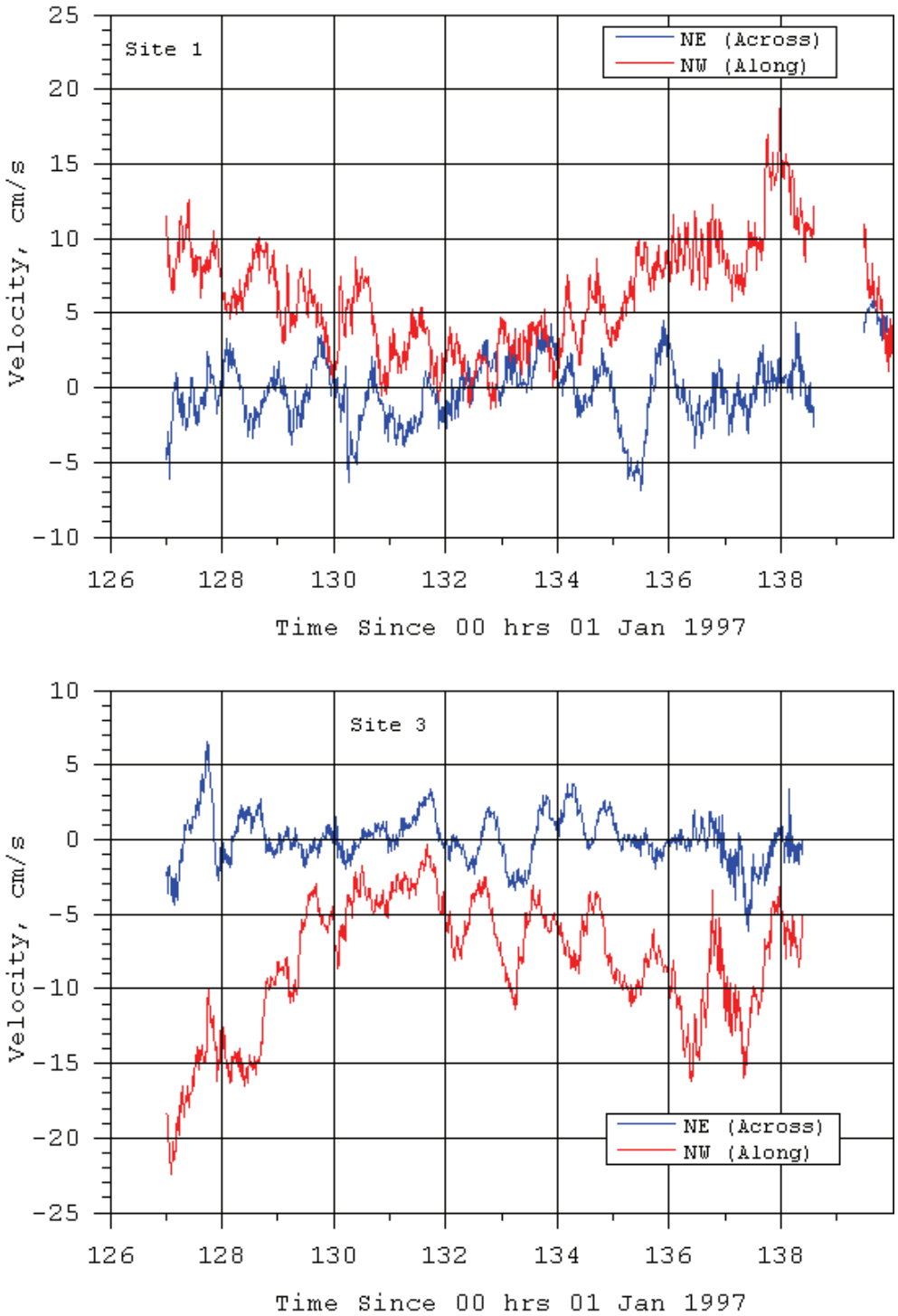

Figure 2-2. Depth average velocity components at sites 1 and 3, May 8-20, 1997.

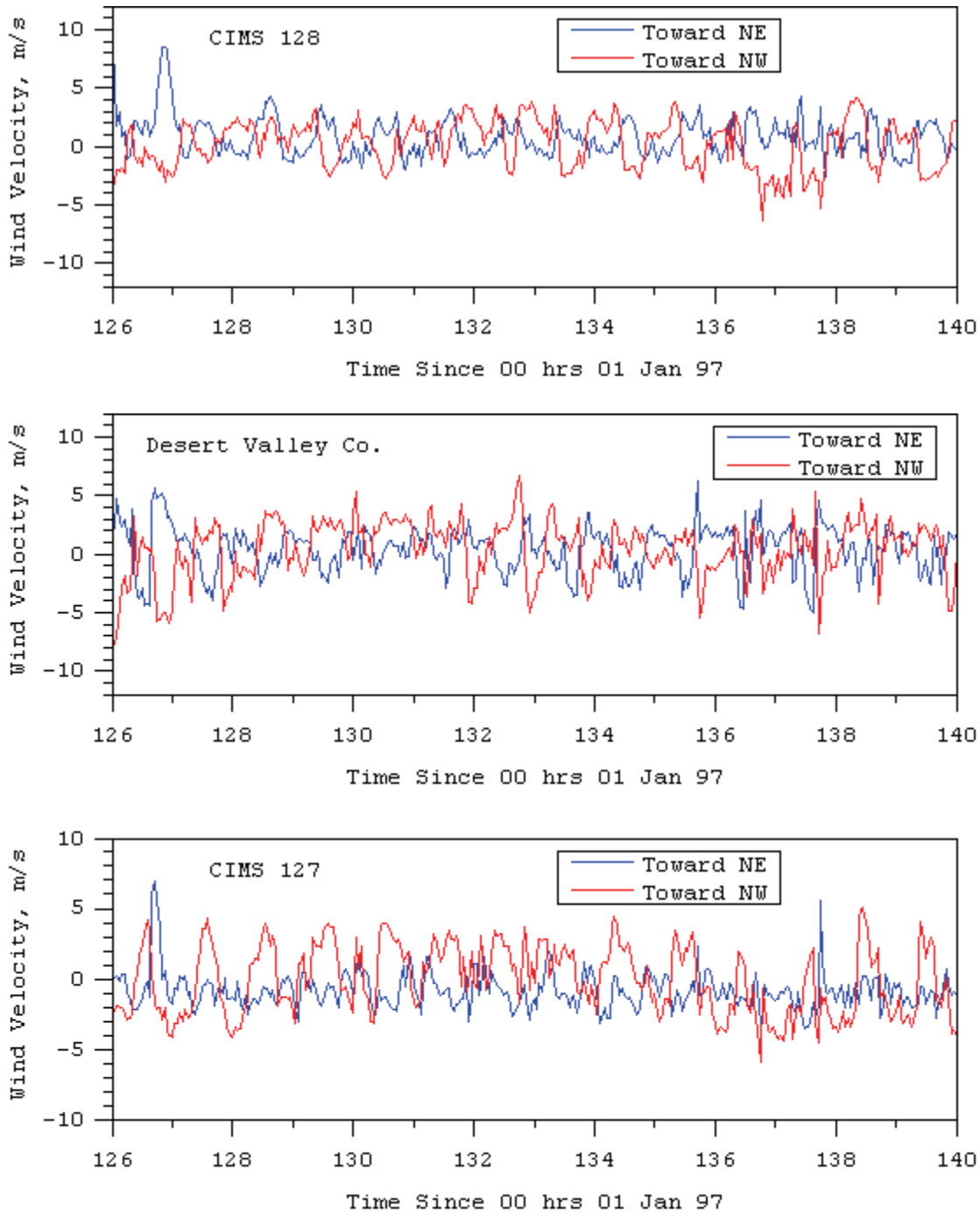

Figure 2-3. Wind velocity components, May 8-20, 1997.

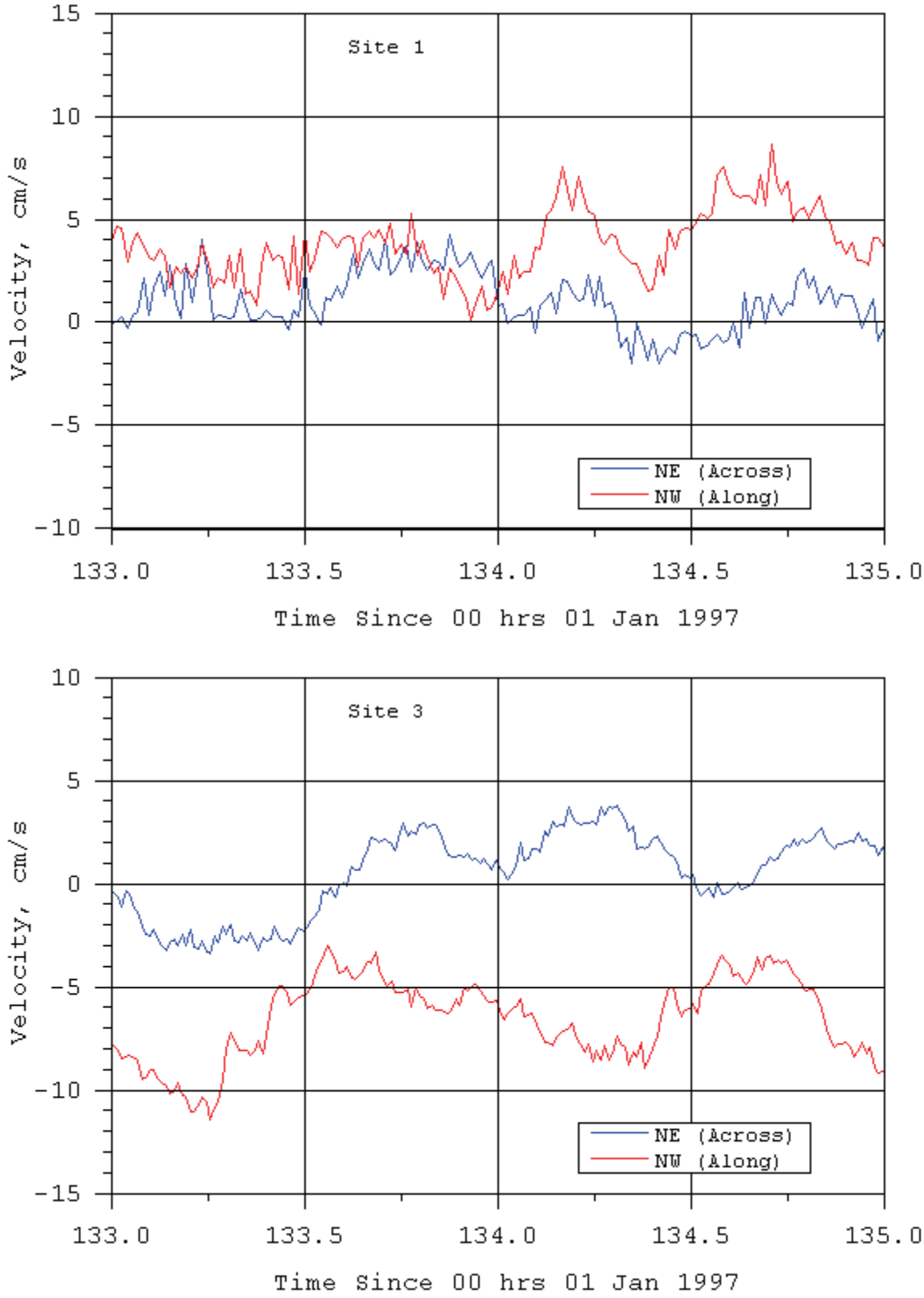

Figure 2-4. Depth average velocity components at sites 1 and 3, May 15-16, 1997

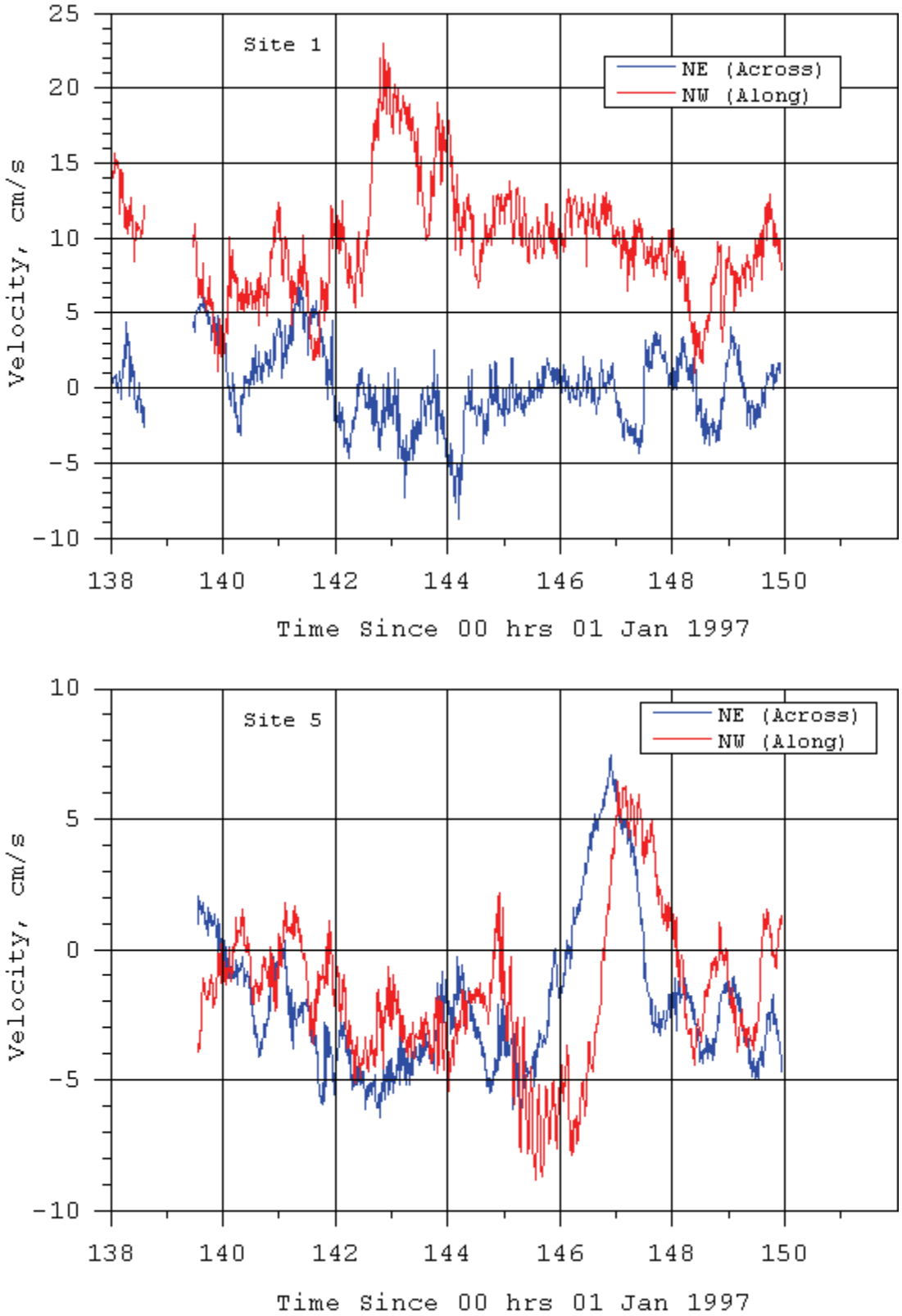

Figure 2-5. Depth average velocity components at sites 1 and 5, May 20-31, 1997

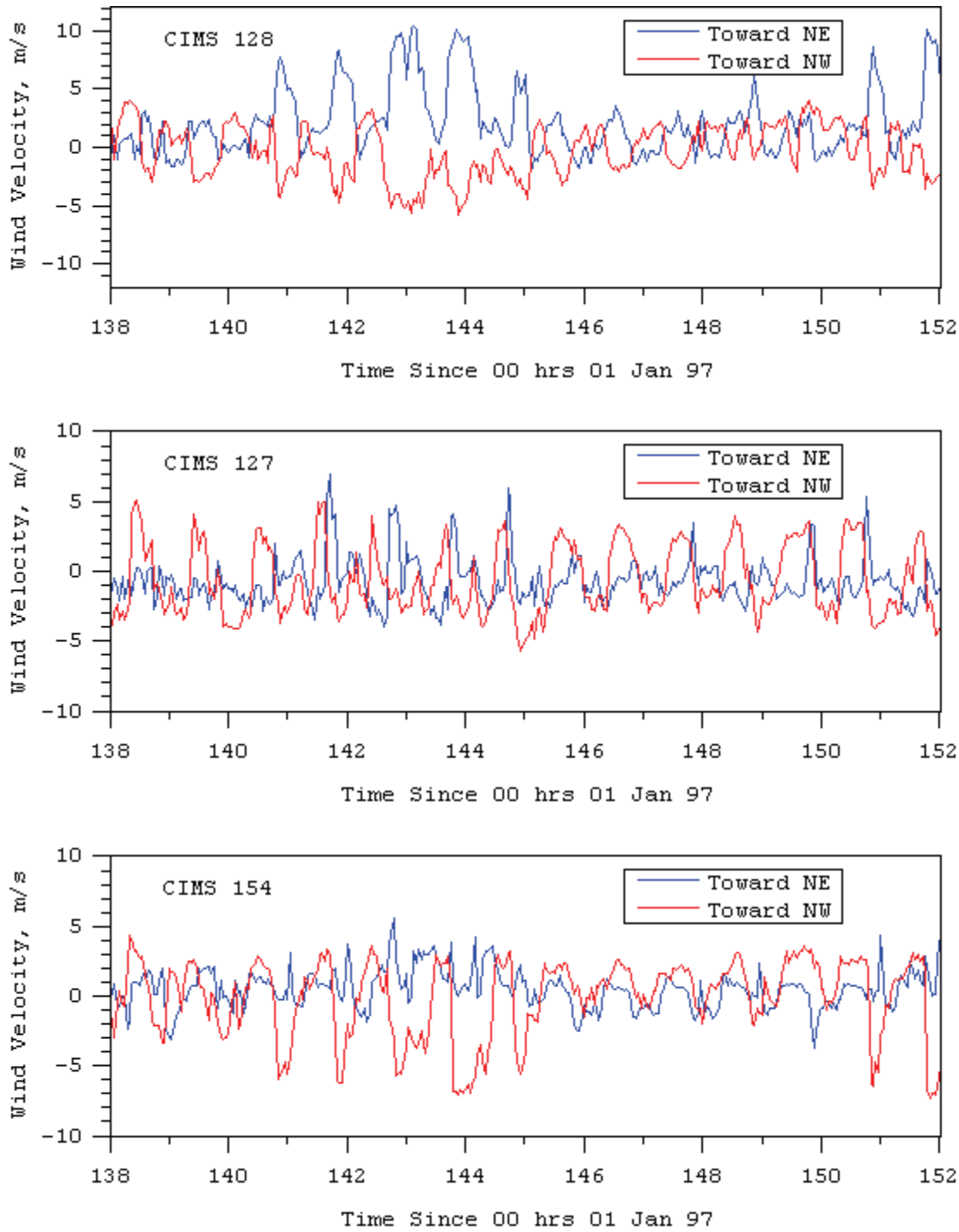

Figure 2-6. Wind velocity components, May 20-31, 1997

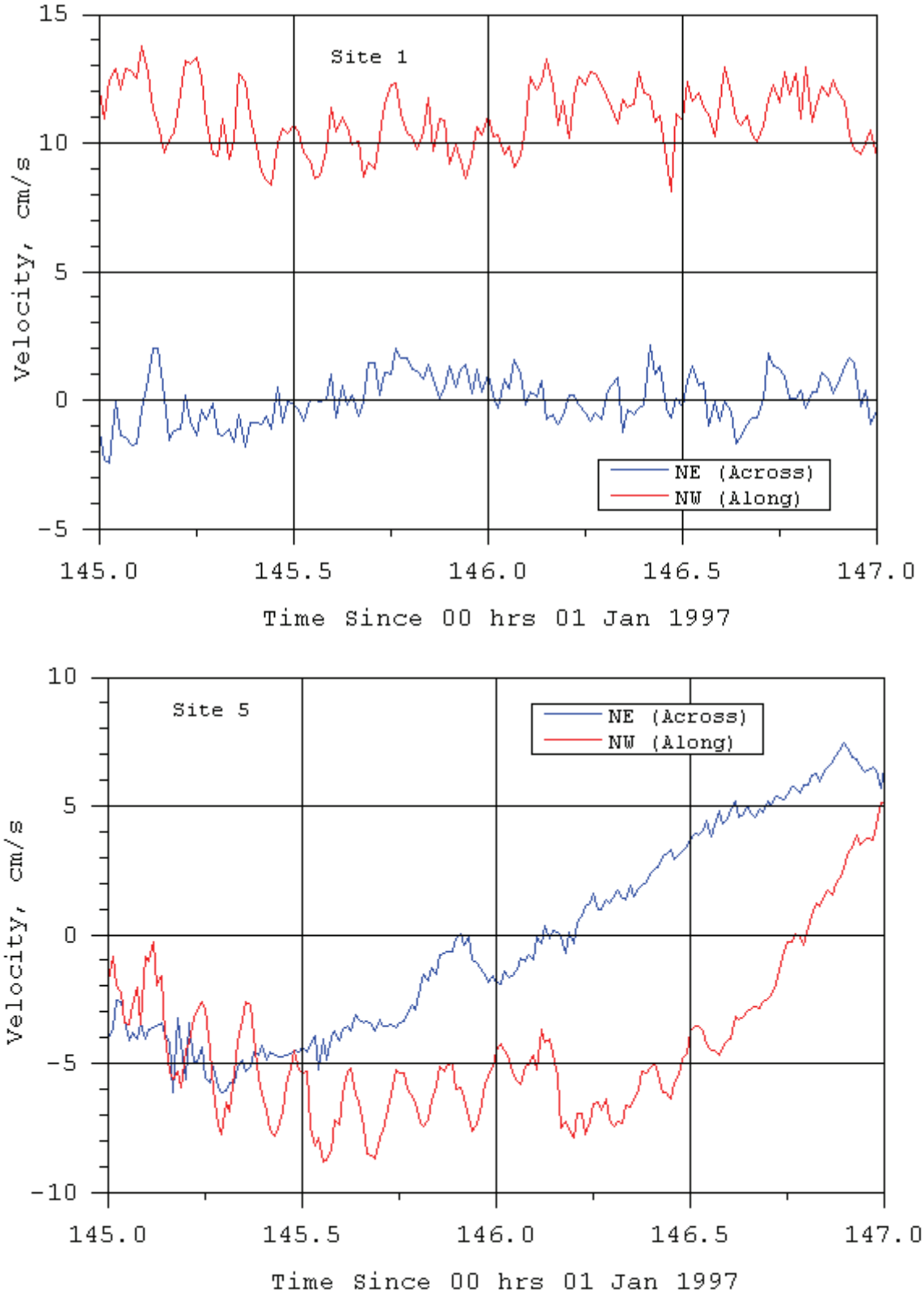

Figure 2-7. Depth average velocity components at sites 1 and 5, May 24-25, 1997

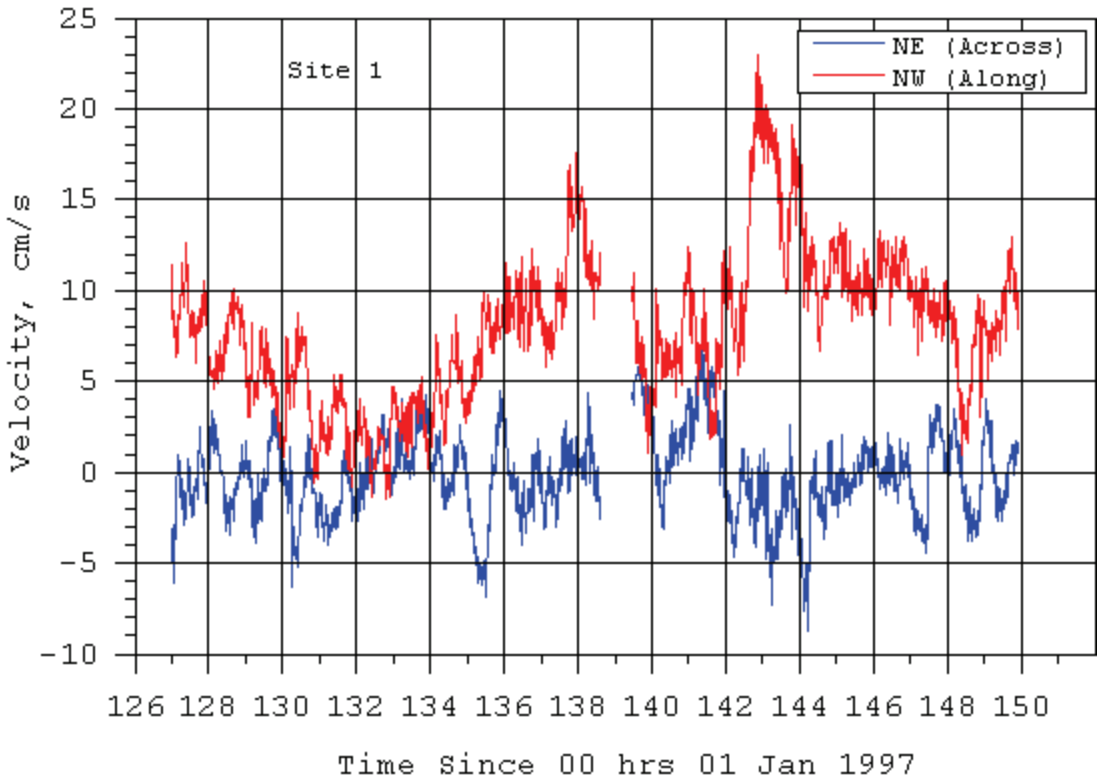

Figure 2-8. Depth average velocity components at site 1, May 8-31, 1997

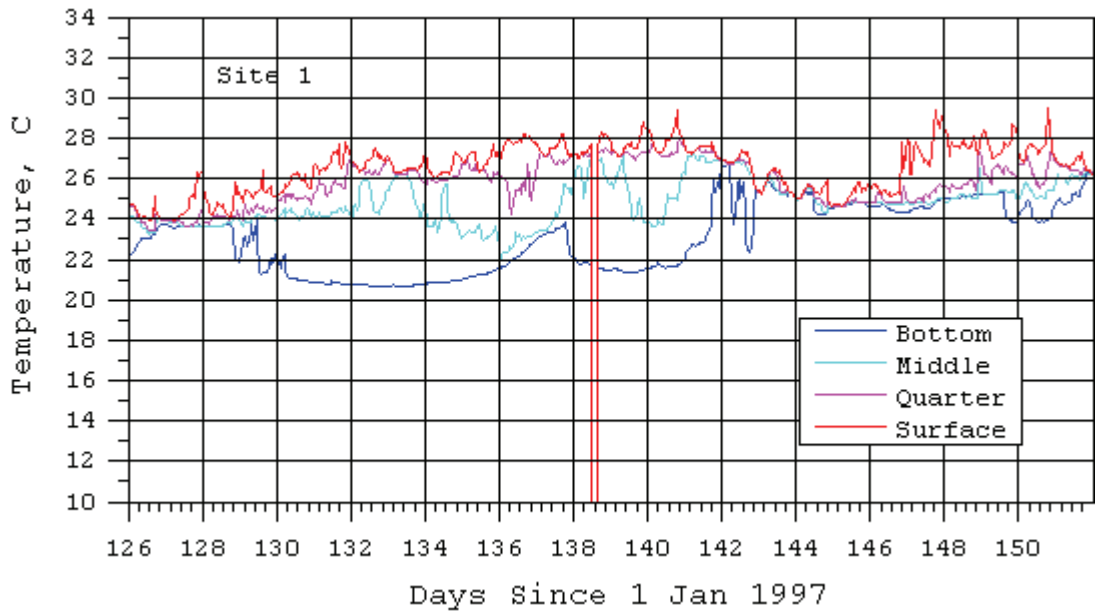

Figure 2-9. Temperature at site 1, May 8-31, 1997

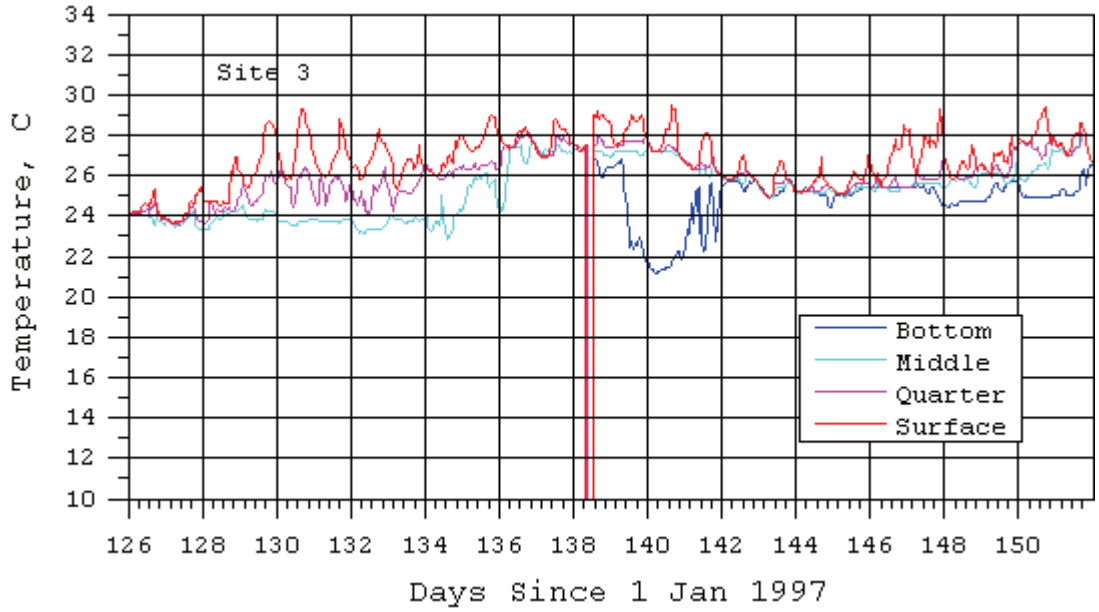

Figure 2-10. Temperature at site 3, May 8-31, 1997

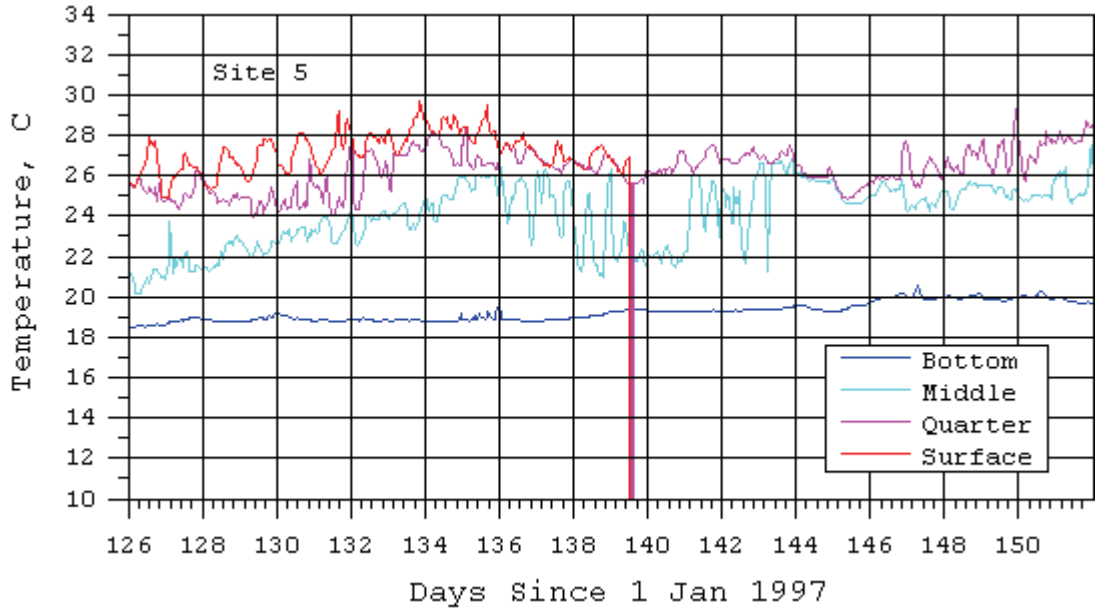

Figure 2-11. Temperature at site 5, May 8-31, 1997

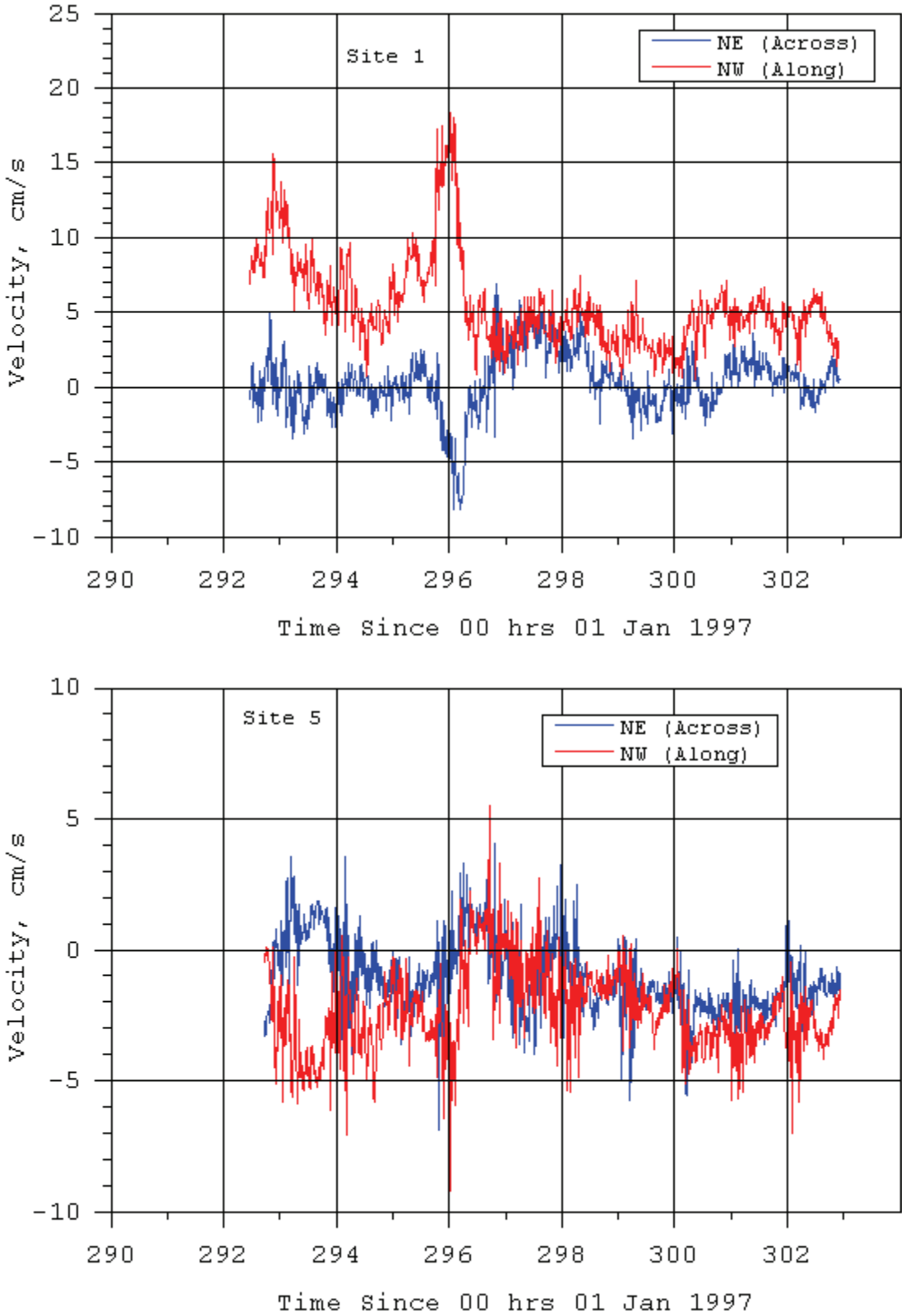

Figure 2-12. Depth average velocity components at site 1, October 17-31, 1997

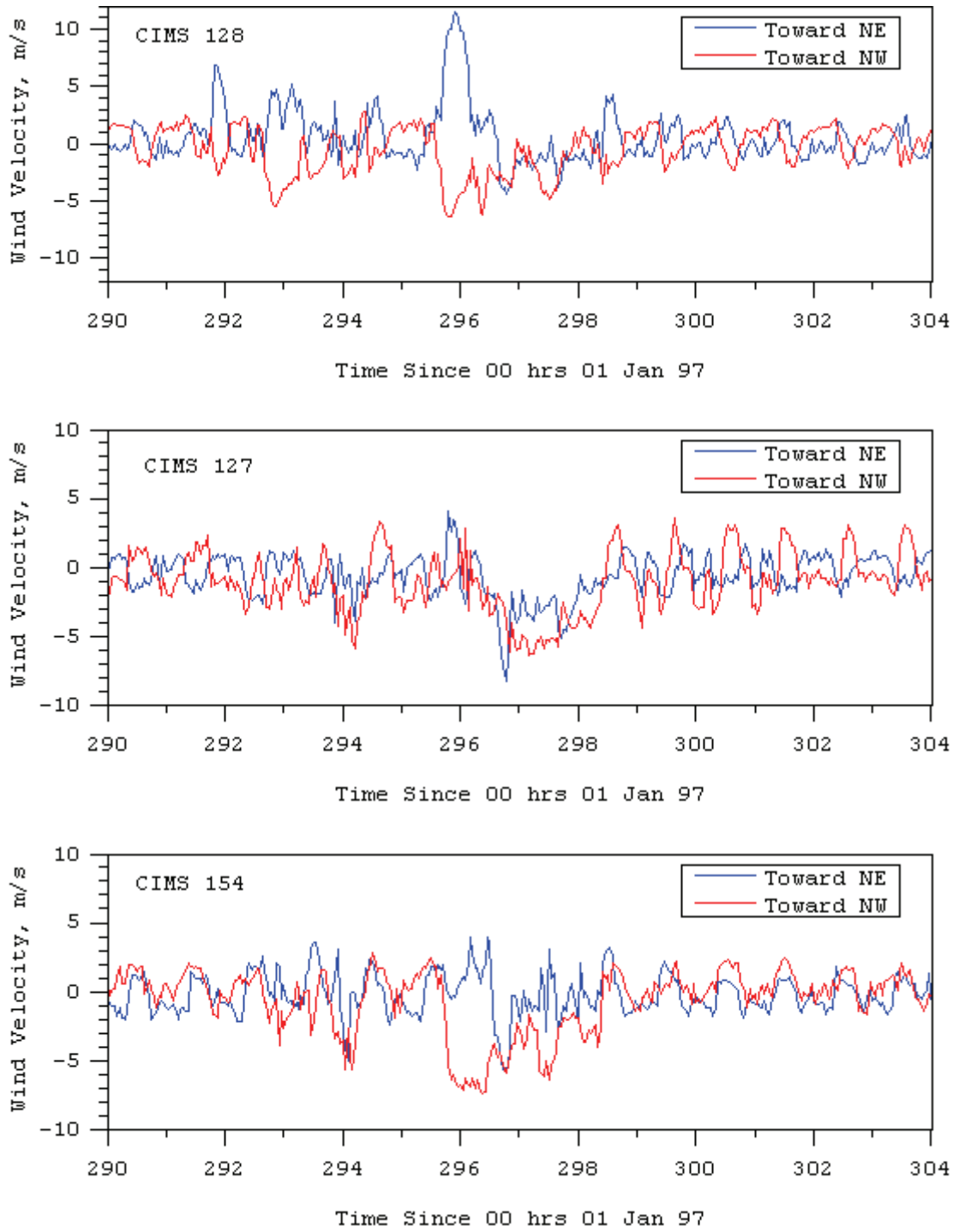

Figure 2-13. Wind velocity components, October 17-31, 1997.

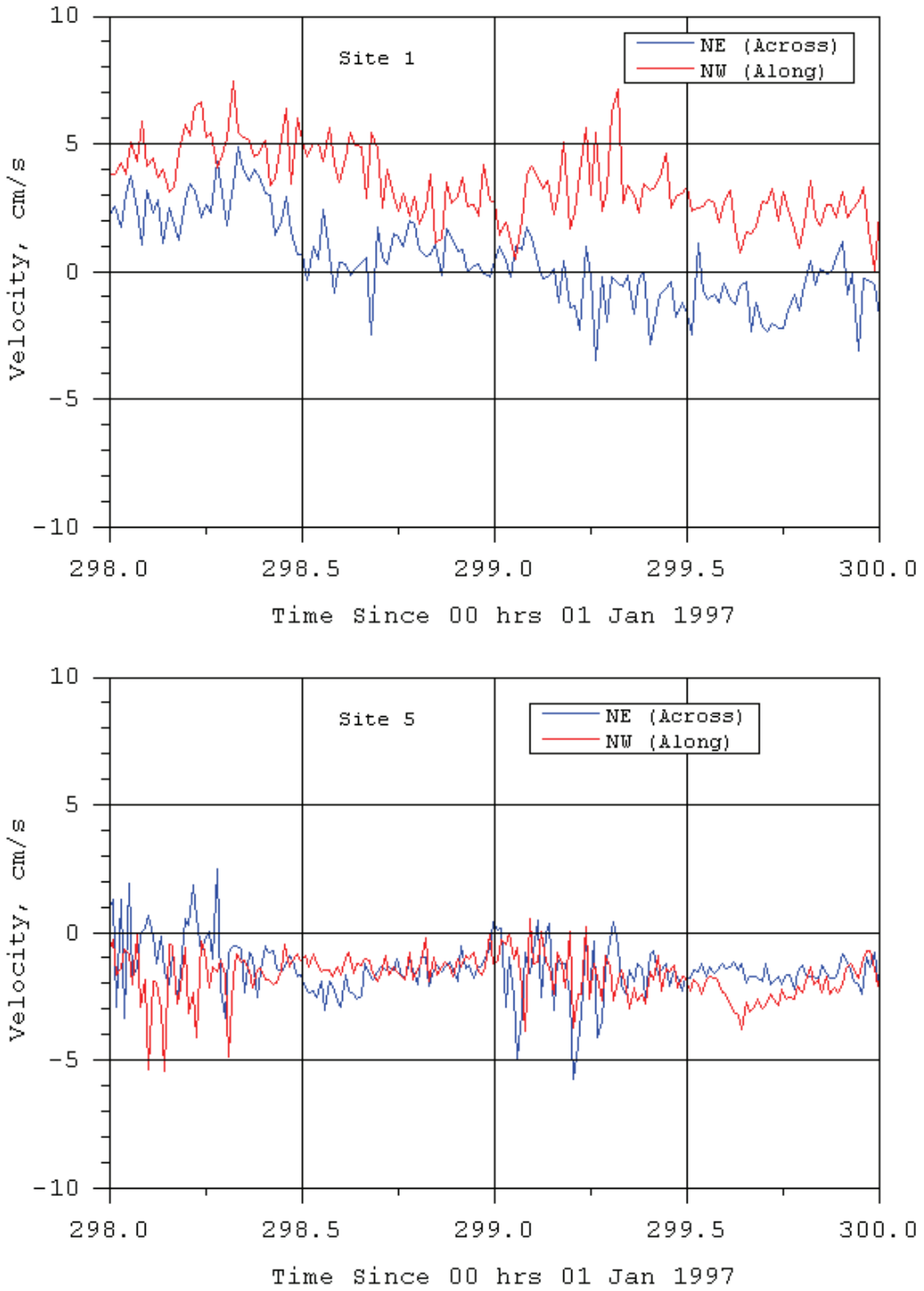

Figure 2-14. Depth average velocity components at sites 1 and 5, October 26-27, 1997

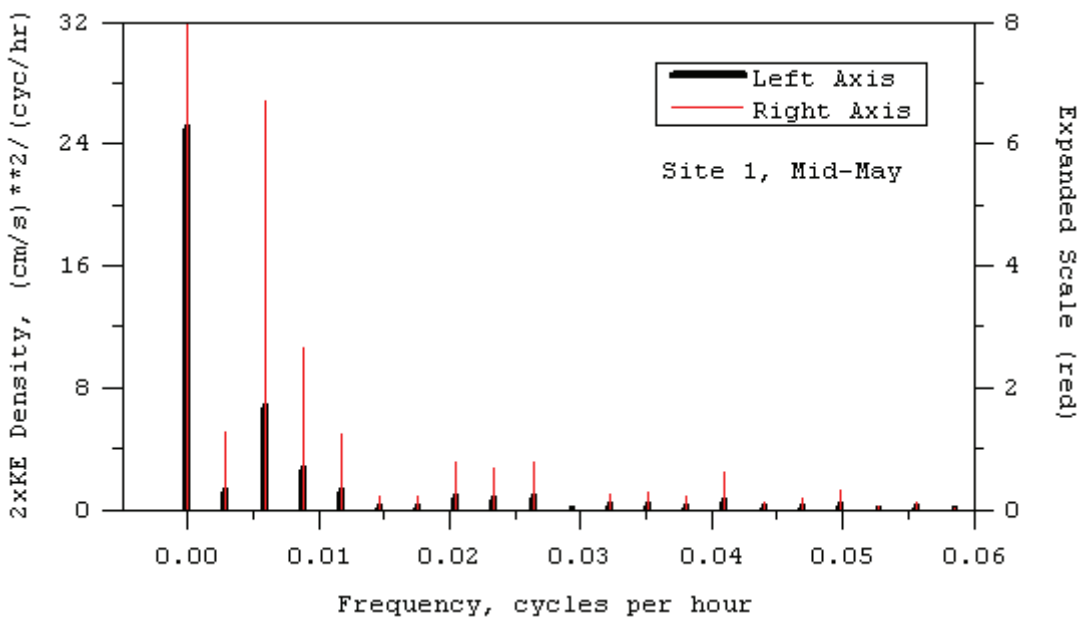

Figure 2-15. Kinetic energy spectral density, site 1, May 8-20, 1997

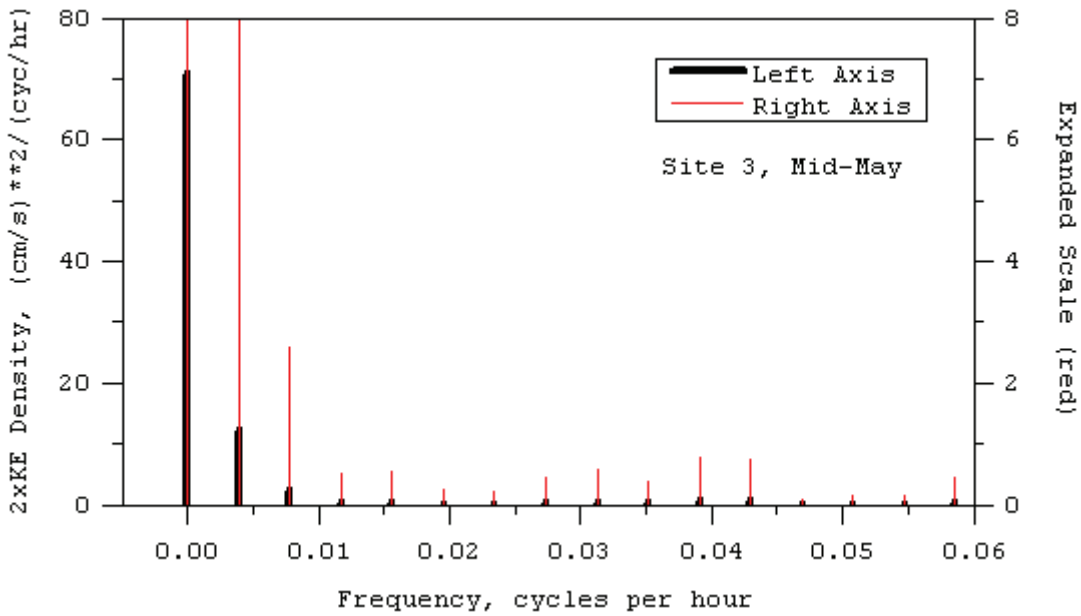

Figure 2-16. Kinetic energy spectral density, site 3, May 8-20, 1997

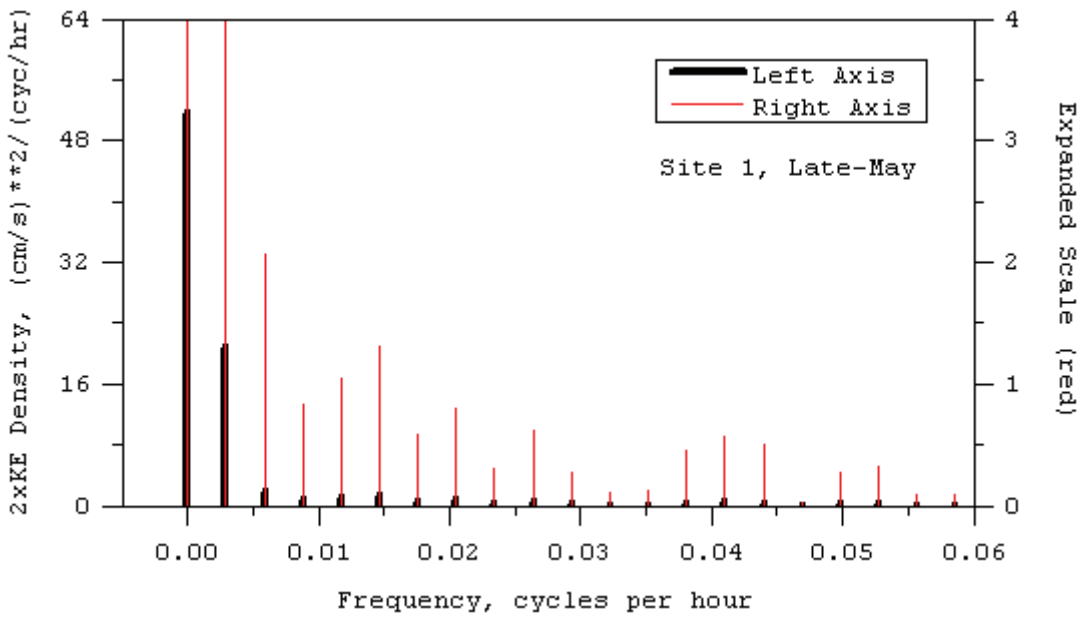

Figure 2-17. Kinetic energy spectral density, site 1, May 20-31, 1997

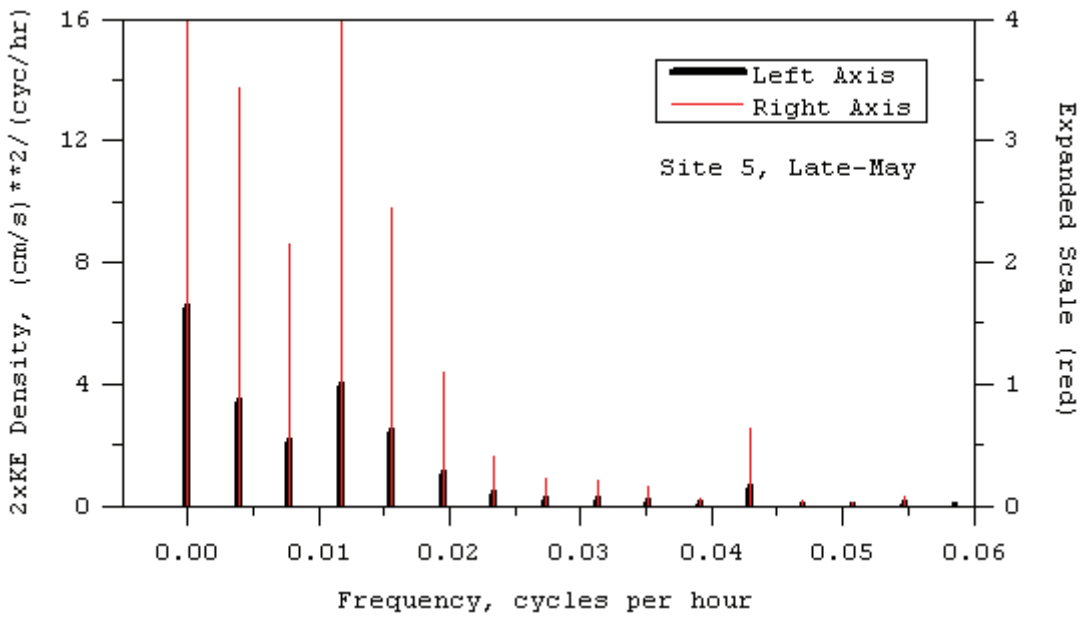

Figure 2-18. Kinetic energy spectral density, site 5, May 20-31, 1997

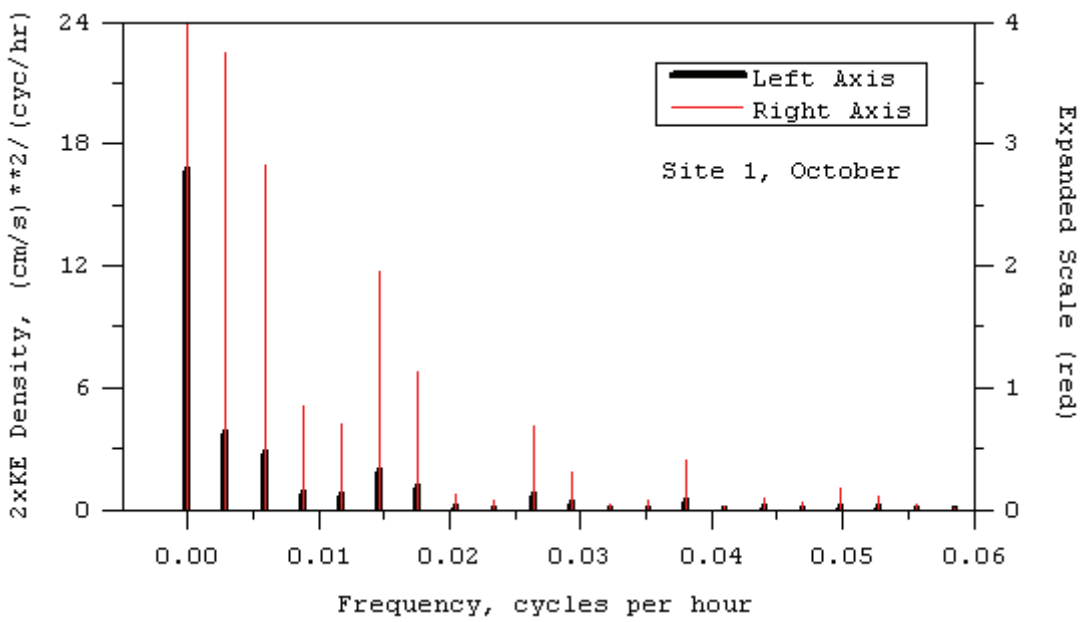

Figure 2-19. Kinetic energy spectral density, site 1, October 20-31, 1997

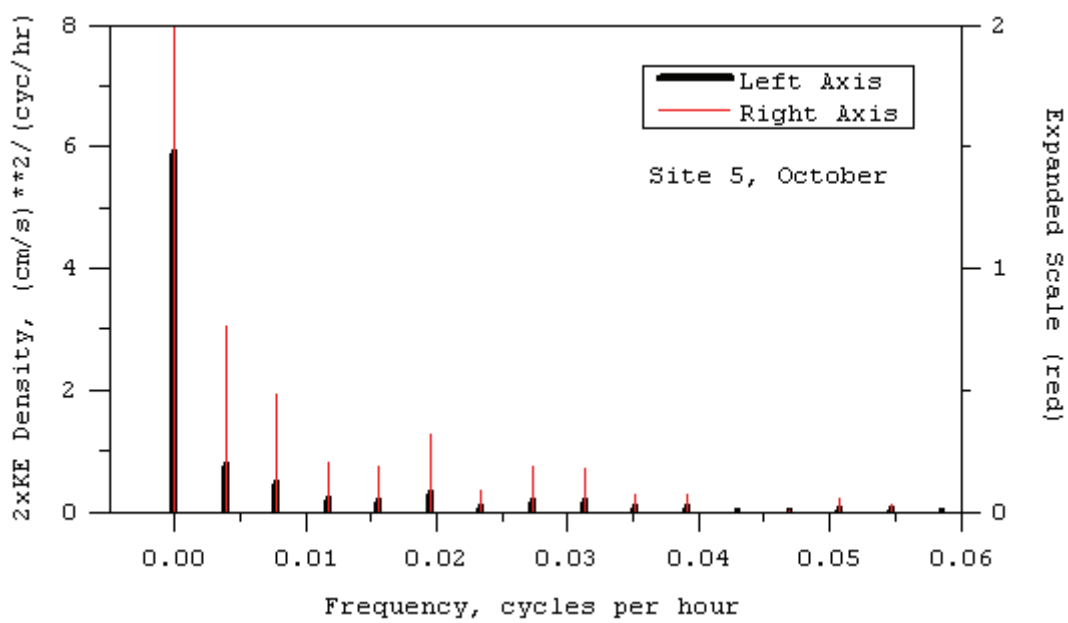

Figure 2-20. Kinetic energy spectral density, site 5, October 20-31, 1997

2.2. Water Quality and Eutrophication

Algae and nutrient dynamics in the Salton Sea are primarily driven by internal recycling with current external loadings being insufficient to drive observed processes. External loadings over that Sea's history are responsible for creating the reservoir of nutrients and organ material resulting the Sea's current hyper-eutrophic conditions and current loading contribute significantly to localized dynamics in the vicinity of the three river inflows.

Eutrophication and nutrient cycling are in the Salton Sea can be conceptualized by first considering algae dynamics. Algae uptake nutrients, ammonium, nitrate, and dissolve orthophosphate for growth. Algae respiration and mortality including predation, result in the release of organic carbon, nitrogen and phosphorous. The aerobic decay of organic carbon in the water column exerts a carbonaceous oxygen demand, while conversion of ammonia to nitrate exerts a nitrogeneous oxygen demand. In the deeper hypoxic or anoxic regions of the water column, there is the potential for anaerobic decomposition of organic carbon by sulfate, with an end product being hydrogen sulfide. Sulfate is produced in the lower water column under aerobic conditions by the oxidation of hydrogen sulfide produced under anaerobic conditions and the flux of hydrogen sulfide from the sediments under anaerobic conditions in the sediment bed.

Ammonia is produced in the water column by algae respiration and decay of dissolved organic nitrogen and consumed by algae uptake for growth and nitrification. Nitrate is consumed by algae for growth when ammonium concentrations are extremely low and can be converted back to ammonium by the process of denitrification. Algae respiration releases dissolved orthophosphate while predation results in the release of dissolved organic phosphorous, which can decay or be mineralized into dissolved orthophosphate. Dissolved orthophosphate can become biologically unavailable by complexation with dissolved metals or adsorbed to inorganic suspended sediments and subsequently desorbed if the dissolve phase concentration becomes low. The combined processes for complexation, adsorption, and desorption can be represented by equilibrium partitioning where the fraction of biologically available dissolved orthophosphate varies with the concentration of adsorption site material. Settling of orthophosphate adsorbed on solids contributes to removal from the water column.

The portions of particulate organic carbon, nitrogen and phosphorus which do react in the water column settle to the sediment bed. Conditions in the sediment bed are typically characterized by a thin surface aerobic layer above a much deeper anaerobic region. Under anoxic conditions at the bottom of the water column, the thin aerobic layer essentially disappears. Organic carbon, nitrogen and phosphorous undergo diagenesis in the sediment bed. Organic carbon can be decomposed in the aerobic layer resulting in a dissolved oxygen flux into the sediment bed referred to as carbonaceous component of the sediment oxygen demand. In the deeper anaerobic region of the sediment organic carbon is oxidized by sulfate to form hydrogen sulfide, which tends to diffuse toward the sediment bed surface. When the surface aerobic layer is present, the hydrogen sulfide reacts with dissolved oxygen to form sulfate and contributes to the flux of oxygen into the bed contributing to the sediment oxygen demand. Sulfide not oxidized in the aerobic layer may be transported into the water column where it can exert an oxygen demand.

The decomposition or diagenesis of organic nitrogen in the sediment bed produces ammonium, which can undergo nitrification in the aerobic layer creating a nitrogenous component of the sediment oxygen demand. The portion of ammonium not nitrified in the aerobic layer and nitrate produced there diffuses into the water column providing a source of

nutrients to algae. In a similar manner, diagenesis of organic phosphorous in the sediment bed produces orthophosphate, a fraction of which may complex or be adsorbed, with the remaining dissolved fraction diffusing into the water column providing a source of orthophosphate for algae. Physical resuspension of particulate and dissolved material can contribute to the flux of nutrients from the sediments into the water column. However, past experience in environments much more energetic than the Salton Sea indicate that physical resuspension is secondary to the diagenetic processes resulting in the fluxes of ammonium, nitrate, dissolved orthophosphate and hydrogen sulfide into the water column.

The internal cycling process in the Salton Sea is essentially self-maintaining with the potential level of algae biomass being proportional to the nutrient pool in the system. Over seasonal time scales, nutrient loads from inflowing tributaries contribute primarily to localized variability near. With complete elimination of external loads, the cycling process can gradually decrease in intensity as certain nutrients, particularly orthophosphate, become less biologically available. Likewise, continued moderate loads can maintain or slightly modify the level of cycling over time, while substantially large external loads will drive the system to a higher level of cycling. A significant characteristic of eutrophic water bodies driven by internal cycling is that organic materials exhibit multiple phase distributions, particulate and dissolved, and multiple reaction time scales, fast or labile and slow or refractory. Partitioning of organic carbon, nitrogen and phosphorous into particulate and dissolved classes is essential for correctly representing reactions in the water column and the flux of organic material to the sediment bed. Similarly, it is essential to account for both fast and slow reaction rates.

Table 2-1 through Table 2-12 summarize the major internal interactions in the conceptual model. Figure 2-21 presents a schematic of nutrient cycling in the water column with organic material partitioned into labile particulate (LPOx), refractory particulate (RPOx) and dissolved (DOx). The dissolved organic material can also be further partitioned in labile and refractory reactive classes. Figure 2-22 shows a schematic of sediment diagenesis where the settling of particulate organic matter and its mineralization in the sediment results in nutrient fluxes to the water column as well as sediment oxygen demand and the flux of hydrogen sulfide into the water column.

An extensive set of water quality observational data were collected by the U.S. Bureau of Reclamation at 3 sites, Figure 2-23, during 1999 (Holdren and Montano, 2002a, b). Observations were collected over the water column at 18 sampling dates. This observational data set is judged to be of sufficient detail to support development and calibration of a three-dimensional water quality model consistent with the conceptualization. A selection of these observational data will be presented in the water quality model calibration section.

Table 2-2.
Water Column Algae Interactions

	Algae Growth	Algae Respiration	Algae Predation
Organic Carbon		secondary source	primary source
Organic Phosphorous		secondary source	primary source
Orthophosphate	sink	primary source	secondary source
Organic Nitrogen		secondary source	primary source
Ammonium	sink	primary source	secondary source
Nitrate	sink	primary source	secondary source
Dissolved Oxygen	source	sink	

Table 2-3.
Water Column Organic Carbon Interactions

Interaction	Source/Sink Process
Algae Respiration and Predation	Source
Aerobic Decay	Sink (Sink of Dissolved Oxygen)
Anaerobic Decay	Sink (Sink of Sulfate, Source of Sulfide)
Denitrification	Sink
Settling including carbon content of settling Algae	Sink (Source Sediment Bed)
Diagenesis in Sediment Bed	Sink (Sink of Dissolve oxygen in bed)

Table 2-4.
Water Column Organic Phosphorous Interactions

Interaction	Source/Sink Process
Algae Respiration and Predation	Source
Decay/Mineralization	Sink (Source of Dissolved Orthophosphate)
Settling including carbon content of settling Algae	Sink Water Column (Source Sediment Bed)
Diagenesis in Sediment Bed	Sink (source of dissolved orthophosphate in bed which can flux to water column)

Table 2-5.
Water Column Dissolved Orthophosphate Interactions

Interaction	Source/Sink Process
Algae Growth	Sink
Algae Respiration and Predation	Source
Decay of Organic Phosphorous	Source
Complexeation and Adsorption	Sink
Desorption	Source
Diagenetic Sediment Flux	Net Source

Table 2-6.
Water Column Particulate Orthophosphate Interactions

Interaction	Source/Sink Process
Complexation and Adsorption	Source
Desorption	Sink
Settling of Adsorbed Phase	Sink
Sediment Bed	Controls Orthophosphate Equilibrium and in turn Dissolve Orthophosphate Flux from Bed

Table 2-7.
Water Column Organic Nitrogen Interactions

Interaction	Source/Sink Process
Algae Respiration and Predation	Source
Decay/Mineralization	Sink (Source of Ammonium)
Settling including nitrogen content of settling Algae	Sink (Source Sediment Bed)
Diagenesis in Sediment Bed	Sink (Source of Ammonium in Bed and in turn Ammonium flux from bed)

Table 2-8.
Water Column Ammonium Interactions

Interaction	Source/Sink Process
Algae Growth	Sink
Algae Respiration and Predation	Source
Decay of Organic Nitrogen	Source
Nitrification	Sink (Source of Nitrate)
Denitrification	Source
Diagenesis in Sediment Bed	Source Sink if nitrified in aerobic layer otherwise flux to water column

Table 2-9.
Water Column Nitrate Interactions

Interaction	Source/Sink Process
Algae Growth	Sink
Algae Respiration and Predation	Source
Nitrification	Source (Sink of ammonium)
Denitrification	Sink
Sediment Flux	Source if nitrification occurs in sediment aerobic layer

Table 2-10.
Water Column Dissolve Oxygen Interactions

Interaction	Source/Sink Process
Algae Growth	Source
Algae Respiration	Sink
Decay of Organic Carbon	Sink (CBOD)
Nitrification	Sink (NBOD)
Oxidation of Hydrogen Sulfide In water column	Sink (COD) Sink of Sulfide, Source of Sulfate
Sediment Oxygen Demand	Sink (SOD having CSOD, NSOD and ChemSOD components)

Table 2-11.
Water Column Hydrogen Sulfide Interactions

Interaction	Source/Sink Process
Anaerobic Decomposition of Organic Matter in Sediment Bed	Source (Sink of Sulfate)
Anaerobic Decomposition of Organic Matter in Water Column	Source (Sink of Sulfate)
Aerobic Oxidation in Bed	Sink (Generates ChemSOD) (Source of Sulfate)
Aerobic Oxidation in Water Column	Sink (ChemOD) (Source of Sulfate)

Table 2-12.
Water Column Sulfate Interactions

Interaction	Source/Sink Process
Anaerobic Decomposition of Organic Matter in Sediment Bed	Sink (Source of Sulfide)
Anaerobic Decomposition of Organic Matter in Sediment Bed	Sink (Source of Sulfide)
Aerobic Oxidation in Bed	Source (Sink of Sulfide)
Aerobic Oxidation Sulfide in Water Column	Source (Sink of Sulfide)

Table 2-13.
Definition of State Variables in Figure 2-21

Water Quality State Variable	Definition
Bc, Bg, Bd	Algae groups c, g, d
LPOC , RPOC	Labile and refractory particulate organic carbon
DOC	Dissolved organic carbon
LPON , RPON	Labile and refractory particulate organic nitrogen
DON	Dissolved organic nitrogen
NH4	Ammonia
NO23	Nitrate + Nitrite
LPOP , RPOP	Labile and refractory particulate organic nitrogen
DOP	Dissolved organic nitrogen
PO4t, PO4d, PO4p	Total, dissolved and particulate phosphate
SU	Unavailable silica
SA, SAd, SAp	Total, dissolved and particulate available silica
DO	Dissolved oxygen
COD	Sulfide component of chemical oxygen demand
TSS	Total suspended solids
TAM	Total active metal

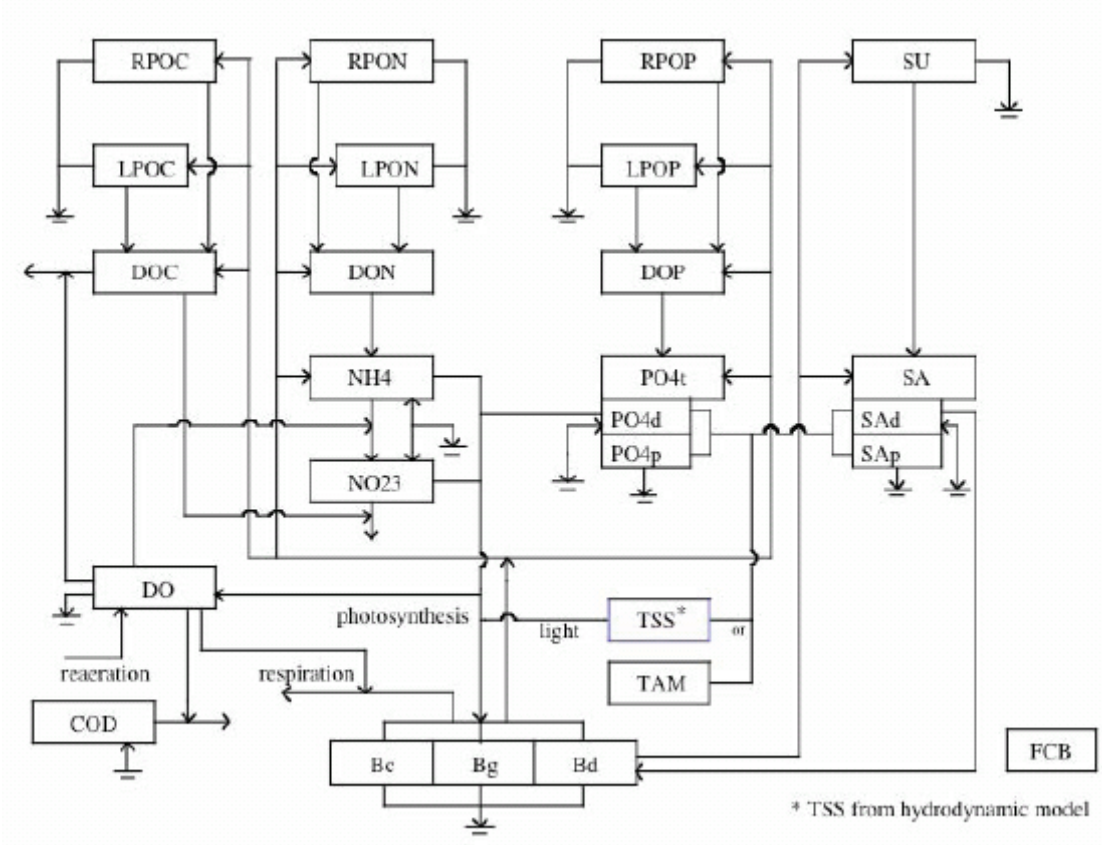

Figure 2-21. Schematic of nutrient cycling in the water column.

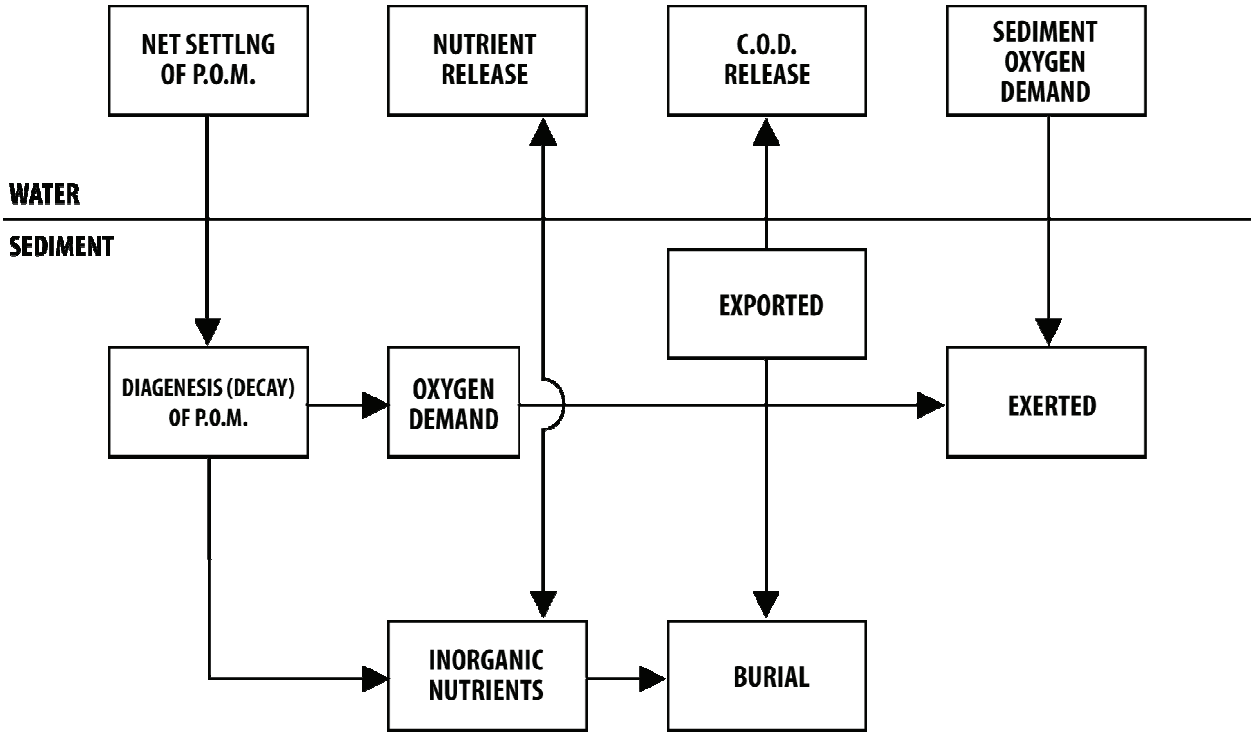

Figure 2-22. Schematic of sediment diagenesis processes (note chemical oxygen demand release, COD, represents chemical oxygen demand associated with sulfide flux from the bed into the water column).

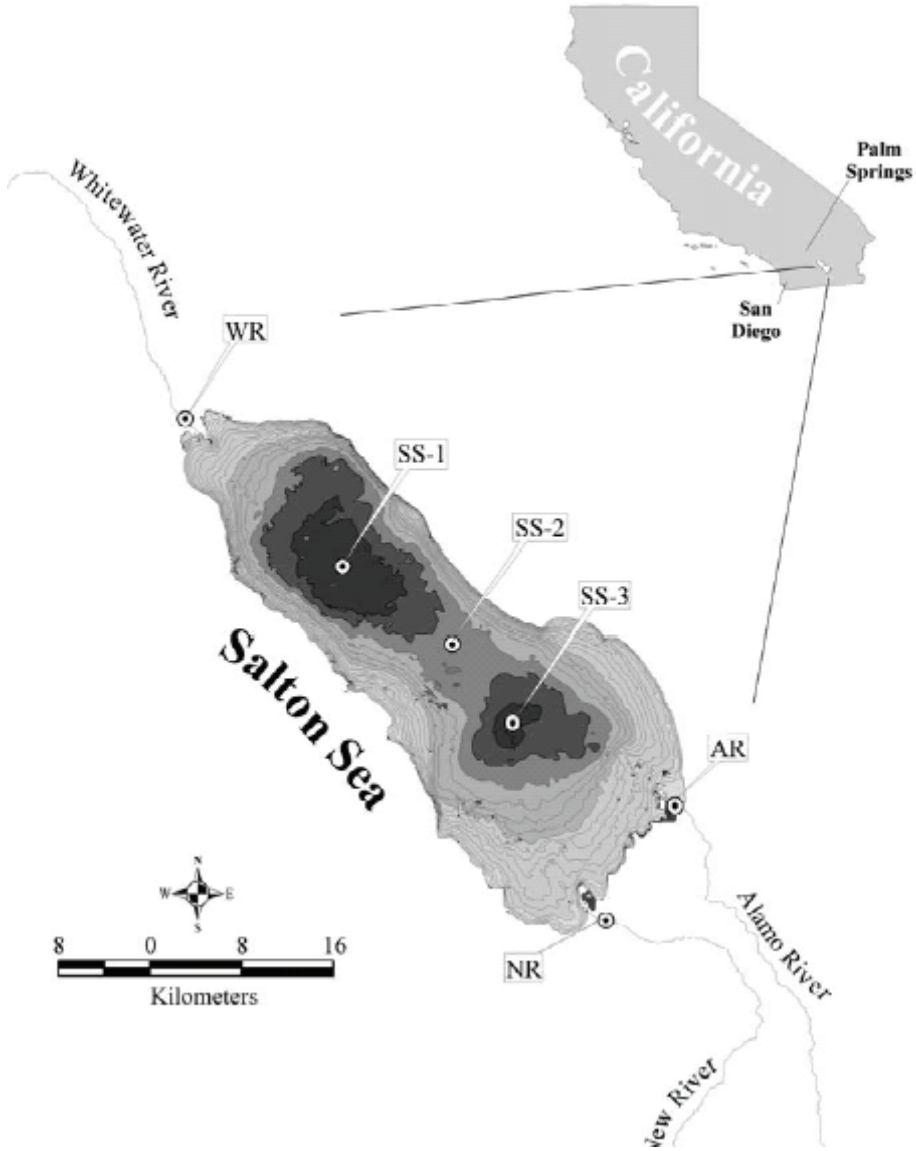

Figure 2-23. Location of water quality monitoring sites in the Salton Sea during 1999. (Holdren and Montano, 2002)

3. Model Selection

The conceptual model presented in the preceding section serves to establish requirements for selecting hydrodynamic and water quality models for the Salton Sea. The fact that circulation and thermal stratification are highly three-dimensional and provide the transport fields for water quality state variable leads to the overarching requirement of three-dimensional models for both hydrodynamics and water quality. Other important considerations include the model's track record of successful application, its availability, supporting documentation and ability to perform simulations on decadal time scales. Decadal time scale simulation is essential since the water quality responses to reduced loadings in systems driven by internal nutrient cycling typical exhibit time scales of 5 to 20 years. Three-dimensional coupled hydrodynamic model application approaches generally fall within two classes, the first being standalone hydrodynamic and water quality models requiring external linkages to pass hydrodynamic transport fields to the water quality model. The second class differs in that a single modeling system, with internal linkages between the hydrodynamic and water quality components exist. When the first approach is used, the ability to easily link the two component models becomes an essential requirement.

The requirement of three-dimensional hydrodynamics with the ability to externally or internally link to a water quality model narrows the choice of appropriate hydrodynamic models to a rather small group. This group includes the CH3D-WES, ECOM, EFDC, and RMA10 models. The CH3D-WES, ECOM and EFDC models are finite differenced based while the RMA10 model is finite element based. The CH3D-WES model can be externally linked to the three-dimensional CE-QUAL-ICM water quality model (Cerco and Cole, 1995), while the ECOM model can be externally linked the RCA water quality model (HydroQual, 2003). The EFDC model can be externally linked to a number of three-dimensional water quality models including CE-QUAL-ICM (Tillman, et al, 2004), RAC, and WASP (Ambrose et al., 1993; Wool et al., 2003) and also includes an internally linked water quality model based on CE-QUAL-ICM (Park, et al., 1995, Tetra Tech, 2006c). The CH3D-WES/CE-QUAL-ICM, ECOM/RCA, and EFDC, with both external and internal linking, modeling systems all have records of successful applications. The RMA10 model has only been linked to the CE-QUAL-ICM model (Cerco et al., 2000). The RMA10 model was also used by Cook (2000) for short term hydrodynamic simulations of the Salton Sea. However, the computational intensity of the RMA10 model limits it application to short time frames on the order of months. For this reason, the RMA10 model can be eliminated from further consideration.

The choice between the CH3D-WES/CE-QUAL-ICM, ECOM/RCA, and EFDC model systems for this study was based on secondary considerations. The CH3D-WES/CE-QUAL-ICM system, although developed by the U.S. Army Corp of Engineers, is not truly public domain and is not readily available. The ECOM/RCA system is public domain, but only commercial support is available. The EFDC modeling system is open source and public domain, as well as being developed by Tetra Tech, who supports the model for the U.S. Environmental Protection Agency.

These considerations lead to the choice of the EFDC (Environmental Fluid Dynamic Code) modeling system and use of its internally linked water quality model component. The EFDC model is supported by extensive documentation (Hamrick, 1992; Tetra Tech, 2002, 2006a, 2006c). EFDC applications have been reported in approximately 20 referred journal publications, more than 30 referred conference proceeding publications, and numerous technical reports, many of which involved reviewed regulatory studies in the U.S. EPA NPDES, TMDL, Superfund and National Estuary programs.

The EFDC hydrodynamic model (Hamrick, 1992) component employs a semi-implicit, conservative finite volume solution scheme for the hydrostatic primitive equations with either two- or three-level time stepping. Salinity and temperature are dynamically coupled which a choice of high accuracy advection schemes including MPDATA and COSMIC. Additional hydrodynamic component features include: simulation of drying and wetting, representation of hydraulic control structures, vegetation resistance, wave-current boundary layers and wave induced currents. An embedded single port buoyant jet module is included for coupled near and far field mixing analysis. The hydrodynamic model has been used extensively for three-dimensional circulation and salinity and temperature transport in estuaries, coastal regions and lakes (Hamrick and Mills, 2001; Jin et al., 2000, 2002; Khangaonkar et al., 2005; Tetra Tech, 2006b, and Wool, et al., 2003).

The EFDC model includes a variable configuration eutrophication model component for simulation of aquatic carbon, nitrogen and phosphorous cycles. The full configuration of state variables is based on the CE-QUAL-ICM model including sediment diagenesis (DiToro, 2000). The configuration can be readily reduced to WASP equivalent configurations. For application to the Salton Sea, dissolved organic carbon, nitrogen and phosphorous have been partitioned into labile and refractory fractions resulting in four sub-fractions for each of the organic materials. Algae were classified into two sub- groups that grow under low and high water temperatures. Kinetics of anaerobic oxidation of organic carbon and associated generation of sulfide in the water column were also incorporated into the model to represent the Salton Sea system, where extended period of low DO and high sulfate exist. Sulfate is not simulated as a separate state variable because its concentration is several orders of magnitude higher than other relevant water quality constituents such as hydrogen sulfide and organic carbon. The 23 water column state variables are summarized in Table 3-1.

Table 3-1.
EFDC Water Column State Variables

Water Quality State Variable	Sub-Classes
Algae	Low temperature group High temperature group
Organic Carbon	Labile and Refractory Particulate Labile and Refractory Dissolved
Organic Phosphorous	Labile and Refractory Particulate Labile and Refractory Dissolved
Ortho-phosphorous	Dissolved and Particulate (Equilibrium Sorption Formulation)
Organic Nitrogen	Labile and Refractory Particulate Labile and Refractory Dissolved
Ammonium	NA
Nitrate	NA
Silica	Available and Un-available
Hydrogen Sulfide (as Oxygen equivalent Chemical Oxygen Demand)	NA
Sulfate (as Oxygen equivalents)	NA
Dissolved Oxygen	NA

4. Model Configuration

The EFDC model was configured to simulate the 1997-1999 historical period. Two horizontal grids were developed, a fine grid with a 600 meter horizontal resolution, shown in Figure 4-1, and a coarse grid with a 1200 meter horizontal resolution. One-foot contour interval bathymetric data was interpolated onto both girds with the fine resolution grid bathymetry shown in Figure 4-2. Vertical resolution for both grids used 25 vertical layers approximately 0.61 meters thick at mean Sea surface level. The number of vertical layers varies in the horizontal dimension consistent with variations in bottom elevation.

Model forcing functions include fresh water inflow, the atmospheric wind field and atmospheric information necessary to specify incident solar radiation and air-water heat exchange. Inflows for the Alamo, New and Whitewater rivers were based on USGS stream gauging data and adjusted to account for ungauged inflows and are shown in Figure 4-3. Atmospheric forcing data are based on CIMIS records at stations 41, 50, 127, 128, 136, 141, and 154 and a record at the Desert Valley Company site near the Safety Clean site, Figure 2-1. Representative sample unadjusted wind records from these sites were shown in Figure 2-3, Figure 2-6, and Figure 2-13. The wind speed from these stations was adjusted to a reference 10 meter height and interpolated over the grid to create a spatially and temporally varying wind field with water surface wind stresses computed internally in the model. Weighted average temporally varying atmospheric temperature, relative humidity, rainfall, water surface incident solar short wave radiation, and cloud cover forcing functions were constructed from CIMIS observational stations records. The hourly atmospheric temperature record is shown in Figure 4-4. The EFDC model internally computes evaporative water loss and associated air-water heat exchange. The model includes a bed thermal mass and heat exchange between the bed thermal mass. The bed thermal mass was assumed to extend to 5 meters below the deepest point in the Sea, approximately 15 meters, or approximately 20 meters below the surrounding shoreline land surface. The temperature at the bottom of the thermal mass layer is held constant at 22 degrees C, the approximate annual average atmospheric temperature. Inflowing concentrations of water quality model state variables are based on observational data collected near the mouth of the three rivers during 1999, and also used for the two subsequent years by applying shifts in the collection dates. Concentrations and flows are interpolated on a daily basis to provide mass loadings of the state variables.

Both the hydrodynamic and coupled hydrodynamic and water quality simulations can be started at any point during the three year configuration period although starts on midnight January 1, 1997 are typical since the water column tends to be well mixed and the annual temperature cycle is near its minimum temperature of 13 ^{o}C. Initial conditions for the water quality state variables were based on January 21, 1999 observations (Holdren and Montano, 2002a). As the performance of the thermal simulation improved, the temperature distribution at the end of 1997 was used to replace the original constant initial temperature conditions. For the water quality model simulations, the sediment diagenesis or flux model requires a few years to reach dynamic equilibrium and the 1997 and 1998 simulation period can be viewed as a spin-up to the 1999 calibration period. Similarly as the water quality model performance improved, the end of year sediment bed conditions were subsequently used for beginning of the year initial conditions.

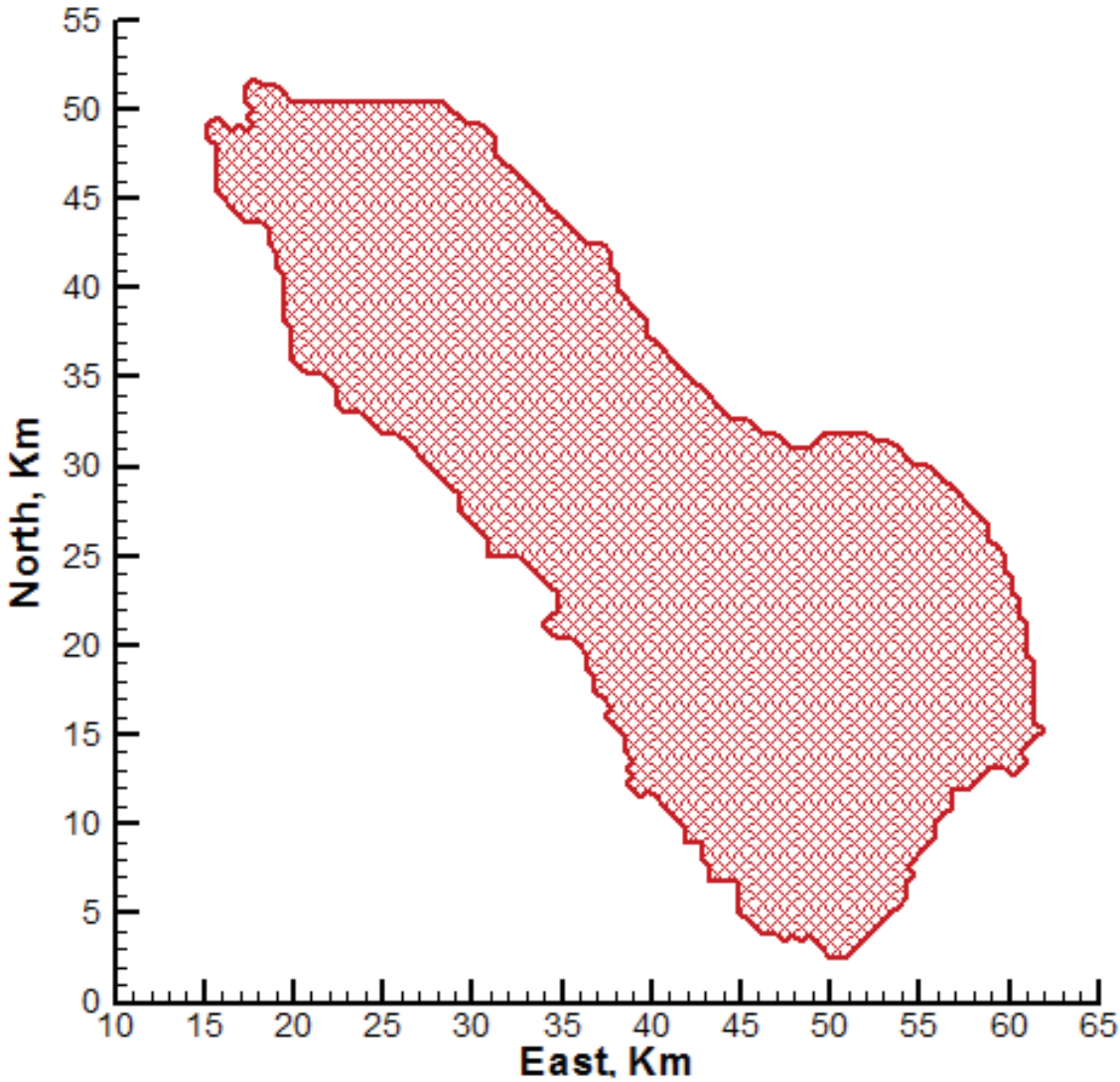

Figure 4-1. Horizontal grid of the Salton Sea with 600 meter square cells.

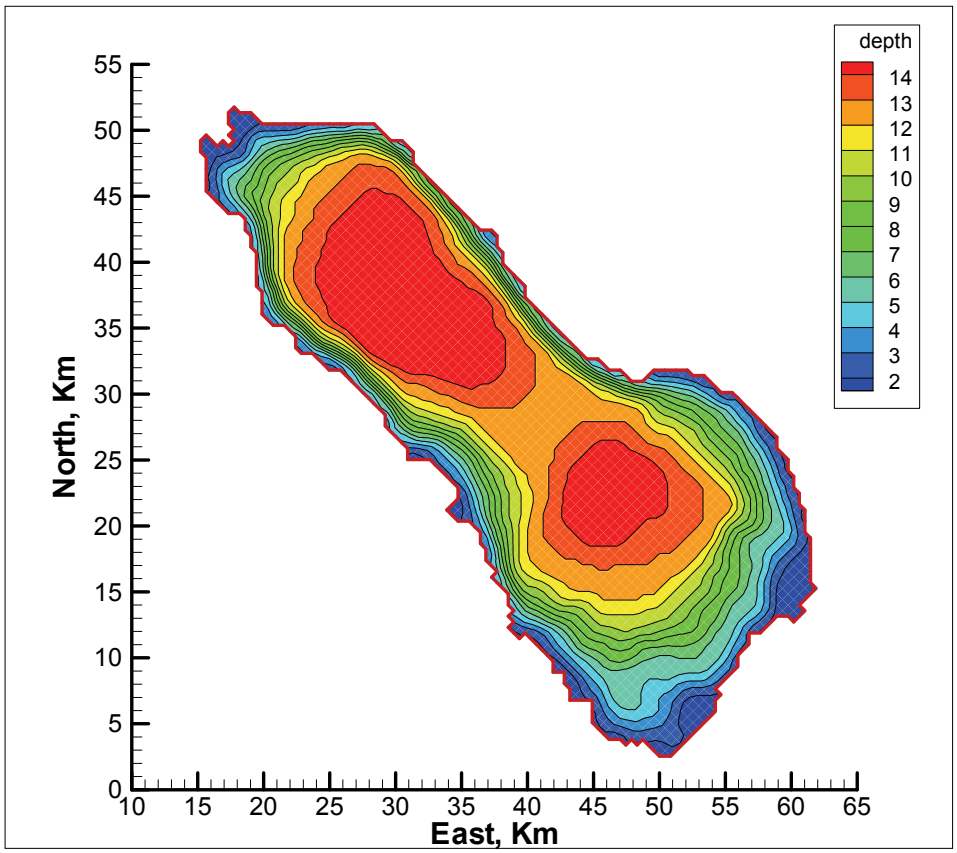

Figure 4-2. Bathymetry of the Salton Sea on 600 meter horizontal grid.

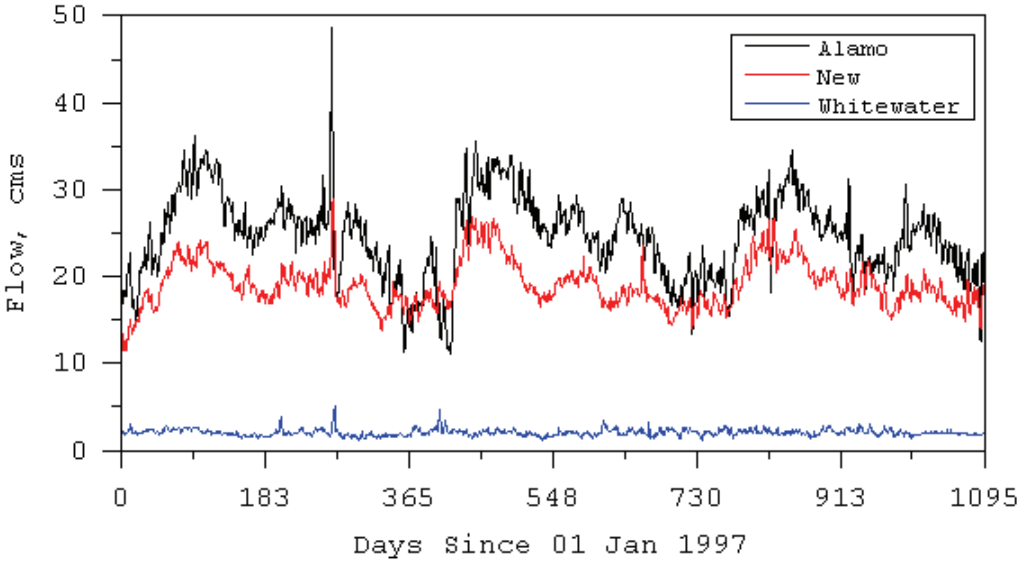

Figure 4-3. Inflow to the Salton Sea, 1997-99.

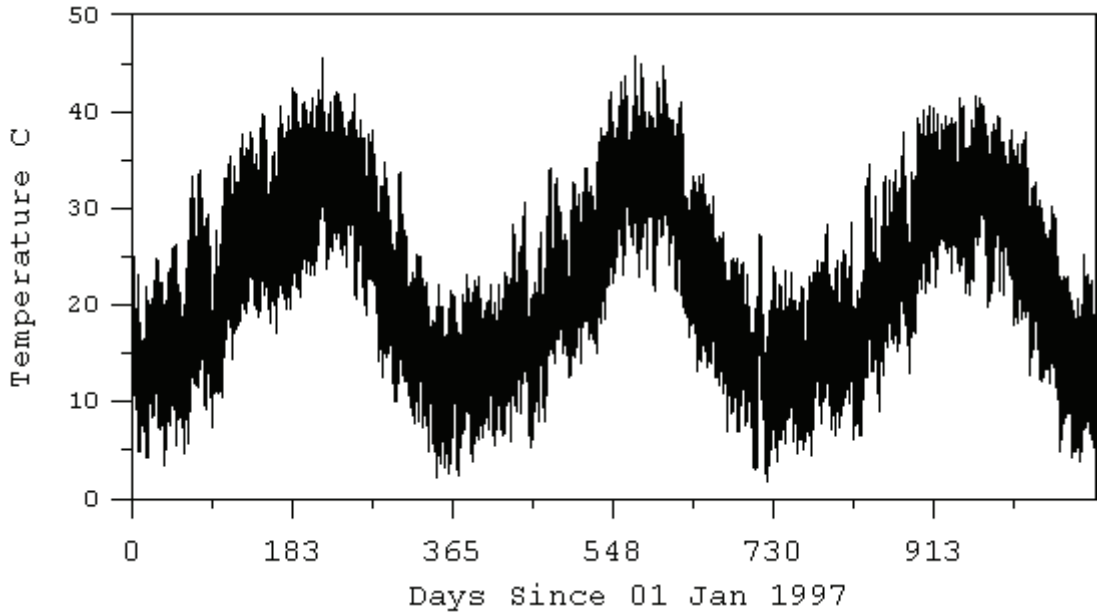

Figure 4-4. Atmospheric temperature in vicinity of Salton Sea, 1997-99.

5. Hydrodynamic and Thermal Calibration and Validation

This chapter describes the calibration and validation of the hydrodynamic and thermal component of the modeling system. Calibration is based on 1997 current and temperature observations, while validation is based on 1999 temperature observations. An analysis of the sensitivity of temperature prediction to accurate velocity prediction using velocity data assimilation is also included.

5.1. Hydrodynamic and Thermal Calibration

The calibration of the hydrodynamic component of the EFDC based model involved comparison of model predicted currents and temperature with observations taken during 1997 by Cook (2000), Figure 2-1. Observational data for the comparison was provided by Cook (2006). Primary calibrations parameters included the adjustment factor for scaling observed CIMIS wind velocities to the reference 10 meter height, an adjustment of the observed incident solar short wave radiation magnitude, the solar shortwave radiation attenuation rated, and the thickness and bottom temperature of the bed thermal mass. Wind velocities at the CIMIS observations stations, 2 meters above ground level were increased to by a factor of 1.5 to the 10 meter reference level required by the model. Incident solar radiation observations were adjusted by a factor of 0.8, and which is consistent with a number of previous applications using radiometer data. The solar short wave radiation attenuation rate was set to 1.5 per meter which is consistent with observational data for light penetration (Holdren and Montano, 2002a). Bottom roughness was specified by a 0.01 meter log-law roughness height with results being relatively insensitive to values in the range of 0.005 to 0.02 meters.

Model predictions of observed depth average current components, discussed in Chapter 2, are presented in Figure 5-1 through Figure 5-3. Observed vertical profiles at 20-minute time intervals at Site 1 and 15 minute intervals at sites 3 and 5 were depth averaged for comparison with corresponding model predictions output at the same time interval. The top panel of Figure 28 shows a comparison for Site 1, see Figure 2-1, during mid-May 1997. The model produces the slow modulation over the observation period, but model predicted velocities are somewhat lower in magnitude. Model predicted variability at time scales less than one day is considerably weaker than observations and can be attributed to the temporally smooth and spatially interpolated hourly wind field forcing the model. Results at Site 3 during the same mid-May period are shown in the bottom panel of Figure 5-1. For this site the model does somewhat better in predicting the current magnitude at scales in access of one day, but exhibits similar characteristics as those for Site 1. The top panel of Figure 5-2 shows a comparison for Site 1 during late May. The model's predictive ability is somewhat improved during this period, but higher frequency responses are not fully represented. A comparison of observations and predictions at Site 5 during late May is shown in the bottom panel of Figure 5-2. The model's predictive ability at this site is quite poor, with model predicted current component magnitudes being too small and the observed event response between days 145 and 148 being absent or delayed. The top panel of Figure 5-3 shows a comparison at Site 1 during late October. Again, model predicted current component magnitudes tend to be lower than observed and too smooth, although the event response at day 296 is reasonably well represented. Comparisons for the same late October period at Site 5 are shown in the lower panel of Figure 5-3. Model predictive ability for this site is relatively poor.

The model's ability to predict depth average current components exhibits a number of deficiencies. At Sites 1 and 3 in the southern basin, component magnitudes are generally to low and excessively smoothed in time in comparison with observations, although directional

response at time scales exceeding one or two days is reasonable. As noted, temporal and spatial specification of the wind field could contribute to this and merits additional discussion. Since observational wind data was available only at hourly averaged increments, there is temporal smoothing or gust removal inherent in the wind field which could account for higher frequency smoothing of the model predictions. Similarly, the interpolation of the shoreline and further landward point observations over a large water body such as the Salton Sea represents spatial smoothing and the neglect of possible microclimatological variations between land and open water. Microclimate variations could possibly account for the absence of diurnal response in the model, if sea breeze effects over the large lake area are not well represented by shoreline and further landward observations. Similar arguments apply to Site 5.

Observed and model predicted temperatures at the five 1997 sites, Figure 2-1, are shown in Figure 5-4–Figure 5-13. The top panels of these figures shows observed temperatures near the water surface, at one quarter and one half of the local depth below the water surface and near the bottom. The bottom panels show corresponding model predictions. Observational data is at one-hour intervals during periods of sensor operation, and model predictions were also output at one hour intervals. Results at Site 1 on the eastern side of the southern basin are shown in Figure 5-4 and Figure 5-5. Model predicted temperature during spring and summer tends to be somewhat higher than observations in the upper water column and lower than observations in the lower water column. The model correctly predicts the vertical mixing event occurring near the end of May at day 152. Vertically mixed conditions occurring near early October, day 274, and persisting for the remainder of the year are also accurately predicted. Results at Site 2 on the south side of the southern basin are shown in Figure 5-6 and Figure 5-7. Model predicted temperature during late winter and early spring are quite consistent with observations which show intermittent period of stratification and nearly complete vertical mixing. The model correctly predicts nearly vertically mixing conditions occurring after mid-October (day 290). Interestingly, the model also predicts the observed periods of unstable stratification in the fall, when water surface temperatures are lower than bottom temperatures. Results at Site 3 on the western side of the southern basin are shown in Figure 5-8 and Figure 5-9. Model predicted thermal stratification during March (days 6-91) is consistent with observations, although the model predicts lower bottom temperatures during most of the spring period. However, by the end of July (day 213) model predicted bottom temperature is consistent with observations. Model predictions under vertically mixed conditions, after day 273, are consistent with observations.

Temperature results at Site 4 in the middle of the Sea are shown in Figure 5-10 and Figure 5-11. Model predicted temperature stratification compares well with observations during March (days 61-91) compares well with observations. During late spring and early summer, the model tends to over predict stratification and does not capture the series of observed mixing events in the vicinity of day 152. Model predictions under vertically mixed conditions after day 274 agree well with observations. Results for Site 5 in the northern basin are shown in Figure 5-12 and Figure 5-13. Observations at Site 5 show strong, persistent stratification through the end of June (day 182). The model generally reproduces these conditions with the exception of the rate of increase in bottom temperature being too great between the middle of April and the middle of May. The model also does not reproduced mixing events occurring between days 152 and 182. The model predictions agree well with observations after the onset of vertically mixed conditions in the fall.

Overall, the model's temperature predictive ability is reasonably good, particularly during late winter-early spring and fall and early winter. At the Southern and mid-Sea sites,

stratification tends to be over predicted during late Spring and early Summer, while at the northern Site 5 stratification is somewhat under predicted. Unfortunately, observational data during warmest months of August and September (days 213-274) are not available for 1997. The model shows very moderate stratification at all sites during August which is eliminate by mid September.

The temperature calibration activity revealed that temperature prediction is most sensitive to the solar short wave radiation and its attenuation rate, and the wind field. The selected attenuation rate of 1.5 per meter is well supported by observational measurements. Adjustment in the magnitude on the solar short wave radiation tends to move temperatures at all stations and depths uniformly upward or downward and the selected adjustment factor of 0.8 was chosen to achieve the best agreement between observed and model predicted surface temperatures. The adjustment of observed wind speed to the reference 10 meter level and the interpolation of the adjusted wind speeds and directions at the observational sites to create a spatially variable wind field proved to result in the greatest temperature stratification prediction sensitivity.

The calibration results indicate that the model tends to perform better at predicting temperature than velocity. This is not unexpected in that temperature and dissolved material tend to have more slowly varying horizontal distributions than velocity. Also consistent with this is the fact that model predicted velocities represent averages in this case over hundreds of meters in contract to the point based characteristic of the observations. For the Salton Sea, model predictions of velocity are poorest at Site 5 in the northern sea. Since under the SSA Plan, Site 5 will become the center of the restored northern marine Sea, it is important to gain some insight into the relationship between predictive ability of velocity and temperature stratification which is addressed in the following section.

5.2. Sensitivity of Temperature Prediction to Velocity Prediction

A velocity data assimilation experiment was conducted to determine the impact of velocity prediction accuracy on temperature prediction, the full details of which will be elaborated in the final report. Basically, velocity data assimilation adds a forcing term to the hydrodynamic momentum equations which nudge the model-predicted velocity to the observed. The forcing term can be viewed as a correction to the surface wind stress such that the corrected wind stress results in accurate prediction of the velocity. Since the model's velocity prediction is poorest at Site 5 in the northern sea, assimilation experiment results for that site will be presented. Figure 5-14 shows the comparison of model predicted and observed currents at site 5 during late May without and with data assimilation. Figure 5-15 shows the corresponding comparison of model predicted and observed temperature with and without velocity data assimilation. Although assimilation results in forcing agreement with observed velocity, the change in temperature prediction is insignificant. Similar comparisons at Site 5 for late October are shown in Figure 5-16 and Figure 5-17. These results, as well as similar results at Sites 1 and 3, indicate that vertical temperature structure and in turn vertical mixing is relatively insensitive to the exact prediction of velocity magnitude and direction. This is consistent with turbulent mixing theory which indicates that the surface stress and resulting vertical shear as well as nocturnal mixing associated with unstable temperature profiles near the water surface are the sources of vertical mixing

5.3. Thermal Validation

A second set of temperature observations taken during the 1999 water quality monitoring study (Holdren and Montano, 2002a) were also compared with model predictions. The observational data set consists of discrete vertical temperature profiles at three stations, Figure 2-23, taken 18 times during 1999. Results for site SS-1, in the northern basin, are shown in Figure 5-18. The top and bottom panel are near the water surface and bottom, while the intermediate panels represent temperatures at 6 and 10 meters below the surface. The results show a tendency of the model to slightly over predict surface temperatures during August and September. Similar to the results at the 1997 Site 5, bottom temperatures are over predicted during late spring and early summer. Results for Station SS-2 near the middle of the Sea are shown in Figure 5-18. Surface and bottom temperature prediction is quite good at this site with the exception of early winter temperatures being slightly over predicted. Results for Station SS-3 in the southern basin are shown in Figure 5-19. As was the case for Station 2, surface and bottom temperature prediction is good at this site with the exception of early winter temperatures being slightly over predicted.

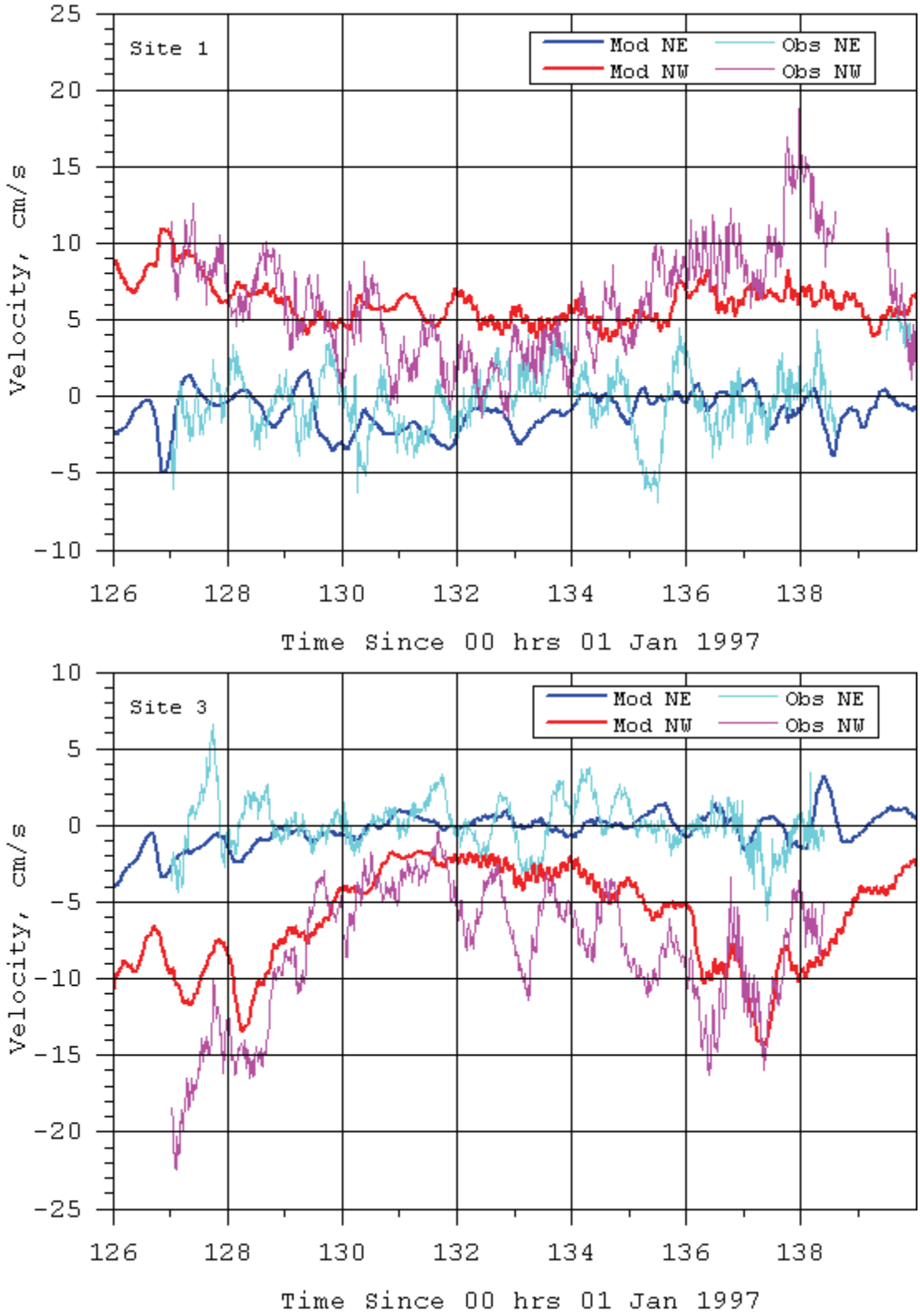

Figure 5-1. Depth average current velocity comparison at Sites 1 and 3 during early May.

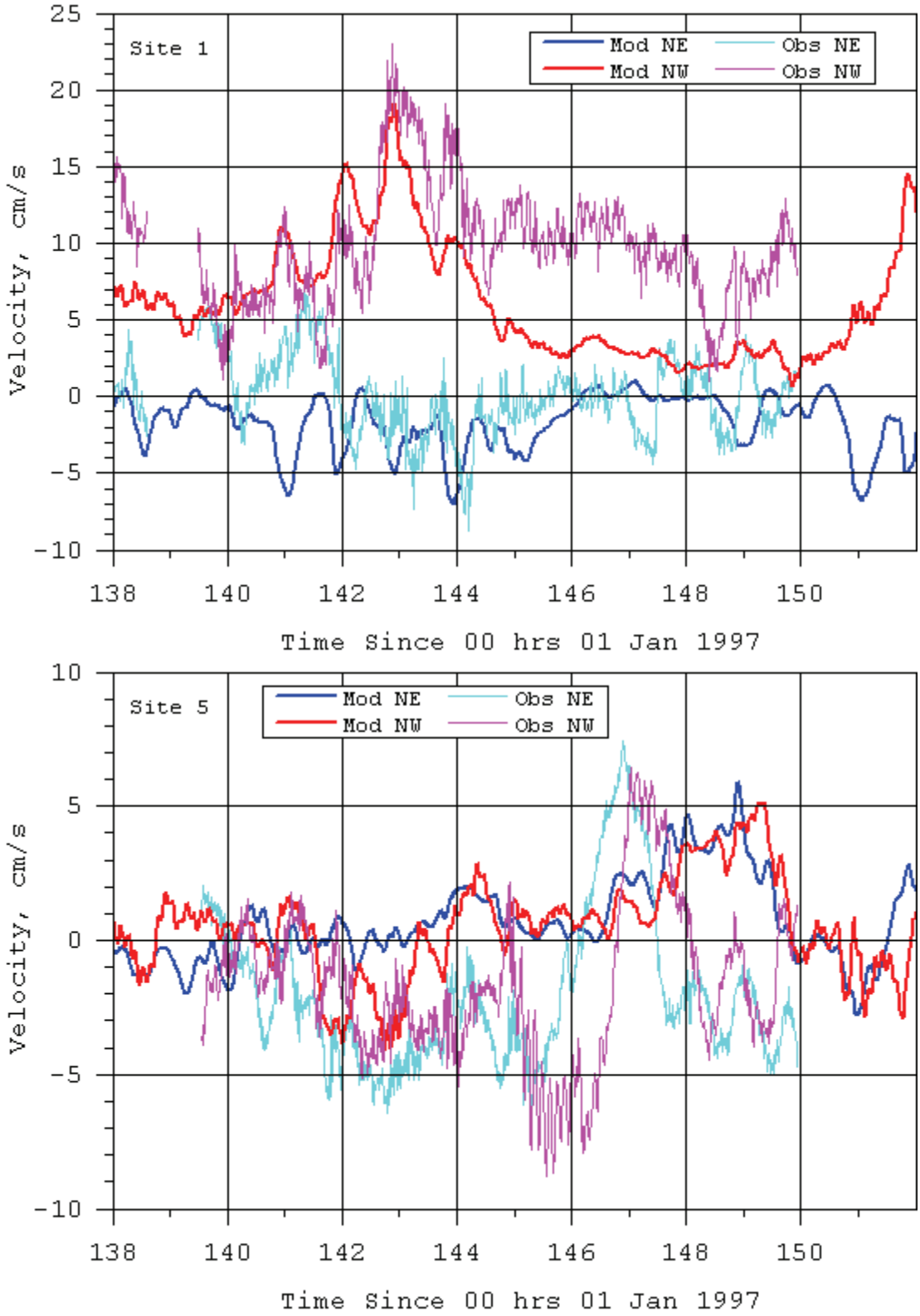

Figure 5-2. Depth average current velocity comparison at Sites 1 and 5 during late May.

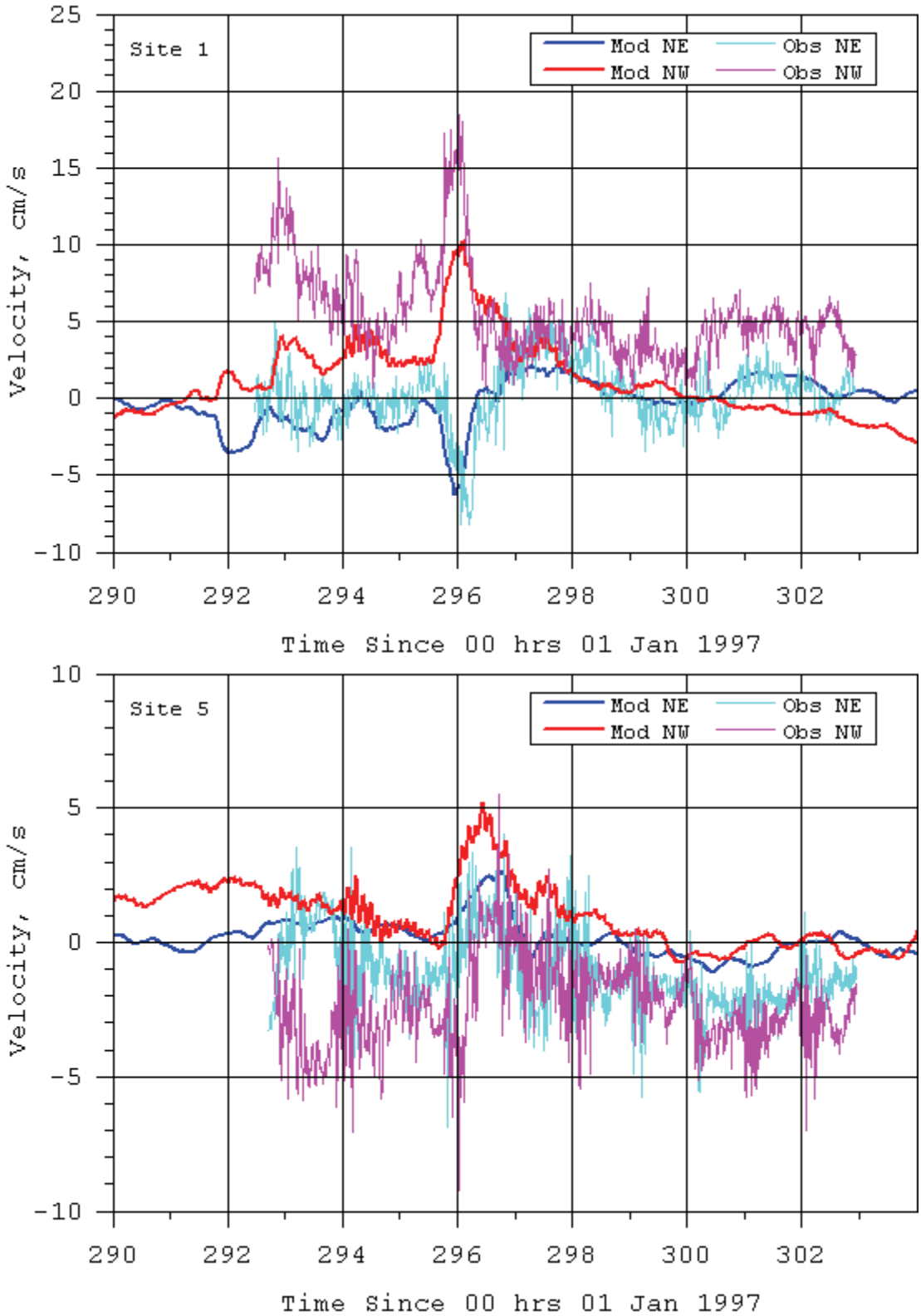

Figure 5-3. Depth average current velocity comparison at Sites 1 and 5 during late October.

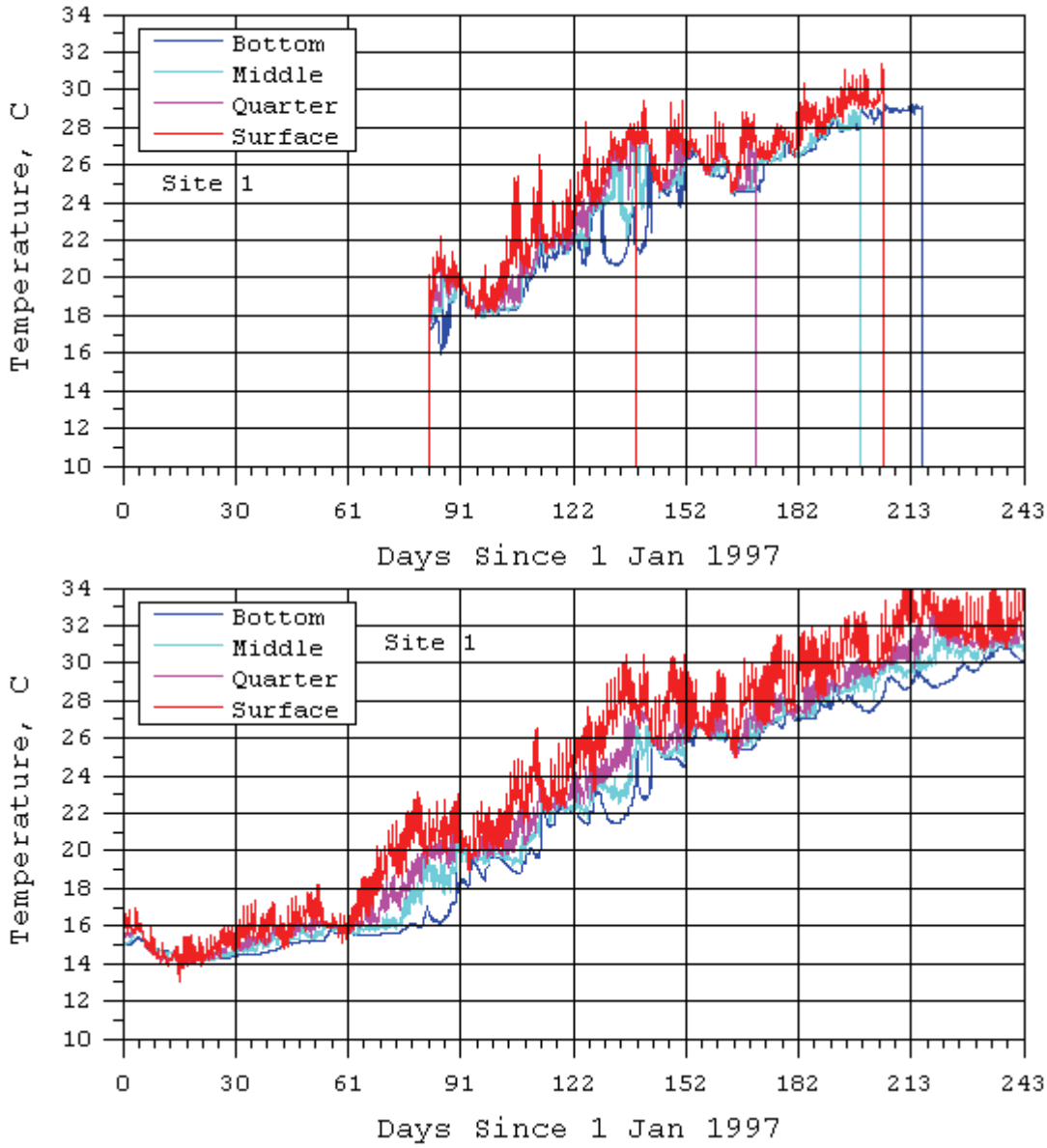

Figure 5-4. Comparison of observed temperature (top panel) with model predicted temperature for the first eight months of 1997 at Site 1.

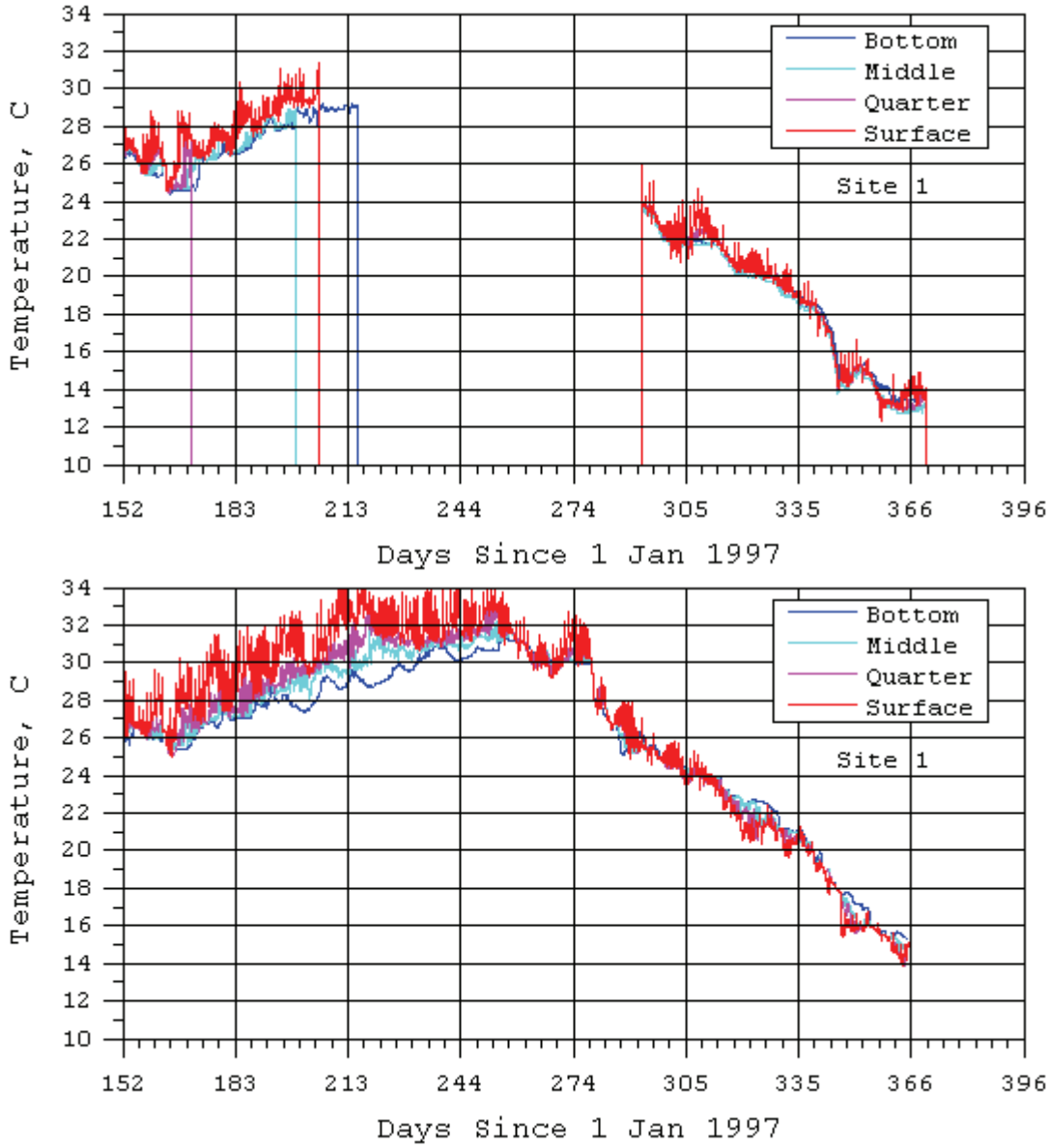

Figure 5-5. Comparison of observed temperature (top panel) with model predicted temperature for the last seven months of 1997 at Site 1.

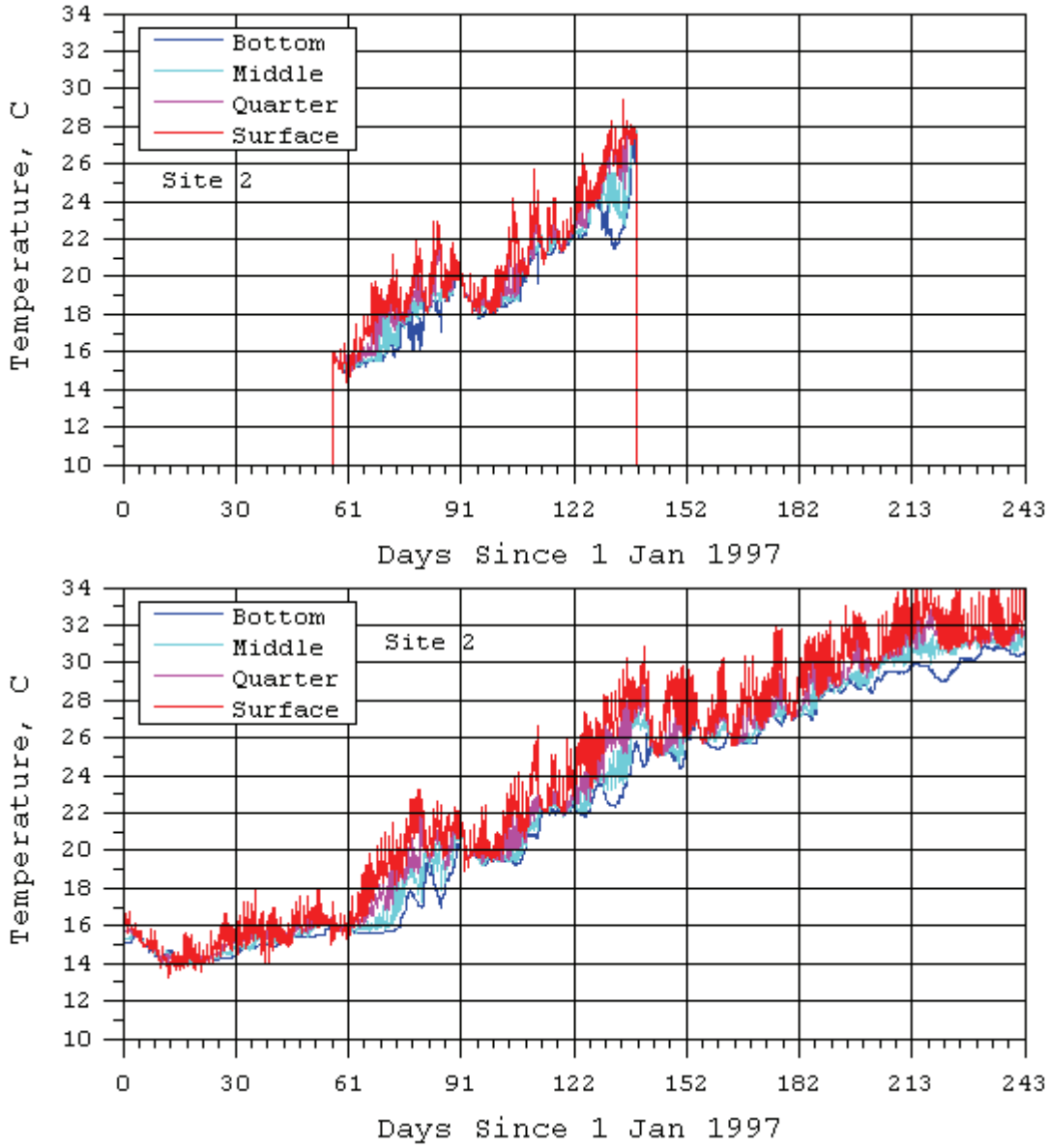

Figure 5-6. Comparison of observed temperature (top panel) with model predicted temperature for the first eight months of 1997 at Site 2.

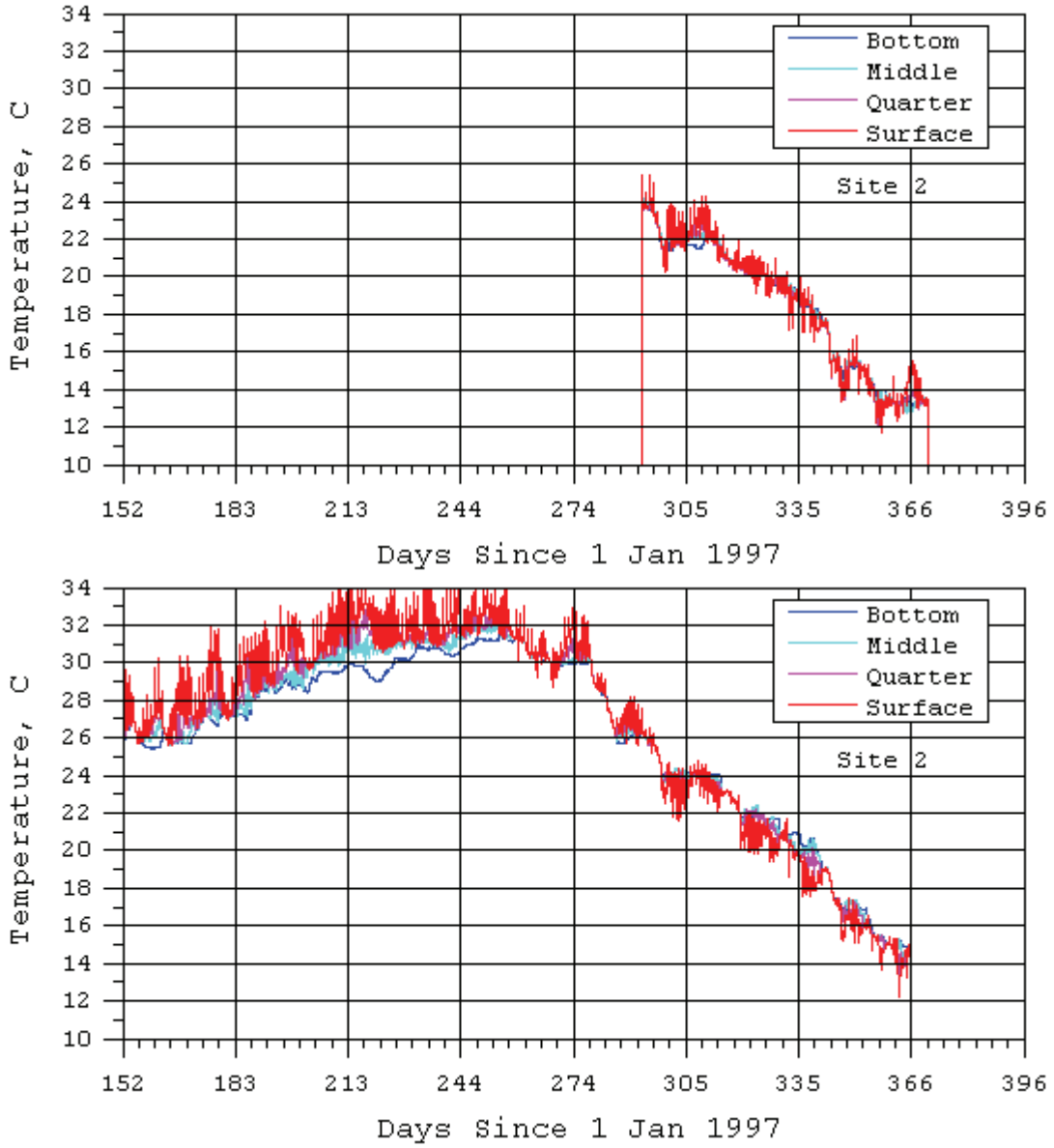

Figure 5-7. Comparison of observed temperature (top panel) with model predicted temperature for the last seven months of 1997 at Site 2.

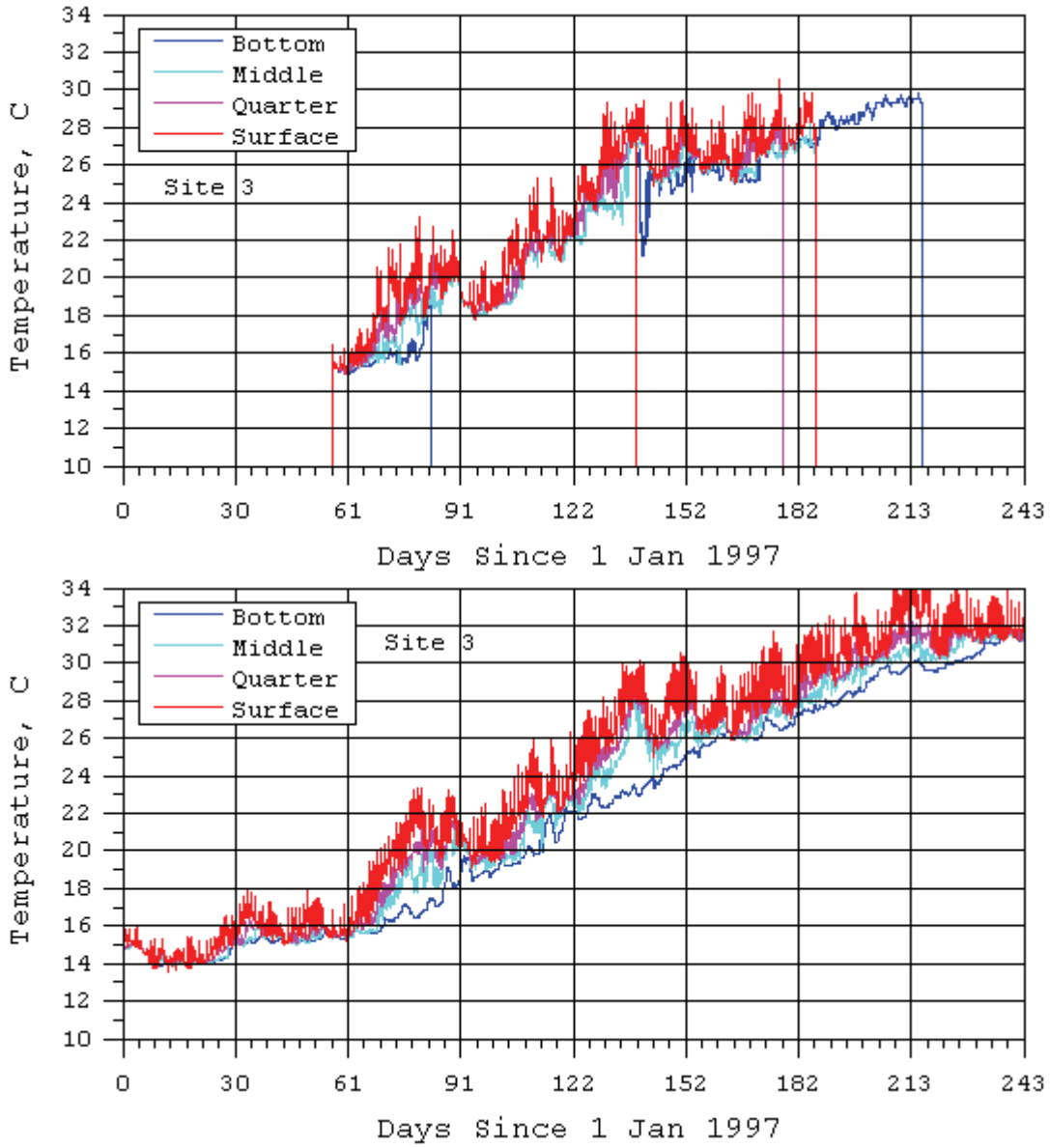

Figure 5-8. Comparison of observed temperature (top panel) with model predicted temperature for the first eight months of 1997 at Site 3.

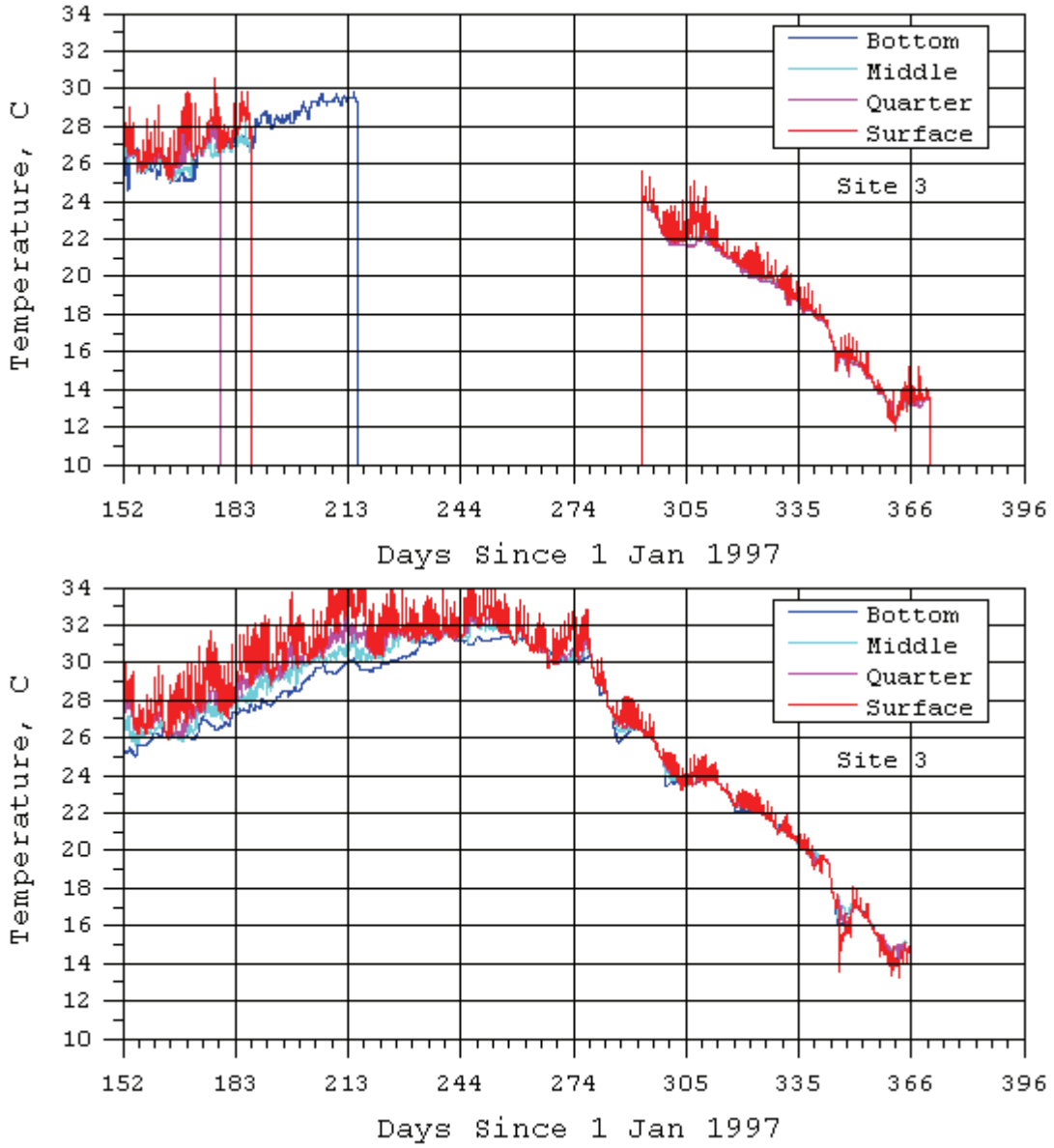

Figure 5-9. Comparison of observed temperature (top panel) with model predicted temperature for the last seven months of 1997 at Site 3.

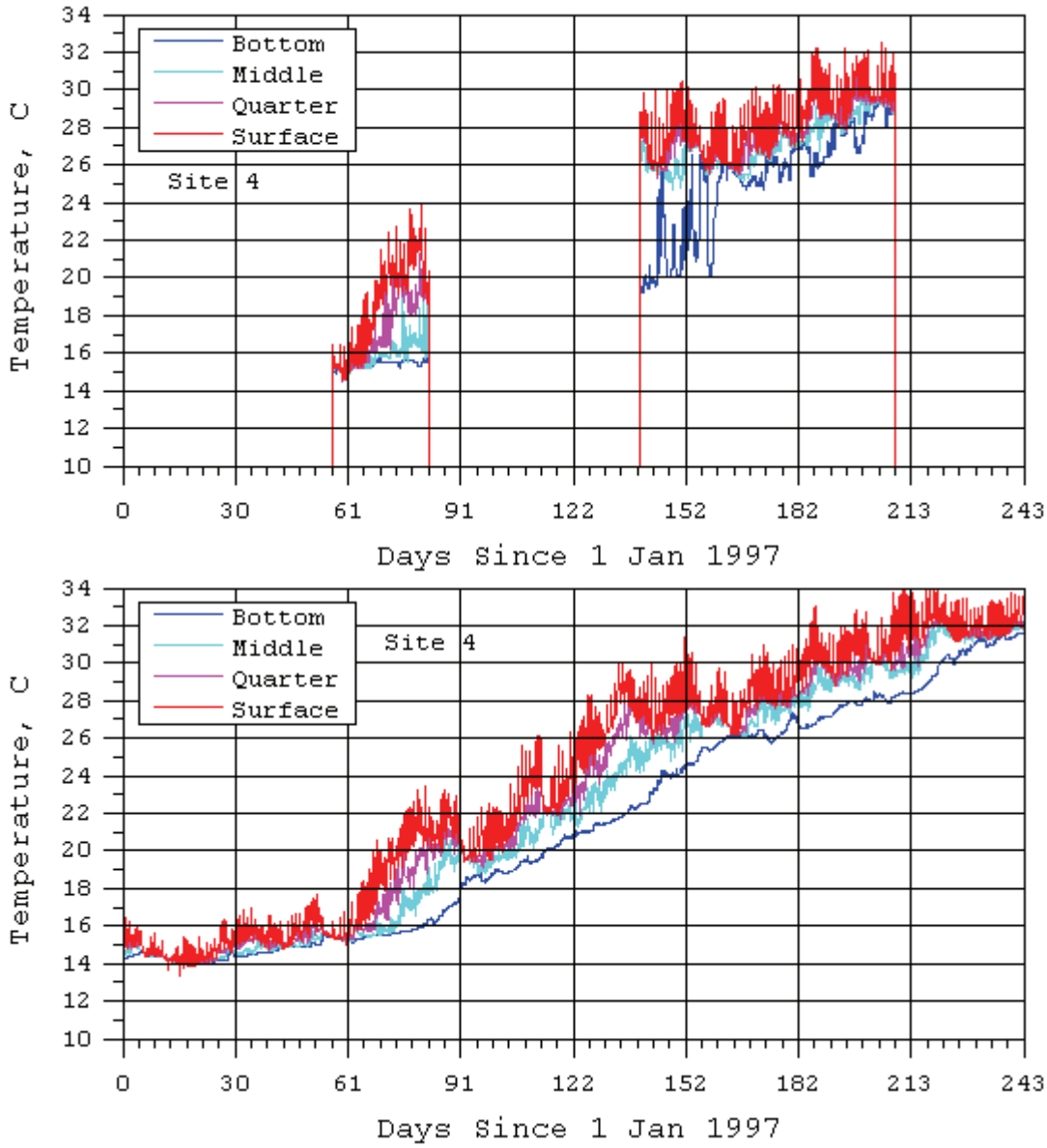

Figure 5-10. Comparison of observed temperature (top panel) with model predicted temperature for the first eight months of 1997 at Site 4.

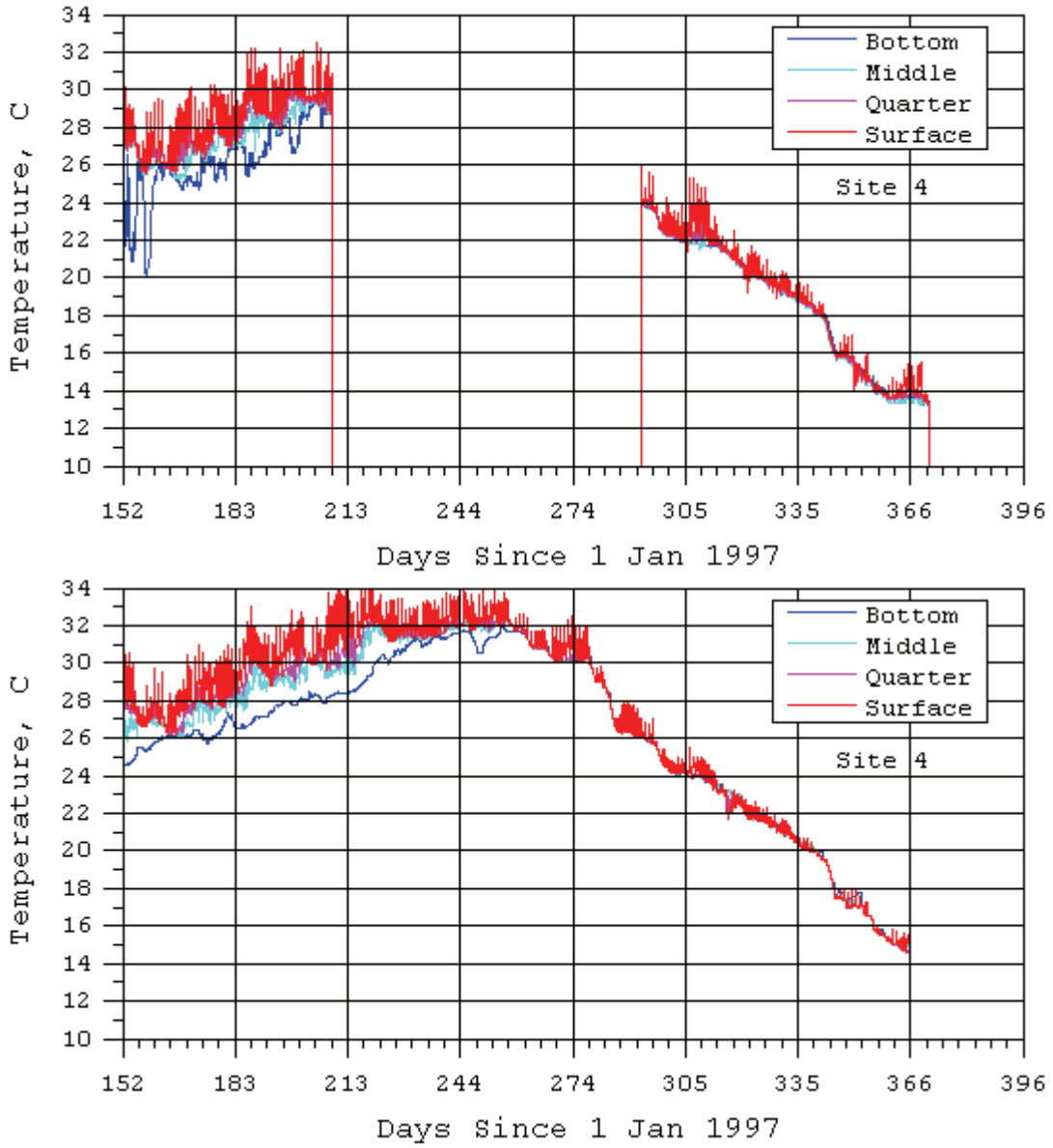

Figure 5-11. Comparison of observed temperature (top panel) with model predicted temperature for the last seven months of 1997 at Site 4.

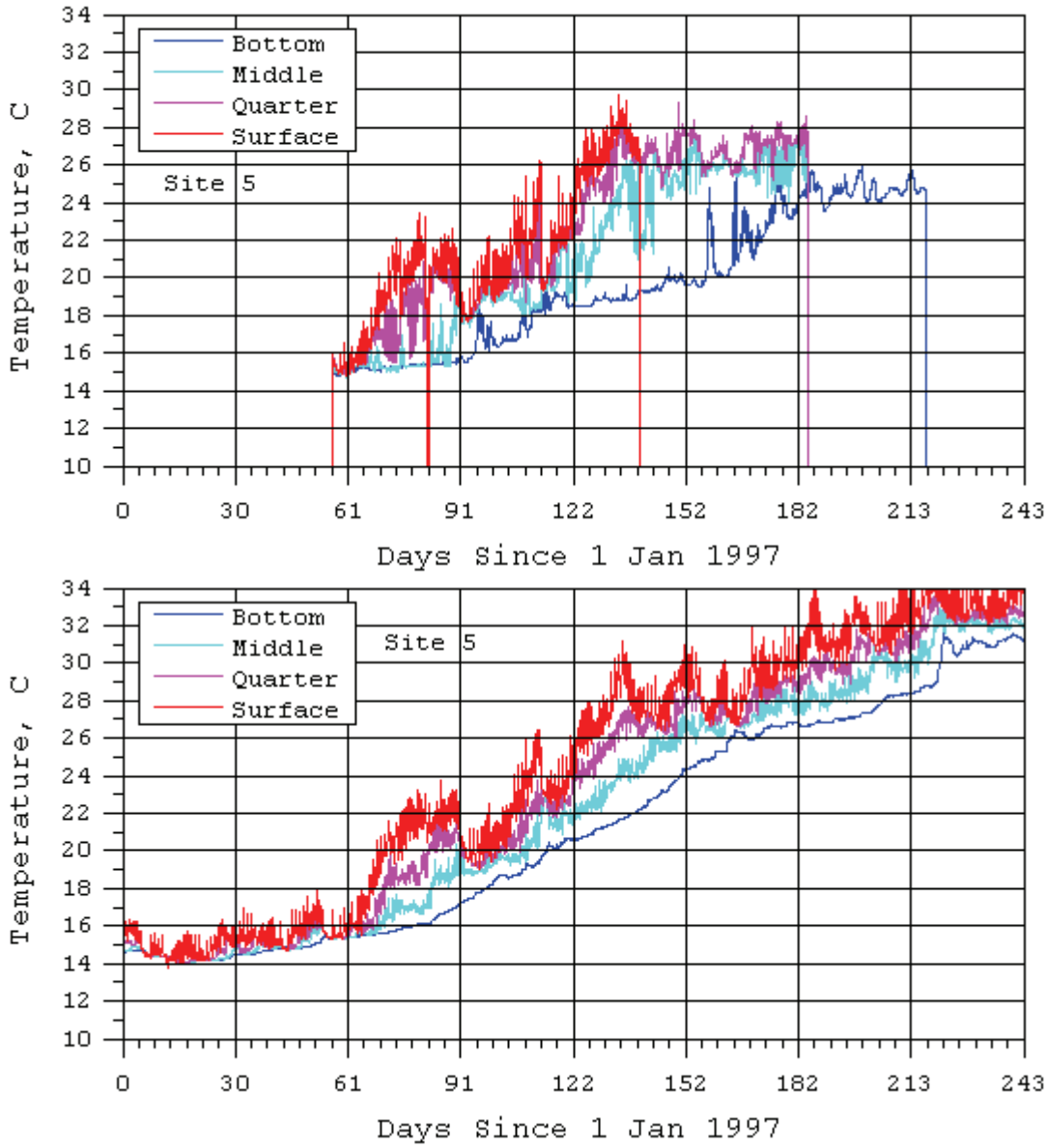

Figure 5-12. Comparison of observed temperature (top panel) with model predicted temperature for the first eight months of 1997 at Site 5.

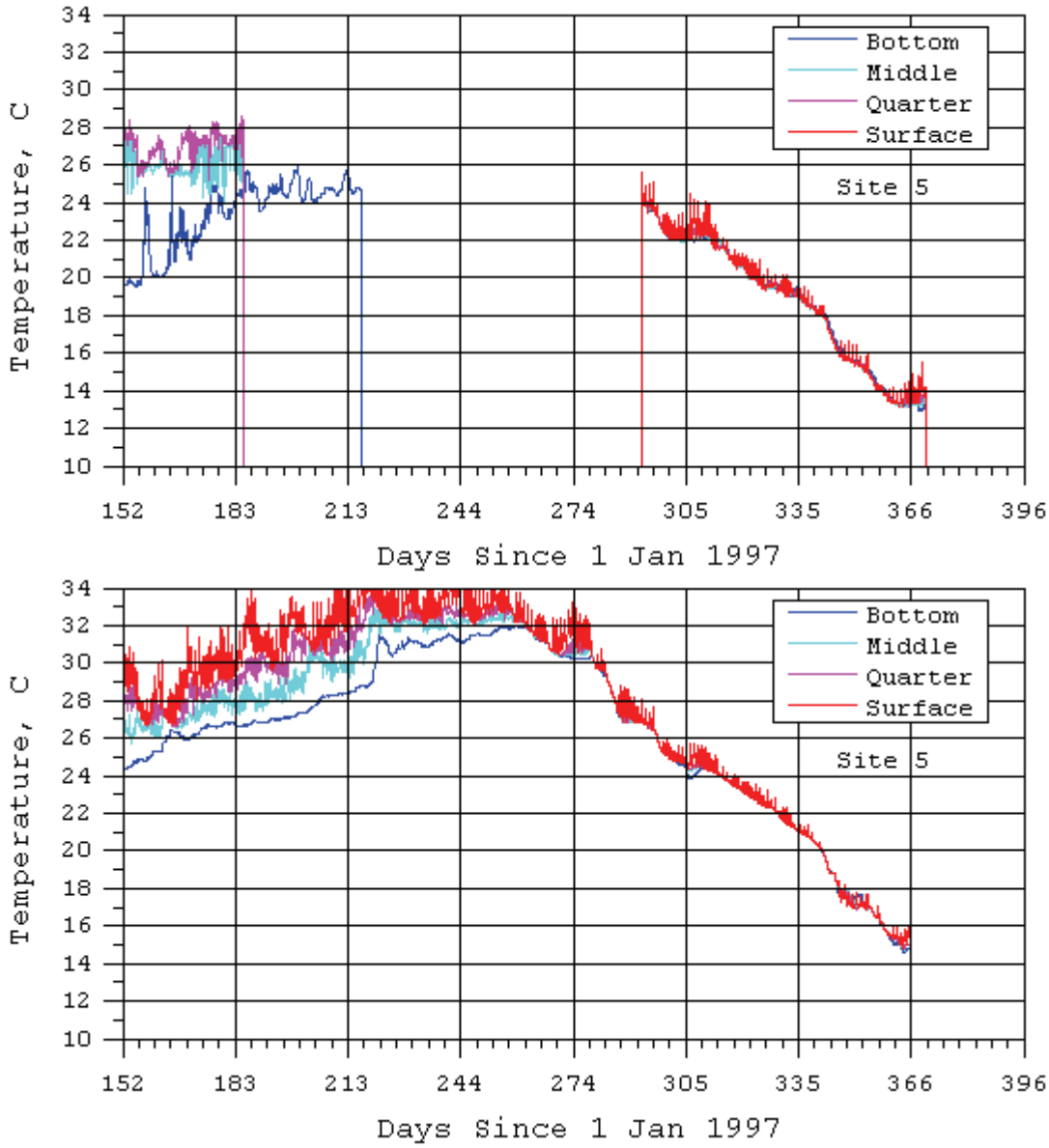

Figure 5-13. Comparison of observed temperature (top panel) with model predicted temperature for last 7 months of 1997 at Site 5.

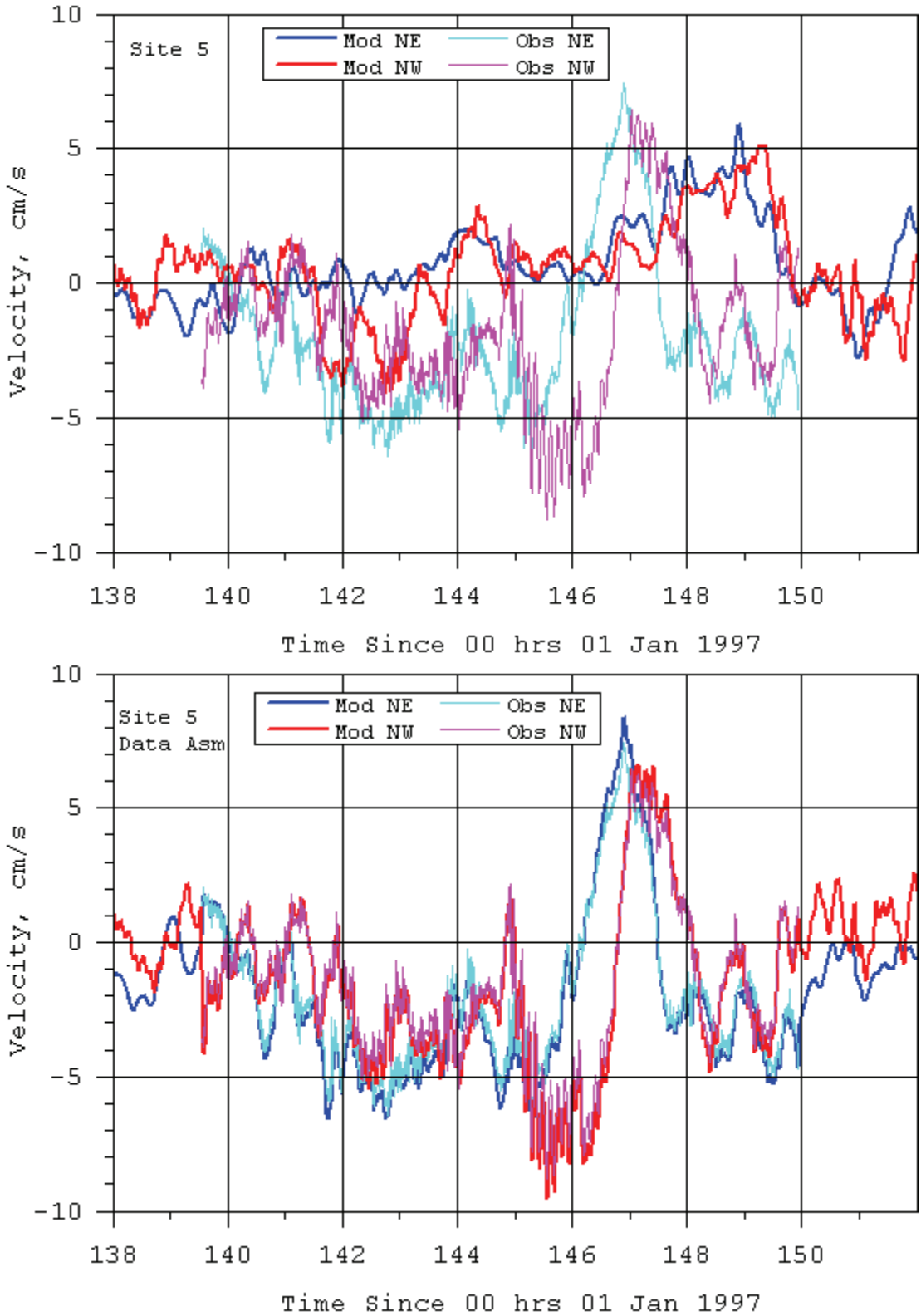

Figure 5-14. Velocity at Site 5 in late May. Top panel without data assimilation. Bottom panel with data assimilation

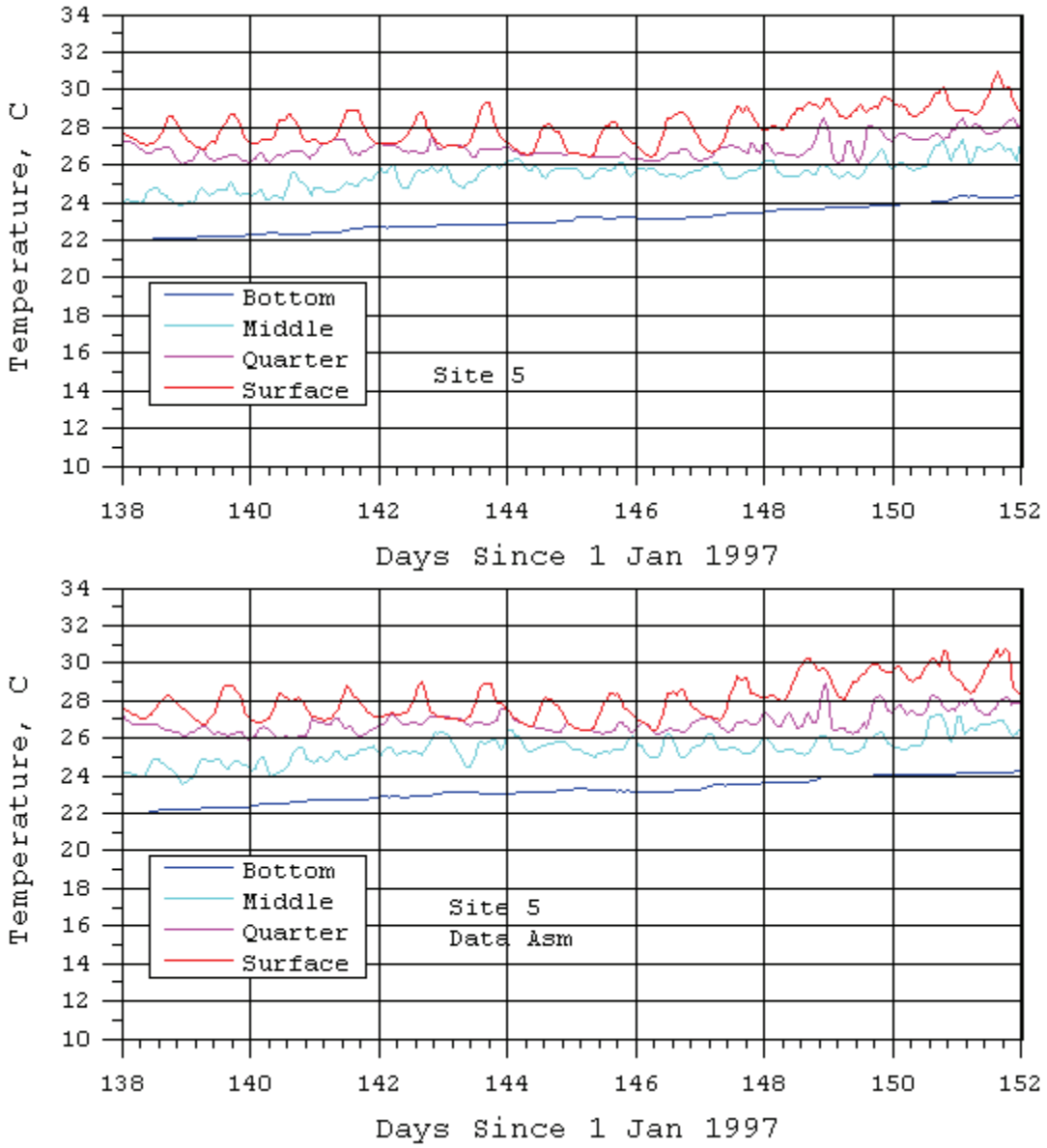

Figure 5-15. Model predicted temperature at Site 5 in late May. Top panel without velocity data assimilation. Bottom panel with velocity data assimilation

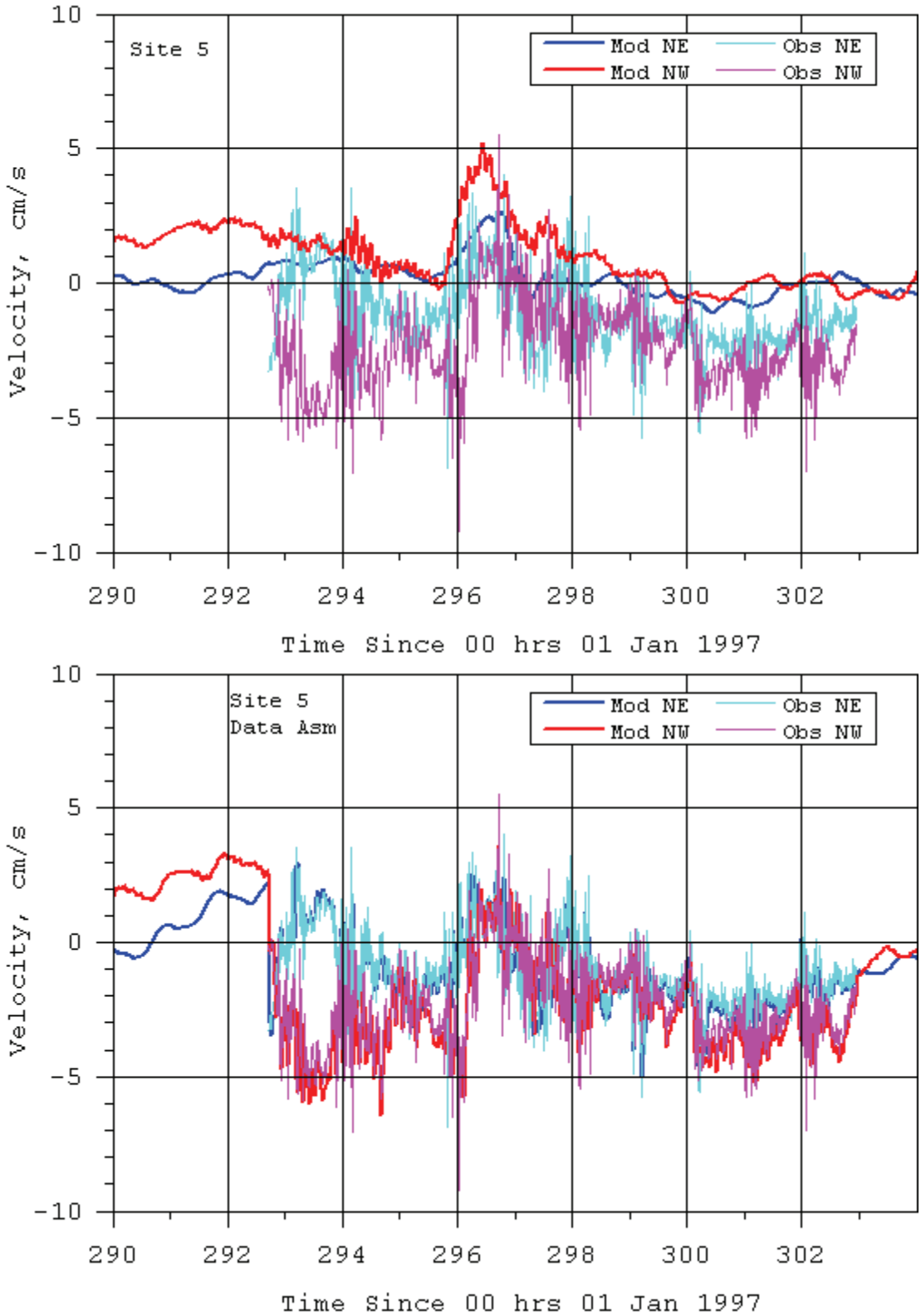

Figure 5-16. Velocity at Site 5 in late October. Top panel without data assimilation. Bottom panel with data assimilation

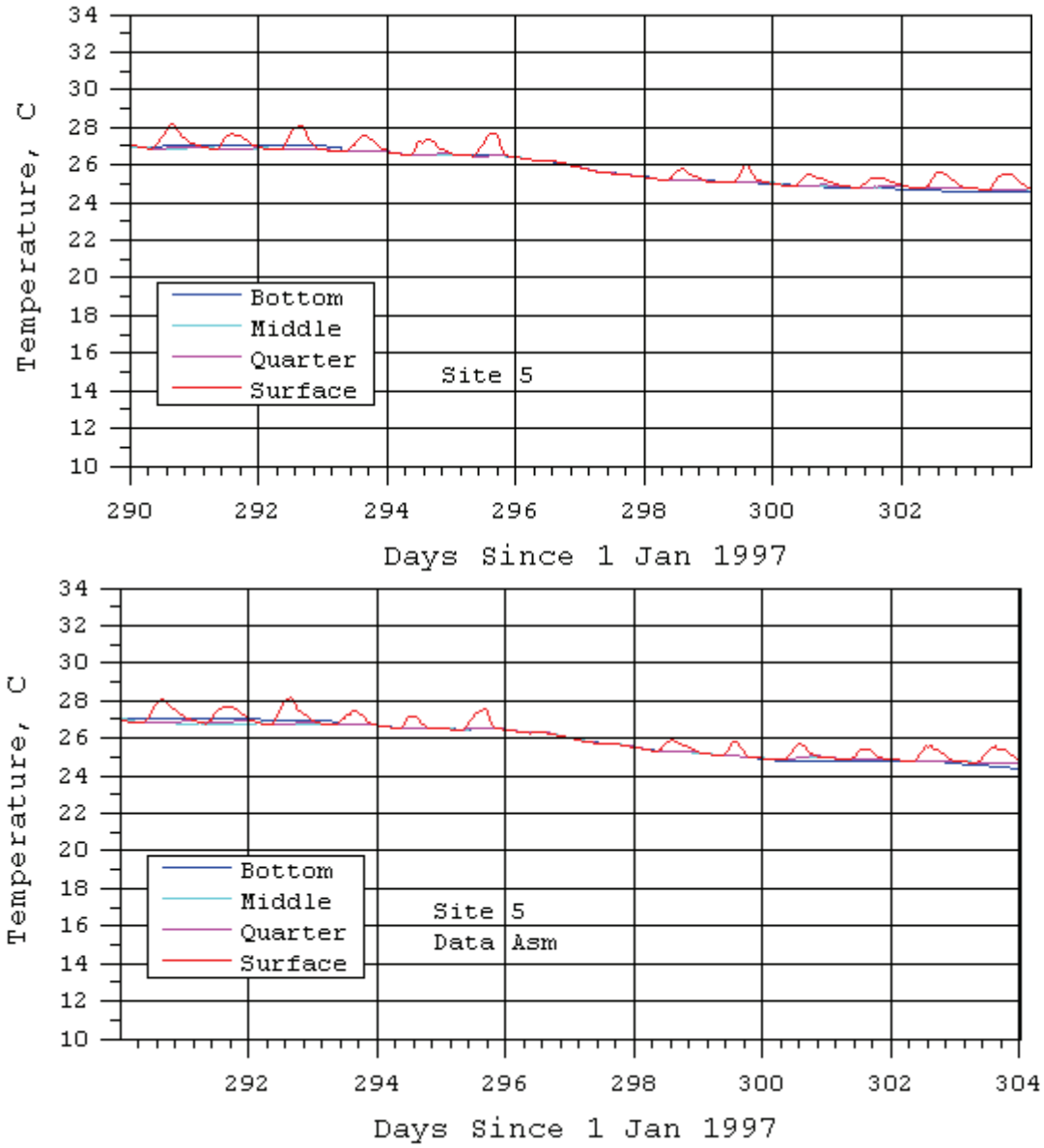

Figure 5-17. Model predicted temperature at Site 5 in late October. Top panel without velocity data assimilation. Bottom panel with velocity data assimilation

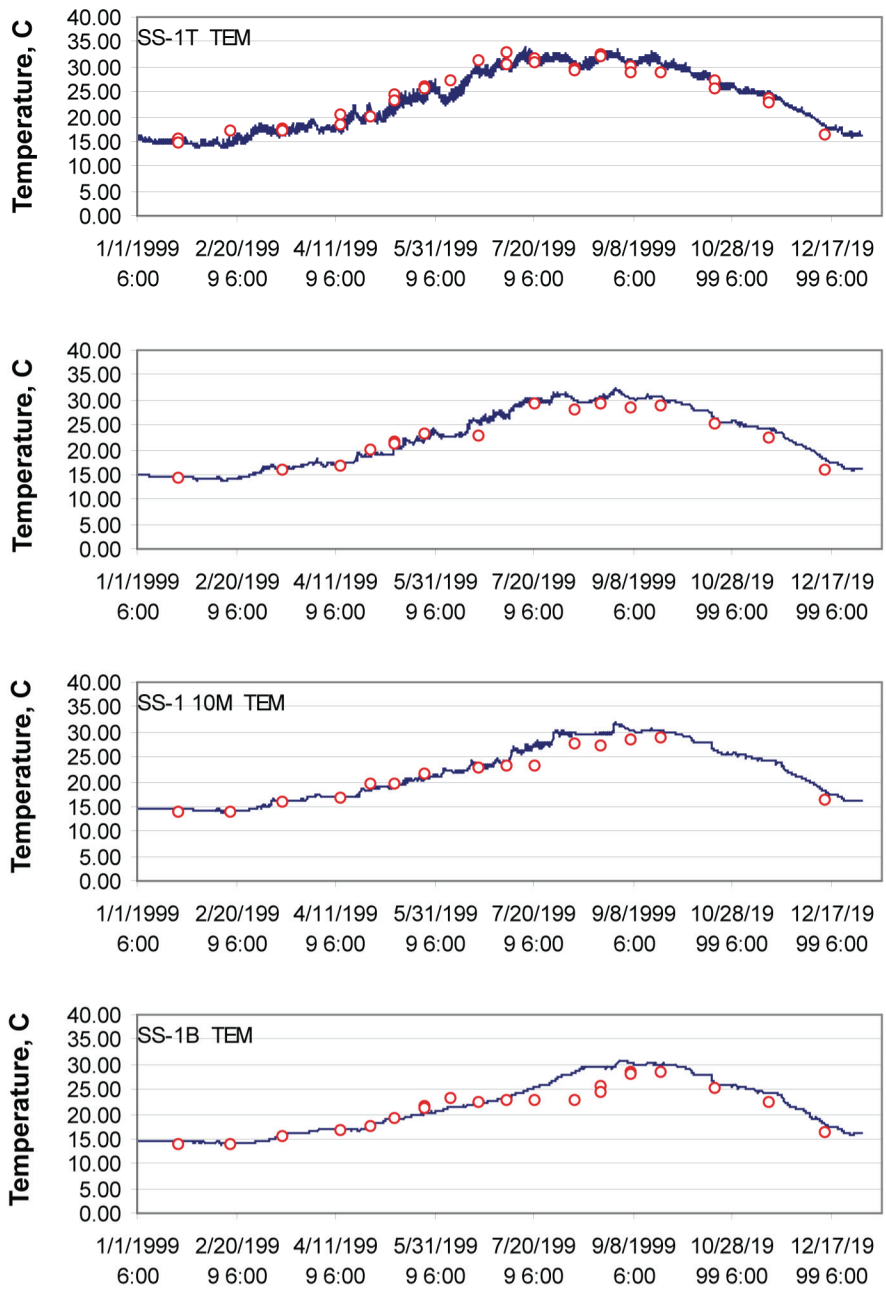

Figure 5-18. Comparison of observed temperature (circles) with model predicted temperature for 1999 at BOR Stations SS1.

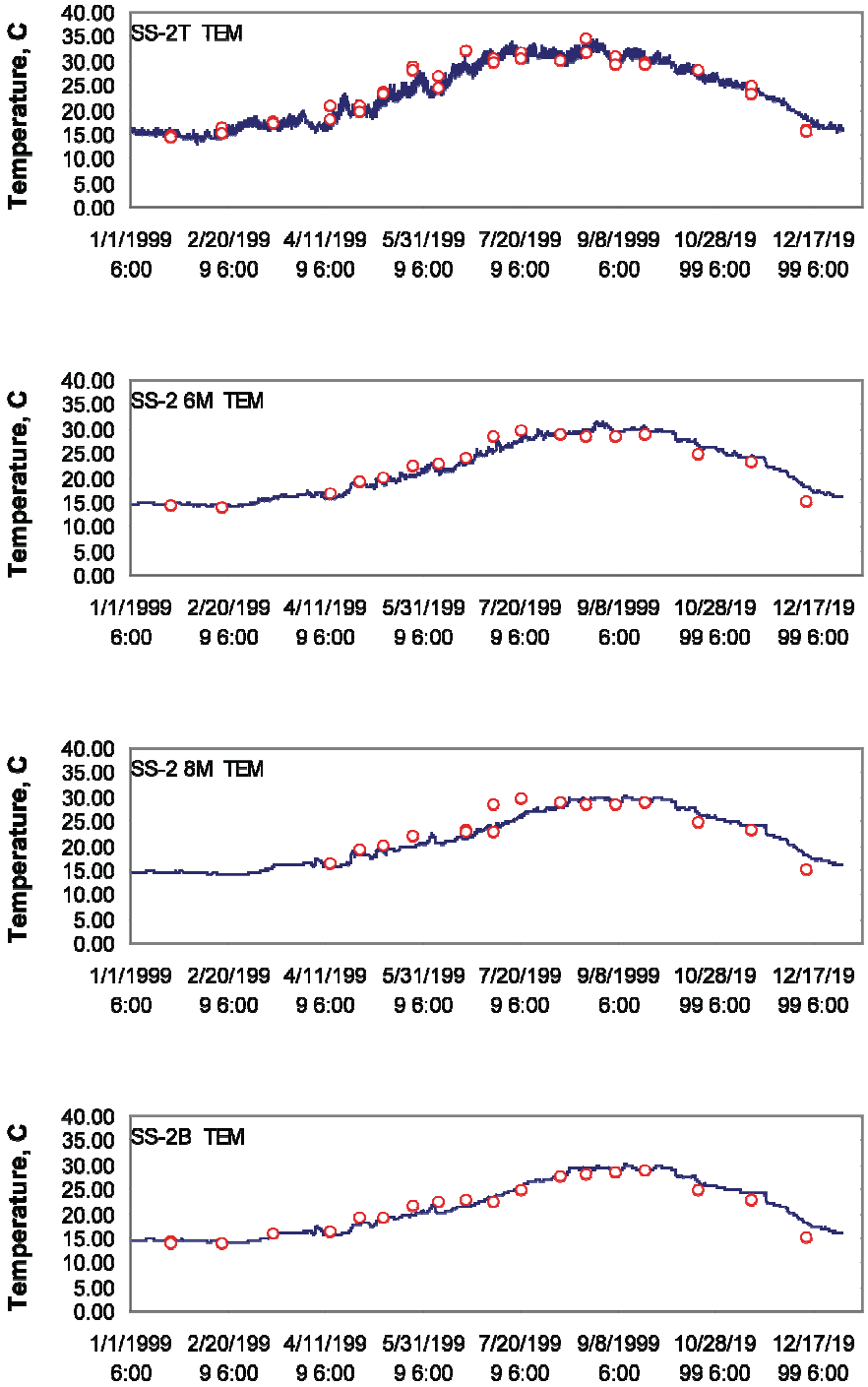

Figure 5-19. Comparison of observed temperature (circles) with model predicted temperature for 1999 at BOR Stations SS2.

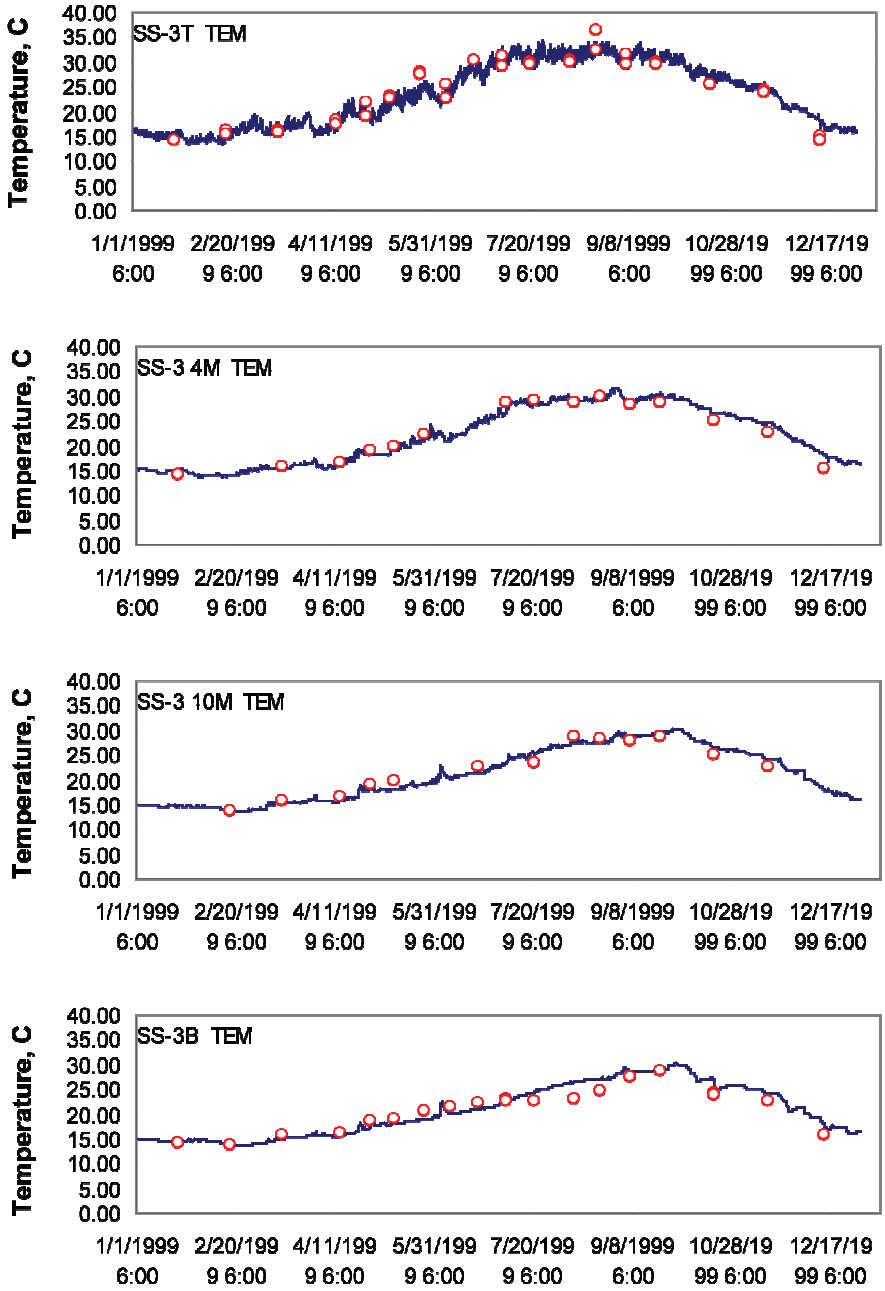

Figure 5-20. Comparison of observed temperature (circles) with model predicted temperature for 1999 at BOR Stations SS2

6. Water Quality Calibration and Validation

The calibration of the water quality component of the model is based on comparison of model predictions with 1999 observational data (Holdren and Montano, 2002a) at three stations shown in Figure 2-23. Chemical samples were taken over the water column depth at each station 18 times during the years. Observations and model predictions of dissolved oxygen (DO), dissolved organic carbon (DOC), dissolved orthophosphate (PO_4), total phosphorous (TP), ammonium (NH_4), nitrate (NO_3), and total nitrogen (TN) are compared near the water column surface and the bottom of the water column. In addition, observations and predictions of dissolved oxygen at approximately one quarter depth from the surface and mid-depth are compared. Water quality model parameters for algae, carbon, phosphorous, nitrogen, chemical oxygen demand and dissolved oxygen are summarized in Table 6-1–Table 6-3. Appropriate sections in the EFDC water quality theory manual (Tetra Tech, 2006a) providing further details of the model formula are noted for each table.

Comparisons of surface and bottom observations and model predictions for dissolved oxygen, dissolved organic carbon, and phosphorous and nitrogen state variables at Station SS-1 in the northern basin are presented in Figure 6-1 and Figure 6-2 respectively. These figure panels also include plots of chemical oxygen demand due to hydrogen sulfide although no data were available for comparison. Similar comparisons for Station SS-2 are presented in Figure 6-3 and Figure 6-4 and for SS-3 in Figure 6-5 and Figure 6-6. Comparisons of dissolved oxygen at the surface, quarter depth, mid-depth, and bottom for these three stations are shown in Figure 6-7 and Figure 6-8.

The model tends to perform quite well for dissolved oxygen prediction at all three stations. The stations show similar characteristics of highly variable but relatively high mean surface DO with the variability and mean decreasing at quarter depth. At mid-depth and near the bottom, low dissolved oxygen levels are present most of the year with conditions becoming anoxic at the bottom in late Spring and persisting until early Fall. Model predictions of dissolved organic carbon are also very good at all three stations. Both the model and observations show similar levels of DOC near the surface and bottom. Surface DOC results from particulate organic carbon decomposition, algae mortality and predation while the major source of DOC near the bottom is due to decomposition of settling particulate matter. Predictions of total phosphorous and nitrogen, at both the surface and bottom at all three station is also reasonable, although there is more relative variability of observed TP about the more slowly varying model predicted levels than for TN. The prediction of nutrient concentrations, PO_4, NH_4 and NO_3 is more variable but generally within reasonable range of the observations. It is observed that there are a number of spikes in the observed data that are not reproduced by the model. These spikes of data may represent some localized conditions, such as the patchy growth of algae. If these observations are not the result of localized conditions, the spike up of nutrient data would imply a huge increase in nutrient loading in the sea which cannot be explained in any mechanistic way.

Due to limited availability of observational data between 1997 and 2006 for years other than 1999, a formal validation of the water quality model was not undertaken. Instead, a fifteen year baseline simulation corresponding to current loading conditions was conducted. The 15 year simulation repeated 1999 hydrologic, atmospheric and nutrient loading conditions periodically. This base line simulation served two purposes. The first was to demonstrate that the water quality model calibration is robust with respect to kinetic parameterization and that the sediment flux prediction has reached a dynamic steady state. The second purpose is to

provide a comparative long-term baseline simulation of the existing sea for comparison with long-term simulations of alternate restoration alternatives including the SSA Plan.

A comparison of surface and bottom DO prediction for the calibration simulation and the last year of a 15 year base-line simulation at Station SS-1 in the north lake are shown in Figure 6-9. The annual pattern of the calibration is maintained quite well over the 15 year period. If unrealistic reaction parameters or initial conductions were used for the 15 year simulation, a significant divergence from the annual pattern would have occurred. Figure 6-11 shows the near bottom dissolved oxygen, the near bottom sulfide component of the chemical oxygen demand, and the sediment oxygen demand for the last year of the 15 year baseline simulation. The sediment oxygen demand closely follows the near bottom dissolved oxygen, with SOD being exerted only during periods when the bottom water is oxygenated. The range of model predicted sediment oxygen demand in the northern sea of 0 to 1.75 $g/m^2/day$ is consistent with the range of 0.5 to 2.5 g/m^2day estimated from laboratory analysis of field sediment cores (Reese, Anderson, and Amrhein, 2007). During periods of anoxic bottom conditions, sediment oxygen demand is not exerted and sulfide flux from the sediment significantly increases and exerts a chemical oxygen demand in the water column. This oxygen demand is tracked as the chemical oxygen demand variable (COD) in the EFDC water quality model. Figure 6-11 indicates model predicted COD ranges from approximately 7 to 14 mg/L between June and September, corresponding to sulfide concentrations of approximately 3.5 to 7 mg/L. This range is quite consistent with the range of 3.1 to 6.8 mg/L reported for 1998-99 (Watts et al., 2001) but significantly lower than peak total sulfide values in excess of 30 mg/L observed during Summer 2006 (Reese, Anderson, and Amrhein, 2007).

Table 6-1.
Water Quality Parameters Related to Algae in the Water Column
(Section 2.4.1 of water quality theory manual)

Parameter	Salton Sea Calibration	Definition
PMc (day-1)	3.2	maximum growth
PMd (day-1)	3.0	
KHNx (g N m-3)	0.01	half-saturation for N
KHPx (g P m-3)	0.001	half-saturation for P
Keb (m-1)	0.01	background light extinction
KeISS (m-1 per g m-3)	0.05	light extinction coefficient for inorganic suspended solid
KeVSS (m-1 per g m-3)	0.0	light extinction coefficient for volatile suspended solid
KeChl (m-1 / mg Chl m-3)	0.017	light extinction coefficient for algae chlorophyll
CChlx (g C / mg Chl)	0.06	algal carbon-to-chlorophyll ratio
(Dopt)x (m)	0.5	depth of maximum algal growth for algal group x
TMlowc, TMuppc (°C)	25, 35	lower and upper optimal temperature for algal group x growth
TMlowd, TMuppd (°C)	14, 23	
KTG1c , KTG2c (°C-2)	0.009, 0.006	effect of temperature below TM1x and above TMux on growth for algal group x
KTG1d , KTG2d (°C-2)	0.004, 0.007	
BMRc (day-1)	0.07	basal metabolism rate at TRx for algal group x
BMRd (day-1)	0.06	
TRx (°C)	20	reference temperature for basal metabolism for algal group x
KTBx (°C-1)	0.069	effect of temperature on metabolism for algal group x
PRRc (day-1)	0.01	reference predation rate at BxP and TRx for algal group x
PRRd (day-1)	0.25	
WSc (m day-1)	0.10	Settling velocity for algal group x
WSd (m day-1)	0.12	

Table 6-2
Parameters Related to Organic Carbon in the Water Column
(Section 2.4.2 of water quality theory manual)

Parameter	Salton Sea Calibration	Definition
FCRP	0.1	fraction of predated carbon produced as refractory POC
FCLP	0.7	fraction of predated carbon produced as labile POC
FCDP	0.2	fraction of predated carbon produced as DOC
FCD	0.0	fraction of basal metabolism exuded as DOC at infinite dissolved oxygen concentration for algal group
KHRx (g O2 m-3)	0.5	half-saturation constant of dissolved oxygen for algal dissolved organic carbon excretion for group x
WSRP (m day-1)	0.3	settling velocity of refractory particulate organic matter
WSLP (m day-1)	0.3	settling velocity of labile particulate organic matter
KHORDO (g O2 m-3)	2.0	oxic respiration half-saturation constant for dissolved oxygen
KRC (day-1)	0.005	dissolution rate of refractory particulate organic carbon
KLC (day-1)	0.05	dissolution rate of labile particulate organic carbon
KDC (day-1)	0.08	heterotrophic respiration rate of dissolved organic carbon at infinite dissolved oxygen concentration
KRCalg (day-1/ g C m-3) KLCalg (day-1/ g C m-3) KDCalg (day-1/ g C m-3)	0.001	constants that relate dissolution of refractory and labile particulate organic carbon, respectively, to algal biomass
TRHDR (°C)	20	reference temperature for hydrolysis of particulate organic matter
TRMNL (°C)	20	reference temperature for hydrolysis of particulate organic matter
KTHDR (°C-1)	0.069	effect of temperature on hydrolysis of particulate organic matter
KTMNL (°C-1)	0.069	reference temperature for mineralization of dissolved organic matter
KHDNN (g N m-3)	0.1	denitrification half-saturation constant for nitrate

Table 6-3.
Parameters Related to Phosphorus in the Water Column
(Section 2.4.3 of water quality theory manual)

Parameter	Salton Sea Calibration	Definition
FPRP	0.05	fraction of predated phosphorus produced as refractory POP
FPLP	0.10	fraction of predated phosphorus produced as labile POP
FPDP	0.70	fraction of predated phosphorus produced as DOP
FPIP	0.15	fraction of predated phosphorus produced as inorganic phosphorus
FPRx	0.0	fraction of metabolized phosphorus by algal group x produced as refractory POP
FPLx	0.0	fraction of metabolized phosphorus by algal group x produced as labile POP
FPDx	0.8	fraction of metabolized phosphorus by algal group x produced as DOP
FPIx	0.2	fraction of metabolized phosphorus by algal group x produced as inorganic phosphorus
APCx (g P per g C)	0.0025	algal phosphorus-to-carbon ratio for algal group x
WSs(m/day)	0.5	inorganic sediment settling velocity
KPO4p(m3/g) for TSS	0.01	Partition coefficient for PO4
CPprm1(g C per g P)	400	minimum carbon-to-phosphorus ratio
CPprm2(g C per g P)	0	difference between minimum and maximum carbon-to-phosphorus ratio
CPprm3 (per g P m-3)	0	effect of dissolved phosphate concentration on carbon-to-phosphorus ratio
KRP(day-1)	0.001	hydrolysis rate of refractory POP
KLP(day-1)	0.05	hydrolysis rate of labile POP
KDP(day-1)	0.05	mineralization rate of dissolved organic phosphorus
KRPalg(day-1 per g C m-3)	0.0005	constants that relate hydrolysis of refractory POP to algal biomass
KLPalg(day-1 per g C m-3)	0.001	constants that relate hydrolysis of labile POP to algal biomass
KDPalg(day-1 per g C m-3)	0.001	constant that relates mineralization to algal biomass

Table 6-4.
Parameters Related to Nitrogen in the Water Column
(Section 2.4.4 of water quality theory manual)

Parameter	Salton Sea Calibration	Definition
FNRP	0.20	fraction of predated nitrogen produced as refractory PON
FNLP	0.30	fraction of predated nitrogen produced as labile PON
FNDP	0.25	fraction of predated nitrogen produced as DON
FNIP	0.25	fraction of predated nitrogen produced as inorganic nitrogen
FNRx	0.0	fraction metabolized nitrogen by algal group x as refractory PON
FNLx	0.0	fraction metabolized nitrogen by algal group x as labile PON
FNDx	0.7	fraction of metabolized nitrogen by algal group x produced as DON
FNIx	0.3	fraction of metabolized N by algal group x produced as inorganic N
ANCx (g N per g C)	0.14	nitrogen-to-carbon ratio in algal group x
ANDC (g N per g C)	0.933	mass of nitrate nitrogen reduced per mass of DOC oxidized
KRN (day-1)	0.001	hydrolysis rate of refractory PON
KLN (day-1)	0.05	hydrolysis rate of labile PON
KDN (day-1)	0.07	mineralization rate of DON
KRNalg (day-1 /g C m-3)	0.001	constants that relate hydrolysis of refractory PON to algal biomass
KLNalg (day-1 /g C m-3)	0.001	constants that relate hydrolysis of labile PON to algal biomass
KDNalg (day-1 /g C m-3)	0.001	constant that relates mineralization to algal biomass
Nitm (g N m-3 day-1)	0.04	maximum nitrification rate
KHNitDO (g O2 m-3)	0.5	nitrification half-saturation constant for dissolved oxygen
KHNitN (g N m-3)	0.1	nitrification half-saturation constant for ammonium
TNit1 (°C) TNit2 (°C)	35	lower and upper optimum temperature for nitrification
KNit1 (°C-2) KNit2 (°C-2)	0.012	effect of temperature below /above TNit on nitrification rate

Table 6-5
Parameters Related to Chemical Oxygen Demand and Dissolved Oxygen in the Water Column (Sections 2.4.6 and 2.4.7 of water quality theory manual)

Parameter	Salton Sea Calibration	Definition
KHCOD (g O2 m-3)	2.0	half-saturation constant of dissolved oxygen required for oxidation of chemical oxygen demand
KCD (day-1)	1.0	oxidation rate of chemical oxygen demand
TRCOD (°C)	20	reference temperature for oxidation of chemical oxygen demand
KTCOD (°C-1)	0.03	effect of temperature on oxidation of chemical oxygen demand
AOCR (g O2 per g C)	2.67	dissolved oxygen-to-carbon ratio in respiration
AONT (g O2 per g N)	4.33	mass of dissolved oxygen consumed per unit mass of ammonium nitrogen nitrified
Kro (in MKS unit)	0.20	proportionality constant
KTr	1.024	constant for temperature adjustment of dissolved oxygen reaeration rate

a)

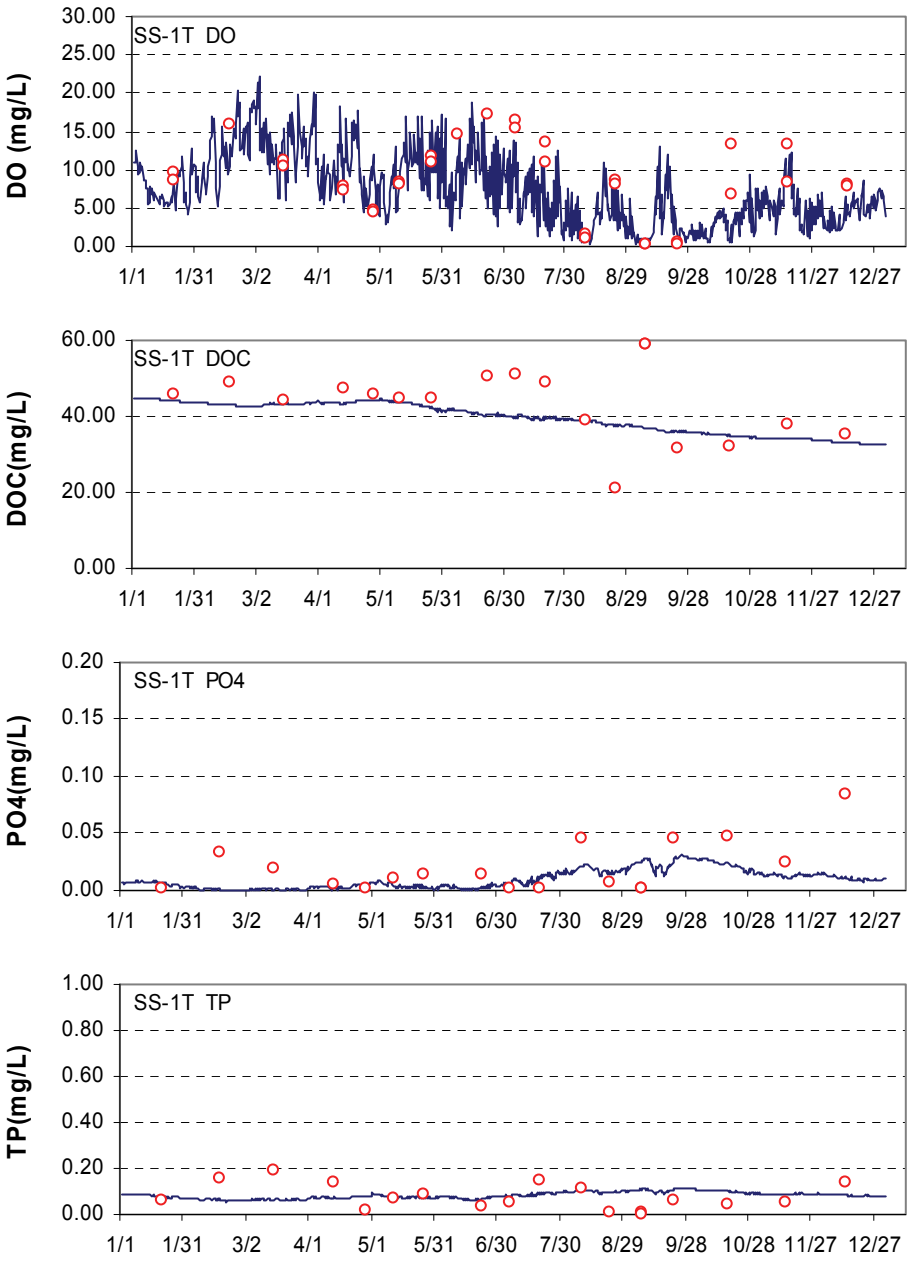
SS-1T DO
DO (mg/L)
30.00
25.00
20.00
15.00
10.00
5.00
0.00
SS-1T DOC
DOC(mg/L)
60.00
40.00
20.00
0.00
SS-1T PO4
PO4(mg/L)
0.20
0.15
0.10
0.05
0.00
SS-1T TP
TP(mg/L)
1.00
0.80
0.60
0.40
0.20
0.00
1/1 1/31 3/2 4/1 5/1 5/31 6/30 7/30 8/29 9/28 10/28 11/27 12/27

b)

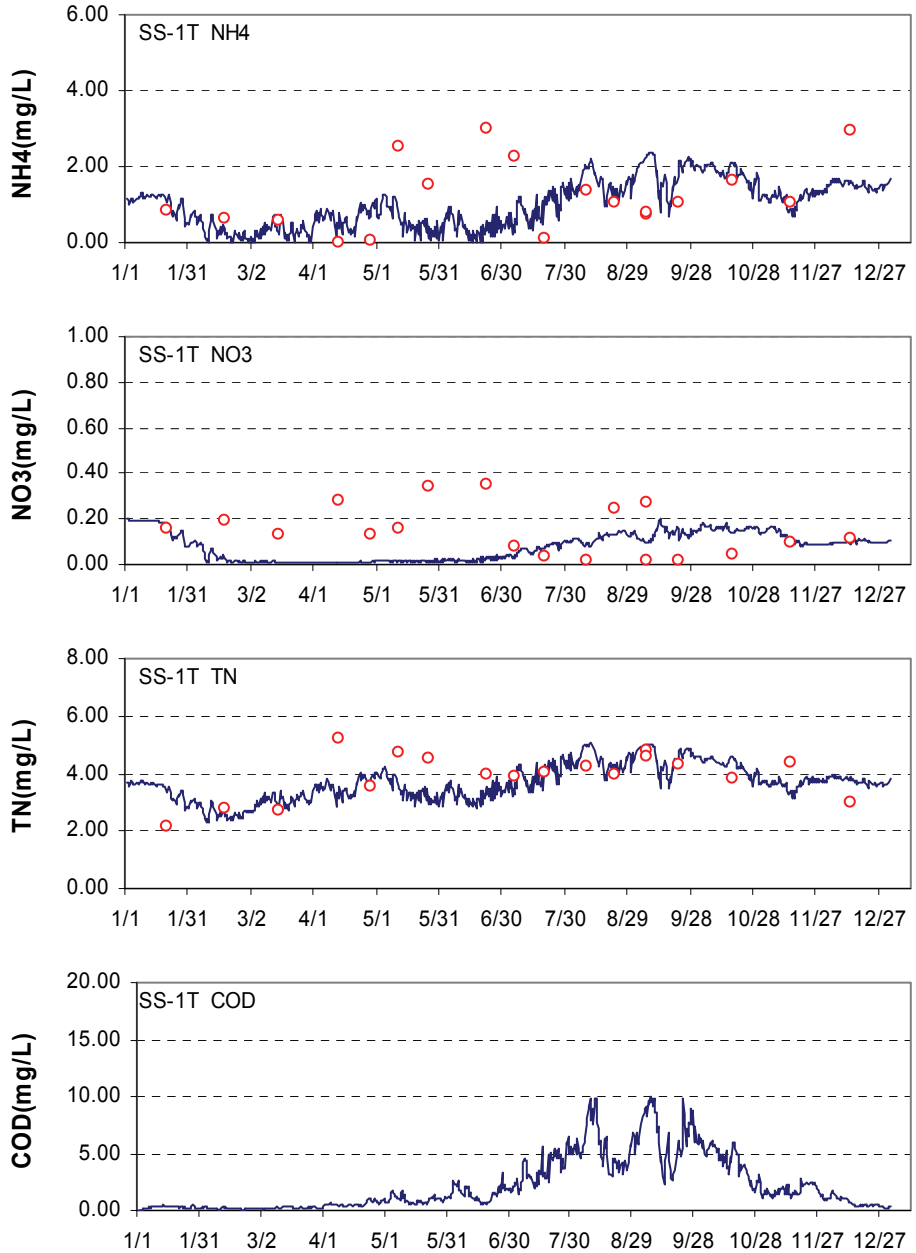

Figure 6-1. Comparison of observed and predicted water quality constituent concentrations near the water surface at USBOR Site SS-1 during 1999 ("T" in the station label refers to the top of the water column).

a)

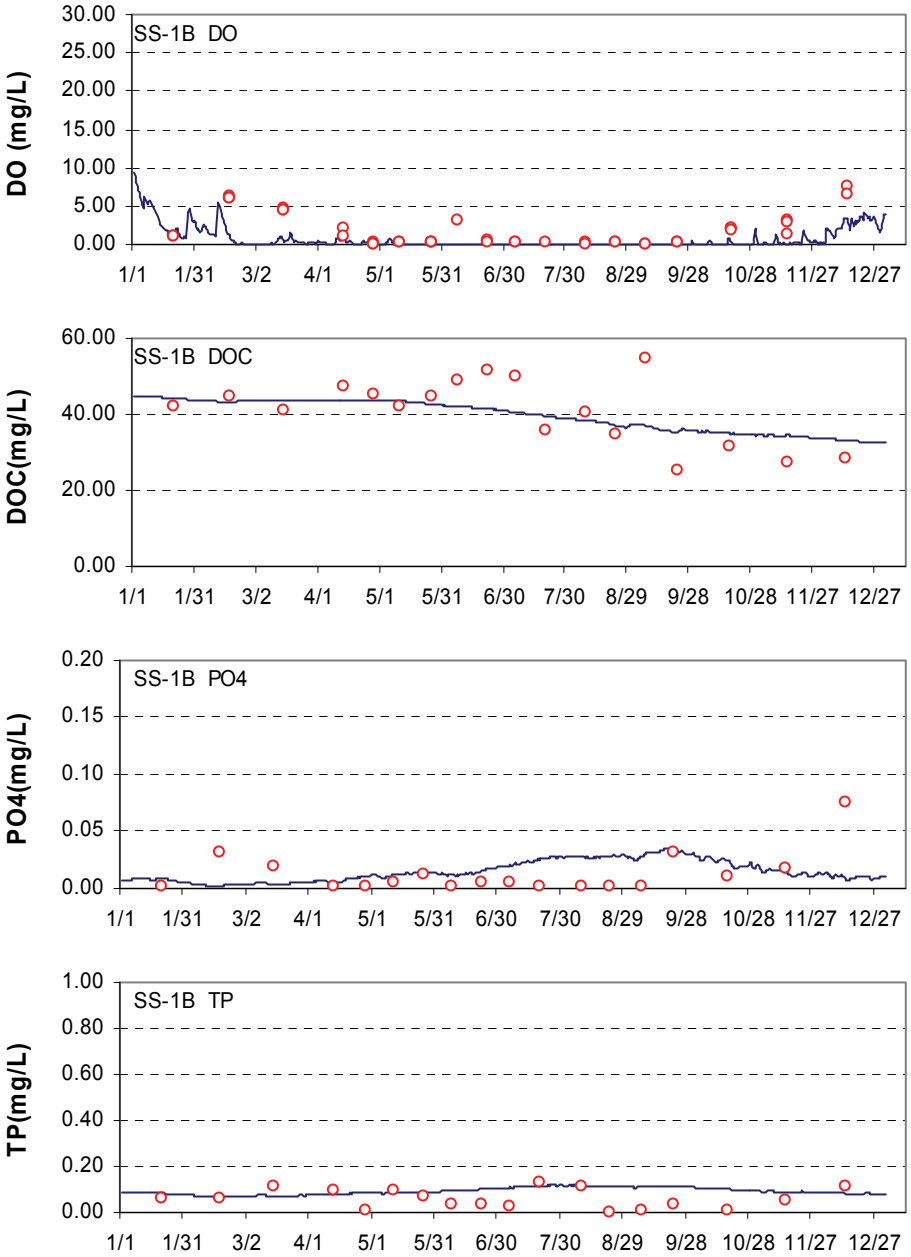
SS-1B DO
DO (mg/L)
30.00
25.00
20.00
15.00
10.00
5.00
0.00
SS-1B DOC
DOC(mg/L)
60.00
40.00
20.00
0.00
SS-1B PO4
PO4(mg/L)
0.20
0.15
0.10
0.05
0.00
SS-1B TP
TP(mg/L)
1.00
0.80
0.60
0.40
0.20
0.00
1/1 1/31 3/2 4/1 5/1 5/31 6/30 7/30 8/29 9/28 10/28 11/27 12/27

b)

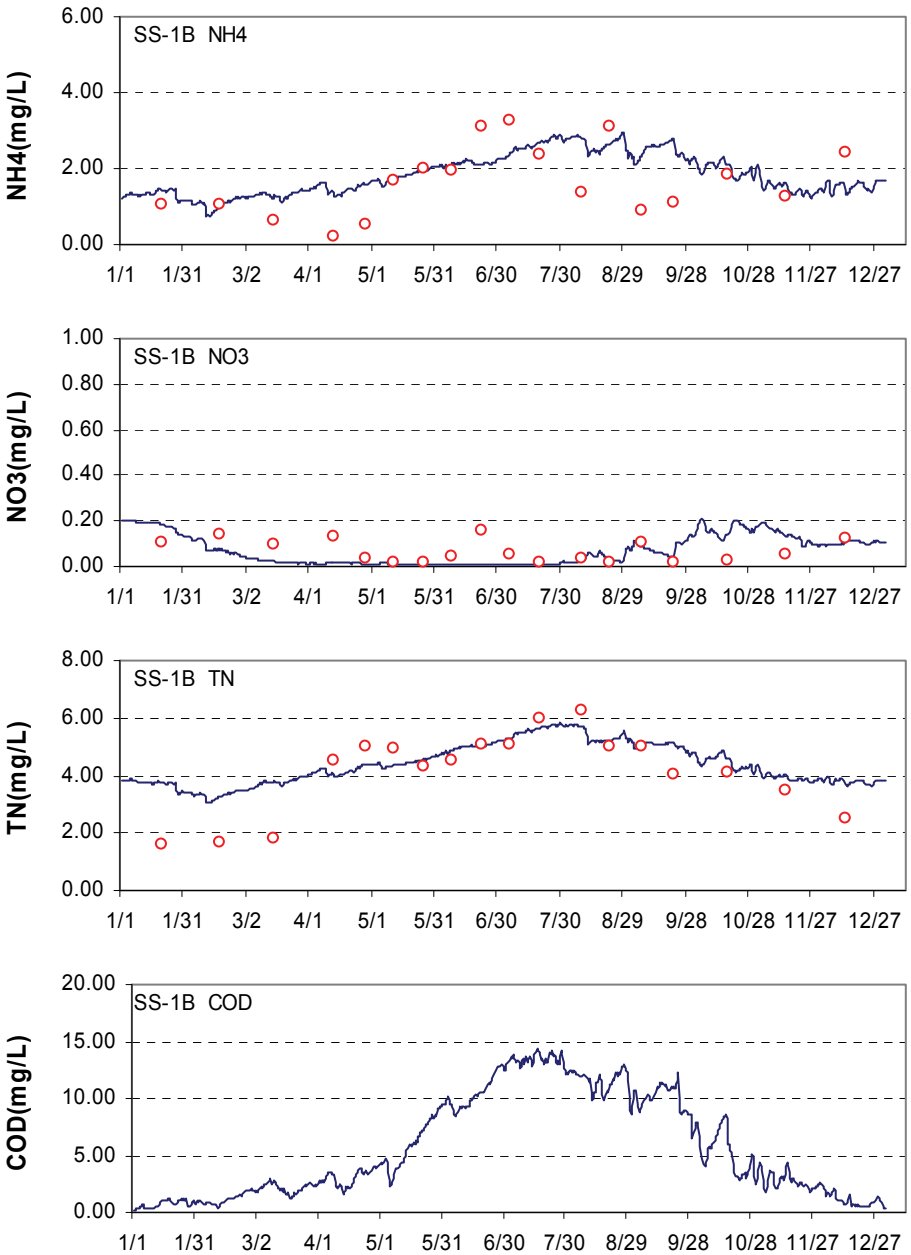

Figure 6-2. Comparison of observed and predicted water quality constituent concentrations near the water column bottom at USBOR Site SS-1 during 1999. ("B" in the station label refers to the bottom of the water column)

a)

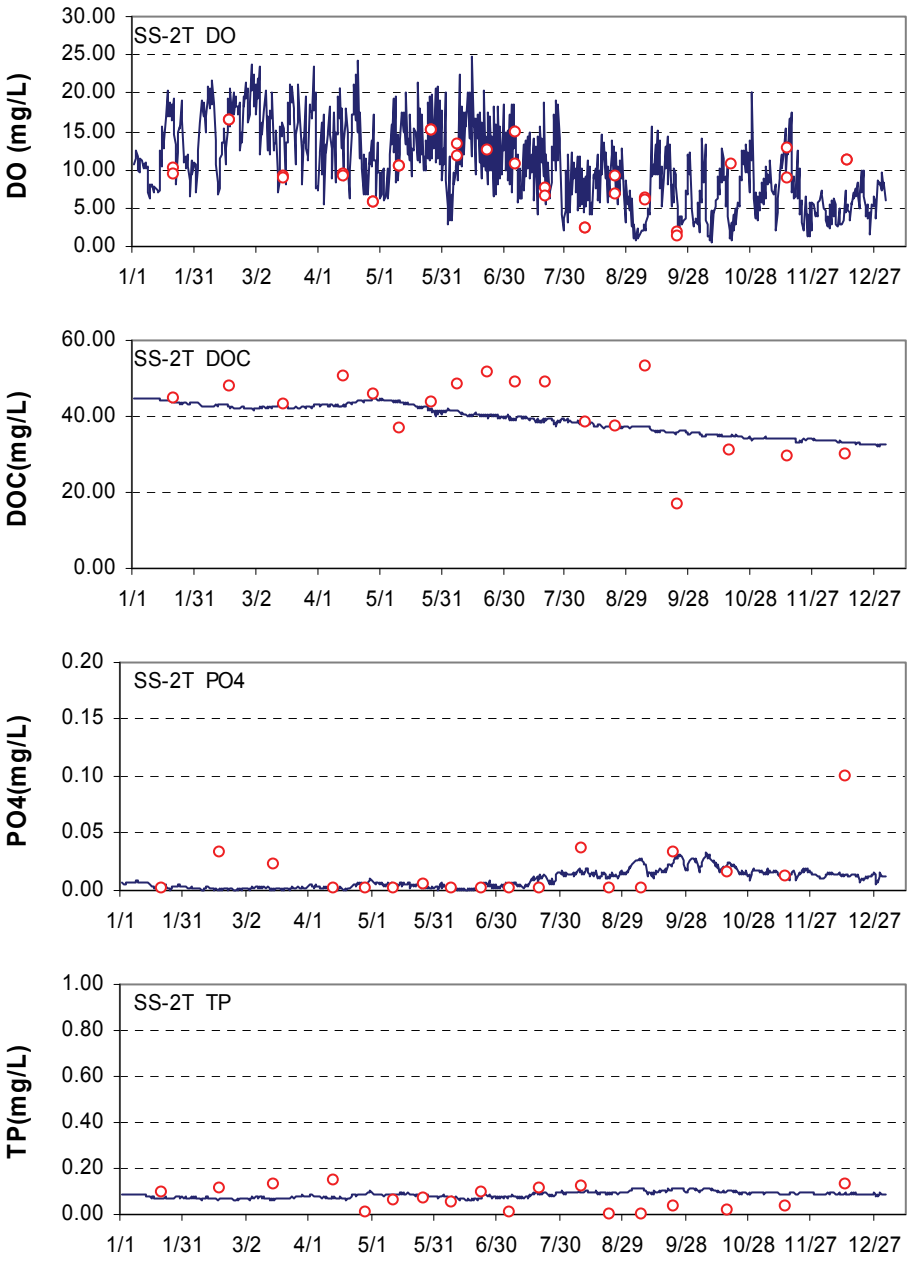
SS-2T DO
DO (mg/L)
30.00
25.00
20.00
15.00
10.00
5.00
0.00
1/1 1/31 3/2 4/1 5/1 5/31 6/30 7/30 8/29 9/28 10/28 11/27 12/27
SS-2T DOC
DOC(mg/L)
60.00
40.00
20.00
0.00
1/1 1/31 3/2 4/1 5/1 5/31 6/30 7/30 8/29 9/28 10/28 11/27 12/27
SS-2T PO4
PO4(mg/L)
0.20
0.15
0.10
0.05
0.00
1/1 1/31 3/2 4/1 5/1 5/31 6/30 7/30 8/29 9/28 10/28 11/27 12/27
SS-2T TP
TP(mg/L)
1.00
0.80
0.60
0.40
0.20
0.00
1/1 1/31 3/2 4/1 5/1 5/31 6/30 7/30 8/29 9/28 10/28 11/27 12/27

b)

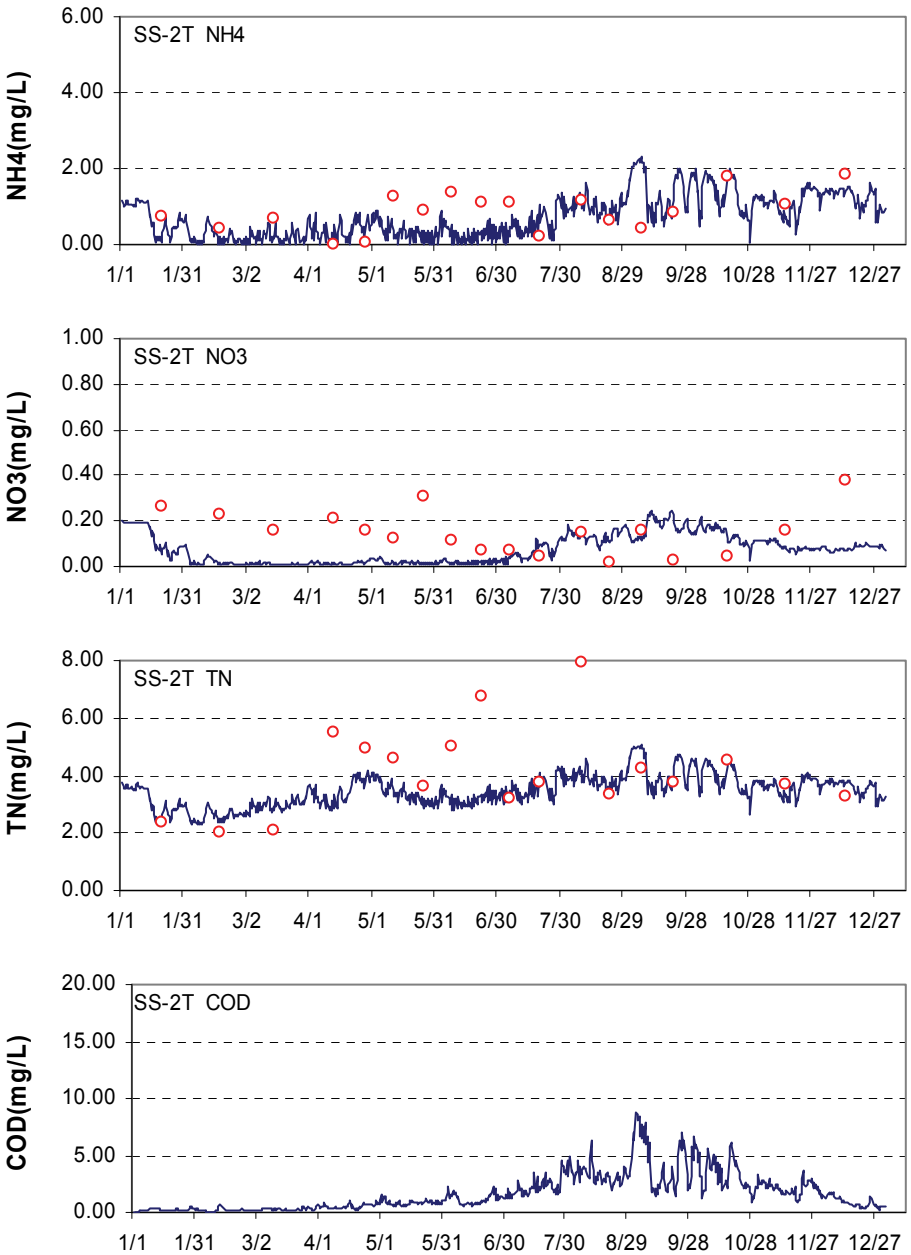

Figure 6-3. Comparison of observed and predicted water quality constituent concentrations near the water surface at USBOR Site SS-2 during 1999. ("T" in the station label refers to the top of the water column)

a)

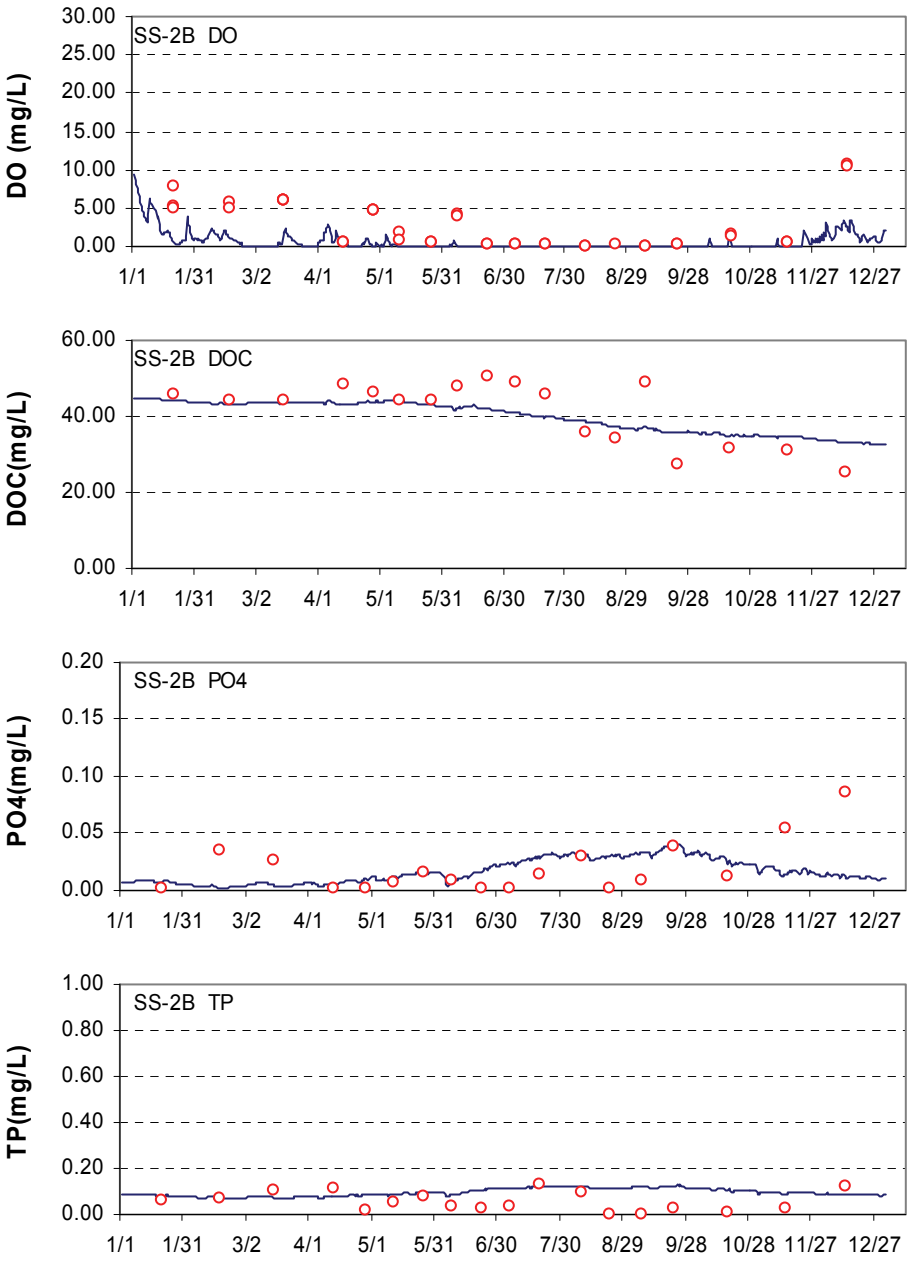
SS-2B DO
DO (mg/L)
30.00
25.00
20.00
15.00
10.00
5.00
0.00
1/1 1/31 3/2 4/1 5/1 5/31 6/30 7/30 8/29 9/28 10/28 11/27 12/27
SS-2B DOC
DOC(mg/L)
60.00
40.00
20.00
0.00
1/1 1/31 3/2 4/1 5/1 5/31 6/30 7/30 8/29 9/28 10/28 11/27 12/27
SS-2B PO4
PO4(mg/L)
0.20
0.15
0.10
0.05
0.00
1/1 1/31 3/2 4/1 5/1 5/31 6/30 7/30 8/29 9/28 10/28 11/27 12/27
SS-2B TP
TP(mg/L)
1.00
0.80
0.60
0.40
0.20
0.00
1/1 1/31 3/2 4/1 5/1 5/31 6/30 7/30 8/29 9/28 10/28 11/27 12/27

b)

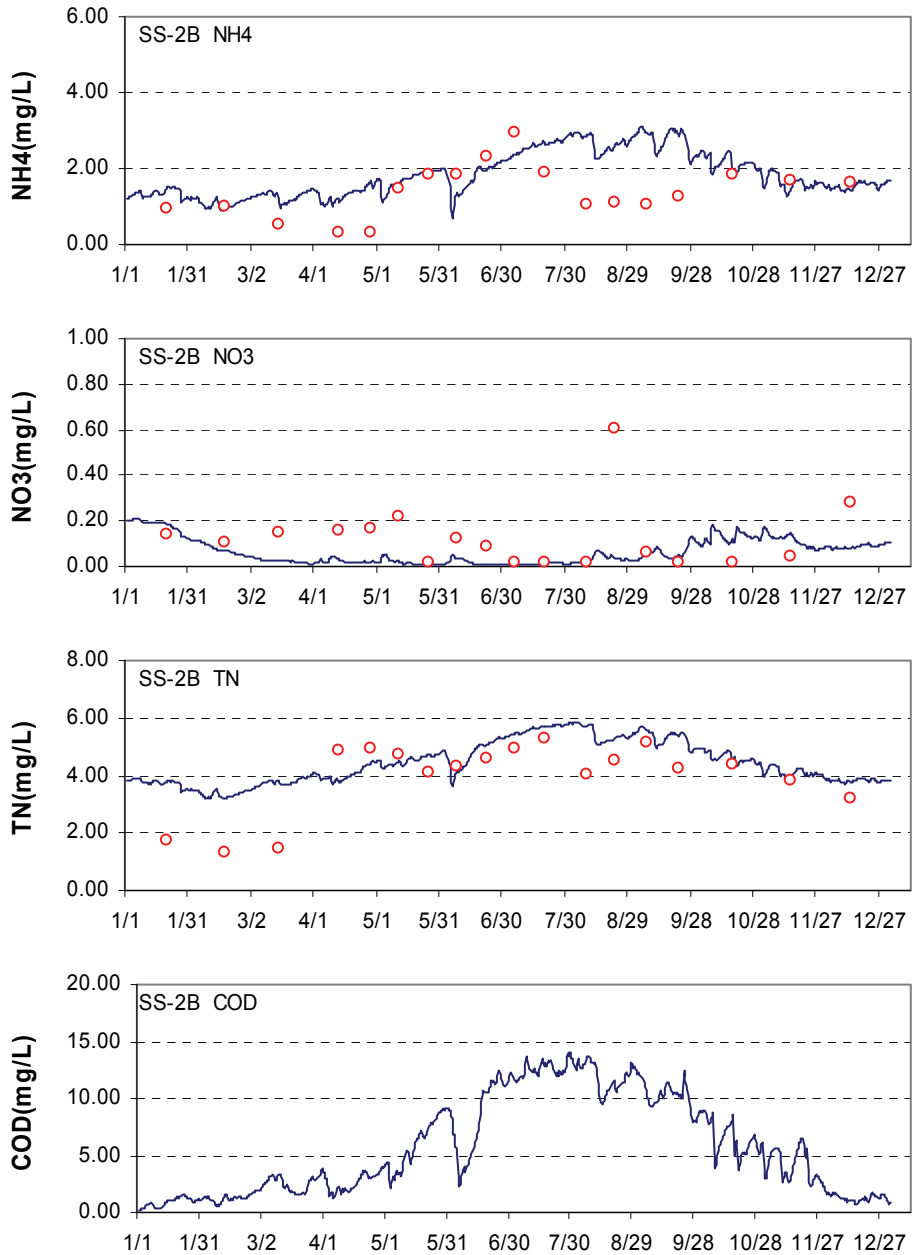

Figure 6-4. Comparison of observed and predicted water quality constituent concentrations near the water column bottom at USBOR Site SS-2 during 1999. ("B" in the station label refers to the bottom of the water column)

a)

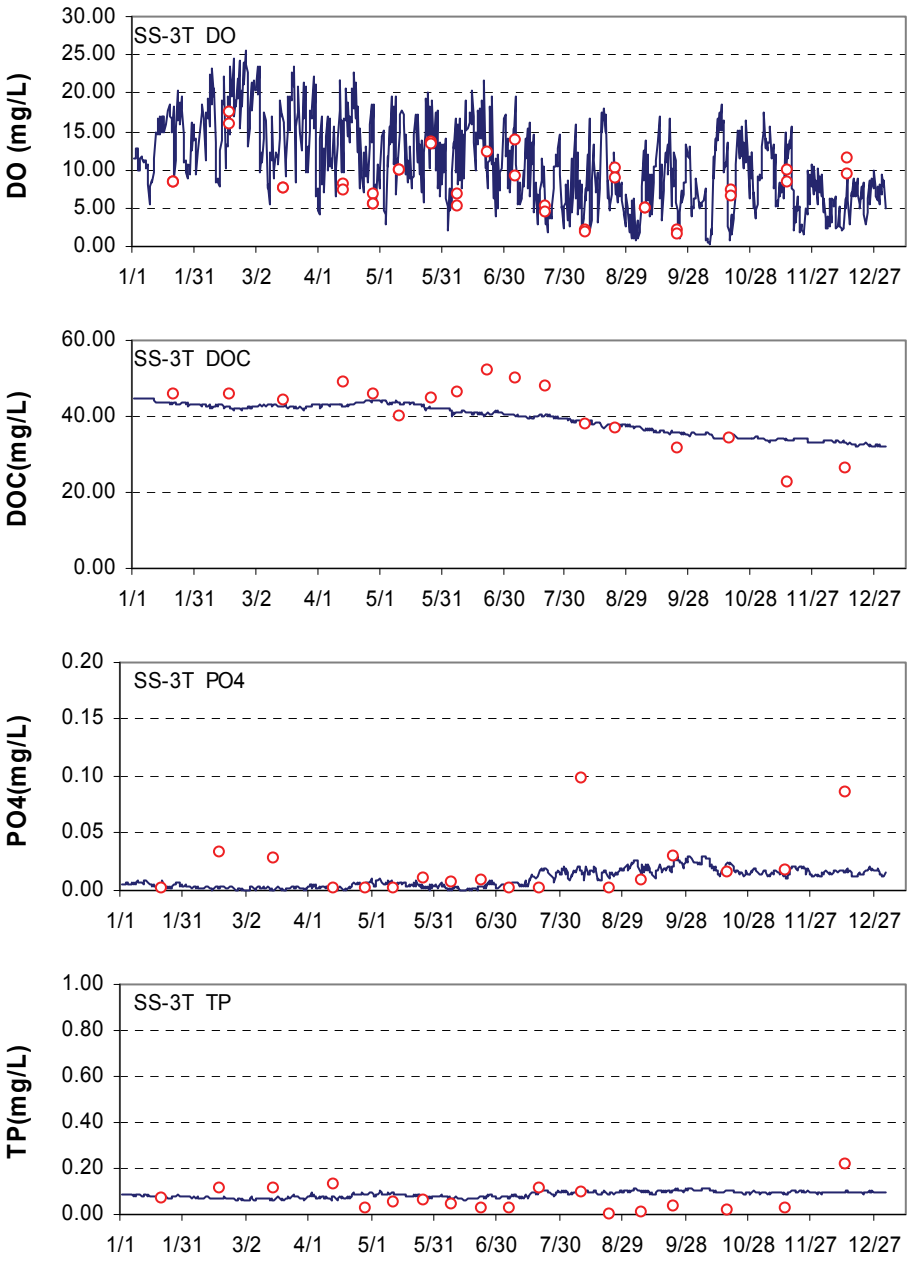
SS-3T DO
DO (mg/L)
30.00
25.00
20.00
15.00
10.00
5.00
0.00
1/1 1/31 3/2 4/1 5/1 5/31 6/30 7/30 8/29 9/28 10/28 11/27 12/27
SS-3T DOC
DOC(mg/L)
60.00
40.00
20.00
0.00
1/1 1/31 3/2 4/1 5/1 5/31 6/30 7/30 8/29 9/28 10/28 11/27 12/27
SS-3T PO4
PO4(mg/L)
0.20
0.15
0.10
0.05
0.00
1/1 1/31 3/2 4/1 5/1 5/31 6/30 7/30 8/29 9/28 10/28 11/27 12/27
SS-3T TP
TP(mg/L)
1.00
0.80
0.60
0.40
0.20
0.00
1/1 1/31 3/2 4/1 5/1 5/31 6/30 7/30 8/29 9/28 10/28 11/27 12/27

a)

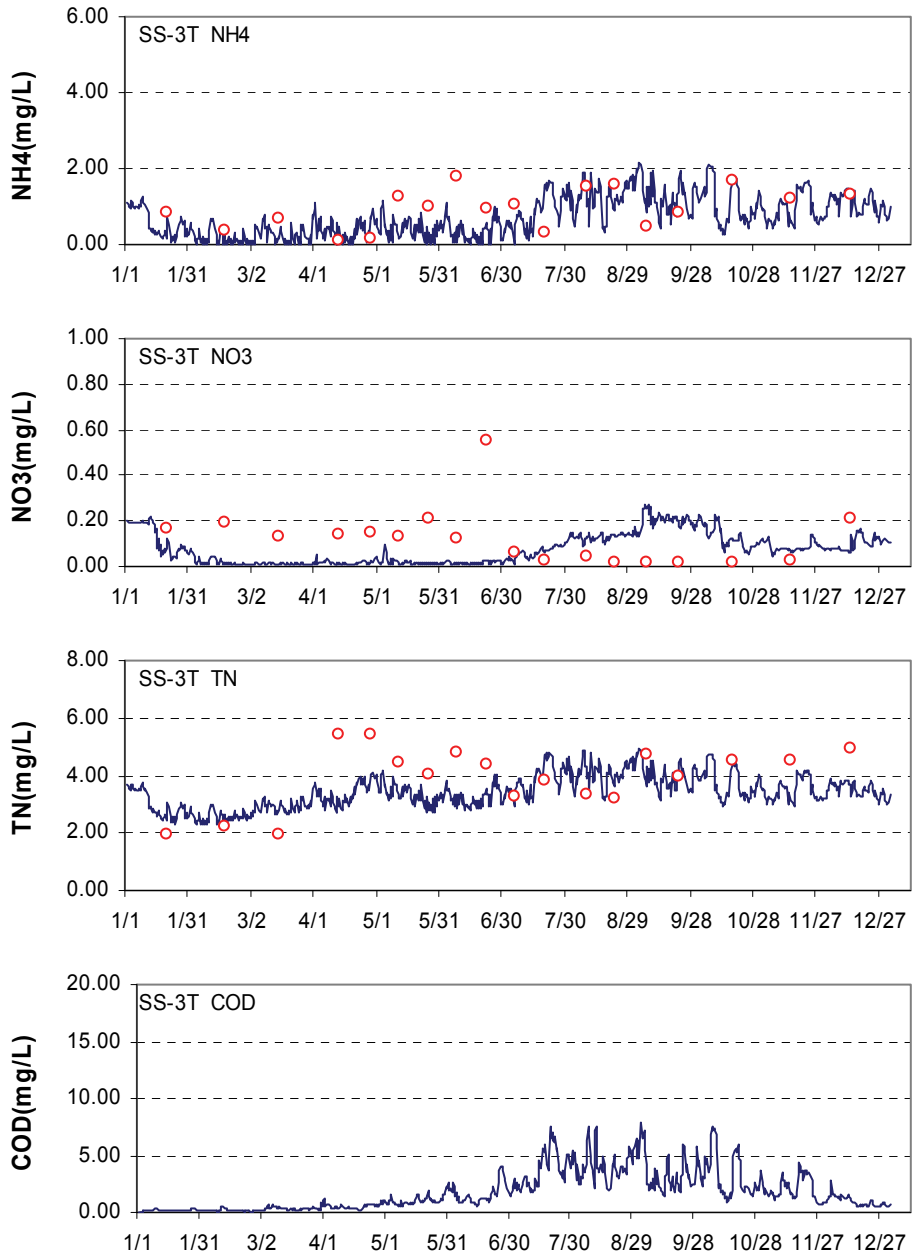

Figure 6-5. Comparison of observed and predicted water quality constituent concentrations near the water surface at USBOR Site SS-3 during 1999. ("T" in the station label refers to the top of the water column)

a)

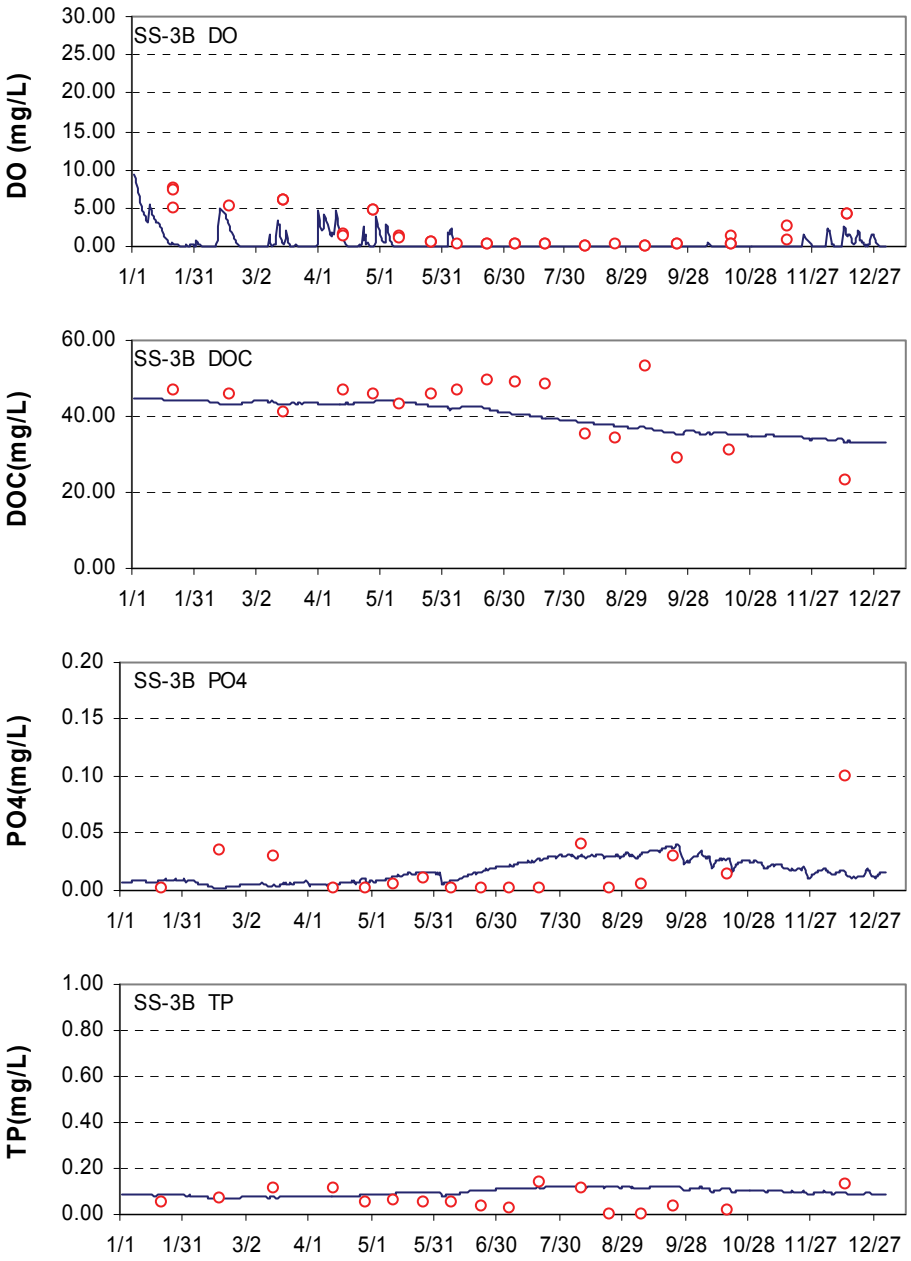
SS-3B DO
DO (mg/L)
30.00
25.00
20.00
15.00
10.00
5.00
0.00
SS-3B DOC
DOC(mg/L)
60.00
40.00
20.00
0.00
SS-3B PO4
PO4(mg/L)
0.20
0.15
0.10
0.05
0.00
SS-3B TP
TP(mg/L)
1.00
0.80
0.60
0.40
0.20
0.00
1/1 1/31 3/2 4/1 5/1 5/31 6/30 7/30 8/29 9/28 10/28 11/27 12/27

b)

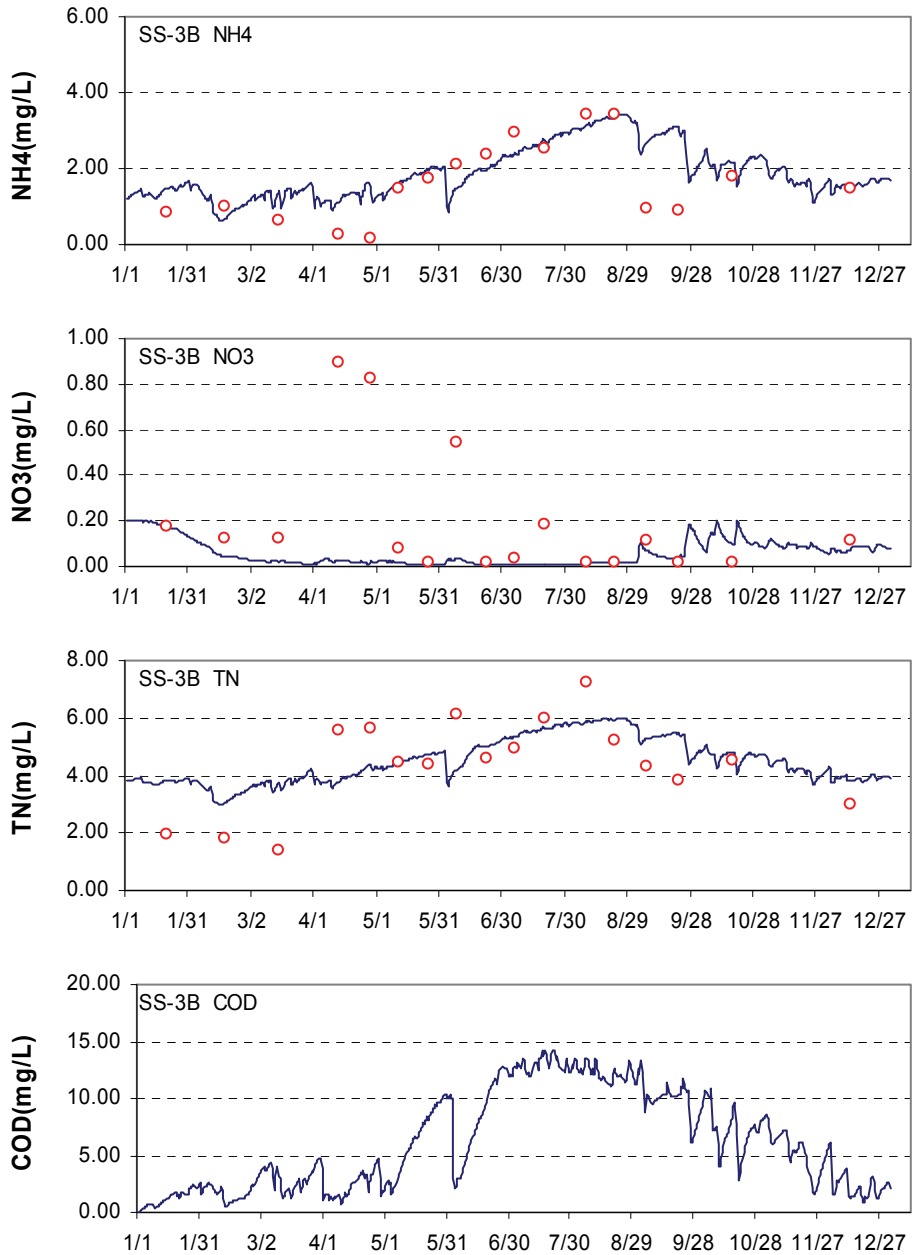

Figure 6-6. Comparison of observed and predicted water quality constituent concentrations near the water column bottom at USBOR Site SS-3 during 1999. ("B" in the station label refers to the bottom of the water column)

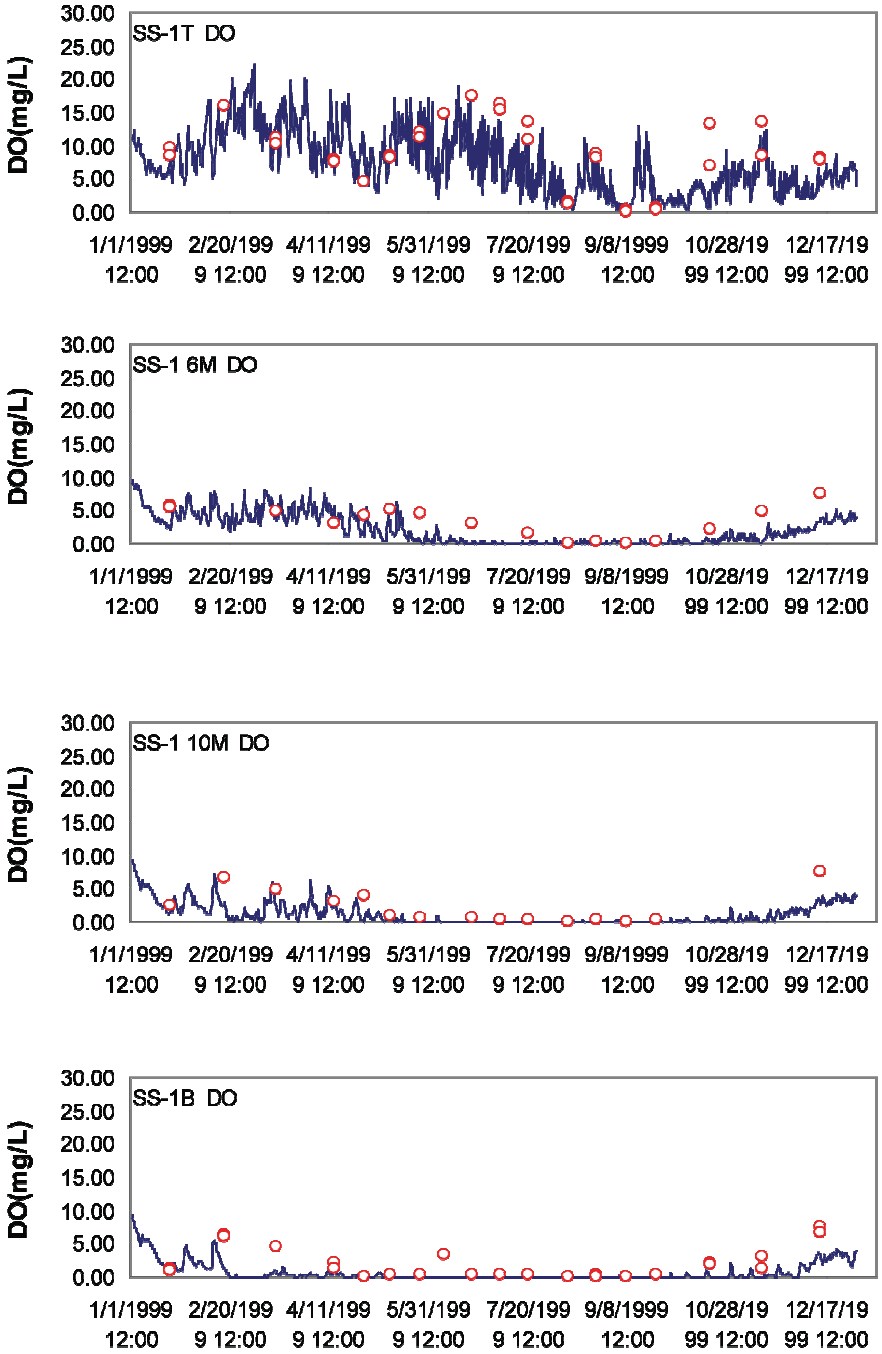

Figure 6-7. Comparison of observed and predicted dissolved oxygen at the water surface (label T), quarter depth (label 6M), mid-depth (label 10M) and bottom (label B) at USBOR Site SS-1 during 1999.

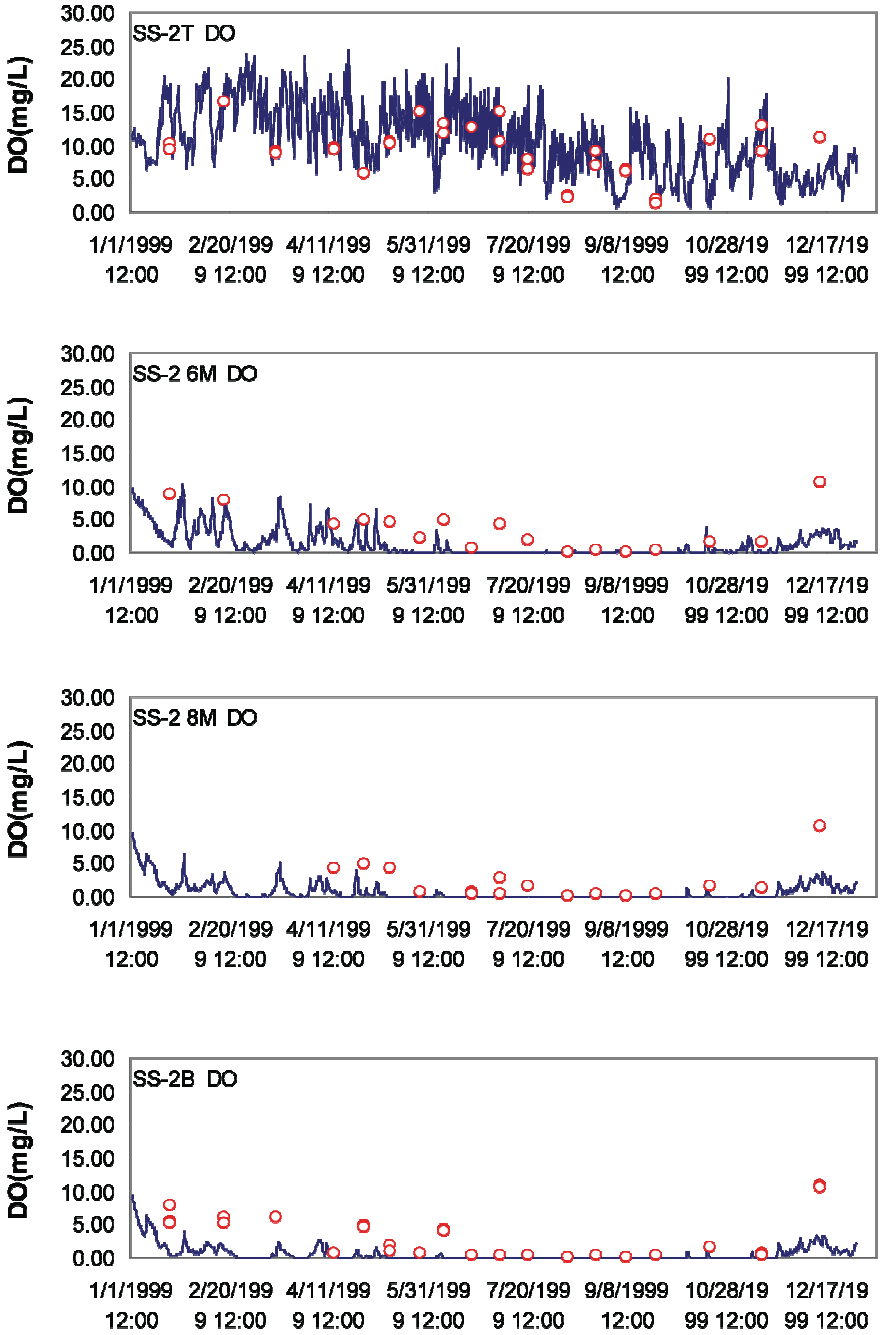

Figure 6-8. Comparison of observed and predicted dissolved oxygen at the water surface (label T), quarter depth (label 6M), mid-depth (label 8M) and bottom (label B) at USBOR Site SS-2 during 1999.

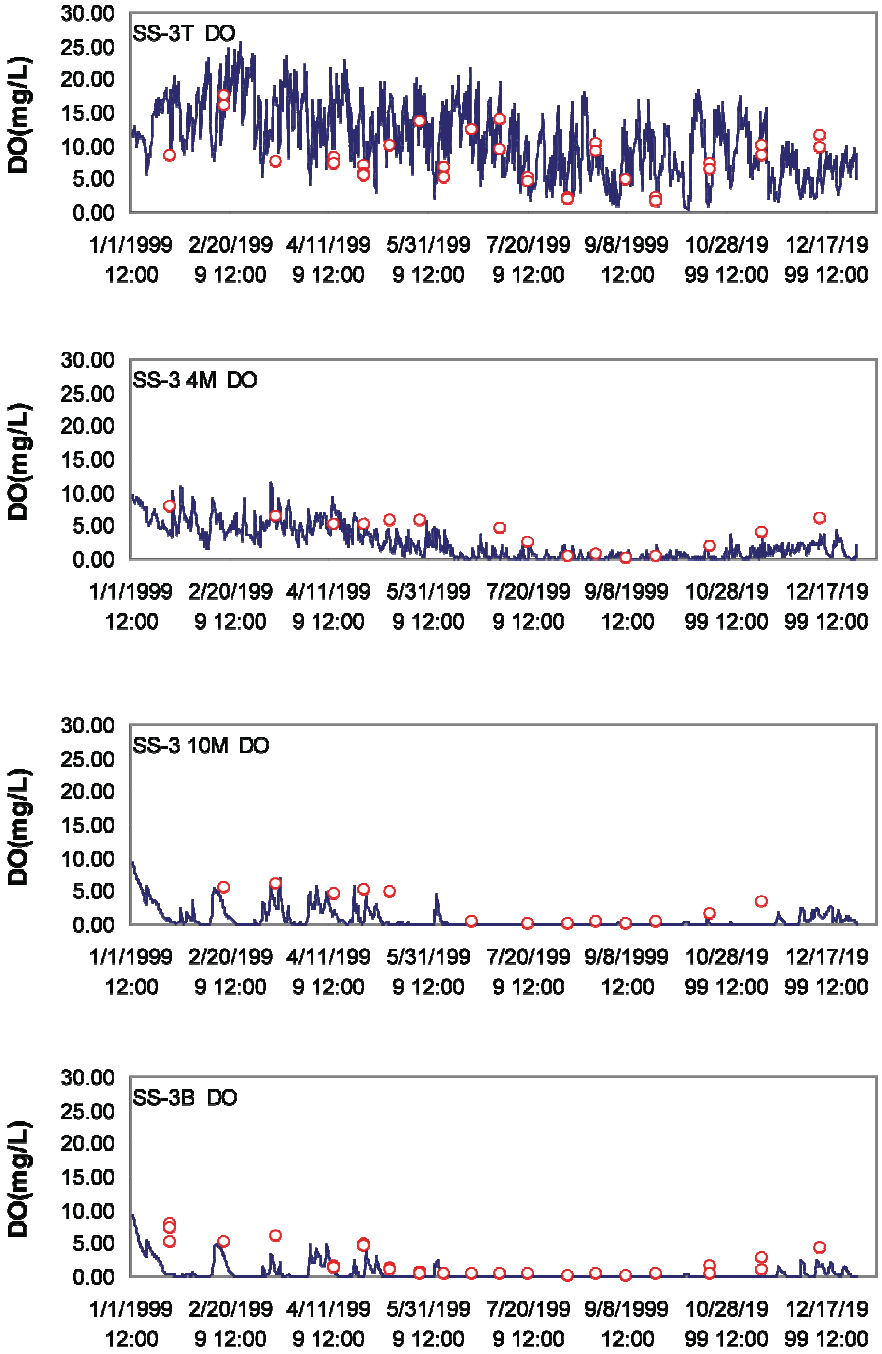

Figure 6-9. Comparison of observed and predicted dissolved oxygen at the water surface (label T), quarter depth (label 4M), mid-depth (label 10M) and bottom (label B) at USBOR Site SS-3 during 1999.

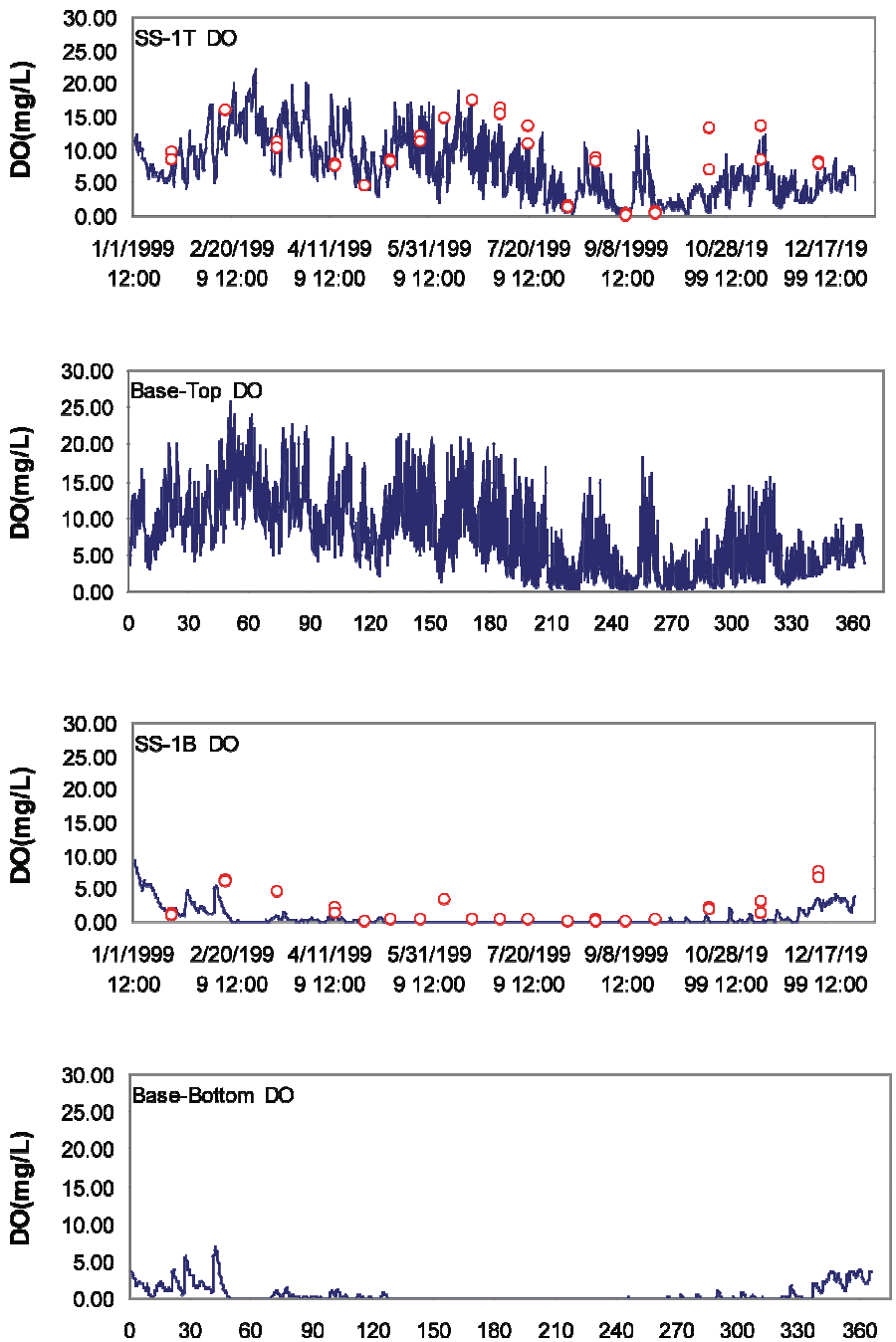

Figure 6-10. Comparison of calibration and 15 year base-line simulation predicted surface and bottom dissolved oxygen at USBOR Station SS-1.

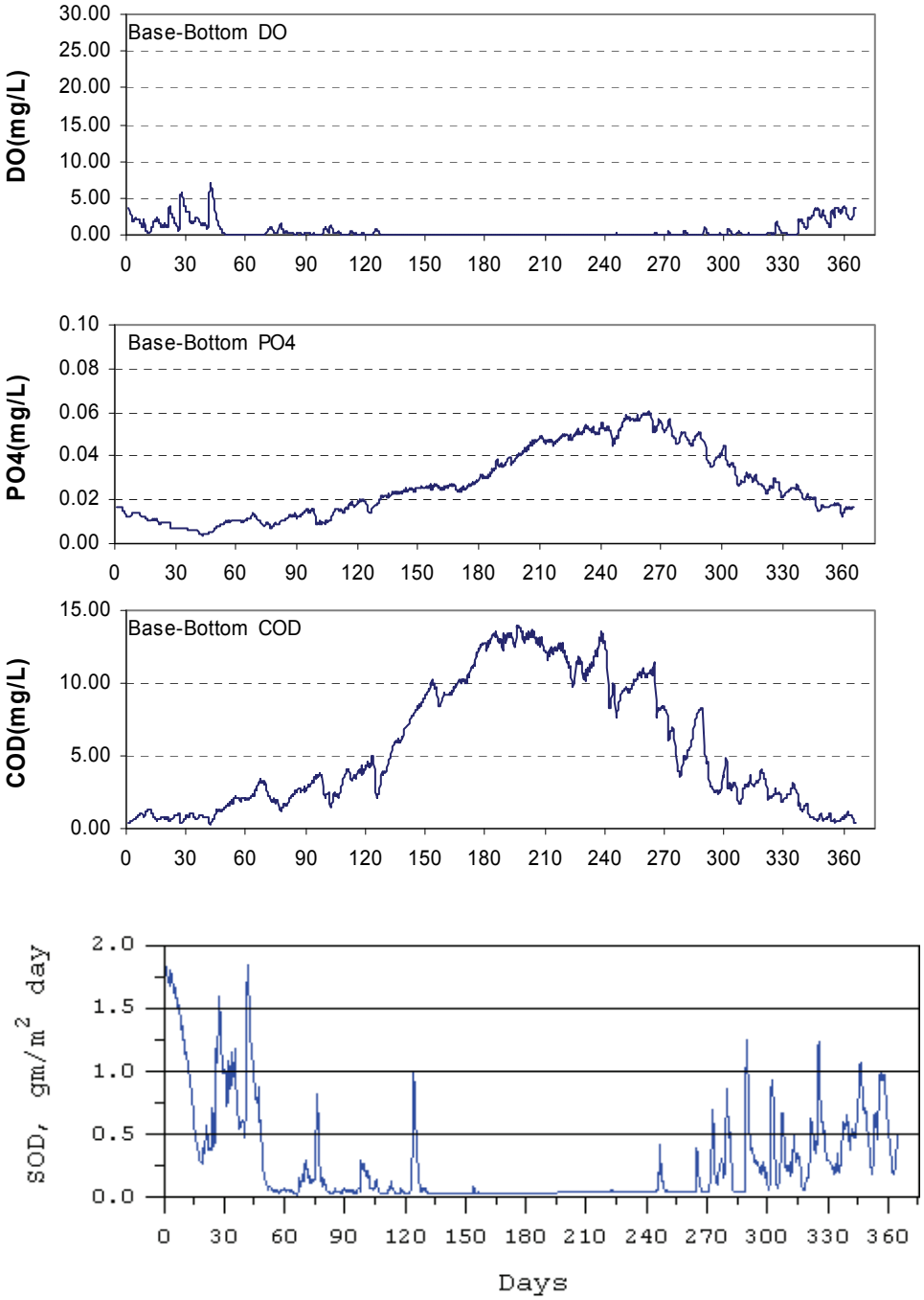

Figure 6-11. Near bottom dissolved oxygen, phosphate, sulfide component of chemical oxygen demand and sediment oxygen demand, for the fifteenth year of a 15 year base-line simulation at USBOR Station SS-1. The simulations assume that no restoration actions are implemented.

7. Evaluation of the Salton Sea Authority Restoration Plan

The calibrated and validated hydrodynamic and water quality model provides an essential tool for evaluating the effectiveness of alternate restoration plans. This chapter specifically evaluates the Salton Sea Authority's Plan, but the procedure outlined herein is readily extended to other alternative plans. The general approach taken is to compare hydrodynamic and water quality responses of restoration plans with existing conditions of long-term projections of existing conditions such as the 15-year baseline simulation discussed in the preceding chapter.

7.1. The Salton Sea Authority Plan

The SSA Plan has numerous components conceptually designed to improve water and air quality and aquatic habitat. Figure 7-1 shows the general concept with respect to structural and hydraulic modifications. The major components to be considered in the modeling-based evaluation are the recreational saltwater lake, including a dedicated habitat zone northwest of the across sea dike and the connected recreational estuary lake and its adjacent dedicated habitat zone. As shown in the figure, the northern and southern lakes are connected by a channel along the southwest shoreline of the existing sea. The design also includes a controlled conveyance channel flowing form the southeastern corner of the northern lake to the southern habitat zone, which openly connects to the southern lake. Flow into this channel is maintained by pumping stations. The conceptual design provides for recirculation of northern lake water by the eastern canal with and without treatment, using two withdrawals. A deepwater intake withdraws water from the northern lake and treats it by oxidation and filtration before discharging the treated water into the eastern canal for return to the southern lake. A second surface intake pumps water from the southeast corner of the northern lake into the eastern canal where it flows to the southern lake. The intended purpose of the treatment of the deep water withdrawn from the northern lake is the reduction of oxygen demand by filtration of particulate organic material and oxidation of sulfide. The SSA plan also includes treatment of the southern river inflows to the estuary lake and habitat zone to remove phosphorous.

Model configurations for simulating the SSA plan were developed for both the coarse and fine horizontal grid configurations of the entire sea such that the SSA Plan grids of the northern saltwater lake remained identical to the current conditions grid. Inflows from the three primary tributaries continue to flow into the southern lake and habitat area and the northern lake. Since repeated historical inflows, corresponding to the baseline simulation, were used, a control device was introduced to discharge excess water form the northern lake such that the water surface elevation did not rise significant above the current annual mean elevation. Historical wind and atmospheric forcing developed for the existing sea conditions were readily used for the SSA plan configuration. Three scenarios were simulated to evaluate individual and combined components of the SSA Plan. Scenario 1 evaluated only the area reduction with no withdrawals and treatment. Scenario 2 includes a 11.74 cms (268 mgd) surface withdrawal and a 15.64 cms (357 mgd) deepwater withdrawal from the northern lake. Oxidation of 50 per cent of sulfide in the deep water withdrawal was simulated by reducing the model's COD state variable by a factor of 0.5 before the deep withdrawal water was introduced into the southern restored area. Scenario 3 evaluated the effect of reducing phosphorous loadings from the inflowing rivers with no withdrawals and treatment of water from the northern lake. Scenario 3 represented a 90 per cent reduction in phosphorous load.

7.2. Hydrodynamic and Thermal Response Evaluation

A primary concern associated with deep reduced surface area restored lakes, such as the SSA Plan's northern saltwater lake, is alteration of vertical mixing dynamics and thermal stratification. These concerns have been raised based on the results of simple one-dimensional vertical temperature model which uses highly empirical parameterizations of vertical mixing (California DWR, 2006) rather than fully three-dimensional hydrodynamic and thermal transport modeling incorporating widely accepted turbulent closure formulations. Comparison of transient vertical temperature structure at Site 5, Figure 2-1, in the northern sea under current conditions and conditions with the north saltwater lake alternative and current wind and atmospheric forcing provide a means for evaluating mixing characteristics of the northern sea alternative. Figure 7-2 shows model predictions for the current conditions, top panel, and the SSA Plan's northern saltwater lake alternative, bottom panel, on the annual time scale. Figure 7-3 shows a similar comparison for two weeks in late May 1997. These figures indicated that vertical mixing and density stratification, as manifest by the vertical temperature profile, are not significantly unchanged from current conditions as is further substantiated by the stratification histograms shown in Figure 7-4. Vertical temperature structure in the northern saltwater lake was insensitive to the Scenario 2 withdrawals.

Although model predictions of velocity at Site 5 for current conditions are not particularly good, it is useful to compare model predictions at Site 5 for current conditions and the SSA northern saltwater lake alternative. This comparison is shown in Figure 63 for the same late May 1997 period corresponding to Figure 7-3. The results in Figure 7-4 indicate that velocity variability amplitude in response to diurnal wind variability is actual increased for the northern saltwater lake alternative. However the fact that the vertical temperature structure is relatively unchanged is consistent with the sensitivity analysis of Chapter 5 which indicated that vertical mixing is not sensitive to the exact magnitude and direction of horizontal current but rather to the surface stress and shear.

The preceding results for the northern saltwater lake are quite different form those projected by the one-dimensional vertical temperature modeling effort (California DWR, 2006) which made arguments that reduction in wind fetch would decrease mixing in a northern sea alternative. The understanding gained in this modeling study indicates that the fetch limitations are of secondary importance, if at all, and that vertical mixing is primarily associated with local current shear response to the local wind stress and nocturnal atmospheric cooling induced convective instability. These arguments can be further substantiated by analysis of turbulent mixing dynamics using non-empirical closure models such as the one incorporated in the EFDC model.

7.3. Water Quality Response Evaluation

The procedure for evaluating the water quality response of the SSA Plan was to conduct three 15 year scenario simulations incorporating various component of the SSA Plan, as previously discuss, and compare these simulations with the 15 year baseline simulation of current conditions in the entire sea. The rationale for the long-term 15 year simulation period is to allow the sediment flux sub-model, which predicts sediment oxygen demand and fluxes of ammonium, dissolved ortho-phosphorous, and sulfide from sediments into the water column, to reach a dynamic equilibrium. Dissolved oxygen is the most often used single indicator of water quality in eutrophic systems and change in the volume-days of low DO water provides a useful temporal and spatially integrated measure (Thomann, et al., 1994).

To provide quantitative measures of the difference between the baseline and three SSA Plan scenario simulations, the percent of total volume-days during the last year of simulation having dissolved oxygen lower than a range of threshold values was calculated in place in the model. For the baseline simulation, the entire current volume of the sea is considered. For the three SSA Plan scenarios the combined volume of the north saltwater lake, south estuarine lake and the two dedicated habitat zones are used. Table 7-1 shows the results for threshold values of 1, 2, and 4 mg/L of dissolved oxygen. Most immediately evident from the table is the result that the all three low dissolved oxygen volume days (LDOVD) measures are smaller for the SSA Plan scenarios than the baseline. The reason for this is likely a flushing effect incorporated into the three SSA Plan scenarios. Since the reduce surface area system is receiving the same volumetric inflow as the full sea, excess water is withdrawn from the SSA Plan configuration such that the sea elevation remains in the vicinity of the current annual mean elevation of the course of the 15 year simulation. Although this may not be consistent with a more exact operational projection, it does provide an insightful. That insight is that dissolve oxygen level are most effectively increased by flushing the sea with excess inflow having current water quality conditions. This is evident in Figure 7-6 and Figure 7-7 which compares surface and bottom dissolved oxygen during the last year of the 15 year baseline and Scenario simulations. In this respect, it is more appropriate to inter compare the four scenarios rather than the baseline and four scenarios.

Considering only the three scenario simulations, the most significant result is that Scenario 2 which includes withdrawal and treatment of water form the northern saltwater lake shows no improvement in dissolved oxygen relative to Scenario 1. One possible explanation for this is that the withdrawal results in downward advection of higher DO water with correspondingly lower COD toward the bottom which accelerates the rate of remineralization in the sediment bed and in turn decreases the overall DO. The other interesting results of the scenarios is reduction in external phosphorous loading is the most effective strategy for improving water quality in the restored water body. Figure 7-8 shows that the 90 per cent phosphorous load reduction results in a corresponding reduction in algae chlorophyll. The reduced algae levels are manifest by less variability in surface dissolved oxygen and a significant increase in bottom dissolved oxygen as shown in Figure 7-6 and Figure 7-7. The elimination of anoxic conditions in the bottom of the water column also eliminate sulfide flux form the sediment and its associated chemical oxygen demand as shown in Figure 7-9. A final and likely the most important result of the scenario simulations is that water quality in the deeper regions of the SSA Plan northern saltwater lake is not significantly different from current conditions based on comparison of Figure 6-10, Figure 7-6, and Figure 7-7. This is entirely consistent with the finding that vertical mixing and stratification, as manifest by the vertical temperature structure, in the northern saltwater lake do not significantly differ from present conditions.

Complete annual time scale plots of all water quality state variables for the last year of the 15 baseline and scenario simulations are provided in Appendix B.

Table 7-1
Per Cent Volume-Days with Dissolved Oxygen Lower than Threshold Value

Scenario	Mid Sea Barrier	Water Withdrawal And Treatment	Per Cent Removal of Inflow Phosphorous	Per Cent Vol-Days Less Than 1 mg/L	Per Cent Vol-Days Less Than 2 mg/L	Per Cent Vol-Days Less Than 4 mg/L
Baseline	N/A	N/A	N/A	36.80%	46.70%	63.20%
1	Yes	No	0	23.80%	31.30%	42.30%
2	Yes	Yes	0	25.30%	33.10%	44.10%
3	Yes	No	90	0.00%	0.00%	5.30%

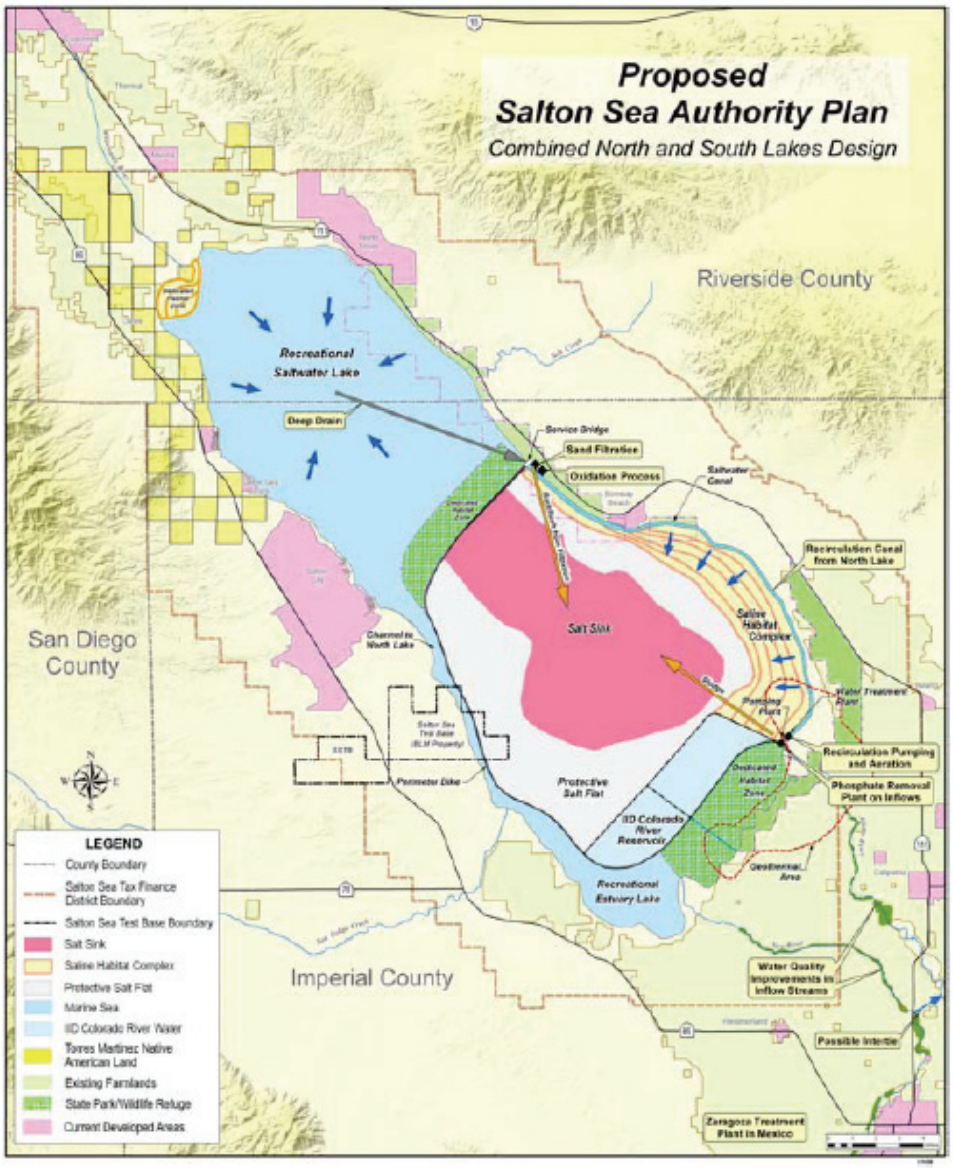

Figure 7-1. Major components of the Salton Sea Authority's restoration plan.

a)

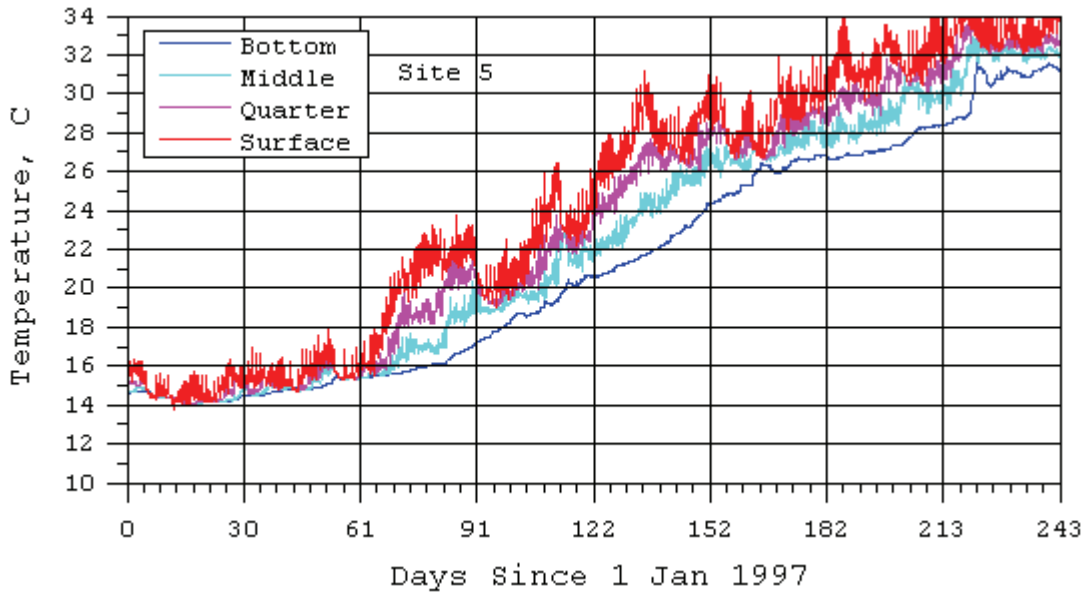
Bottom
Middle
Quarter
Surface
Site 5
Temperature, C
Days Since 1 Jan 1997

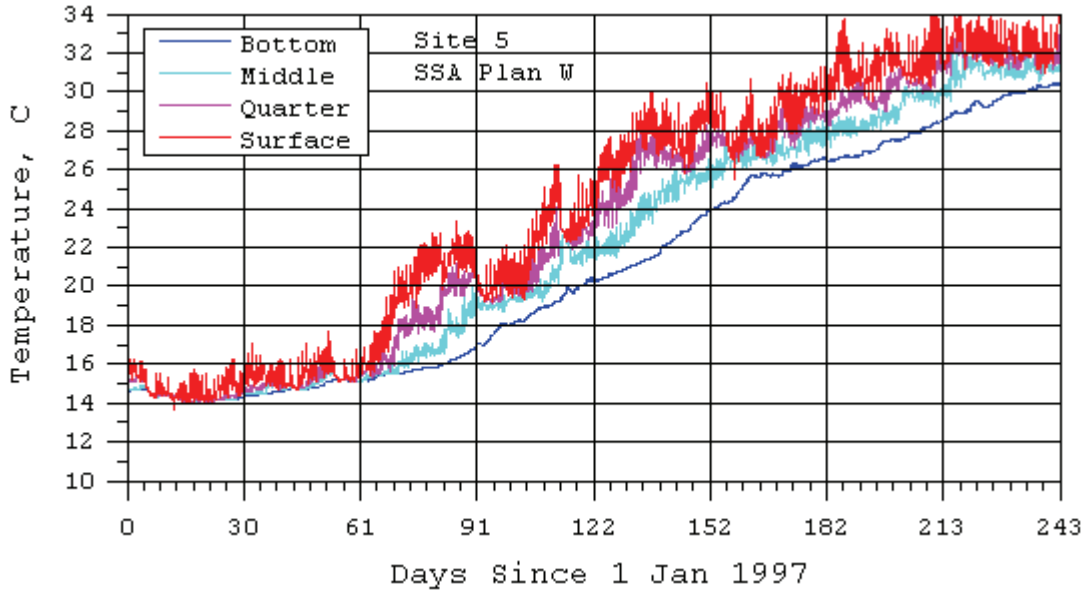
Bottom
Middle
Quarter
Surface
Site 5
SSA Plan W
Temperature, C
Days Since 1 Jan 1997

b)

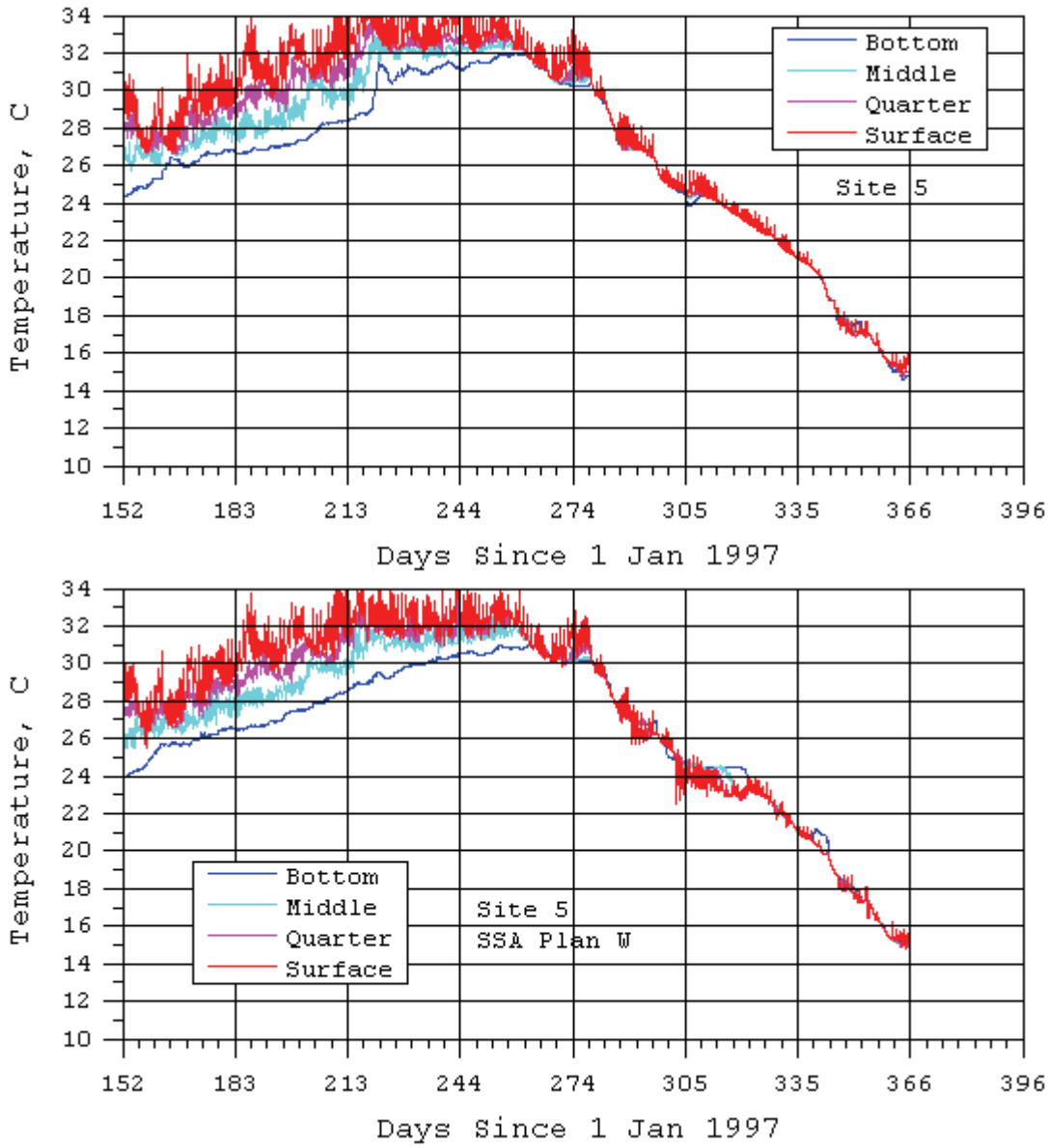

Figure 7-2. Model predicted temperature at Site 5. Top panel is current conditions. Bottom panel is SSA restoration alternative

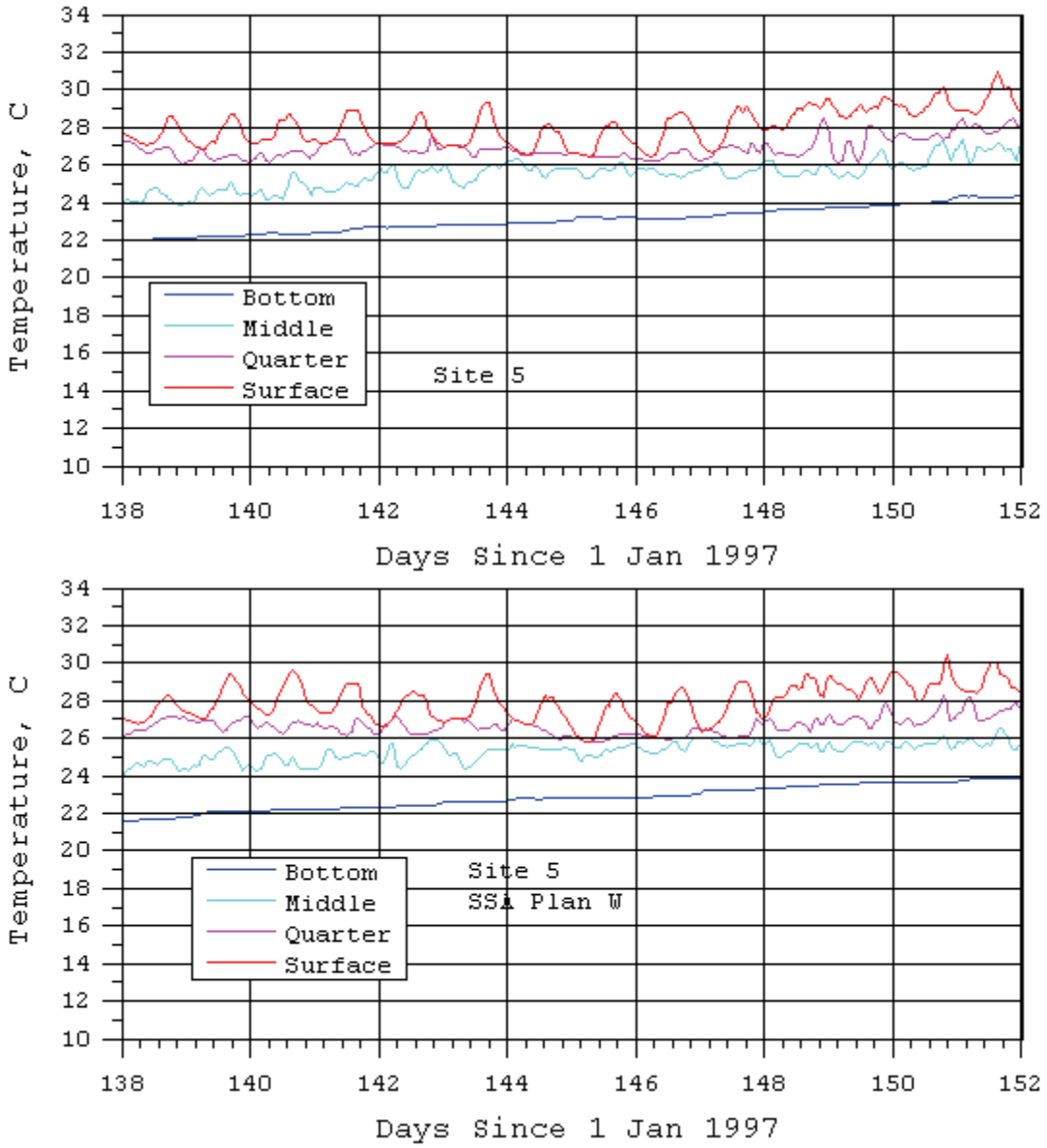

Figure 7-3. Model predicted temperature at Site 5. Top panel is current conditions. Bottom panel is SSA restoration alternative

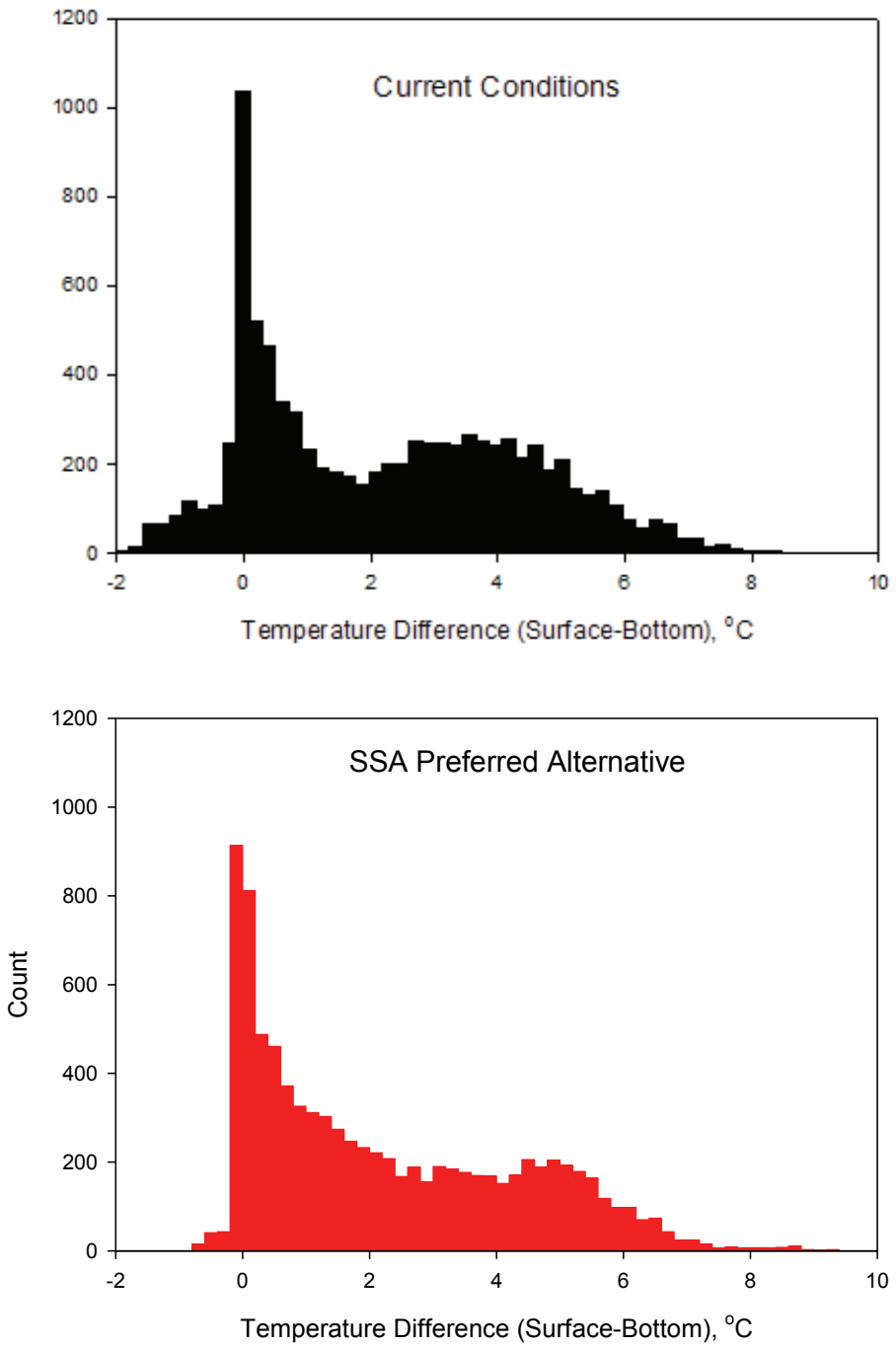

Figure 7-4. Histogram of Temperature Stratification. Top panel is current conditions. Bottom panel is SSA restoration alternative.

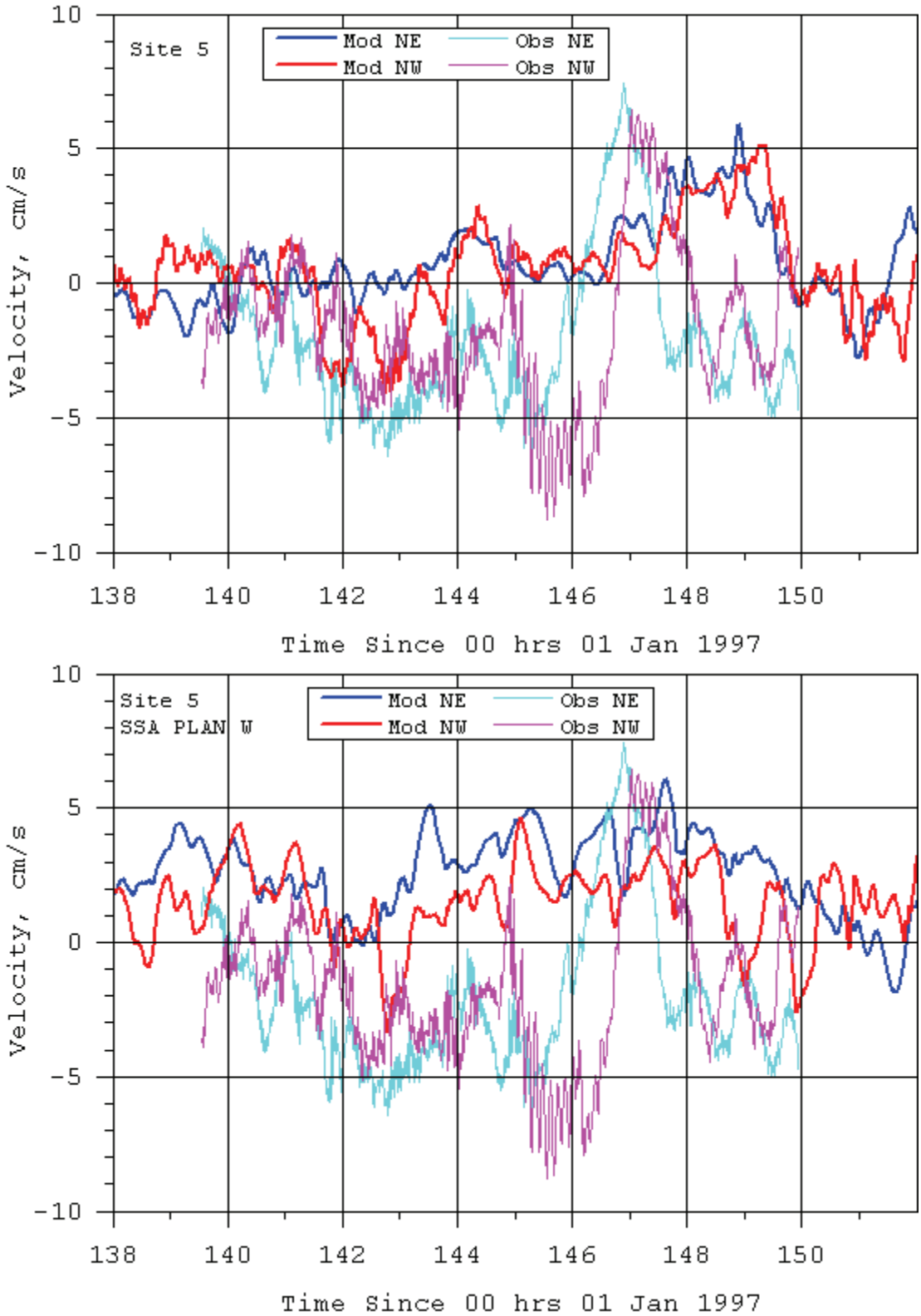

Figure 7-5. Model predicted velocities at Site 5 in late May. Top panel is current conditions. Bottom panel is SSA restoration alternative

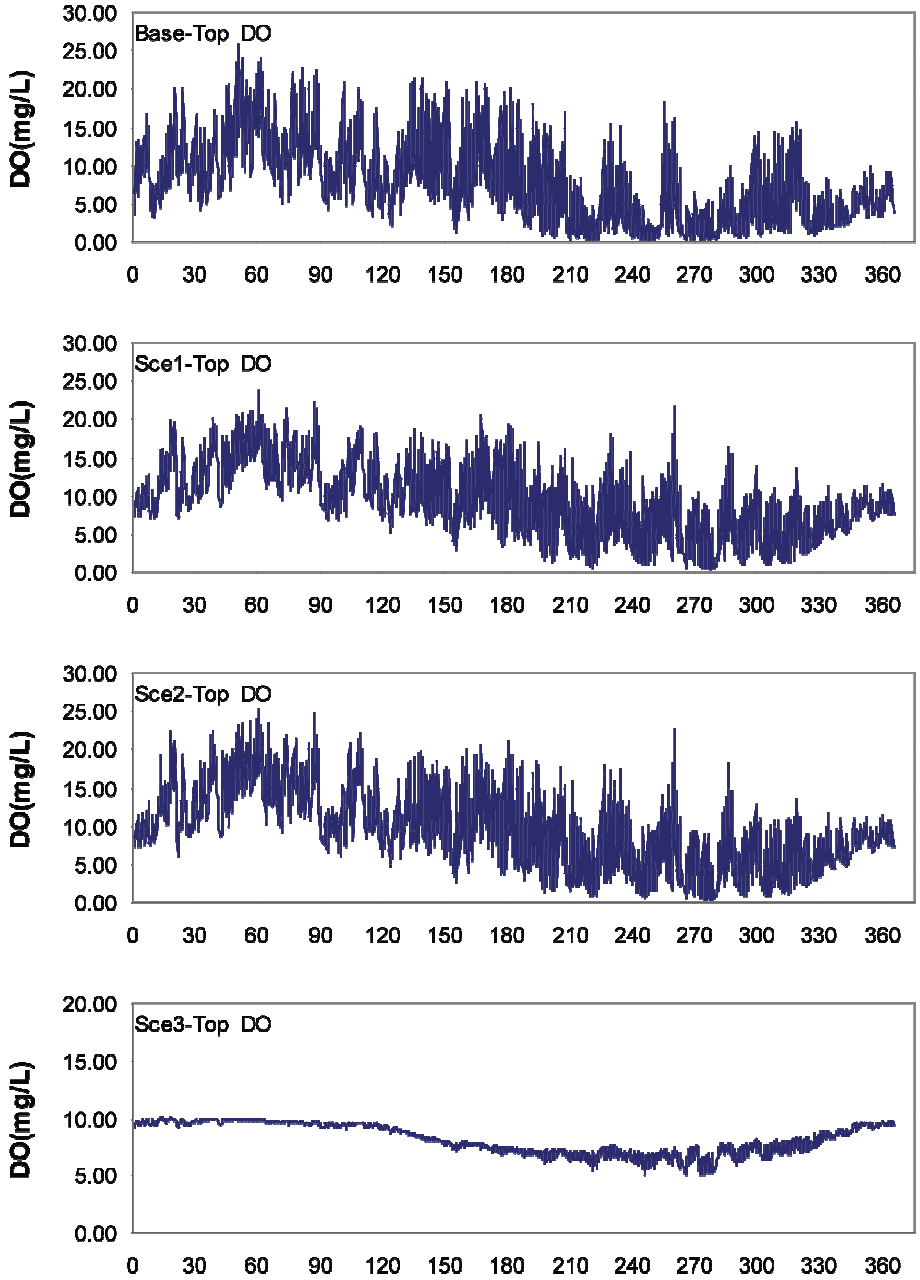

Figure 7-6. Comparison surface dissolve oxygen at USBOR Station SS-1 for 15 year baseline and restoration scenario simulations. The three restoration scenarios in Table 7-1 are labeled as Sce1, Sce2, and Sce3.

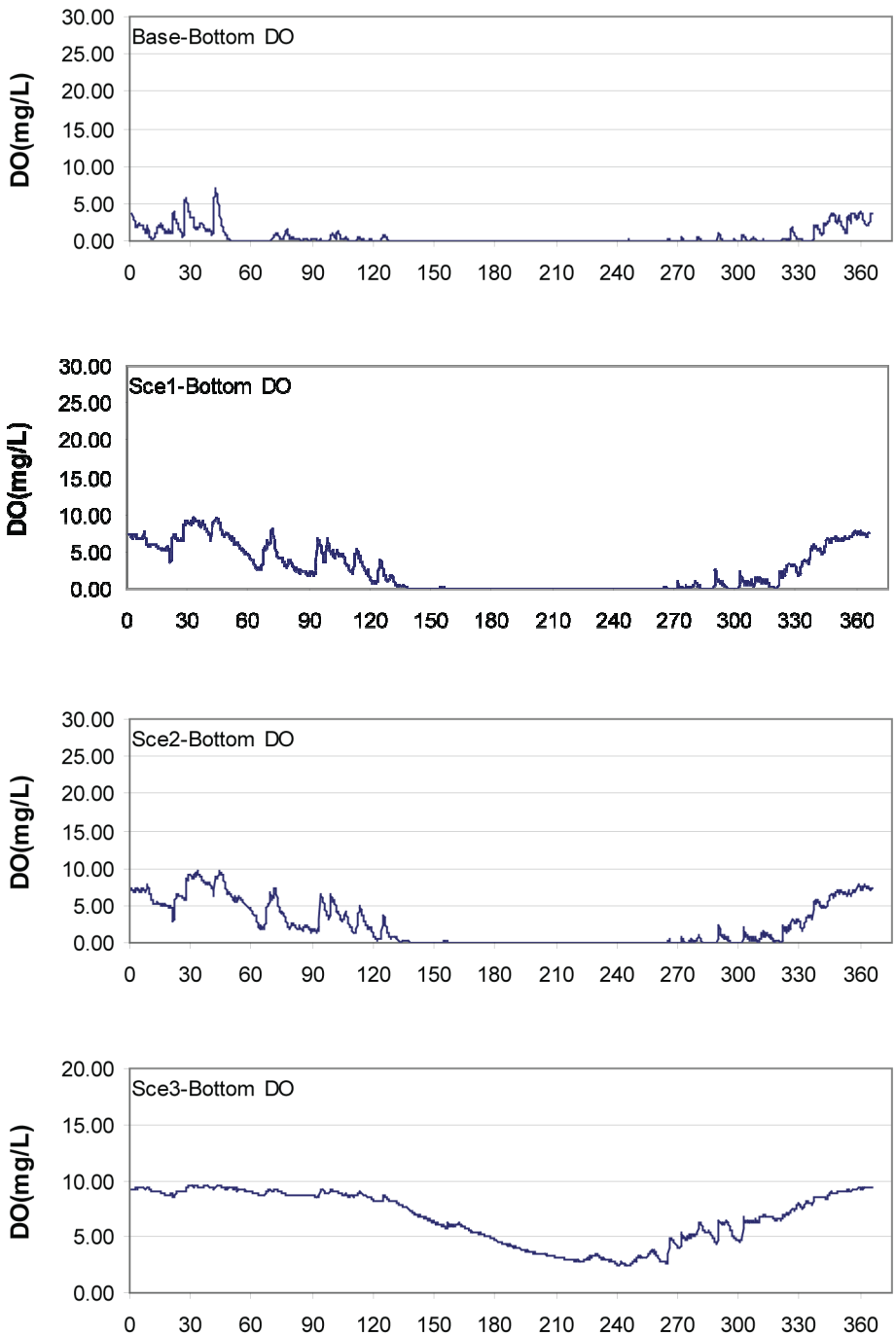

Figure 7-7. Comparison bottom dissolve oxygen at USBOR Station SS-1 for 15 year baseline and restoration scenario simulations. The three restoration scenarios in Table 7-1 are labeled as Sce1, Sce2, and Sce3.

a)

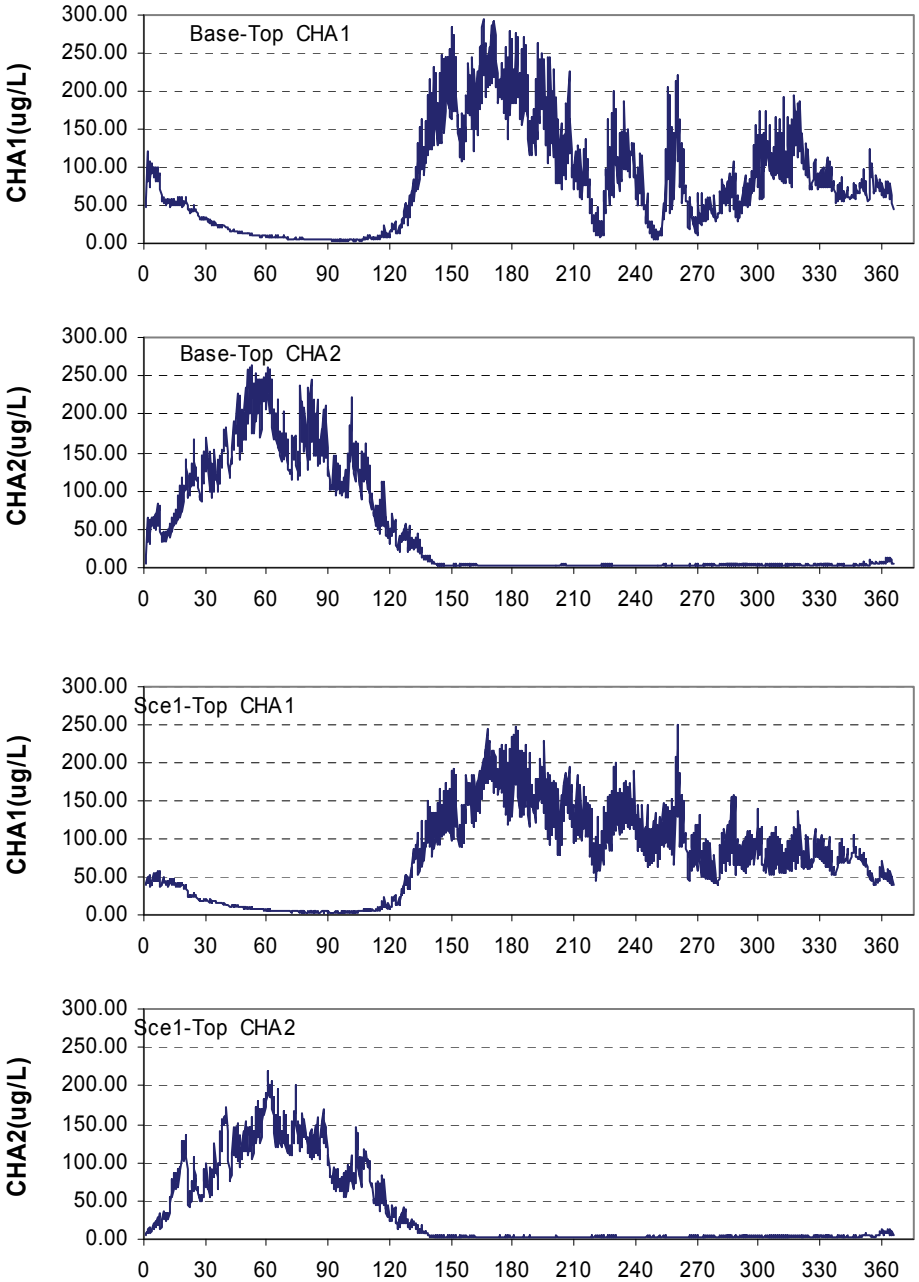
Base-Top CHA1
CHA1(ug/L)
Base-Top CHA2
CHA2(ug/L)
Sce1-Top CHA1
CHA1(ug/L)
Sce1-Top CHA2
CHA2(ug/L)
300.00
250.00
200.00
150.00
100.00
50.00
0.00
0 30 60 90 120 150 180 210 240 270 300 330 360

b)

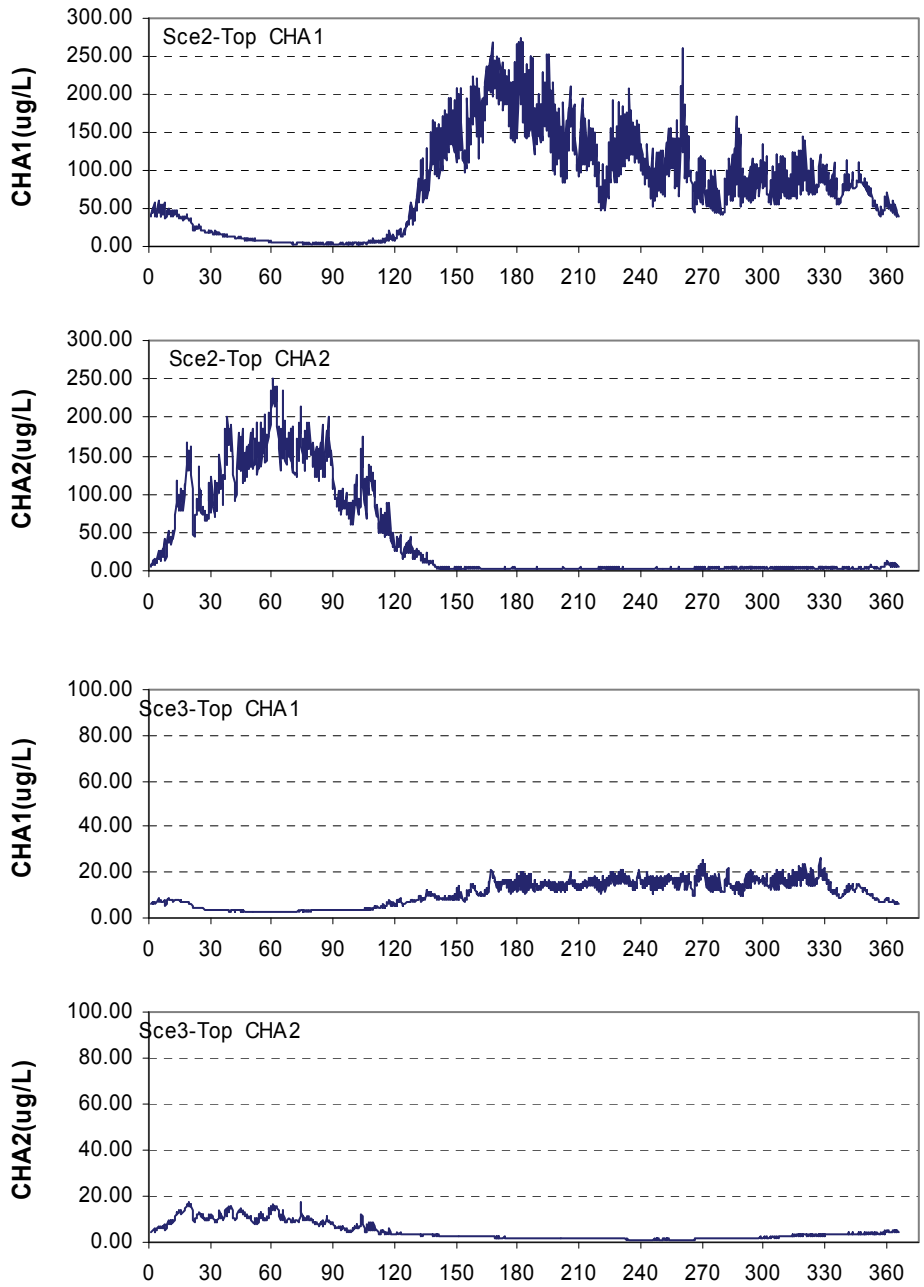

Figure 7-8. Comparison surface chlorophyll 'a' at USBOR Station SS-1 for 15 year baseline and restoration scenario simulations. The three restoration scenarios in Table 7-1 are labeled as Sce1, Sce2, and Sce3.

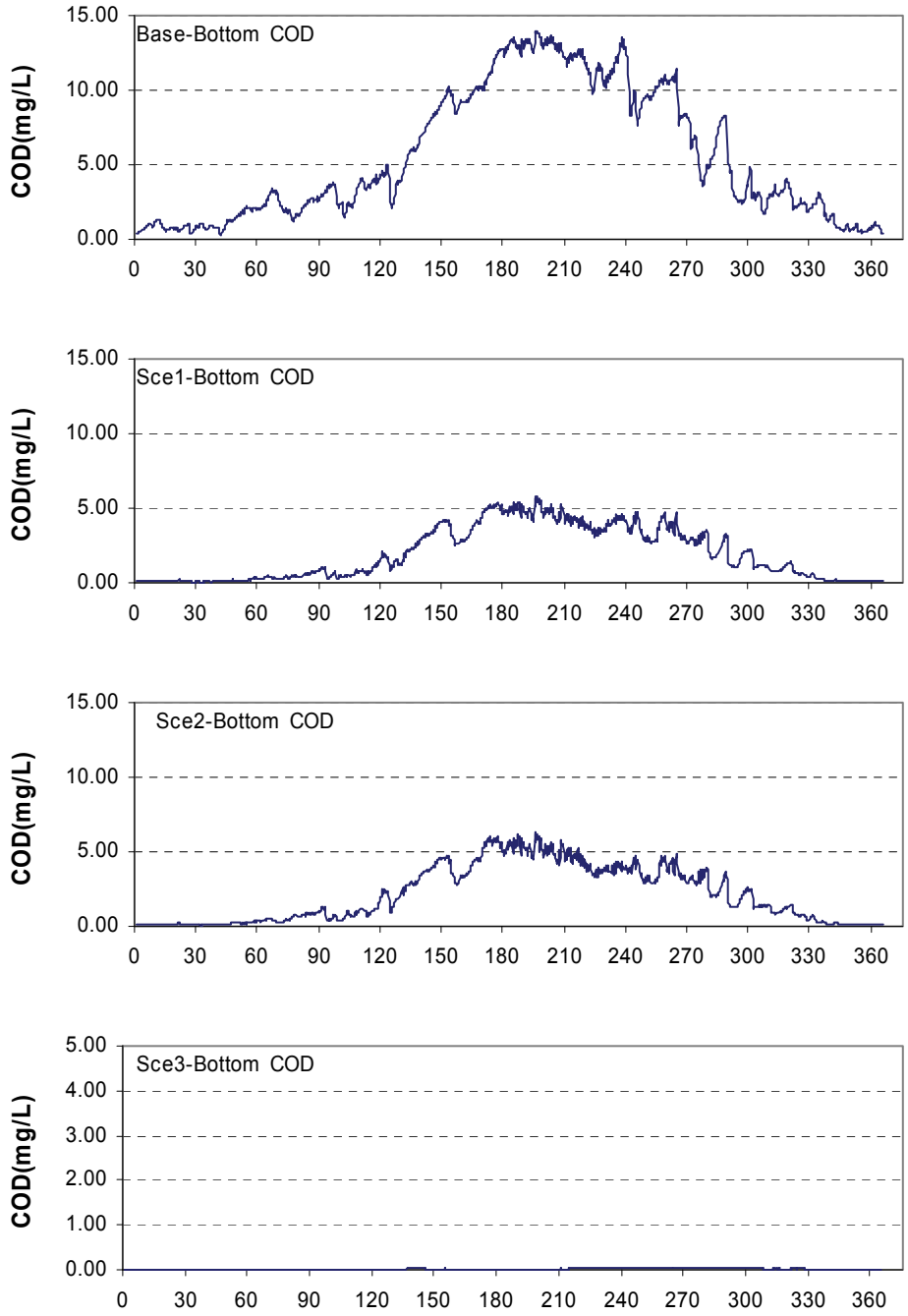

Figure 7-9. Comparison bottom chemical oxygen demand due to hydrogen sulfide at USBOR Station SS-1 for 15 year baseline and restoration scenario simulations. The three restoration scenarios in Table 7-1 are labeled as Sce1, Sce2, and Sce3.

8. Summary

The development of a hydrodynamic and water quality model of the Salton Sea for use in assessing recent hydrodynamic and water quality conditions and evaluating changes resulting from various restoration plans including the Salton Sea Authority Plan has been presented. Consistent with the wide acceptance that physical and biogeochemical processes in the Salton Sea are fundamentally three-dimensional in space and highly variable in time, a three-dimensional modeling system, EFDC, was selected, configured and calibrated for recent conditions. The EFDC based model was configured to simulate and evaluate the major components of the Salton Sea Authority's preferred restoration plan. The major findings of that evaluation are that mixing and stratification in the SSA Plan's northern saltwater lake are not significantly different than current conditions and that under extended current loading conditions water quality in the northern saltwater lake is not significantly different from current conditions. Reduction of external phosphorous loads was determined to be more effective than treatment of hypolimnetic water to remove sulfide and associated oxygen demand.

9. References

Ambrose, R. B., T. A. Wool, and J. L. Martin, 1993: The water quality analysis and simulation program, WASP5: Part A, model documentation version 5.1. U. S. EPA, Athens Environmental Research Laboratory, 210 pp.

California Department of Water Resources, 2006: Salton Sea Ecosystem Restoration Program: Draft Programmatic Environmental Impact.

Cerco, C. F., and Cole, T. 1995. User's guide to the CE-QUAL-ICM three-dimensional eutrophication model; Release Version 1.0, Technical Report EL-95-15, U.S. Army Engineer Waterways Experiment Station, Vicksburg, MS.

Cerco, C. F., Bunch, B. W., Teeter, A. M., and Dortch, M. S. (2000). Water Quality Model of Florida Bay, ERDC/EL TR-00-10, U.S. Army Engineer Research and Development Center, Vicksburg.

Cook, C. B., 2000: Internal Dynamics of a Terminal Basin Lake: A Numerical Model for Management of the Salton Sea, Ph.D. Dissertation, University of California, Davis.

Cook, C. B. 2006: Personal communication of 1997 Salton Sea ADCP and temperature observational data to Tetra Tech, Inc.

Cook, C. B., G. T. Orlob, and D. W. Huston, 2002: Simulation of wind- driven circulation in the Salton Sea: Implications for indigenous ecosystems. Hydrobiologia 473: 59- 75.

DiToro, D. M. 2000. Sediment Flux Modeling, Wiley-Interscience.

Hamilton, D. P. and Schladow, S. G., 1996: Prediction of water quality in lakes and reservoirs: Part I - Model Description. Ecological Modelling 96: pp91-110.

Hamrick, J.M., 1989: Excitation response analysis of estuarine circulation. Circulation Patterns in Estuaries, B.J. Neilson et al., Eds., Humana Press, Clifton, NJ, 157-182.

Hamrick, J. M., 1992: A three-dimensional environmental fluid dynamics computer code: Theoretical and computational aspects. The College of William and Mary, Virginia Institute of Marine Science, Special Report 317, 63 pp.

Hamrick, J. M., and Wm. B. Mills, 2001: Analysis of temperatures in Conowingo Pond as influenced by the Peach Bottom atomic power plant thermal discharge. Environmental Science and Policy, 3, s197-s209.

Holdren, G. C. and A. Montano, 2002a: Chemical and physical limnology of the Salton Sea, California – 1999. Technical Memorandum No. 8220-03-02. U.S. Bureau of Reclamation, Denver, CO.

Holdren, G. C. and A. Montano, 2002b: Chemical and physical characteristics of the Salton Sea, California. Hydrobiologia, 473: 1- 21.

HydroQual, Inc. 2003: User's Guide for RCA (Row-Column Advanced Ecological Systems Modeling Program). Mahwah, NJ.

Jin, K. R., J. M. Hamrick, and T. S. Tisdale, 2000: Application of a three-dimensional hydrodynamic model for Lake Okeechobee, Journal of Hydraulic Engineering, 106, 758-772.

Jin, K. R., Z. G. Ji, and J. M. Hamrick, 2002: Modeling winter circulation in Lake Okeechobee, Florida. Journal of Waterway, Port, Coastal, and Ocean Engineering, 128, 114-125.

Khangaonkar T. P., Z. Yang, C. DeGasperi, and K. Marshall. 2005: Modeling hydrothermal response of a reservoir to modifications at a high-head dam. Water International, 30, 378-388.

Park, K., A. Y. Kuo, J. Shen, and J. M. Hamrick, 1995: A three-dimensional hydrodynamic-eutrophication model (HEM3D): description of water quality and sediment processes submodels. The College of William and Mary, Virginia Institute of Marine Science. Special Report 327, 113 pp.

Rao, D. B. and D. J. Schwab, 1976: Two-dimensional normal modes in arbitrary enclosed basins on a rotation earth: Application to Lake Ontario and Superior. Phil. Trans. Royal Society, Series A, 281, 63-96.
Saylor, J. H., J. C. K. Huang, and R. O. Reid, 1980; Vortex modes in Southern Lake Michigan. J. Physical Oceanography, 10, 1814-1823.

Reese, B.K., M.A. Anderson and C. Amrhein, 2007: Hydrogen Sulfide Production and Volatilization in the Salton Sea. Final Report to Tetra Tech, Inc., Dept. of Environmental Sciences, University of California, Riverside.

Schladow, S. G., et al., 2004: Salton Sea Nutrients TMDL Modeling, SWRCD No. 01-265-170-0, Draft Final submitted to Colorado River Basin Regional Water Quality Control Board by Environmental Dynamics Laboratory, Department of Civil and Environmental Engineering, University of California, Davis.

Schwab, D. J., 1977: Internal free oscillations of Lake Ontario. Limnology and Oceanography, 22, 700-708.

Schladow, S. G. and Hamilton, D. P., 1996: Prediction of water quality in lakes and reservoirs: Part II – Model calibration, sensitivity analysis and application. Ecological Modelling 96: pp111-123.

Tetra Tech, 2002: User's Manual for Environmental Fluid Dynamics Code: Hydrodynamics, prepared for the US Environmental Protection Agency, Region 4, Tetra Tech, Inc. Fairfax, VA.

Tetra Tech, 2006a: User's Manual for Environmental Fluid Dynamics Code: Water Quality, prepared for the US Environmental Protection Agency, Region 4, Tetra Tech, Inc. Fairfax, VA.

Tetra Tech, 2006b: A Hydrodynamic and Water Quality Model for the Lower Charles River Basin, Massachusetts. A report to the US Environmental Protection Agency, Region 1, Tetra Tech, Inc. Fairfax, VA.

Tetra Tech, Inc., 2006c: The Environmental Fluid Dynamics Code, Theory and Computation: Volume 3: Water Quality Module. Tetra Tech, Inc. Fairfax, VA.

Thomann, R.V., J.R. Collier, A. Butt, E. Casman, L.C. Linker, 1994: Response of the Chesapeake Bay water quality model to loading scenarios. Report of the Modeling Subcommittee, CBP/TRS 101/94. U. S. EPA, Chesapeake Bay Program, Annapolis, MD.

Tillman, D.H., Cerco, C.F., Noel, M.R., Martin, J.L., and Hamrick, J. (2004). Three-Dimensional Eutrophication Model of the Lower St. Johns River, Florida., ERDC/EL TR-04-13, U.S. Army Engineer Research and Development Center, Vicksburg, MS.

Watts, J.M., B.K. Swan, M.A. Tiffany, S.H. Hurlbert, 2001: Thermal, mixing, and oxygen regimes of the Salton Sea, California, 19997-1999. Hydrobiologia. 466:159-176.

Wool, T. A., S. R. Davie, and H. N. Rodriguez, 2003: Development of three-dimensional hydrodynamic and water quality models to support TMDL decision process for the Neuse River estuary, North Carolina. Journal of Water Resources Planning and Management, 129, 295-306.

10. Appendix A. Excitation-Response Analysis of Circulation

Some additional insight into the circulation can be gained from an excitation-response point of view which describes the response of the Sea in terms of its normal or natural mode spatial response patterns having associated natural frequencies. Spatial and temporal variations in the wind field, the excitation, having similar structures as the normal modes produce resonant circulation responses. Exact calculation of the modal structure and frequencies for arbitrary shaped closed basins with topography using the linear shallow water equations

$$\begin{aligned} \partial_t u - fv &= -g\partial_x \zeta - \sigma u \\ \partial_t v + fu &= -g\partial_y \zeta - \sigma v \\ \partial_t \zeta + \partial_x (hu) + \partial_y (hv) &= 0 \end{aligned} \tag{A1}$$

(Rao and Schwab, 1976) is complex, but approximate frequencies for various external barotropic modes can be readily estimated (Hamrick, 1988). For large enclosed basins such as the Salton Sea, two classes of wave normal modes exist, the first class being gravity-inertia waves or irrotational modes and the second class corresponding to rotational modes or topographic Rossby waves. Representative parameters for the Salton Sea include a mean depth, H, of 10 meters, longitudinal axis length of 60 km and average width of approximately 25 km, and a Coriolis parameter, f, of 8E-5/sec. Based on these parameters, the external Rossby radius is approximately 125 km, compared with the mean sea width of approximately 25 km, indicating that rotation is can be of secondary significances. Estimates of the natural frequencies for long surface gravity waves can be made using the dispersion relationship for constant depth linear shallow water equations in a plane, rotation coordinate system

$$\begin{gathered} i\omega\left((i\omega-\sigma)^2 + f^2\right) + C^2\left(k_x^2 + k_y^2\right)(i\omega-\sigma) = 0 \\ \operatorname{Re}\omega = \frac{2\pi}{T}, \quad k_x = \frac{2\pi}{L_x}, \quad k_y = \frac{2\pi}{L_y} \\ C^2 = gH, \quad \sigma = c_b \frac{q}{H} \end{gathered} \tag{A2}$$

where is the complex frequency, kx and ky are the horizontal wave numbers, and is the inverse dampening or frictional time scale. Representative values of the resistance coefficient, cb , and the velocity magnitude scale, q, for the Salton Sea are 0.0025, and 10 cm/s. In the limit of infinite wave lengths, corresponding to non-propagating modes, (1) reduces to

$$\omega\left((i\omega-\sigma)^2 + f^2\right) = 0 \tag{A3}$$

Having roots

$$\omega = 0$$
$$\omega = -i\sigma \pm f \tag{A4}$$

corresponding to steady circulation and a damped inertial oscillation having a period and damping time scale

$$T_I = \frac{2\pi}{f} = 22\ hours$$
$$T_{ID} = \frac{1}{\sigma} = 11\ hours \tag{A5}$$

Normal modes at the inertial period can be show to be spurious. However responses to excitations having periodicity near the inertial period tend to be amplified and the proximity of the inertial period to the diurnal period suggest that the response should be sensitive to diurnal wind variability associate with sea breeze effects.

For surface gravity wave modes, the Coriolis term can to first approximation be neglected with (1) reducing to

$$\omega^2 + i\omega\sigma - C^2\left(k_x^2 + k_y^2\right) = 0 \tag{A6}$$

having the roots corresponding the period and damping time scales

$$T = \frac{1}{\sqrt{gH}\sqrt{\frac{1}{L_x^2} + \frac{1}{L_y^2} - \left(\frac{\sigma}{4\pi C}\right)^2}}$$
$$TD = \frac{2}{\sigma} \tag{A7}$$

Approximating the Salton Sea as a rectangular basin of length L and width B requires that the wave lengths be integer fractions of twice L and twice B with (6) becoming

$$T_{m,n} = \frac{2}{\sqrt{gH}\sqrt{\left(\frac{m}{L}\right)^2 + \left(\frac{n}{B}\right)^2 - \left(\frac{\sigma}{2\pi C}\right)^2}} \tag{A8}$$

The longest period, T1,0, corresponds to a uni-nodal standing wave along the long axis. Using a long axis length of approximately 60 km, (7) gives a period of approximately 3.3 hours with dissipation being negligible due to the short wave length. It can also be readily verified that inclusion of the Coriolis effect does not significantly alter this estimated period. The longest lateral period, T0,1, corresponding to a uni-nodal lateral standing wave is

approximately 1.4 hours. Oscillations in the depth average current having periods in the range of 1.4 to 3.3 hours are readily discernable, but weaker in magnitude than the inertial oscillations.

During period of density stratification, internal standing waves may also be excited. The preceding longitudinal and lateral oscillation period estimates can be approximately extended to internal oscillations by replacing the surface wave speed with the internal wave speed

$$C_i = \sqrt{\frac{\Delta\rho}{\rho} g H_{eff}} \tag{A9}$$

For a 5 oC temperature difference and a crude estimate of the effect layer depth as one half the average depth, Ci is approximately 0.15 m/s compared to the external wave speed for approximately 10 m/s. Thus the longest longitudinal and lateral oscillation period would be increased by a factor of approximately 65, to 9 and 3.8 days, respectively, with higher modes having correspondingly shorter integer factor periods. Investigation of the excitation of internal modes requires analysis of vertical current profiles and is currently in progress.

As noted, second class wave motions consistent with the horizontal scale of the Salton Sea will be topographic Rossby waves. These waves can be analyzed with the rigid lid from of (A1) and the introduction of a transport stream function.

$$\partial_t \left(\partial_x \left(\frac{1}{h} \partial_x \psi \right) + \partial_y \left(\frac{1}{h} \partial_y \psi \right) \right) + \frac{f}{h^2} \left(\partial_x \psi \partial_y h - \partial_y \psi \partial_x h \right) = 0 \tag{A10}$$

Various estimates of normal modes and natural frequencies have been presented in the literature based on analysis of (A10) for idealized water body shapes and depth profiles, with estimates of the shortest oscillation period being of the form

$$T = \gamma \frac{2\pi}{f} \tag{A11}$$

For circular basins with linear and parabolic depth profiles (Saylor et al., 1980) the values of are 5 and 7 respectively, for the gravest mode, while the large wave number limit gives a minimum value of 3 independent of the presumed depth profile. For an elliptical shaped basin, with an elliptic paraboloidal depth profile

$$\gamma = \sqrt{\frac{49 - 9\alpha^2}{1 - \alpha^2}}$$
$$\alpha = \frac{B^2 - L^2}{B^2 + L^2} \tag{A12}$$

which would give a corresponding value of on the order of 10 for the entire Salton Sea.

For elongated rectangular basins with a cosine lateral depth profile and maximum and minimum depths 1.75 and 2.5 times the mean depth, Hamrick (1989) estimated to be approximately 3.1. These results suggest that the Salton Sea could support topographic Rossby wave modes with periods ranging form 65 to 200 hours. Schwab (1977) discusses analyses of internal topographic waves which would have significantly longer natural periods. Unfortunately the lengths of the current meter records in the Salton Sea prohibit reliable estimation of topographic wave existence.

11. Appendix B. Complete Results for Fifteen Year Water Quality Model Scenarios

B.0 Base Case – Full Sea with results shown for Station SS-1

B.1 Scenario 1 – Northern Sea and Southern Estuary with no withdrawal and treatment and no reduction in external phosphorous load

B.2 Scenario 2 – Northern Sea and Southern Estuary with withdrawal and treatment and no reduction in external phosphorous load

B.3 Scenario 3 – Northern Sea and Southern Estuary with no withdrawal and treatment and 90 % reduction in external phosphorous load

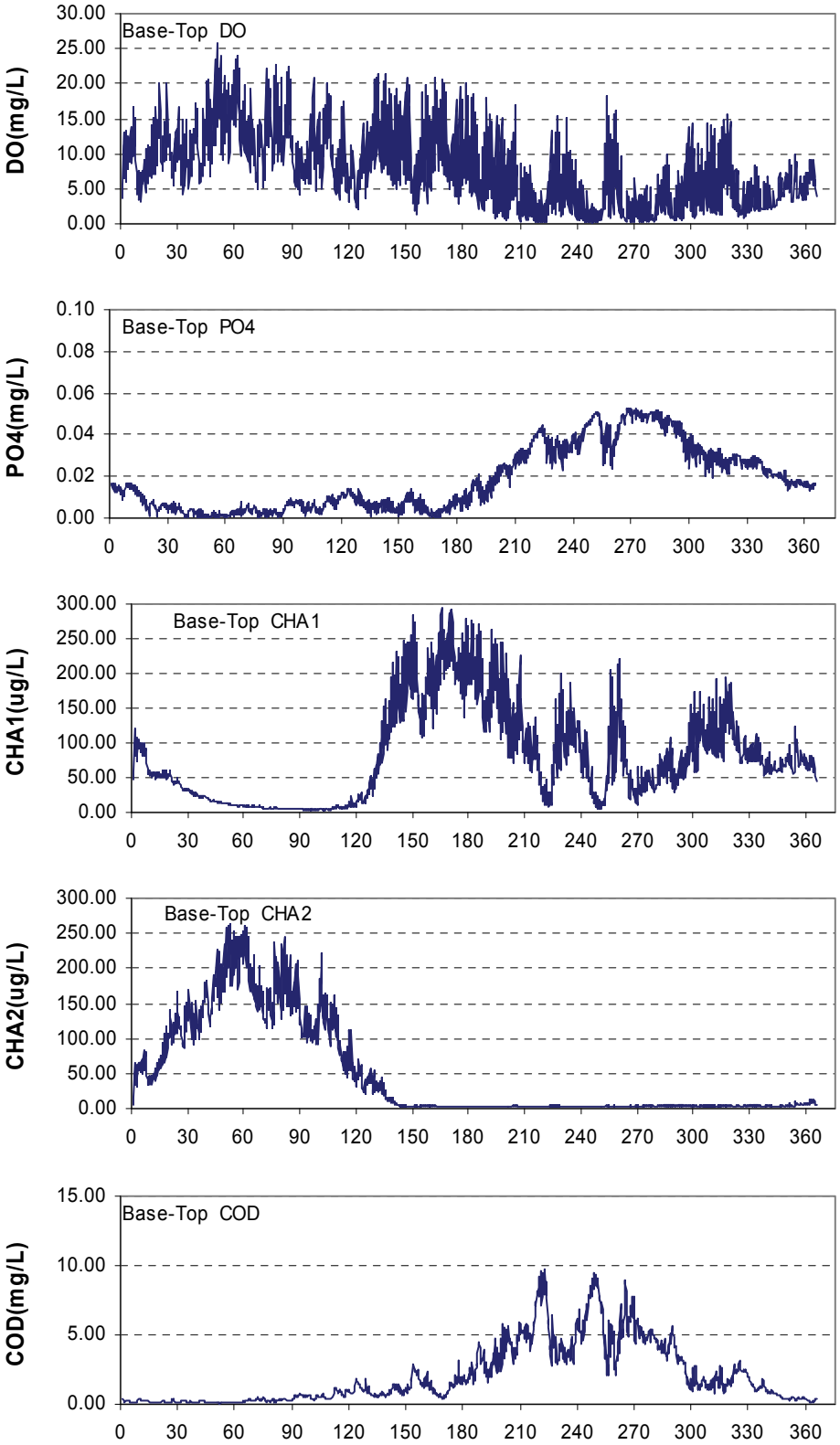
Base-Top DO
DO(mg/L)
30.00
25.00
20.00
15.00
10.00
5.00
0.00
0 30 60 90 120 150 180 210 240 270 300 330 360
Base-Top PO4
PO4(mg/L)
0.10
0.08
0.06
0.04
0.02
0.00
0 30 60 90 120 150 180 210 240 270 300 330 360
Base-Top CHA1
CHA1(ug/L)
300.00
250.00
200.00
150.00
100.00
50.00
0.00
0 30 60 90 120 150 180 210 240 270 300 330 360
Base-Top CHA2
CHA2(ug/L)
300.00
250.00
200.00
150.00
100.00
50.00
0.00
0 30 60 90 120 150 180 210 240 270 300 330 360
Base-Top COD
COD(mg/L)
15.00
10.00
5.00
0.00
0 30 60 90 120 150 180 210 240 270 300 330 360

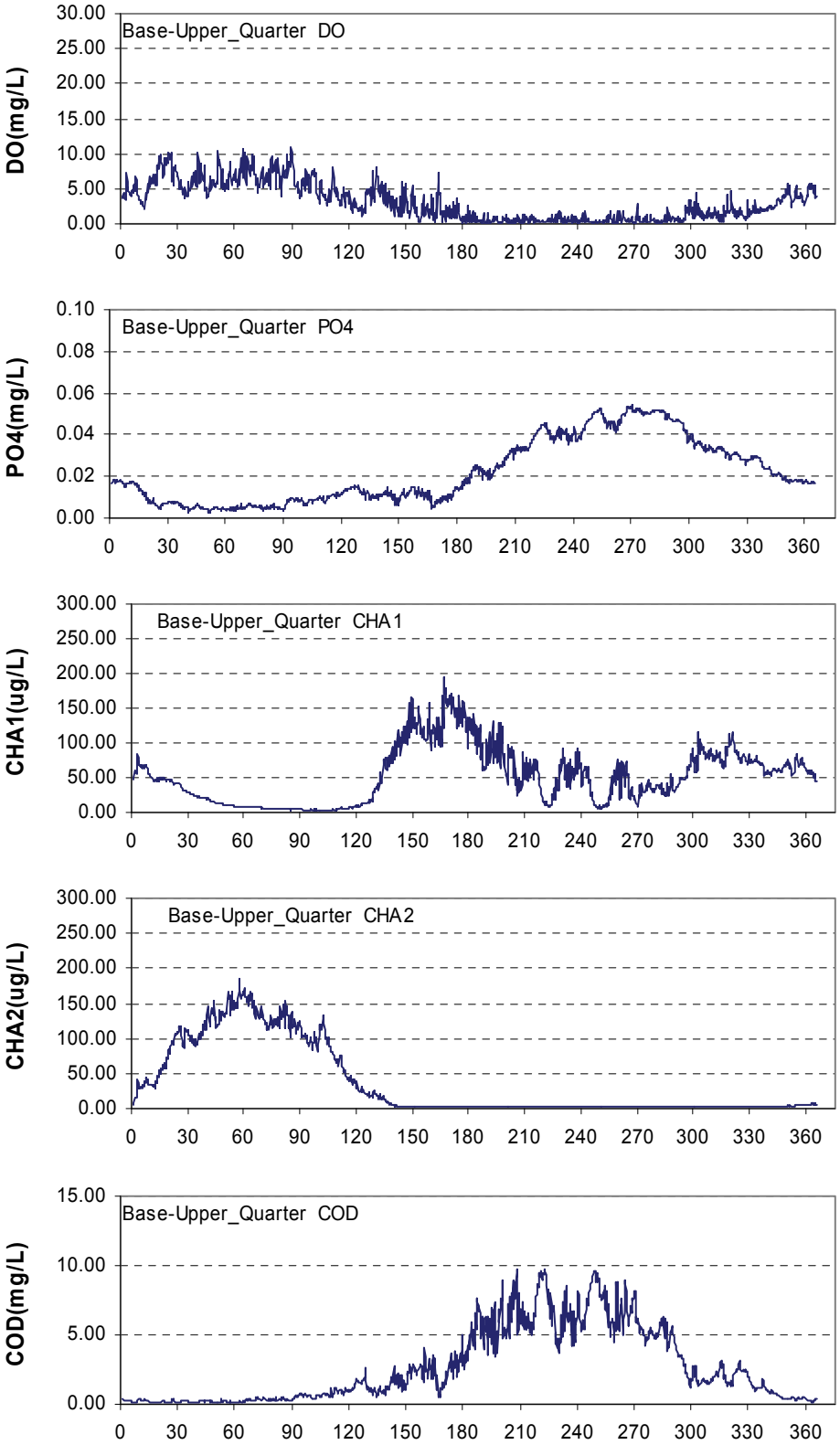
Base-Upper_Quarter DO
DO(mg/L)
30.00
25.00
20.00
15.00
10.00
5.00
0.00
0 30 60 90 120 150 180 210 240 270 300 330 360
Base-Upper_Quarter PO4
PO4(mg/L)
0.10
0.08
0.06
0.04
0.02
0.00
0 30 60 90 120 150 180 210 240 270 300 330 360
Base-Upper_Quarter CHA1
CHA1(ug/L)
300.00
250.00
200.00
150.00
100.00
50.00
0.00
0 30 60 90 120 150 180 210 240 270 300 330 360
Base-Upper_Quarter CHA2
CHA2(ug/L)
300.00
250.00
200.00
150.00
100.00
50.00
0.00
0 30 60 90 120 150 180 210 240 270 300 330 360
Base-Upper_Quarter COD
COD(mg/L)
15.00
10.00
5.00
0.00
0 30 60 90 120 150 180 210 240 270 300 330 360

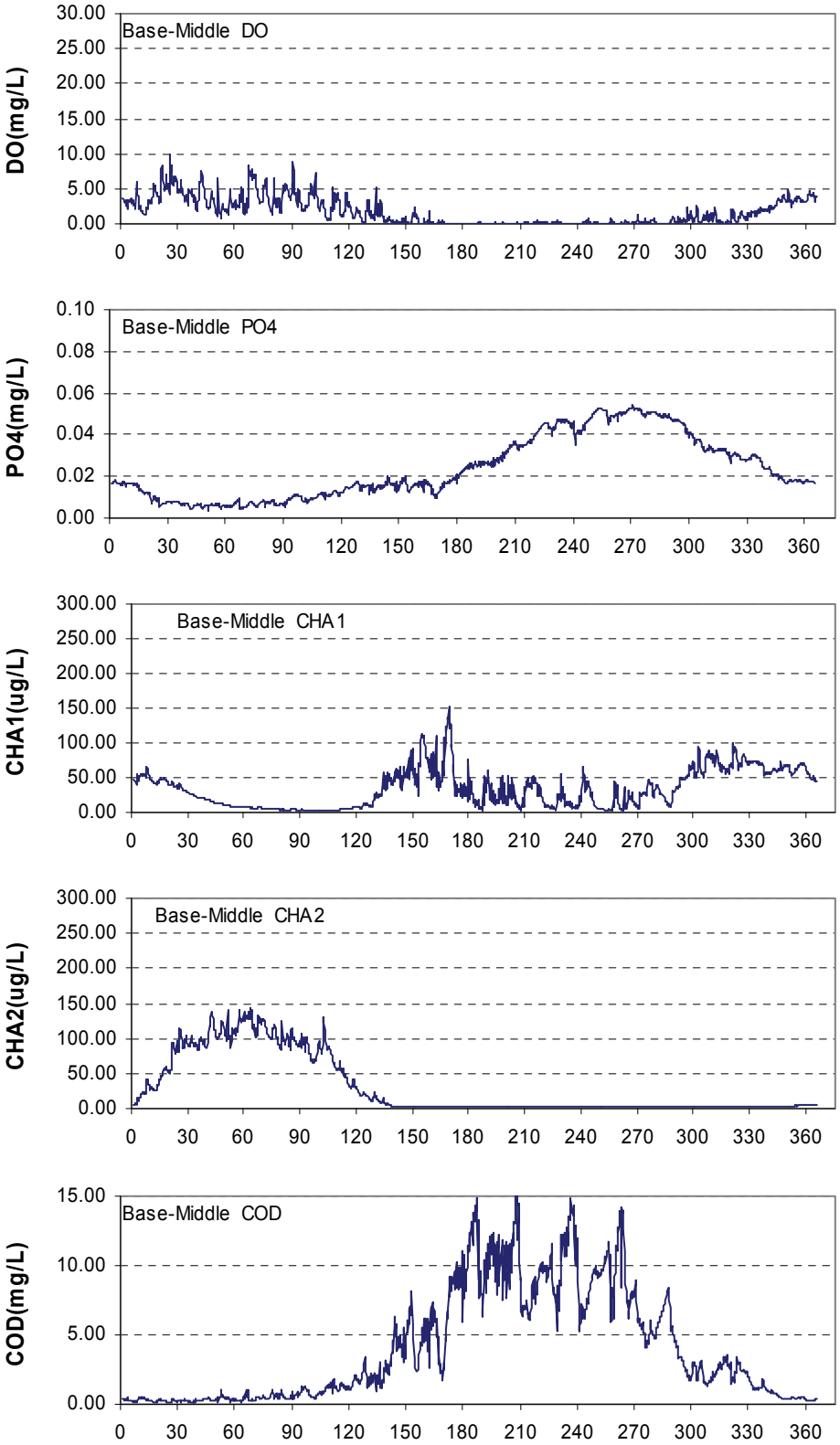
Base-Middle DO
DO(mg/L)
30.00
25.00
20.00
15.00
10.00
5.00
0.00
0 30 60 90 120 150 180 210 240 270 300 330 360
Base-Middle PO4
PO4(mg/L)
0.10
0.08
0.06
0.04
0.02
0.00
0 30 60 90 120 150 180 210 240 270 300 330 360
Base-Middle CHA1
CHA1(ug/L)
300.00
250.00
200.00
150.00
100.00
50.00
0.00
0 30 60 90 120 150 180 210 240 270 300 330 360
Base-Middle CHA2
CHA2(ug/L)
300.00
250.00
200.00
150.00
100.00
50.00
0.00
0 30 60 90 120 150 180 210 240 270 300 330 360
Base-Middle COD
COD(mg/L)
15.00
10.00
5.00
0.00
0 30 60 90 120 150 180 210 240 270 300 330 360

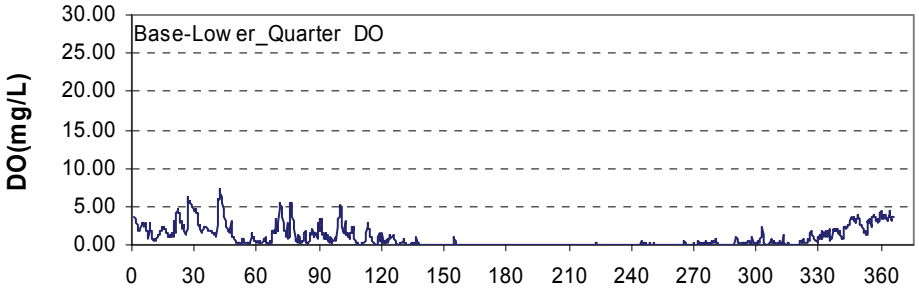
Base-Low er_Quarter DO
DO(mg/L)
30.00
25.00
20.00
15.00
10.00
5.00
0.00
0 30 60 90 120 150 180 210 240 270 300 330 360

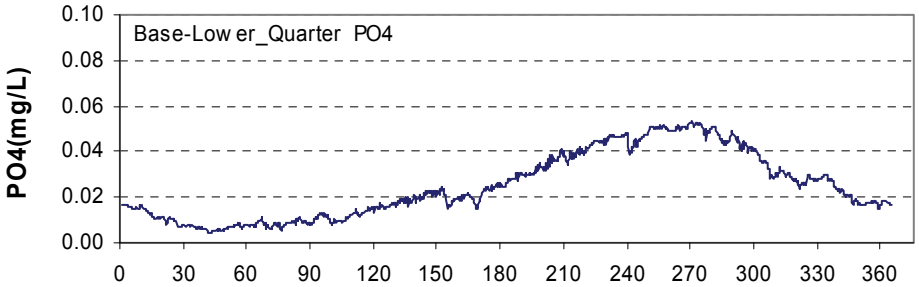
Base-Low er_Quarter PO4
PO4(mg/L)
0.10
0.08
0.06
0.04
0.02
0.00
0 30 60 90 120 150 180 210 240 270 300 330 360

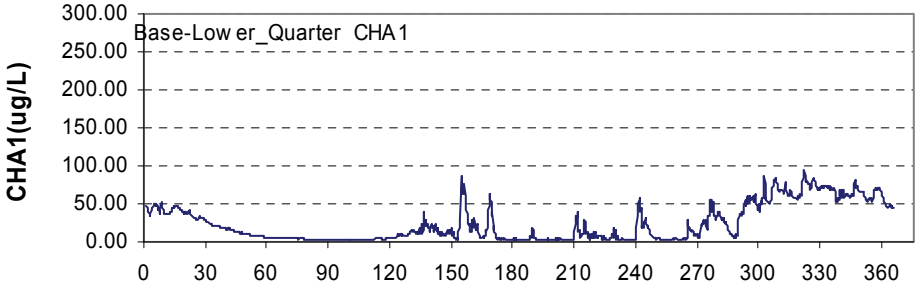
Base-Low er_Quarter CHA1
CHA1(ug/L)
300.00
250.00
200.00
150.00
100.00
50.00
0.00
0 30 60 90 120 150 180 210 240 270 300 330 360

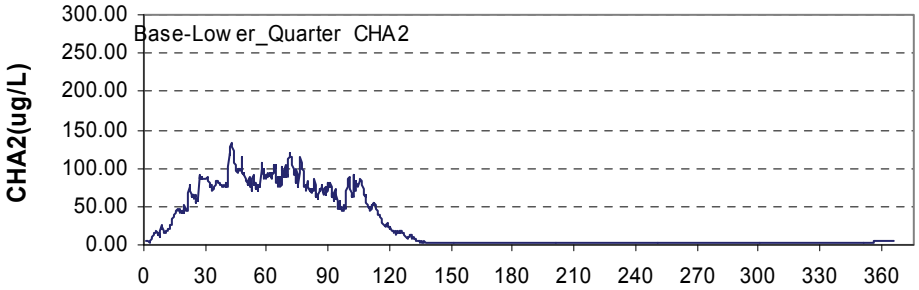
Base-Low er_Quarter CHA2
CHA2(ug/L)
300.00
250.00
200.00
150.00
100.00
50.00
0.00
0 30 60 90 120 150 180 210 240 270 300 330 360

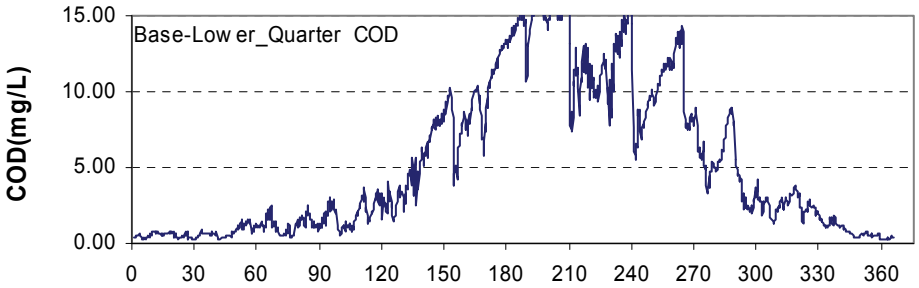
Base-Low er_Quarter COD
COD(mg/L)
15.00
10.00
5.00
0.00
0 30 60 90 120 150 180 210 240 270 300 330 360

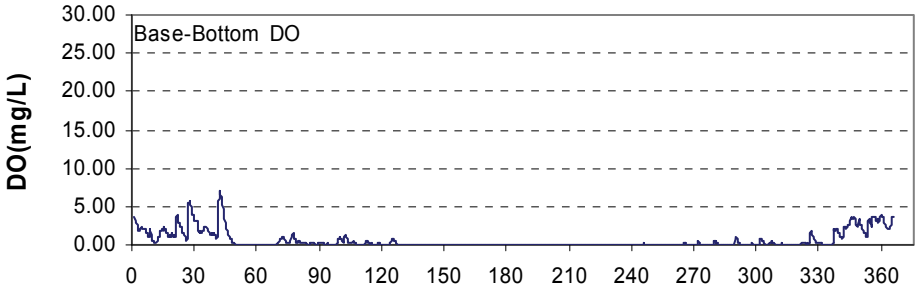
Base-Bottom DO
DO(mg/L)
30.00
25.00
20.00
15.00
10.00
5.00
0.00
0 30 60 90 120 150 180 210 240 270 300 330 360

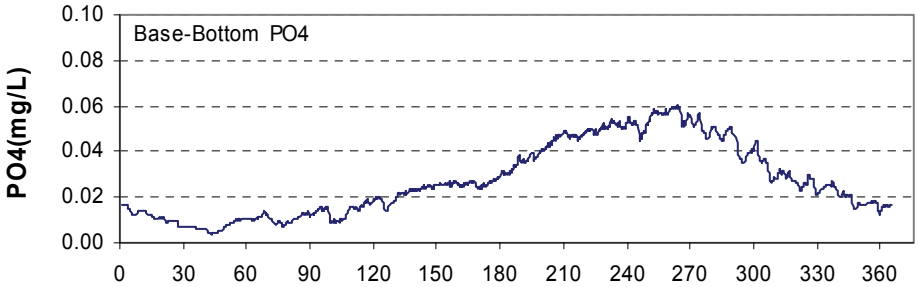
Base-Bottom PO4
PO4(mg/L)
0.10
0.08
0.06
0.04
0.02
0.00
0 30 60 90 120 150 180 210 240 270 300 330 360

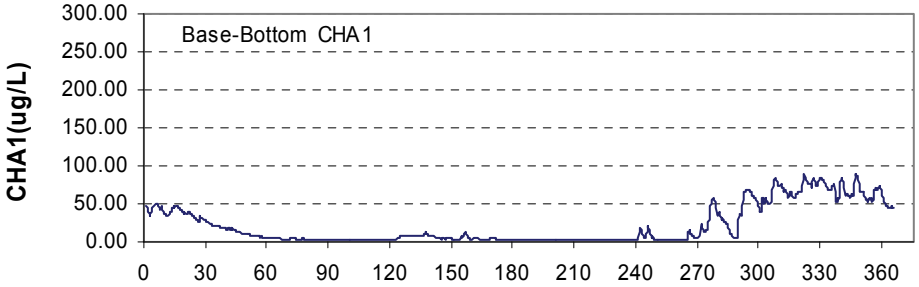
Base-Bottom CHA1
CHA1(ug/L)
300.00
250.00
200.00
150.00
100.00
50.00
0.00
0 30 60 90 120 150 180 210 240 270 300 330 360

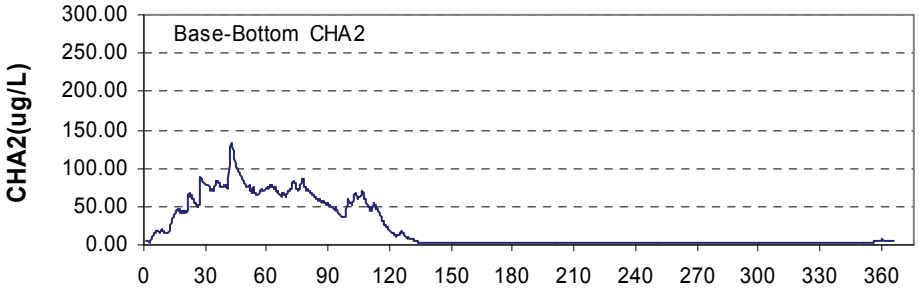
Base-Bottom CHA2
CHA2(ug/L)
300.00
250.00
200.00
150.00
100.00
50.00
0.00
0 30 60 90 120 150 180 210 240 270 300 330 360

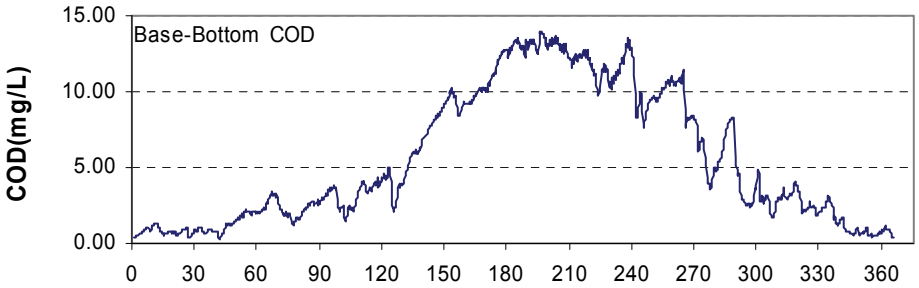
Base-Bottom COD
COD(mg/L)
15.00
10.00
5.00
0.00
0 30 60 90 120 150 180 210 240 270 300 330 360

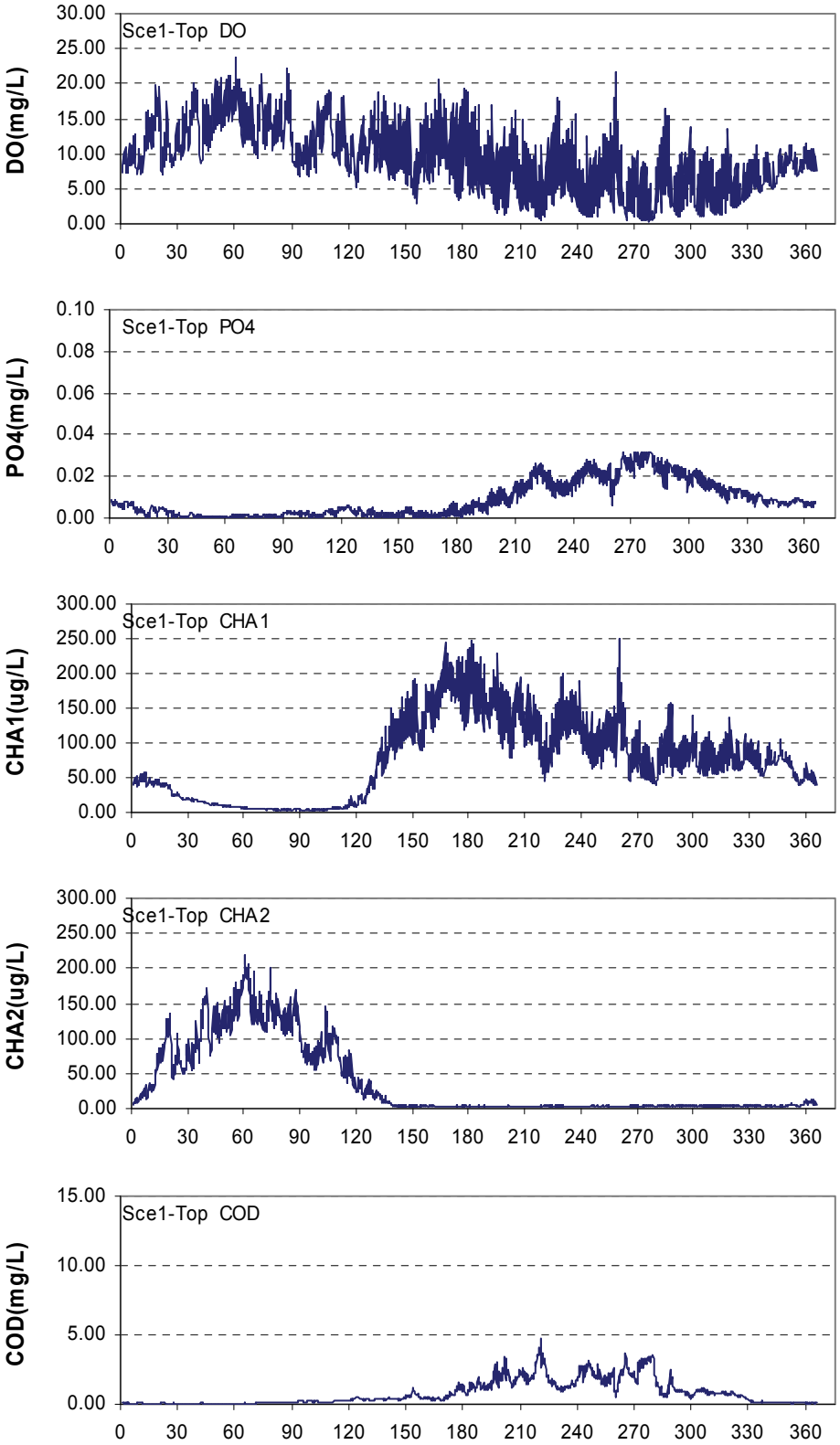
Sce1-Top DO
DO(mg/L)
30.00
25.00
20.00
15.00
10.00
5.00
0.00
0 30 60 90 120 150 180 210 240 270 300 330 360
Sce1-Top PO4
PO4(mg/L)
0.10
0.08
0.06
0.04
0.02
0.00
0 30 60 90 120 150 180 210 240 270 300 330 360
Sce1-Top CHA1
CHA1(ug/L)
300.00
250.00
200.00
150.00
100.00
50.00
0.00
0 30 60 90 120 150 180 210 240 270 300 330 360
Sce1-Top CHA2
CHA2(ug/L)
300.00
250.00
200.00
150.00
100.00
50.00
0.00
0 30 60 90 120 150 180 210 240 270 300 330 360
Sce1-Top COD
COD(mg/L)
15.00
10.00
5.00
0.00
0 30 60 90 120 150 180 210 240 270 300 330 360

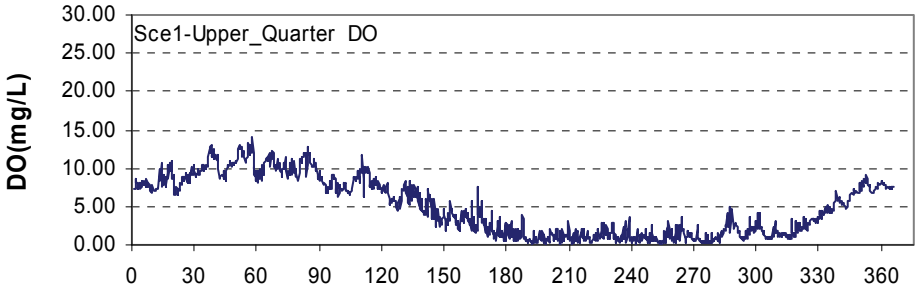
Sce1-Upper_Quarter DO
DO(mg/L)
30.00
25.00
20.00
15.00
10.00
5.00
0.00
0 30 60 90 120 150 180 210 240 270 300 330 360

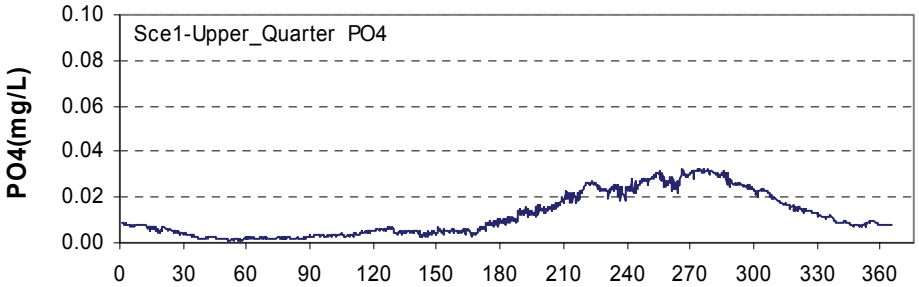
Sce1-Upper_Quarter PO4
PO4(mg/L)
0.10
0.08
0.06
0.04
0.02
0.00
0 30 60 90 120 150 180 210 240 270 300 330 360

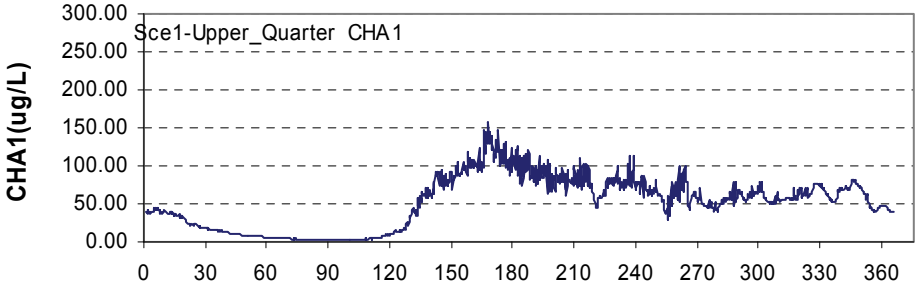
Sce1-Upper_Quarter CHA1
CHA1(ug/L)
300.00
250.00
200.00
150.00
100.00
50.00
0.00
0 30 60 90 120 150 180 210 240 270 300 330 360

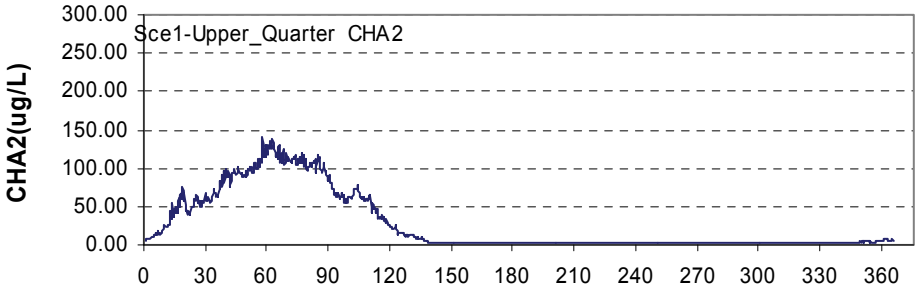
Sce1-Upper_Quarter CHA2
CHA2(ug/L)
300.00
250.00
200.00
150.00
100.00
50.00
0.00
0 30 60 90 120 150 180 210 240 270 300 330 360

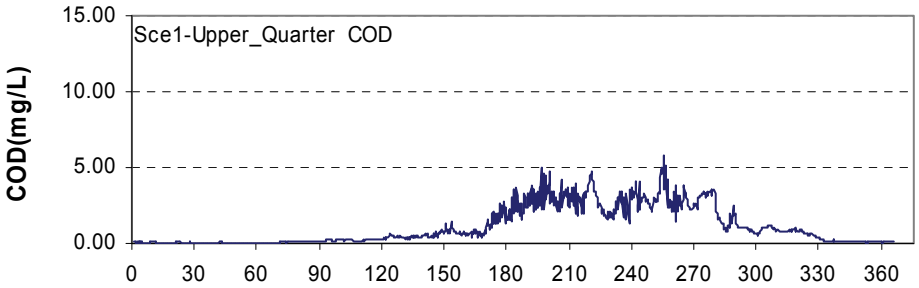
Sce1-Upper_Quarter COD
COD(mg/L)
15.00
10.00
5.00
0.00
0 30 60 90 120 150 180 210 240 270 300 330 360

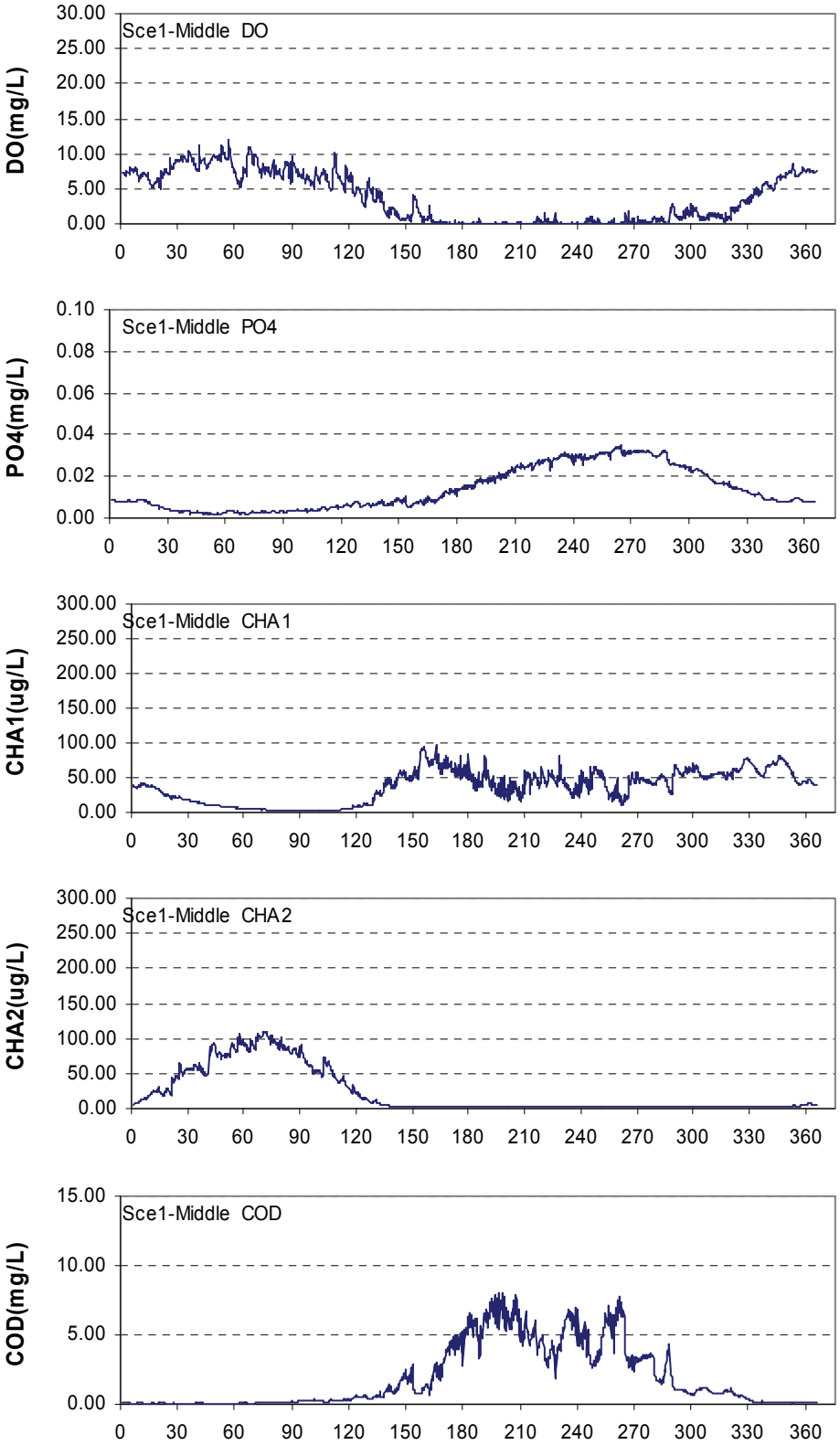
Sce1-Middle DO
DO(mg/L)
30.00
25.00
20.00
15.00
10.00
5.00
0.00
0 30 60 90 120 150 180 210 240 270 300 330 360
Sce1-Middle PO4
PO4(mg/L)
0.10
0.08
0.06
0.04
0.02
0.00
0 30 60 90 120 150 180 210 240 270 300 330 360
Sce1-Middle CHA1
CHA1(ug/L)
300.00
250.00
200.00
150.00
100.00
50.00
0.00
0 30 60 90 120 150 180 210 240 270 300 330 360
Sce1-Middle CHA2
CHA2(ug/L)
300.00
250.00
200.00
150.00
100.00
50.00
0.00
0 30 60 90 120 150 180 210 240 270 300 330 360
Sce1-Middle COD
COD(mg/L)
15.00
10.00
5.00
0.00
0 30 60 90 120 150 180 210 240 270 300 330 360

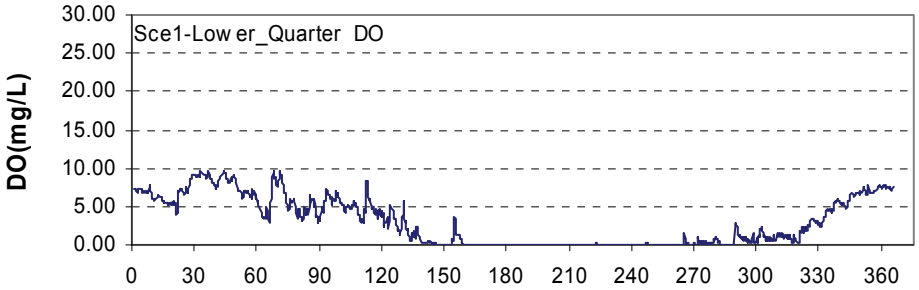
Sce1-Low er_Quarter DO
DO(mg/L)
30.00
25.00
20.00
15.00
10.00
5.00
0.00
0 30 60 90 120 150 180 210 240 270 300 330 360

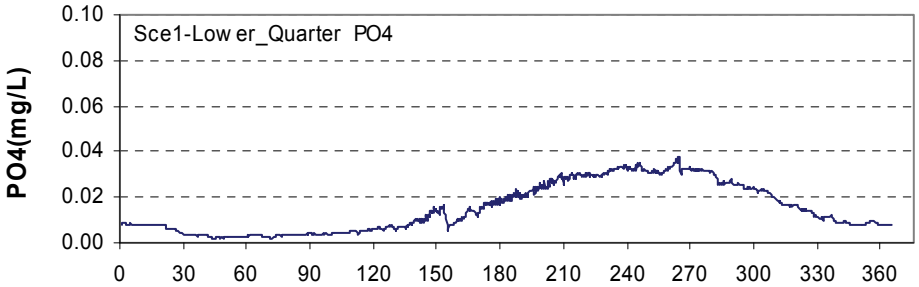
Sce1-Low er_Quarter PO4
PO4(mg/L)
0.10
0.08
0.06
0.04
0.02
0.00
0 30 60 90 120 150 180 210 240 270 300 330 360

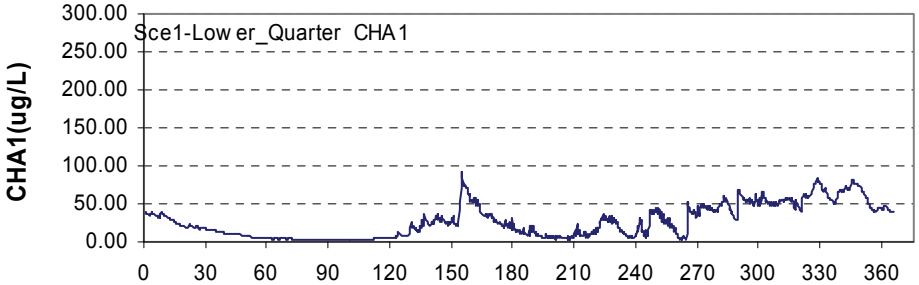
Sce1-Low er_Quarter CHA1
CHA1(ug/L)
300.00
250.00
200.00
150.00
100.00
50.00
0.00
0 30 60 90 120 150 180 210 240 270 300 330 360

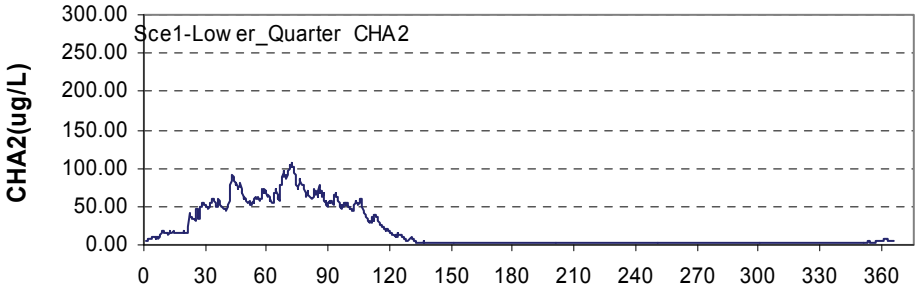
Sce1-Low er_Quarter CHA2
CHA2(ug/L)
300.00
250.00
200.00
150.00
100.00
50.00
0.00
0 30 60 90 120 150 180 210 240 270 300 330 360

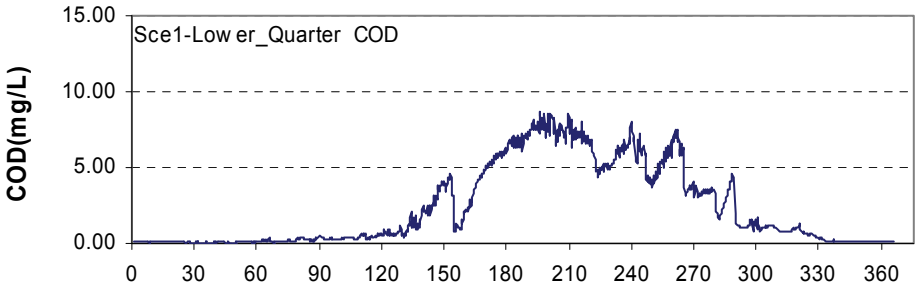
Sce1-Low er_Quarter COD
COD(mg/L)
15.00
10.00
5.00
0.00
0 30 60 90 120 150 180 210 240 270 300 330 360

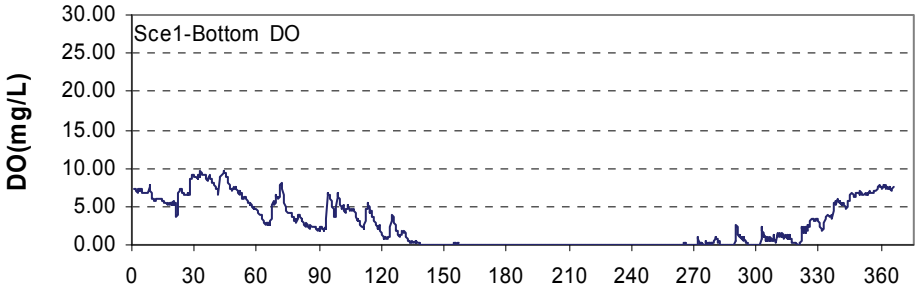
Sce1-Bottom DO
DO(mg/L)
30.00
25.00
20.00
15.00
10.00
5.00
0.00
0 30 60 90 120 150 180 210 240 270 300 330 360

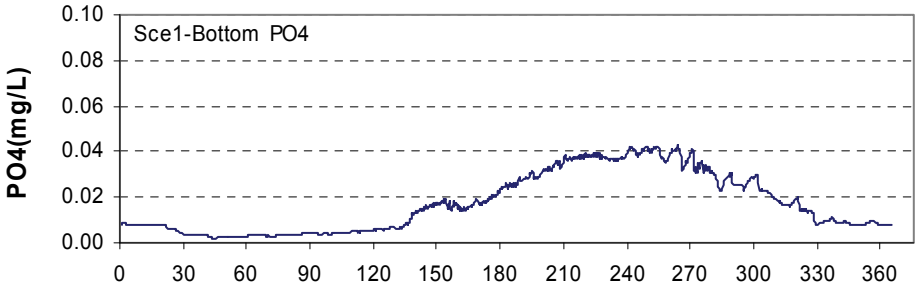
Sce1-Bottom PO4
PO4(mg/L)
0.10
0.08
0.06
0.04
0.02
0.00
0 30 60 90 120 150 180 210 240 270 300 330 360

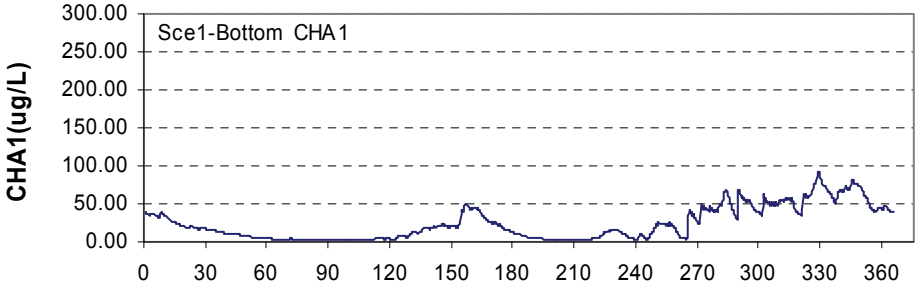
Sce1-Bottom CHA1
CHA1(ug/L)
300.00
250.00
200.00
150.00
100.00
50.00
0.00
0 30 60 90 120 150 180 210 240 270 300 330 360

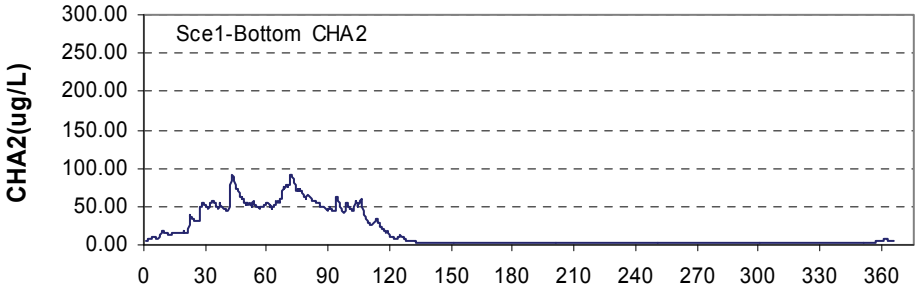
Sce1-Bottom CHA2
CHA2(ug/L)
300.00
250.00
200.00
150.00
100.00
50.00
0.00
0 30 60 90 120 150 180 210 240 270 300 330 360

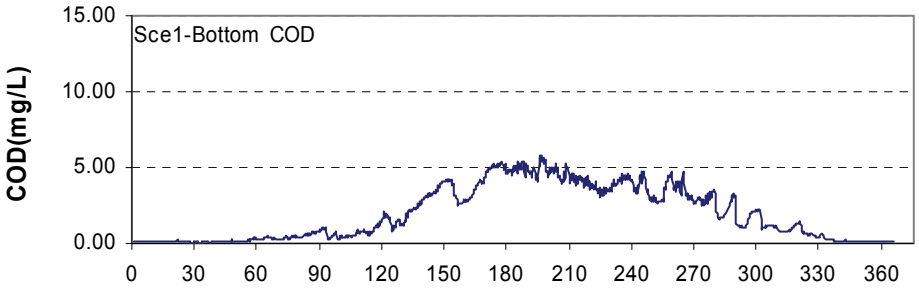
Sce1-Bottom COD
COD(mg/L)
15.00
10.00
5.00
0.00
0 30 60 90 120 150 180 210 240 270 300 330 360

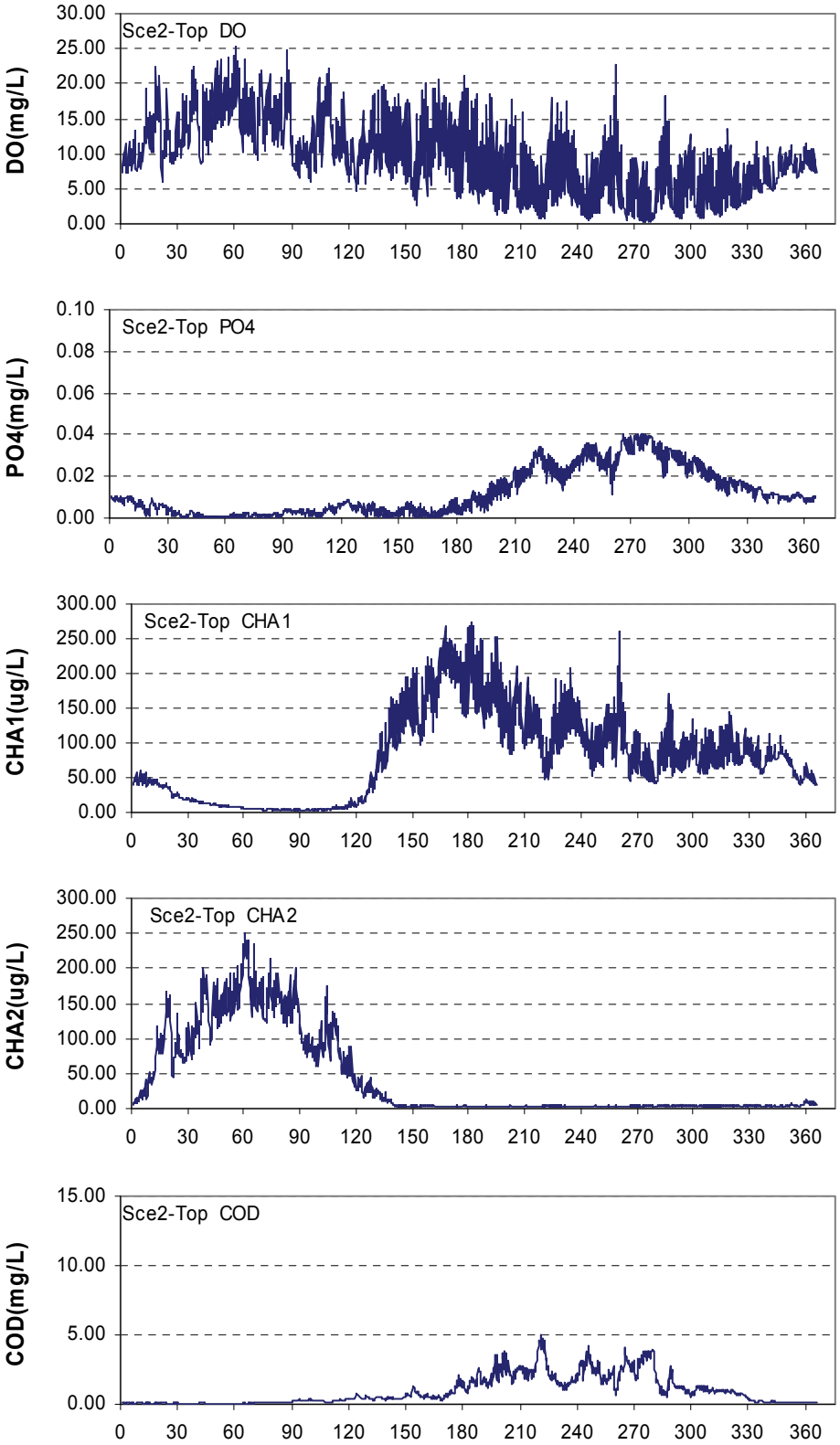
Sce2-Top DO
DO(mg/L)
30.00
25.00
20.00
15.00
10.00
5.00
0.00
0 30 60 90 120 150 180 210 240 270 300 330 360
Sce2-Top PO4
PO4(mg/L)
0.10
0.08
0.06
0.04
0.02
0.00
0 30 60 90 120 150 180 210 240 270 300 330 360
Sce2-Top CHA1
CHA1(ug/L)
300.00
250.00
200.00
150.00
100.00
50.00
0.00
0 30 60 90 120 150 180 210 240 270 300 330 360
Sce2-Top CHA2
CHA2(ug/L)
300.00
250.00
200.00
150.00
100.00
50.00
0.00
0 30 60 90 120 150 180 210 240 270 300 330 360
Sce2-Top COD
COD(mg/L)
15.00
10.00
5.00
0.00
0 30 60 90 120 150 180 210 240 270 300 330 360

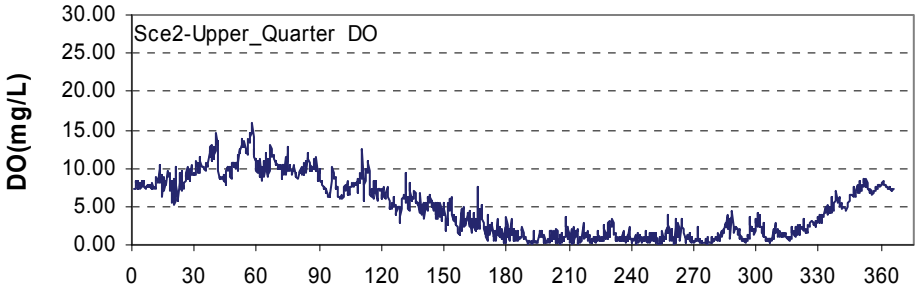
Sce2-Upper_Quarter DO
DO(mg/L)
30.00
25.00
20.00
15.00
10.00
5.00
0.00
0 30 60 90 120 150 180 210 240 270 300 330 360

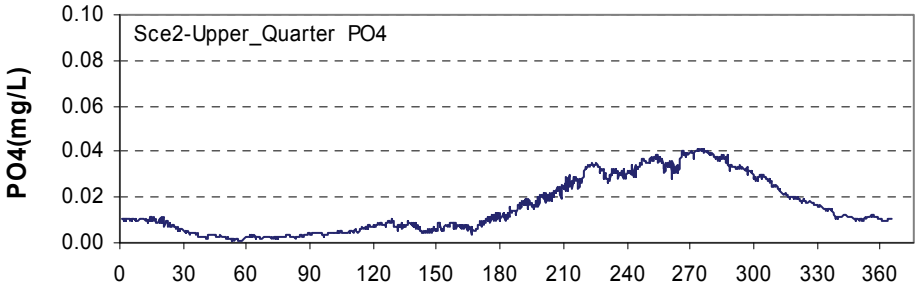
Sce2-Upper_Quarter PO4
PO4(mg/L)
0.10
0.08
0.06
0.04
0.02
0.00
0 30 60 90 120 150 180 210 240 270 300 330 360

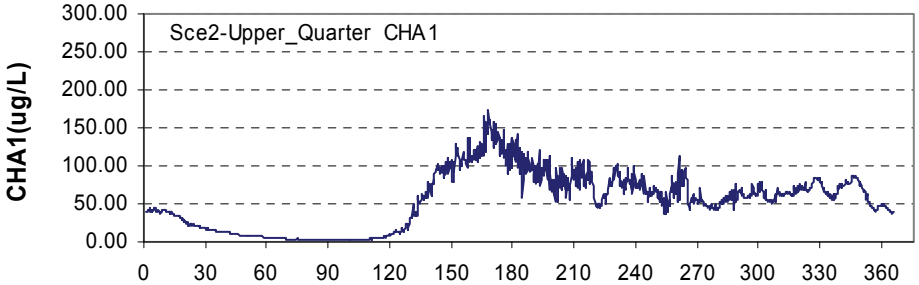
Sce2-Upper_Quarter CHA1
CHA1(ug/L)
300.00
250.00
200.00
150.00
100.00
50.00
0.00
0 30 60 90 120 150 180 210 240 270 300 330 360

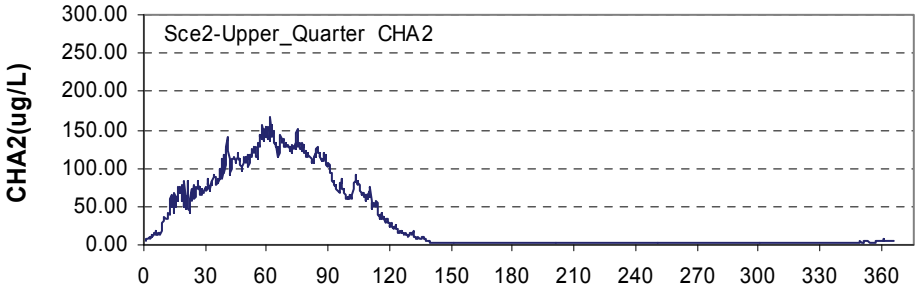
Sce2-Upper_Quarter CHA2
CHA2(ug/L)
300.00
250.00
200.00
150.00
100.00
50.00
0.00
0 30 60 90 120 150 180 210 240 270 300 330 360

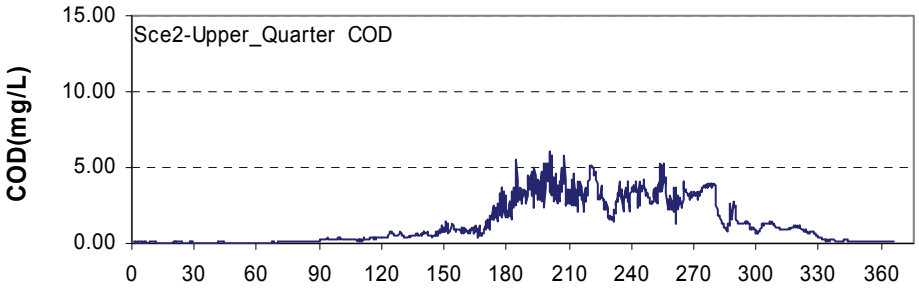
Sce2-Upper_Quarter COD
COD(mg/L)
15.00
10.00
5.00
0.00
0 30 60 90 120 150 180 210 240 270 300 330 360

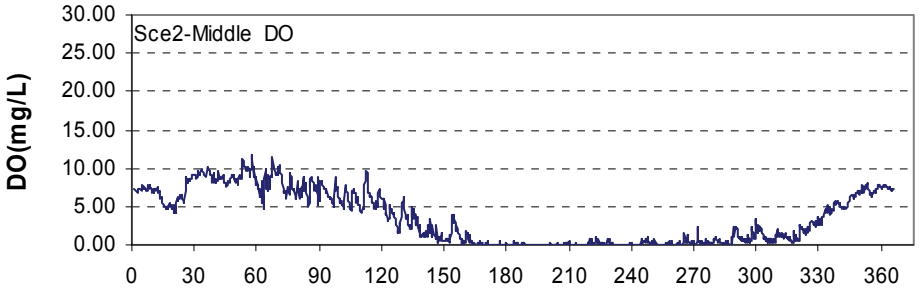
Sce2-Middle DO
DO(mg/L)
30.00
25.00
20.00
15.00
10.00
5.00
0.00
0 30 60 90 120 150 180 210 240 270 300 330 360

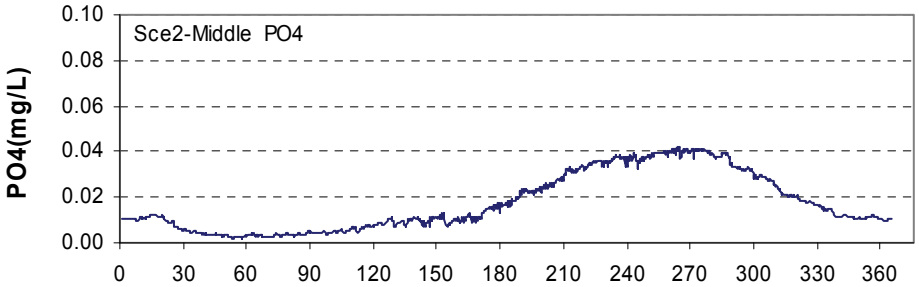
Sce2-Middle PO4
PO4(mg/L)
0.10
0.08
0.06
0.04
0.02
0.00
0 30 60 90 120 150 180 210 240 270 300 330 360

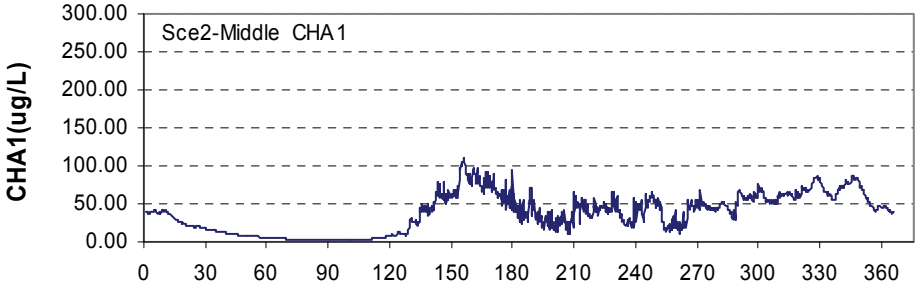
Sce2-Middle CHA1
CHA1(ug/L)
300.00
250.00
200.00
150.00
100.00
50.00
0.00
0 30 60 90 120 150 180 210 240 270 300 330 360

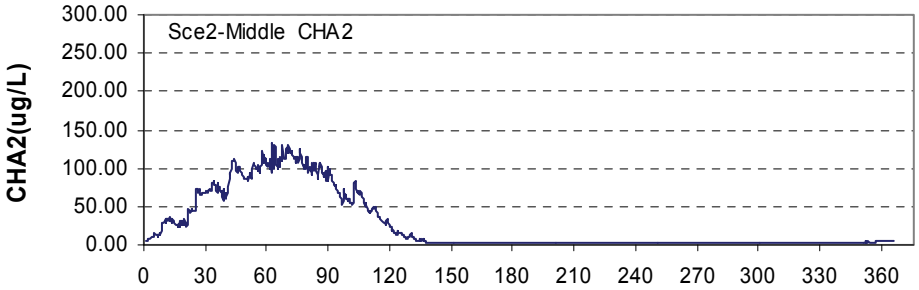
Sce2-Middle CHA2
CHA2(ug/L)
300.00
250.00
200.00
150.00
100.00
50.00
0.00
0 30 60 90 120 150 180 210 240 270 300 330 360

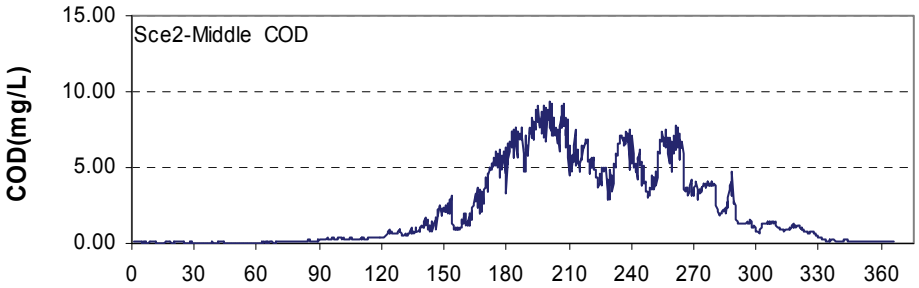
Sce2-Middle COD
COD(mg/L)
15.00
10.00
5.00
0.00
0 30 60 90 120 150 180 210 240 270 300 330 360

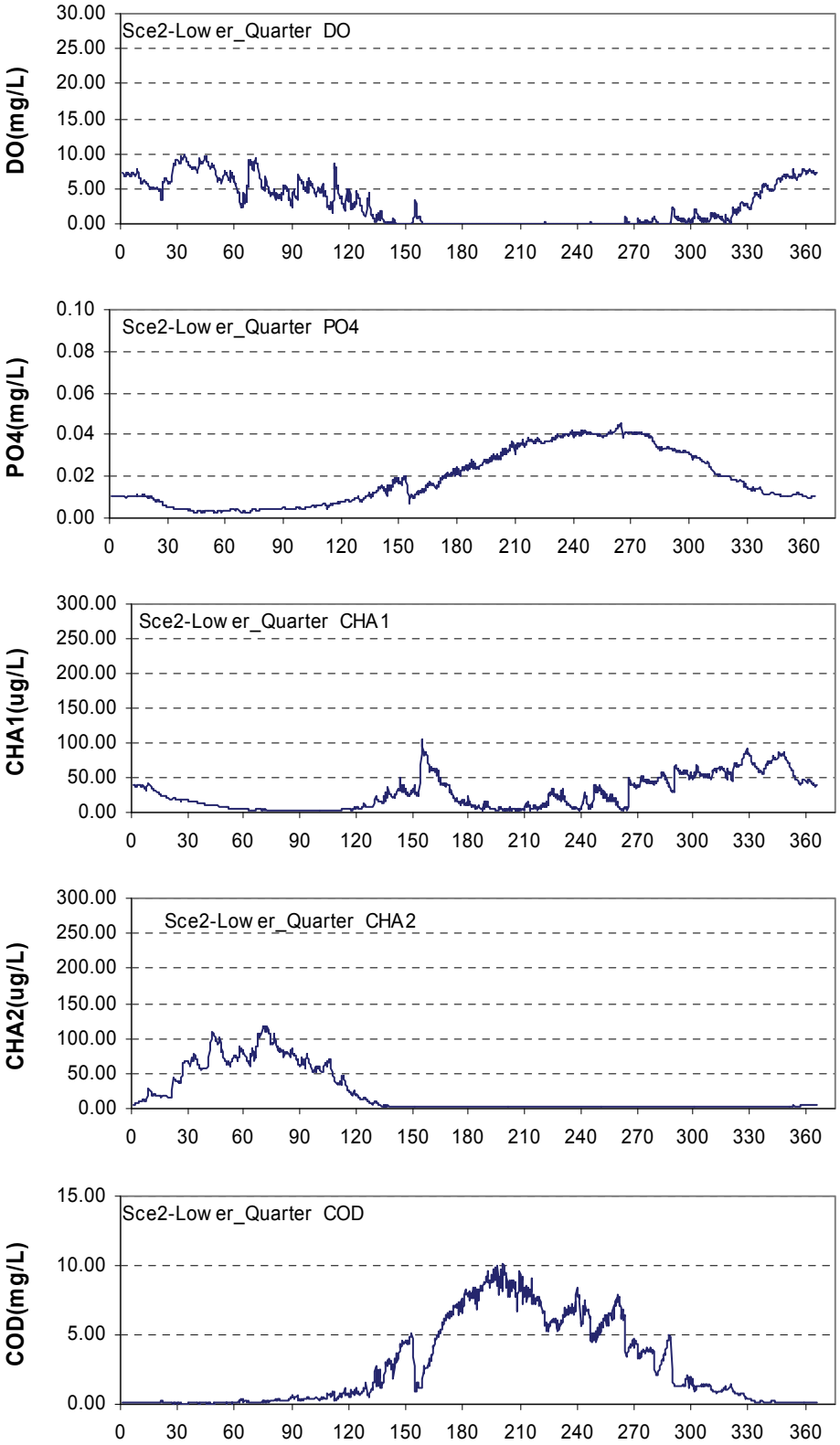
Sce2-Low er_Quarter DO
DO(mg/L)
30.00
25.00
20.00
15.00
10.00
5.00
0.00
0 30 60 90 120 150 180 210 240 270 300 330 360
Sce2-Low er_Quarter PO4
PO4(mg/L)
0.10
0.08
0.06
0.04
0.02
0.00
0 30 60 90 120 150 180 210 240 270 300 330 360
Sce2-Low er_Quarter CHA1
CHA1(ug/L)
300.00
250.00
200.00
150.00
100.00
50.00
0.00
0 30 60 90 120 150 180 210 240 270 300 330 360
Sce2-Low er_Quarter CHA2
CHA2(ug/L)
300.00
250.00
200.00
150.00
100.00
50.00
0.00
0 30 60 90 120 150 180 210 240 270 300 330 360
Sce2-Low er_Quarter COD
COD(mg/L)
15.00
10.00
5.00
0.00
0 30 60 90 120 150 180 210 240 270 300 330 360

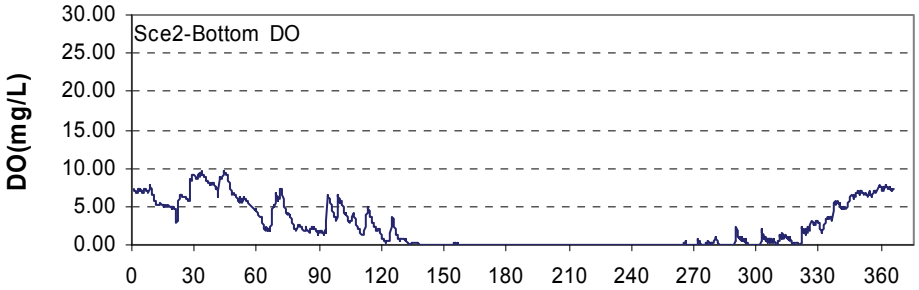
Sce2-Bottom DO
DO(mg/L)
30.00
25.00
20.00
15.00
10.00
5.00
0.00
0 30 60 90 120 150 180 210 240 270 300 330 360

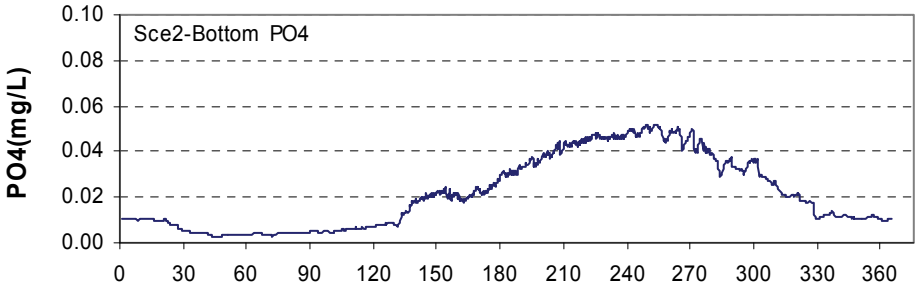
Sce2-Bottom PO4
PO4(mg/L)
0.10
0.08
0.06
0.04
0.02
0.00
0 30 60 90 120 150 180 210 240 270 300 330 360

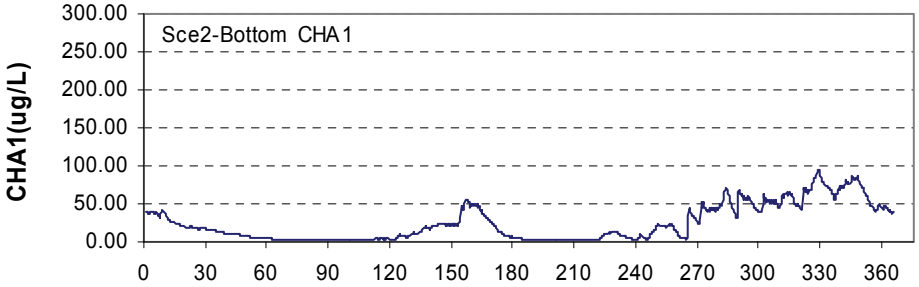
Sce2-Bottom CHA1
CHA1(ug/L)
300.00
250.00
200.00
150.00
100.00
50.00
0.00
0 30 60 90 120 150 180 210 240 270 300 330 360

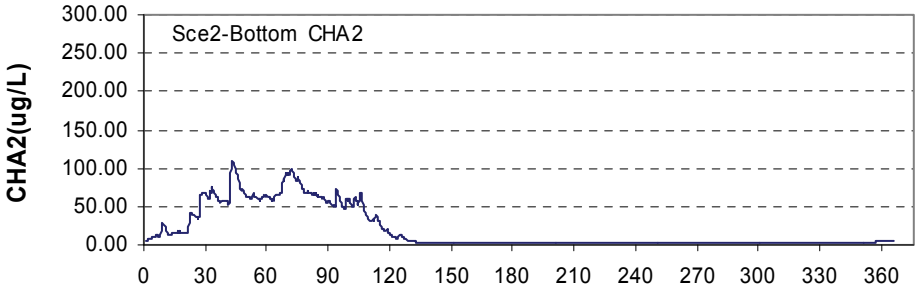
Sce2-Bottom CHA2
CHA2(ug/L)
300.00
250.00
200.00
150.00
100.00
50.00
0.00
0 30 60 90 120 150 180 210 240 270 300 330 360

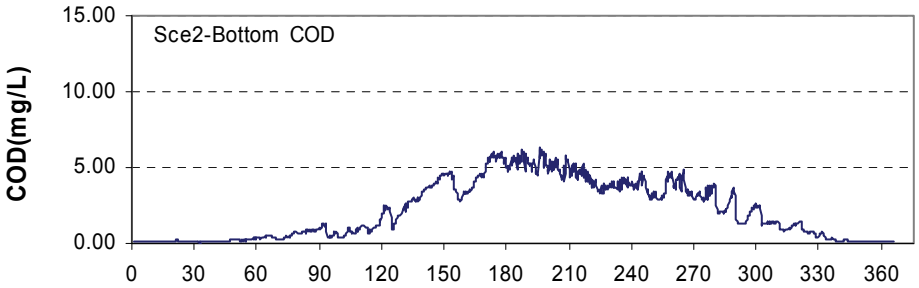
Sce2-Bottom COD
COD(mg/L)
15.00
10.00
5.00
0.00
0 30 60 90 120 150 180 210 240 270 300 330 360

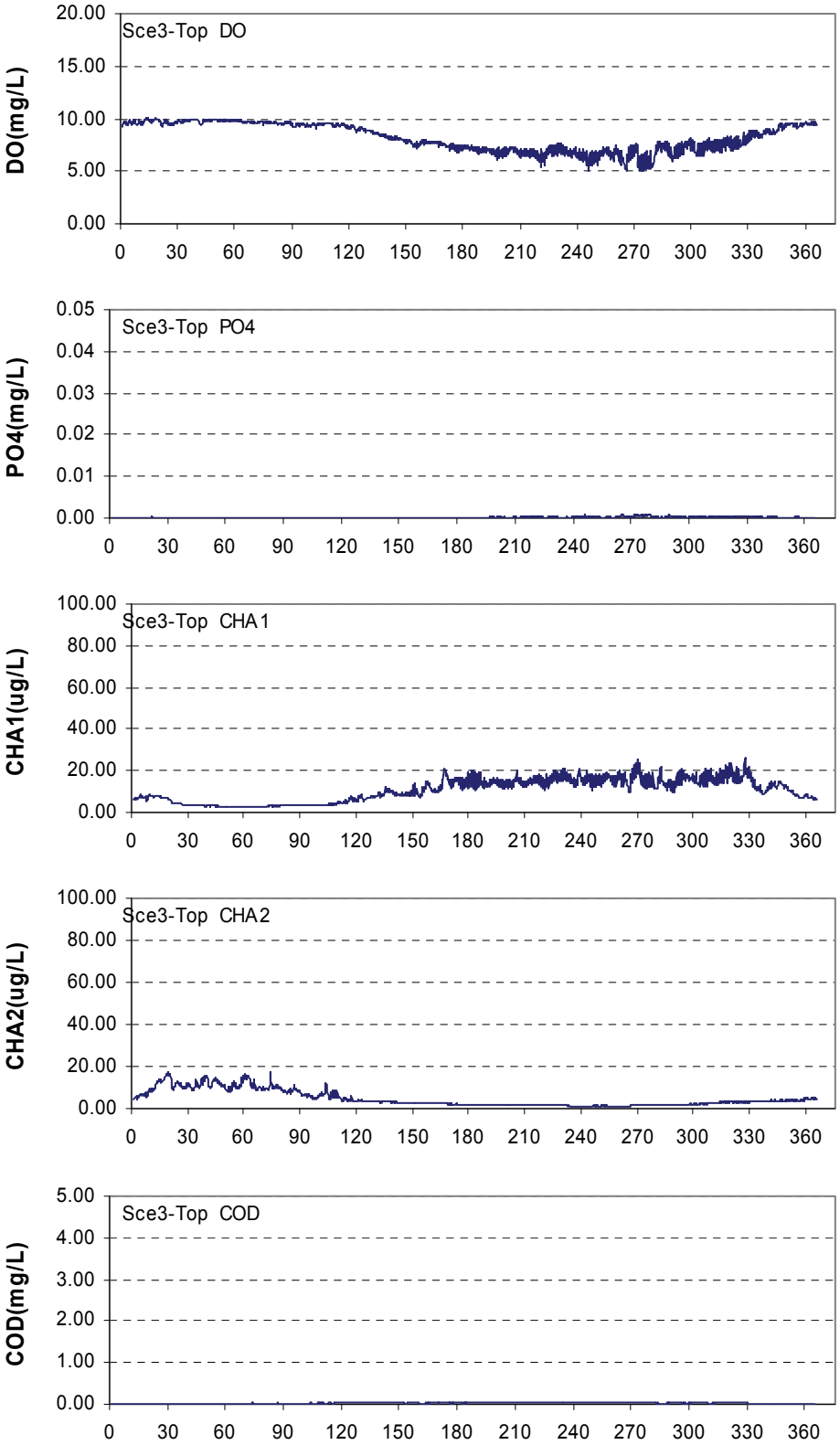
Sce3-Top DO
DO(mg/L)
20.00
15.00
10.00
5.00
0.00
Sce3-Top PO4
PO4(mg/L)
0.05
0.04
0.03
0.02
0.01
0.00
Sce3-Top CHA1
CHA1(ug/L)
100.00
80.00
60.00
40.00
20.00
0.00
Sce3-Top CHA2
CHA2(ug/L)
100.00
80.00
60.00
40.00
20.00
0.00
Sce3-Top COD
COD(mg/L)
5.00
4.00
3.00
2.00
1.00
0.00
0 30 60 90 120 150 180 210 240 270 300 330 360

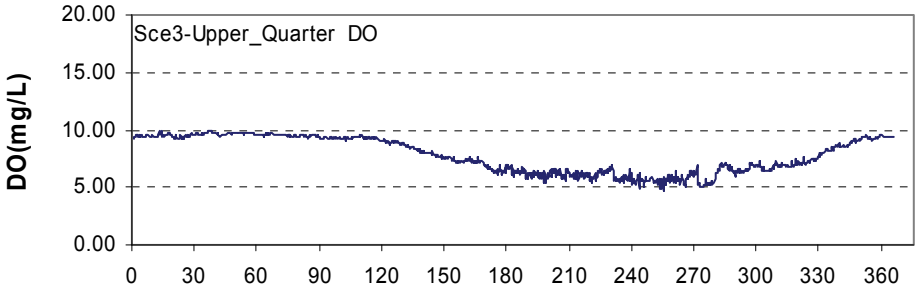
Sce3-Upper_Quarter DO
DO(mg/L)
20.00
15.00
10.00
5.00
0.00
0 30 60 90 120 150 180 210 240 270 300 330 360

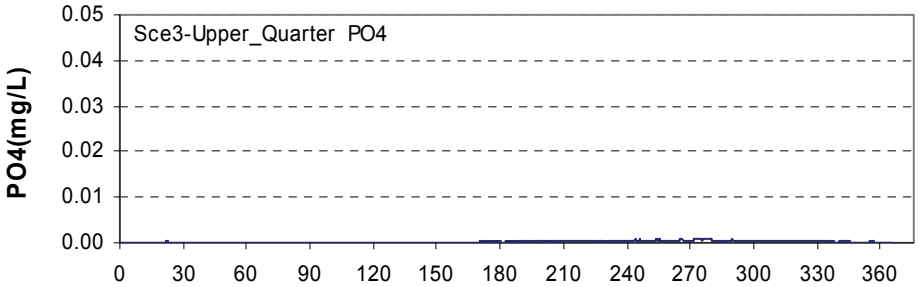
Sce3-Upper_Quarter PO4
PO4(mg/L)
0.05
0.04
0.03
0.02
0.01
0.00
0 30 60 90 120 150 180 210 240 270 300 330 360

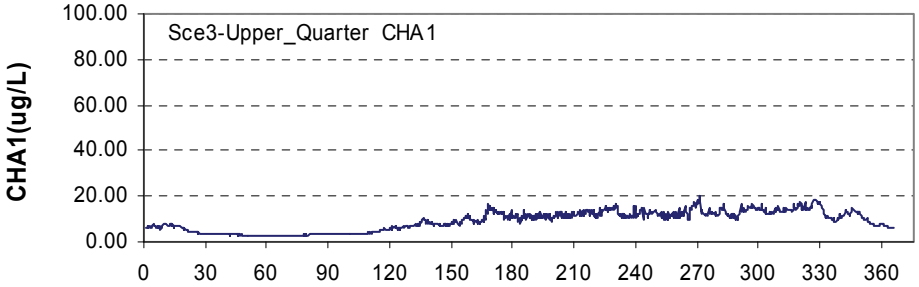
Sce3-Upper_Quarter CHA1
CHA1(ug/L)
100.00
80.00
60.00
40.00
20.00
0.00
0 30 60 90 120 150 180 210 240 270 300 330 360

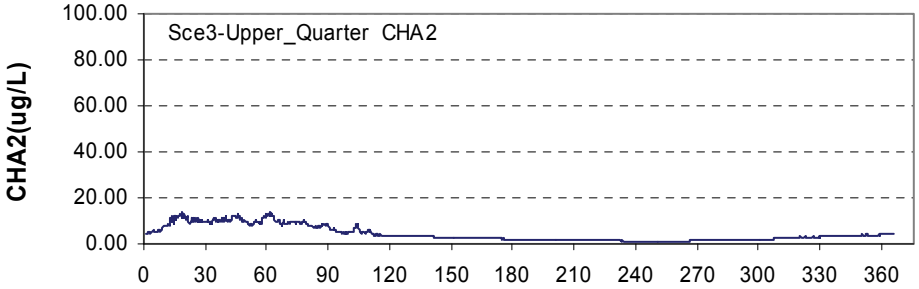
Sce3-Upper_Quarter CHA2
CHA2(ug/L)
100.00
80.00
60.00
40.00
20.00
0.00
0 30 60 90 120 150 180 210 240 270 300 330 360

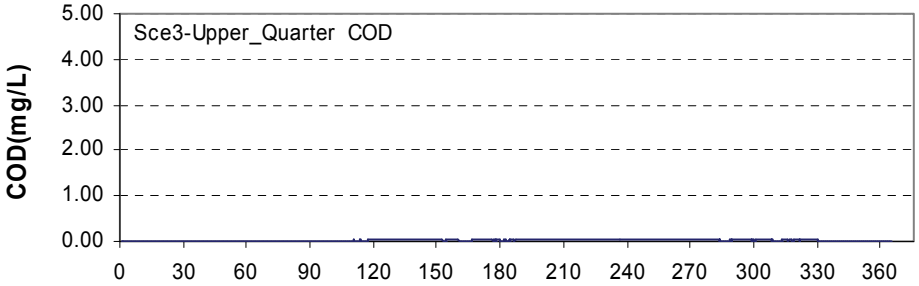
Sce3-Upper_Quarter COD
COD(mg/L)
5.00
4.00
3.00
2.00
1.00
0.00
0 30 60 90 120 150 180 210 240 270 300 330 360

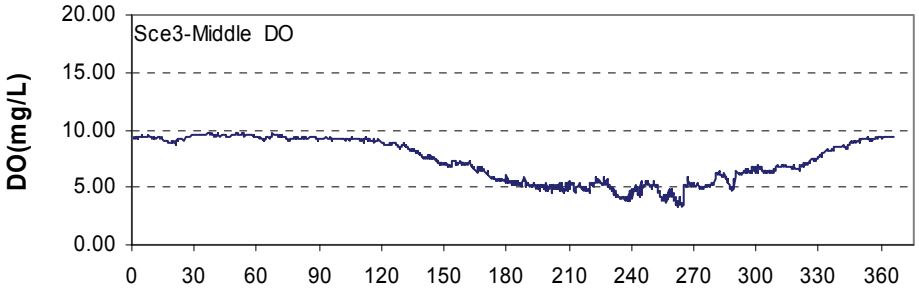
Sce3-Middle DO
DO(mg/L)
20.00
15.00
10.00
5.00
0.00
0 30 60 90 120 150 180 210 240 270 300 330 360

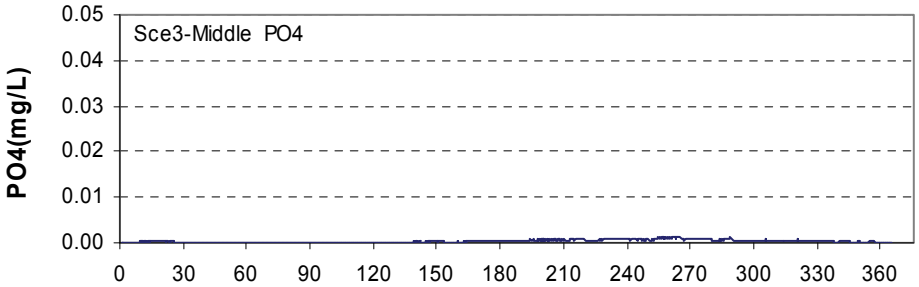
Sce3-Middle PO4
PO4(mg/L)
0.05
0.04
0.03
0.02
0.01
0.00
0 30 60 90 120 150 180 210 240 270 300 330 360

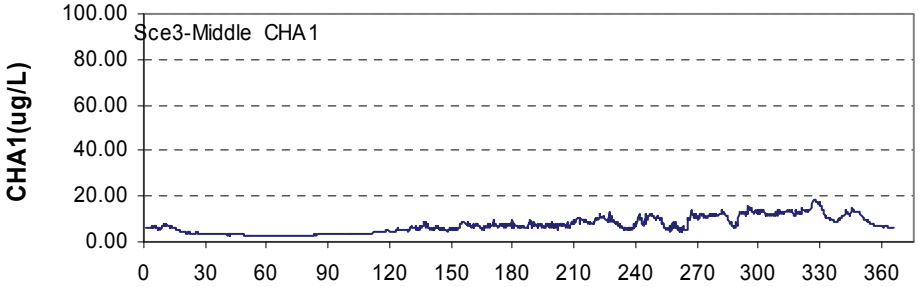
Sce3-Middle CHA1
CHA1(ug/L)
100.00
80.00
60.00
40.00
20.00
0.00
0 30 60 90 120 150 180 210 240 270 300 330 360

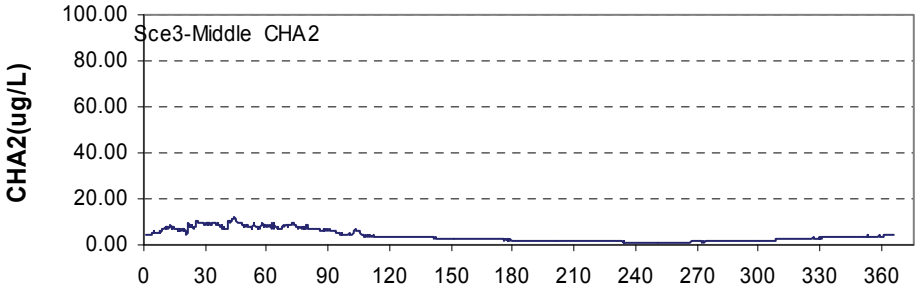
Sce3-Middle CHA2
CHA2(ug/L)
100.00
80.00
60.00
40.00
20.00
0.00
0 30 60 90 120 150 180 210 240 270 300 330 360

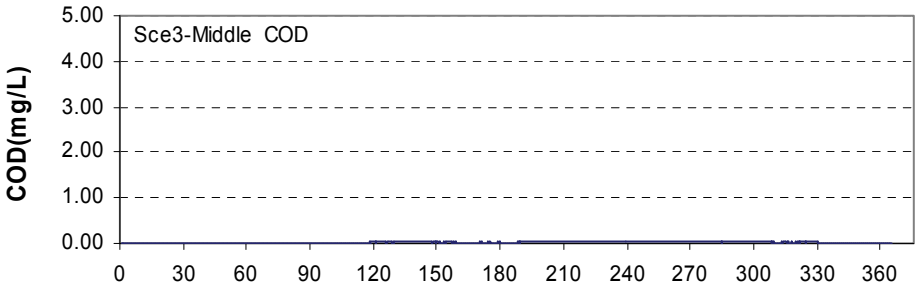
Sce3-Middle COD
COD(mg/L)
5.00
4.00
3.00
2.00
1.00
0.00
0 30 60 90 120 150 180 210 240 270 300 330 360

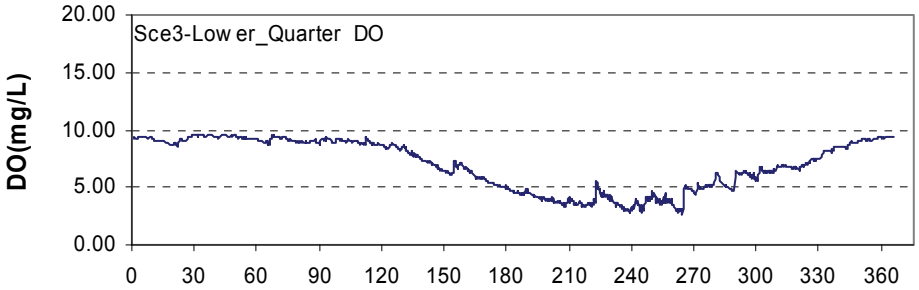
Sce3-Low er_Quarter DO
DO(mg/L)
20.00
15.00
10.00
5.00
0.00
0 30 60 90 120 150 180 210 240 270 300 330 360

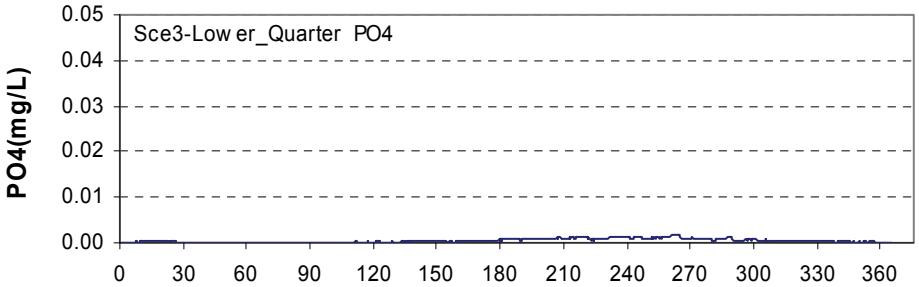
Sce3-Low er_Quarter PO4
PO4(mg/L)
0.05
0.04
0.03
0.02
0.01
0.00
0 30 60 90 120 150 180 210 240 270 300 330 360

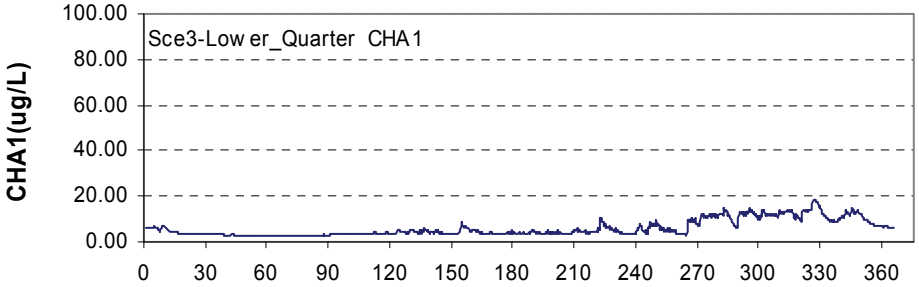
Sce3-Low er_Quarter CHA1
CHA1(ug/L)
100.00
80.00
60.00
40.00
20.00
0.00
0 30 60 90 120 150 180 210 240 270 300 330 360

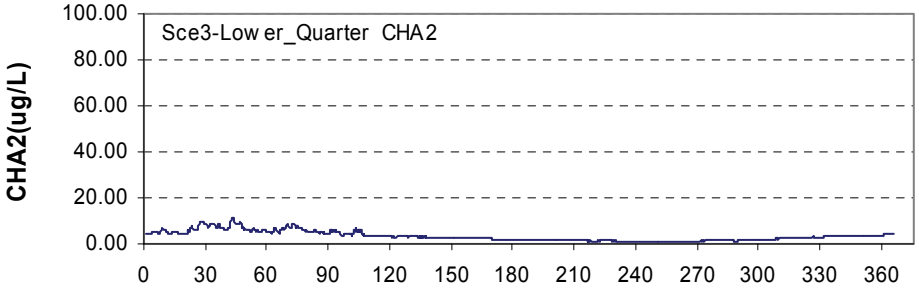
Sce3-Low er_Quarter CHA2
CHA2(ug/L)
100.00
80.00
60.00
40.00
20.00
0.00
0 30 60 90 120 150 180 210 240 270 300 330 360

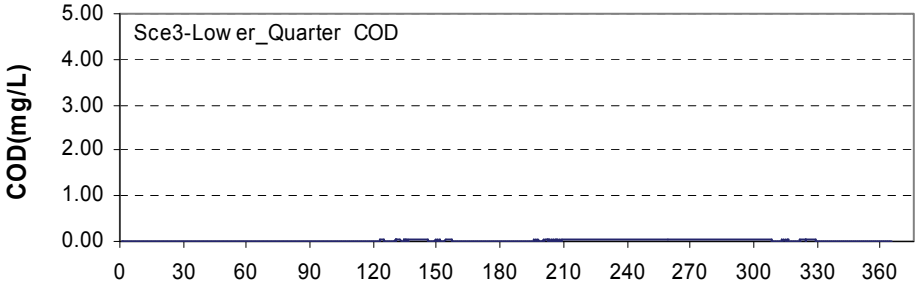
Sce3-Low er_Quarter COD
COD(mg/L)
5.00
4.00
3.00
2.00
1.00
0.00
0 30 60 90 120 150 180 210 240 270 300 330 360

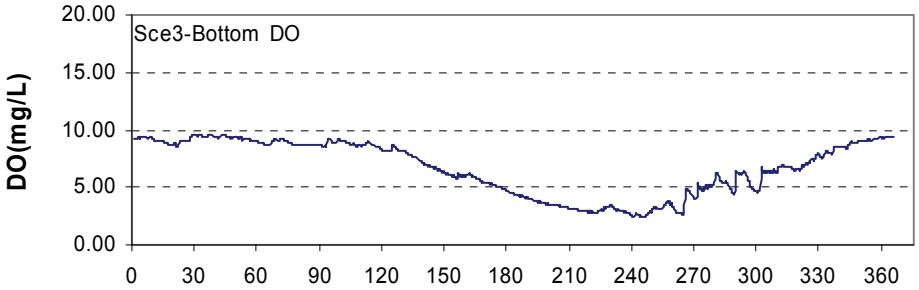
Sce3-Bottom DO
DO(mg/L)
20.00
15.00
10.00
5.00
0.00
0 30 60 90 120 150 180 210 240 270 300 330 360

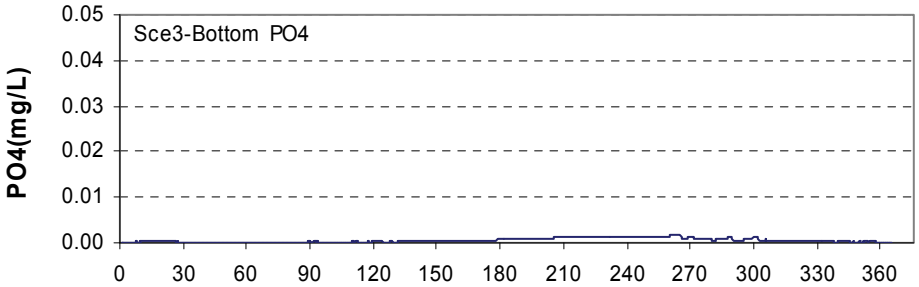
Sce3-Bottom PO4
PO4(mg/L)
0.05
0.04
0.03
0.02
0.01
0.00
0 30 60 90 120 150 180 210 240 270 300 330 360

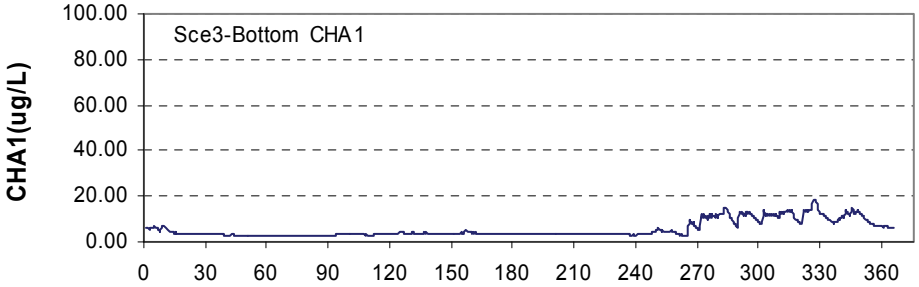
Sce3-Bottom CHA1
CHA1(ug/L)
100.00
80.00
60.00
40.00
20.00
0.00
0 30 60 90 120 150 180 210 240 270 300 330 360

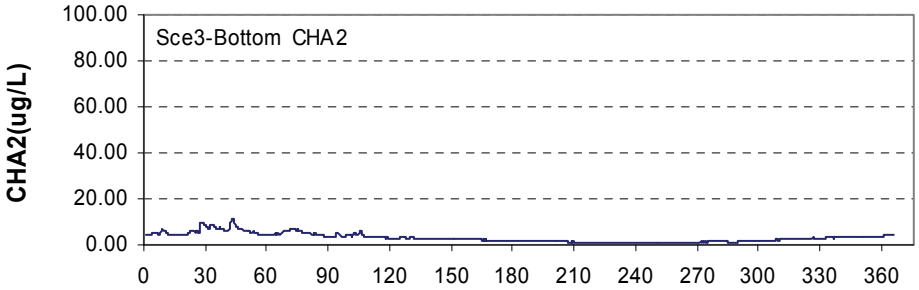
Sce3-Bottom CHA2
CHA2(ug/L)
100.00
80.00
60.00
40.00
20.00
0.00
0 30 60 90 120 150 180 210 240 270 300 330 360

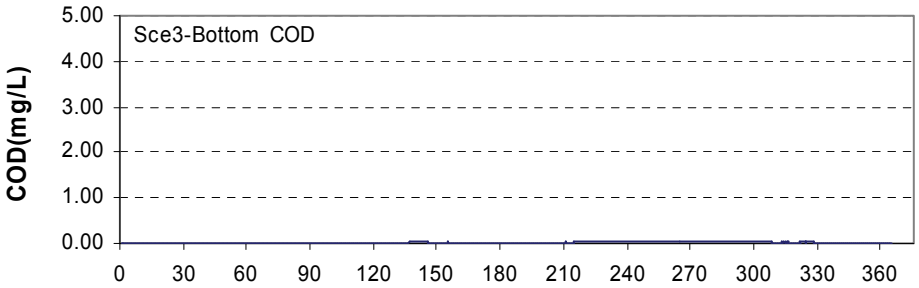
Sce3-Bottom COD
COD(mg/L)
5.00
4.00
3.00
2.00
1.00
0.00
0 30 60 90 120 150 180 210 240 270 300 330 360

Task 3:
Pilot Testing of an Advanced Oxidation Water Treatment System for Sulfide Control

Prepared by:

TETRA TECH

1. Project Site Description and Background

This task describes the operation of a pilot treatment system to oxidize the hydrogen sulfide present in the waters of the hypolimnion in the Salton Sea. The pilot system used ozone and hydrogen peroxide to oxidize the hydrogen sulfide. As described under Task 1, the hydrogen sulfide is produced as a result of organic matter decay and oxygen depletion, and is a particular problem in the Salton Sea. Although the advanced ozonation system tested here is commonly used in water treatment, there are no data on its use under hypersaline conditions that occur in the Salton Sea. The high dissolved organic carbon and oxygen demand of the Salton Sea waters also make it different from most previous reports of ozonation treatment. The goal of the pilot test was to obtain performance data on oxidation of hydrogen sulfide under conditions that would apply were the treatment to be employed as part of the Salton Sea Authority's Revitalization and Restoration Plan.

1.1. Summertime Water Quality Concerns

During the warm summer months, but especially during July and August, the Salton Sea regularly stratifies. The deeper waters of the Sea's hypolimnion are depleted of oxygen , especially when wind conditions limit mixing at the surface. The combination of limited lake mixing, low oxygen transfer, high temperatures, and high concentrations of nutrients and organic material produces hydrogen sulfide in the hypolimnion of the lake. Hydrogen sulfide is toxic to wildlife at low concentrations and, when released into the atmosphere, causes odor problems that impact neighboring communities.

1.2. Advanced Oxidation System

The water treatment evaluated as part of the Salton Sea Restoration project is an advanced oxidation system capable of injecting ozone or ozone and peroxide into the water and mixing these oxidizing agents. This mixture forms hydroxyl radicals (·OH). Ozone (O_3), hydrogen peroxide (H_2O_2), and hydroxyl radicals are strong oxidizing agents capable of oxidizing several organic and inorganic compounds including hydrogen sulfide.

Ozone was generated from pure oxygen gas supplied with liquid oxygen dewars. Ozone was produced in two ozone generators by subjecting oxygen gas to an electric arc between two electrodes. The following is the ozone generating reaction:

$$3O_2 \xrightarrow{Electricity} 2O_3$$

Ozone/peroxide was also evaluated to oxidize hydrogen sulfide. The advanced oxidation system was designed to inject controlled ratios of ozone and hydrogen peroxide (H_2O_2) directly into the reactor. The ozone and hydrogen peroxide produced hydroxyl radicals as shown in the following reaction:

$$2O_3 + H_2O_2 \rightarrow 2OH\cdot + 3O_2$$

Hydroxyl radicals are extremely reactive and have higher electrochemical oxidation potential (EOP) than other commonly used oxidizing agents. For example, the EOP of ozone is 2.08 volts (V) and that of the hydroxyl radical (OH·) is 2.8 V. As a reference, the EOP of chlorine, an effective oxidizing agent widely used for disinfection, is 1.36 V.

The following is a reaction mechanism for sulfide and ozone that is central to the pilot test:

$$S^{2-} + 2O_3 \rightarrow SO_4^{2-} + O_2$$

2. The Pilot Plant System

Two teams operated the pilot plant. One team was collected the hypolimnetic water samples while the second team collected and processed water samples then delivered them to the laboratory for chemical analysis.

2.1. Purpose of the Pilot Plant Testing

The advanced oxidation system was designed to process hypolimnetic water from the Salton Sea. The main objectives of the pilot plant testing were to assess the hydrogen sulfide removal efficiency of the advanced oxidation system and to evaluate aesthetic components of the Salton Sea water after water processing.

2.2. Collection of Hypolimnetic Water

The following equipment was used to collect and transport hypolimnetic water samples:

- Pillow Tank and Centrifugal Pump – Environmental Resource Management (ERS) staff collected hypolimnetic water samples at a depth of approximately 35-feet below water surface (bws) using one centrifugal gasoline-powered pump, a flexible pipe, and a screen. A pillow tank stored the hypolimnetic water samples as they were transported to shore.

- Barge and Boat – One barge and one boat, owned and operated by ERS, transported hypolimnetic water samples from the lake to the ERS station.

- Water Quality Monitoring Probe – During collection of hypolimnetic water samples, ERS staff used a water quality monitoring probe to measure water temperature, dissolved oxygen, and conductivity.

2.3. Sulfide Destruction with Ozone and Ozone/Peroxide

The advanced oxidation system selected for this project consisted of a skid mounted HiPOx unit capable of dosing ozone (O_3) or ozone/peroxide into a plug flow reactor. During operation of the pilot plant, varying ozone and ozone/peroxide doses were used to evaluate the oxidation requirements for treating the hypolimnetic water of the Salton Sea.

2.4. Pilot Plant System Components

The Salton Sea pilot plant consisted of the following system components (Attachment A):

- Baker Feed Tank – One 4,500-gallon polyethylene feed tank was stored hypolimnetic water samples. This tank was fitted with flexible hoses and 2-inch camlock fittings. It was also fitted with 2-inch polyvinyl chloride (PVC) piping connected to a variable frequency drive (VFD) feed pump. A low water level switch was installed directly above the outlet valve which was designed to shut down the system at low water levels.

- VFD Feed Pump – The VFD feed pump was designed with sufficient head to circulate water from the feed tank, through the sand filter, and into the advanced oxidation system. The pump also supplied the multimedia filter with backwash water. The flow rates of the VFD feed pump were managed by the programmable logic controller (PLC).

- Multimedia Filter – The fiberglass multimedia filter was 21-inches in diameter (2.4 ft^2) and capable of processing flows of 10-gallons per minute (gpm). The calculated filtration rate for this application is 4.15 gal/ft^2 min. The multimedia filter was designed to remove settleable and suspended solids from the hypolimnetic water samples prior to processing with the advanced oxidation system. The media used in this project consisted of anthracite, sand and gravel.

- Advanced Oxidation System – The advanced oxidation system consisted of a skid-mounted HiPOx system. The HiPOx system has a plug flow reactor modified to operate at a flow of 10 gpm. The volume of the plug flow reactor was 27 gallons, and the residence time was approximately 160 seconds.

- Final Effluent Holding Tank – The processed water from the advanced oxidation system flowed into a final effluent holding tank prior to discharge into the Salton Sea. The capacity of the final effluent holding tank was 700 gallons. The final effluent holding tank was designed to supply the VFD feed pump with backwash water for the multimedia filter and prevent discharge of processed water during startup, process upsets, and water processing at low ozone concentrations.

- Bag Filtration System – One 10-micron bag filtration system was installed to filter backwash water from the multimedia filter prior to discharge into the Salton Sea.

- Power Generator – One 30-kilovolt Ampere (kVA) 3-phase power generator was used at 210 V to power the VFD feed pump and the advanced oxidation system.

2.5. Functionality of the Advanced Oxidation System

The advanced oxidation system selected for this project consists of one HiPOx unit supplied by Applied Process Technologies (APT Water) in Pleasant Hill, California. The advanced oxidation system consisted of the following equipment:

- Ozone Generation System – The HiPOx unit was equipped with two solid-state ozone generators capable of delivering maximum ozone concentrations of 12% by weight. Liquid oxygen dewars (supplied by Praxair Distribution Inc.) was used in the ozone generators.

- Hydrogen Peroxide System – A double-walled tank stored the hydrogen peroxide solution. The hydrogen peroxide solution used during the pilot test was of 35% by weight. One hydrogen peroxide metering pump injected hydrogen peroxide into the inlet of the advanced oxidation system's plug flow reactor.

- Integrated Control System – All functions of the advanced oxidation system were monitored and controlled by an integrated PLC, designed to operate in a fail-safe mode. Operating parameters were continuously monitored by the PLC.

- Process Control – Operating set points (i.e., VFD feed pump flow, ozone dose, hydrogen peroxide dose, etc.), valve sequencing and timing, and other process parameters were changed locally through an operator interface terminal (OIT).

- Equipment Enclosure – The ozone generators and equipment were housed in a climate controlled National Electrical Manufacturers Association (NEMA) 3R enclosure.

3. Pilot Plant Mobilization and Operation

3.1. Bench Scale Testing

Prior to mobilizing the equipment, Tetra Tech performed bench scale testing of the advanced oxidation system at the APT Water Laboratories in Pleasant Hill, California. The processed water samples were submitted to the Curtis and Tomkins Laboratories in Berkley, California. During the bench scale testing, the Salton Sea sample was divided into four sub-samples. Two sub-samples were processed with ozone, and two sub-samples were processed with ozone/peroxide.

The results associated with the bench scale testing were inconclusive due to one or more of the following factors:

- Sulfide was not detected in samples submitted to the laboratory for chemical analysis. Tetra Tech suspects that samples contained little sulfide, which may have been oxidized during sample collection and transportation.

- High inorganic content caused problems in the analysis of water samples, and chemical oxygen demand (COD) was reported to be very high. The results of analysis did not reveal a reduction in COD, and in some cases showed an increase in COD.

- Based on the results obtained during bench scale testing, the pilot plant work plan was modified to account for procedures that would preserve sulfide in samples and approximate COD values in water samples. In the original work plan, all samples were scheduled for delivery to Calscience Environmental Laboratories (Calscience). The sampling schedule was modified to include sample delivery two days per week to the Department of Environmental Sciences at the University of California in Riverside (UCR) for chemical analysis.

3.2. Mobilization of Process Equipment

Mobilization of rented process equipment, including the polyethylene tanks and the bag filtration system, was conducted on October 5, 2006. On October 11, 2006, APT Water shipped the advanced oxidation system to the Salton Sea, and the unit was received at the ERS station on October 13, 2006.

The electrical installation was finalized on October 16, 2006, and the mechanical installation the HiPOx unit was finalized on October 18, 2006. APT Water staff traveled to the Salton Sea on October 19, 2006, to install the two ozone generators and conduct equipment inspection. On October 20, 2006, functional tests of the system and training were conducted.

3.3. Pilot Plant Operation with Clean Water

The advanced oxidation system was started on October 19, 2006, and the pilot plant was operated with clean water through October 20, 2006.

During clean water tests, the feed tank was filled with municipal drinking water. The system was operated at a flow of 10 gpm to test for adequate operation of the filters, ozone/peroxide dosing systems, and process control. No water samples were collected during pilot plant operations with clean water.

On October 23, 2006, the pilot plant began operating with water collected from the Salton Sea. Since local temperatures had decreased by this time, and the water in Sea had mixed, no sulfide was detected in the hypolimnetic water samples. Task 1 shows temporal data on sulfide concentrations in Sea, and the rapid changes in concentration that occur following mixing. To evaluate the sulfide removal efficiency of the pilot system under these conditions, the hypolimnetic water was spiked with sulfide at the feed tank starting on October 24, 2006, and continued through the end of the project. A benefit of the artificial spiking of Sea water was that there was a controllable sulfide concentration during each experiment.

Once the pilot plant started and adequate functional operation of the system was tested, the operation was geared toward demonstrating that the system was capable of oxidizing hydrogen sulfide. During this phase of the pilot testing unit, the operating parameters were selected to establish the residual ozone concentrations at which the system had removed total and dissolved sulfide in the hypolimnetic water samples. During the last days of operation, the pilot plant was operated at high ozone and ozone/peroxide dosing rates to determine the extent to which the advanced oxidation system could reduce the COD concentrations in hypolimnetic water.

3.4. Hypolimnetic Water Sample Collection by ERS

On October 23, 2006, the first hypolimnetic water samples for pilot testing were collected by ERS using the procedures outlined below. The site locations were based on an August, 2006 survey that was conducted to identify the best location for collection of anoxic hypolimnetic water samples.

- Sample Collection – Hypolimnetic water samples were collected with a gasoline-powered pump by lowering a pipe to a depth of 35 feet bws. The water was pumped into one 700-gallon pillow tank. The pillow tank was transported via barge to the ERS station for sample processing. The pillow tank and pump were equipped with a camlock release system to quickly connect and disconnect the pump to the system. Hypolimnetic water samples were monitored using a portable oxidation-reduction potential (ORP) meter (i.e., Horiba U22 capable of recording turbidity, ORP, salinity, and pH).

- Water Transfer – After the pillow tank was filled with water, it was transported to the ERS station. A 2-inch flexible transfer hose was used to pump water from the pillow tank to the baker feed tank. Depending on the weather conditions, four to six hours were required to fill the baker feed tank with approximately 2,800-gallons of water (62% of the feed tank capacity).

The data accumulated during hypolimnetic water sample collection is included in Attachment B.

3.5. Sample Spiking with Sodium Sulfide

During operation of the advanced oxidation system, dissolved oxygen (DO) concentrations in hypolimnetic water samples varied significantly. Elevated DO concentrations did not maintain dissolved sulfide as a result of aerobic conditions in the hypolimnetic area.

Sulfide concentrations in hypolimnetic water are present during the warm summer months of July and August. Naturally occurring sulfide concentrations in hypolimnetic water were not observed when the advanced oxidation system became available for operation in October. To

test the performance of the advanced oxidation system, the water samples were artificially spiked with 0.5 to 2 pounds of flaked sodium sulfide.

Most of the artificially spiked samples reported dissolved and total sulfide concentrations of up to 25 milligrams per liter (mg/L).

To spike the hypolimnetic water samples, sodium sulfide was pre-dissolved in a container of water then poured into the baker feed tank prior to transferring the last load of hypolimnetic water from the pillow tank into the baker feed tank for mixing.

3.6. Selection of Operating Parameters During Pilot Plant Testing

The purpose of operating the pilot plant at various operating parameters was to determine the ozone dosages required to completely oxidize total and dissolved sulfide in hypolimnetic water samples. To select experimental ozone dosages, operations staff used two Hach colorimetric tests to evaluate dissolved sulfide concentrations in the spiked hypolimnetic water samples (raw water) and ozone concentrations in treated hypolimnetic water samples (treated water). The Hach field test kits were used as follows:

- Hach Dissolved Sulfide Colorimetric Test – A dissolved sulfide colorimetric test was used to confirm sulfide presence in hypolimnetic water samples after spiking and dissolved sulfide absence in treated hypolimnetic water samples. The dissolved sulfide colorimetric test proved to be a successful qualitative test to detect the presence of dissolved sulfide. During pilot plant operation it was noted that some samples which reported no dissolved sulfide in the colorimetric test did report detectable concentrations of total sulfide in the laboratory reports.

- Hach Ozone Colorimetric Test – The ozone colorimetric test was used during the third week of operation to evaluate the residual ozone concentrations in treated water samples. Specifically, the purpose was to estimate ozone concentrations in the effluent (residual ozone) that would be required to completely oxidize dissolved and total sulfide.

3.7. Sample Collection and Transportation

Sampling of the pilot plant process flows began after the water in the baker feed tank was spiked and the system had operated for one hour. Any remaining water in the HiPOx polyethylene tank from the previous day was flushed during this first hour of operation. , Furthermore, the system's processing parameters were verified to be working under adequate conditions (i.e., operating pressures, process flows, and ozone and ozone/peroxide feed rates) at this time. Sampling bottles, chain of custodies and coolers were also prepared during the first hour of operation.

Once the first hour of operation was completed, raw water from the feed tank and filtered water from the multimedia filter were sampled first. The collection of treated water samples was conducted by two people. One person collected the treated water sample, while a second logged the operating parameters of the pilot plant. After the raw and filtered water samples were collected, the team sampled the treated water at the advanced oxidation system effluent. All samples were immediately cooled with ice following collection.

3.7.1 Sample Labeling

During hypolimnetic water sample collection, the raw water samples collected prior to sand filtration were labeled RW. Samples collected after sand filtrations were labeled SF, and samples collected at the advanced oxidation system effluent were labeled TW. To differentiate between samples, the samples were labeled with the date the sample was collected (i.e., a sample collected at the sand filter on October 30, 2006, was labeled SF30).

For treated water samples, the ozone dose in percent was also used to label the samples. For example, a treated water sample collected at the advanced oxidation system on October 30, 2006, while operating with a 1.14% ozone dose (equivalent to 11.4 mg/L) was labeled TW30-1.14%. For samples collected on November 14 and 15, 2006, the hydrogen peroxide dose in mL/L was also added to the sample label after the ozone dose.

3.7.2 Calscience Environmental Laboratory

,The hypolimnetic water samples were transported under chain of custody to Calscience in Garden Grove, California on Mondays, Wednesdays, and Fridays. The samples were analyzed for the following parameters:

- Total suspended solids (TSS)
- Total organic carbon (TOC) and Dissolved Organic Carbon (DOC)
- Chemical oxygen demand (COD)
- Chemical oxygen demand, filtered (COD_f)
- Ammonia (NH_3-N)
- Dissolved sulfide
- Total sulfide
- Nitrites, nitrates, and total Kjeldahl nitrogen (TKN)
- Selenium
- Total phosphate
- Absolute biological oxygen demand (BOD_{20})
- Absolute nitrogenous biological oxygen demand ($NBOD_{20}$)

3.7.3 University of California at Riverside Laboratory

On Tuesdays and Thursdays, the water samples were analyzed for total sulfide and COD by the Department of Environmental Sciences at the University of California at Riverside (UCR). Consistent with UCR laboratory specifications, all samples were cooled immediately after collection and preserved.

The UCR laboratory was selected for analysis of selected dissolved sulfide and COD samples due to their experience with these analyses in the Salton Sea matrix and their ability to perform rapid dissolved sulfide analysis. COD analysis was conducted at UCR due to the high concentrations of inorganics with large COD values (greater than 1,000 mg/L) per standard operating procedures. In prior work with Salton Sea waters, the UCR laboratory has created an analytical procedure for the analysis of COD samples in hypersaline water (Chris Amrhein, personal communication, 2006) that was used for this work.

4. Pilot Plant Results & Discussion

The charts included in Attachment C summarize the results of analysis of samples collected during the pilot test.

4.1. Total Suspended Solids

TSS analysis was conducted in all hypolimnetic water samples submitted to Calscience. The following results were observed for TSS data:

- TSS was significantly reduced by the sand filtration system in all of the water samples. Initial TSS concentrations ranged from 1.4 mg/L to 109 mg/L, and were reduced to an average concentration of 3.5 mg/L.
- There was no apparent decline of TSS concentrations as a result of ozone or ozone/peroxide dosing.
- A deviation in the overall trend of TSS results was observed during the first two days of operation. The variation may have been attributed to inadequate sample mixing within the system. After the second day of processing hypolimnetic water samples, the startup operations were modified to improve mixing at the feed tank prior to initiating daily operations of the system.
- The TSS and COD data indicate that the largest observed COD reductions were obtained by the sand filter.

4.2. Dissolved and Total Sulfide

The following trends were observed for total sulfide and dissolved sulfide data:

- Concentrations of total sulfide and dissolved sulfide generally were not affected by sand filtration.
- Oxidation of sulfide was achieved with ozone, although ozone/peroxide was also used on November 14 and 15, 2006. The most significant reduction in sulfides occurred at low ozone and ozone/peroxide doses.
- Dissolved sulfide was oxidized at a low ozone dose, and total removal of dissolved sulfide and total sulfide was generally observed at residual ozone concentrations of 1.5 mg/L.
- The results of analysis of treated water samples indicated that sulfide is oxidized by ozone. During most operation days, the sulfide concentrations had been reduced to concentrations below the detection limit.
- Although the Hach tests did not detect any sulfide concentrations, UCR and Calscience did detect concentrations of total sulfide, indicating this test may not be a sufficient quantitative test for total sulfide.

Table 4-1 summarizes the ozone demand calculated for selected dates. The dates were selected based on the UCR data.

Table 4-1
Summary of Ozone Requirements and Initial Sulfide Concentrations

Date	Initial Sulfide Concentration in mg/L	Ozone Requirement in mg/L	Sulfide/Ozone Requirement per mg of Sulfide
10/23/2006	0	0	0
10/24/2006	27	85.1	3.15
10/25/2006	17	59.7	3.51
10/26/2006	23.09	67.5	2.92
10/27/2006	29	87.8	3.03
10/30/2006	9.5	32.8	3.45
10/31/2006	20.77	69.4	3.34
11/1/2006	11	22.9	2.08
11/2/2006	4.12	31.6	7.67
11/3/2006	11	33.6	3.05
11/6/2006	12	49.5	4.13
11/7/2006	16.66	56.3	3.38
11/8/2006	13	37.5	2.88
11/9/2006	7.4	47.0	6.35
11/14/2006	12.4	62.9	5.07
11/15/2006	5.9	68.9	11.68

The average sulfide requirement was 3.76 mg of ozone per mg of sulfide. The average was calculated by excluding the data on November 14 and 15. During those days, the operation of the system was focused on reducing COD concentrations.

The increase in the ozone requirements at low initial sulfide concentrations is likely associated with the presence of organic and inorganic material in the water samples.

Tetra Tech performed testing to simulate sulfide losses at the baker feed tank. During those tests, it was determined that sulfide losses were less than 13% in a two hour time span. Testing was performed with a 55-gallon drum which required removing the drum lid for sampling, and sulfide losses at the 55-gallon drum are expected to be higher compared to sulfide losses in the baker feed tank. During pilot plant operation, the baker feed tank remained covered and the tank was allowed to stabilize for 45 minutes before the first sample was collected. Sample collection was generally conducted in a time span of one hour.

4.3. Oxidation-Reduction Potential

UCR also collected oxidation-reduction potential (ORP) data, as part of their COD and total sulfide evaluation. The ORP data trends are consistent with the total and dissolved sulfide data and show that the ORP consistently increased with higher ozone doses. Generally, the ORP was reduced to approximately -850 mV after the water samples were spiked with sodium sulfide and increased with ozone and ozone/peroxide addition. The ORP was observed to remain unchanged when total sulfide concentrations were reduced to approximately 0.2 mg/L or less.

4.4. Total Organic Carbon

The following trends were observed for TOC data:

- TOC values in raw water samples were not consistent during the pilot plant operation. These values were expected to show minor variations from day to day.

- The TOC data did not show a steady reduction of TOC at increasing ozone concentrations.

- The TOC data generally was inconclusive since it did not follow a specific pattern that could be explained as part of the filtration and oxidation process.

- One of the problems noted by the Bureau of Reclamation was that in lake water, the TOC requires analysis with a modification to the EPA method. The modified EPA method should allow longer oxidation times in the laboratory furnace. That modification in lake water analysis has yielded consistent results in other water characterization projects supported by the Bureau of Reclamation.

4.5. Ammonia and Phosphate

The following trends were observed for ammonia data:

- The sand filter had no impact on ammonia concentrations.

- There were six days in which little or no ammonia was detected in the water samples prior to entering the treatment system.

- In three of the six days when ammonia was detected in the water samples, the concentrations of ammonia were reduced to undetectable levels as ozone concentrations increased.

The inconsistency in trends of ammonia data is thought to result from one or several of the following:

1. Ammonia concentrations in water samples collected at the pilot plant operations were close to the methods detection limit.

2. Some ammonia may have been oxidized into nitrites or nitrates; however, an increase in nitrites or nitrates was not detected in the water samples.

3. Part of the ammonia may have been stripped at the oxygen-ozone/water separation unit when dissolved oxygen moved from an aqueous phase into a gas phase.

Phosphate showed little variation as a result of filtration and ozone or ozone/peroxide oxidation. The concentrations of phosphate for hypolimnetic water samples were reported at approximately 0.5 mg/L and were considered to be high when compared to phosphate concentrations reported by UCR (other sources report concentrations of phosphate in the Salton Sea to be 0.1 mg/L).

4.6. Chemical Oxygen Demand, Ultimate Biological Oxygen Demand, and Ultimate Nitrogenous Biological Oxygen Demand

The following trends were observed for COD data:

- The majority of water samples decreased in COD concentrations after filtration.

- There was no clear trend in the reduction of COD concentrations as a result of ozone or ozone/peroxide addition.

- The UCR spectrophotometric method for analysis of COD was modified for chemical analysis of water samples from the Salton Sea. The modified method did not provide a consistent downward trend as ozone or ozone/peroxide doses were increased.

- The method used by Calscience was expected to report higher COD values associated with the oxidation of inorganic compounds. The COD values provided by Calscience did not provide a consistent downward trend.

During a routine conference call to discuss the results of analysis, the Bureau of Reclamation raised concerns that high COD values reported by UCR may indicate that a large amount of substrate remained in treated water samples. Based on the comments made by the Bureau of Reclamation, the pilot plant was operated at high ozone/peroxide doses to determine if a stronger oxidizing agent (i.e., hydroxyl ion) would yield a larger reduction of COD and to evaluate the biodegradable fraction of COD in processed water samples.

The treated water samples submitted to Calscience and UCR on November 14 and 15, 2006, were analyzed for COD, BOD_{20} and $NBOD_{20}$. BOD_{20} was reported in all water samples at concentrations under 30 mg/L, indicating that substrate is a small fraction of the COD values reported by UCR. BOD_{20} was reported in all water samples treated with ozone/peroxide at concentration below 15 mg/L. $NBOD_{20}$ was detected in only one sample collected at the sand filter on November 15, 2006.

The inconsistent trends may have resulted from the difficulty of evaluating COD with standard and modified methods, which in turn were caused by high concentrations of total dissolved solids, including inorganic compounds. The following diagram provides a visual description of the different components of COD.

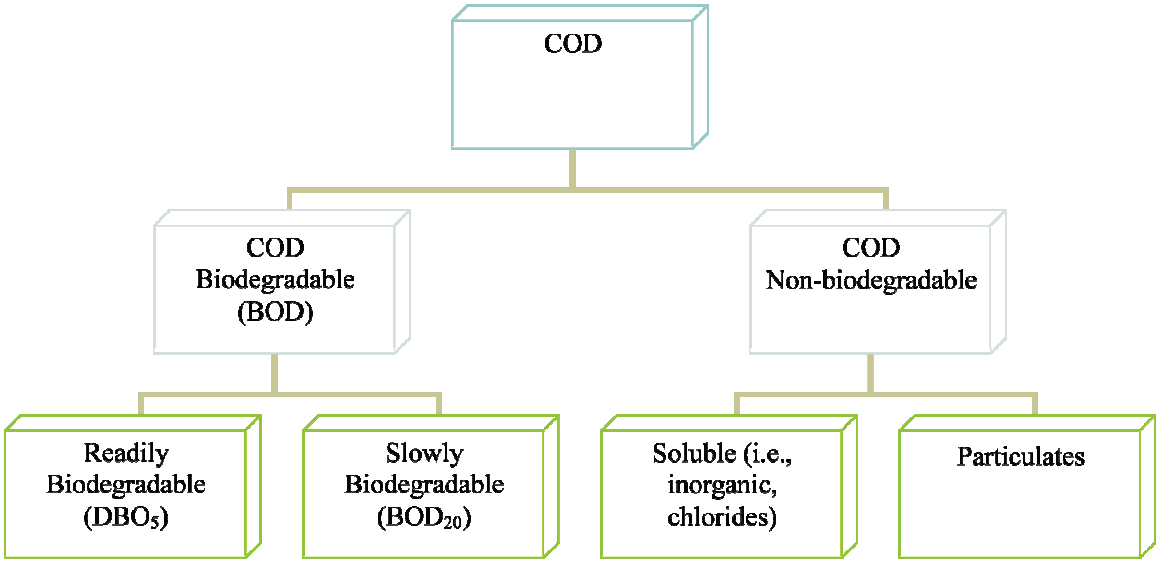

Figure 4-1

4.7. Nitrites, Nitrates, Total Kjeldahl Nitrogen, and Total and Dissolved Organic Nitrogen

Determining nitrogen content through analysis of nitrites, nitrates, and TKN was complicated by the presence of high chlorides in sample water, which required the laboratory to dilute

these samples for analysis of nitrites and nitrates and to prevent damage to the laboratory equipment.

Although there were small fluctuations in TKN concentrations at increasing ozone doses, TKN did not appear to be significantly affected by either the sand filter or the advanced oxidation system.

Nitrites and nitrates were rarely detected in water samples and may have been reduced at the baker feed tank during sulfide addition.

On November 15, 2006, water samples processed with ozone and ozone/peroxide were analyzed by Calscience for total organic nitrogen (TON) and dissolved organic nitrogen (DON). The results of analysis did not illustrate a substantial TON or DON variation at varying ozone or ozone/peroxide doses.

4.8. Foaming

Some foaming was observed at the sampling ports of the advanced oxidation system. Although the foaming was not substantial, it is possible that foaming characteristics of the water may change throughout the year. Foaming may be associated with the organic material in hypolimnetic water, which behave as surfactants. The design of a full scale water treatment system should take into consideration the potential formation of foam within reactors and tanks.

5. Pilot Plant Demobilization

Pilot plant operations concluded on November 15, 2006. The pilot plant, including the onsite generator, tanks, and advanced oxidation system, remained onsite per the Salton Sea Authority's request.

The results of analysis associated with the pilot plant operations were initially summarized and distributed internally to all stakeholders. Once the results of analysis were reviewed, Tetra Tech staff initiated demobilization of the pilot plant. The pilot plant decommissioning was conducted in December 2006, and all process equipment was shipped to the corresponding suppliers by December 19, 2006.

5.1. Physical Condition of the Pilot Plant

During decommissioning of the pilot plant, the following conditions were observed:

- The polyethylene tanks required additional cleaning as a result of algae growth inside the tanks.
- Some ozone injection points required unclogging towards the end of the pilot plant operation period. The clogging at the ozone injection points is expected to have been caused mainly by water hardness.

A full scale system would require a design that allows adequate cleaning of unitary process equipment such as reactors, holding tanks, and ozone injection points. Clean-in-place systems should be designed into the system to prevent buildup of organic material that may cause process failure.

6. Summary of Results

Based on the results of analysis of water samples collected during pilot plant operation, the following general observations were made (Attachment D):

- The sand filter was able to remove most of the TSS reported in water samples and in many cases demonstrated higher COD removal efficiencies when compared to the advanced oxidation system.

- The oxidation of dissolved sulfide and total sulfide was demonstrated with the addition of ozone and ozone/peroxide. A residual concentration of 1.5 mg/L of ozone at the effluent was required to fully oxidize all sulfide in the water samples.

- The results indicated that approximately 3.76 mg/L of ozone were required to oxidize 1 mg/L of total sulfide. The ozone demand was expected to be associated mainly with the ozone required to oxidize total sulfide. However, other non-targeted inorganic and organic compounds in the hypolimnetic water were also expected to be oxidized by ozone, thus increasing ozone demand. Not all compounds in the Salton Sea water can be oxidized by ozone (i.e., chlorides), which was evident in the data where COD concentrations at the effluent were higher than 200 mg/L. Treated water samples contained approximately 15 mg/L of BOD and no NBOD. Confirmation sampling of BOD and NBOD results of analysis are still pending.

- A reduction of COD in treated water samples was not consistently observed at increased ozone doses. This may have resulted from the interference of inorganic compounds in the matrix of the water samples.

- Generally speaking, the high concentration of dissolved solids in the water samples caused problems during chemical analysis. However, the data demonstrated that the advanced oxidation system is effective in oxidizing dissolved sulfide and total sulfide.

Attachment A: Pilot Plant System Photos

1 SYSTEM PHOTOS

Photo 1 – Barge and 700-gallon pillow tank used for collection of Salton Sea water and transfer to Baker Tank.

Photo 2 – Baker tank used to store Salton Sea water sample and to mix sodium sulfide (tank shown during installation).

Photo 3 – Feed pump with a variable frequency drive (forefront) and sand filter and final discharge tank (background), prior to installation.

Photo 4 – Advanced Oxidation Unit for ozone and ozone/peroxide.

Photo 5 – Bag filtration unit for backwash water prior to installation.

Photo 6 – Treatment system assembled.

Photo 7 – Power generator was used to power the advanced oxidation system and the VFD feed pump.

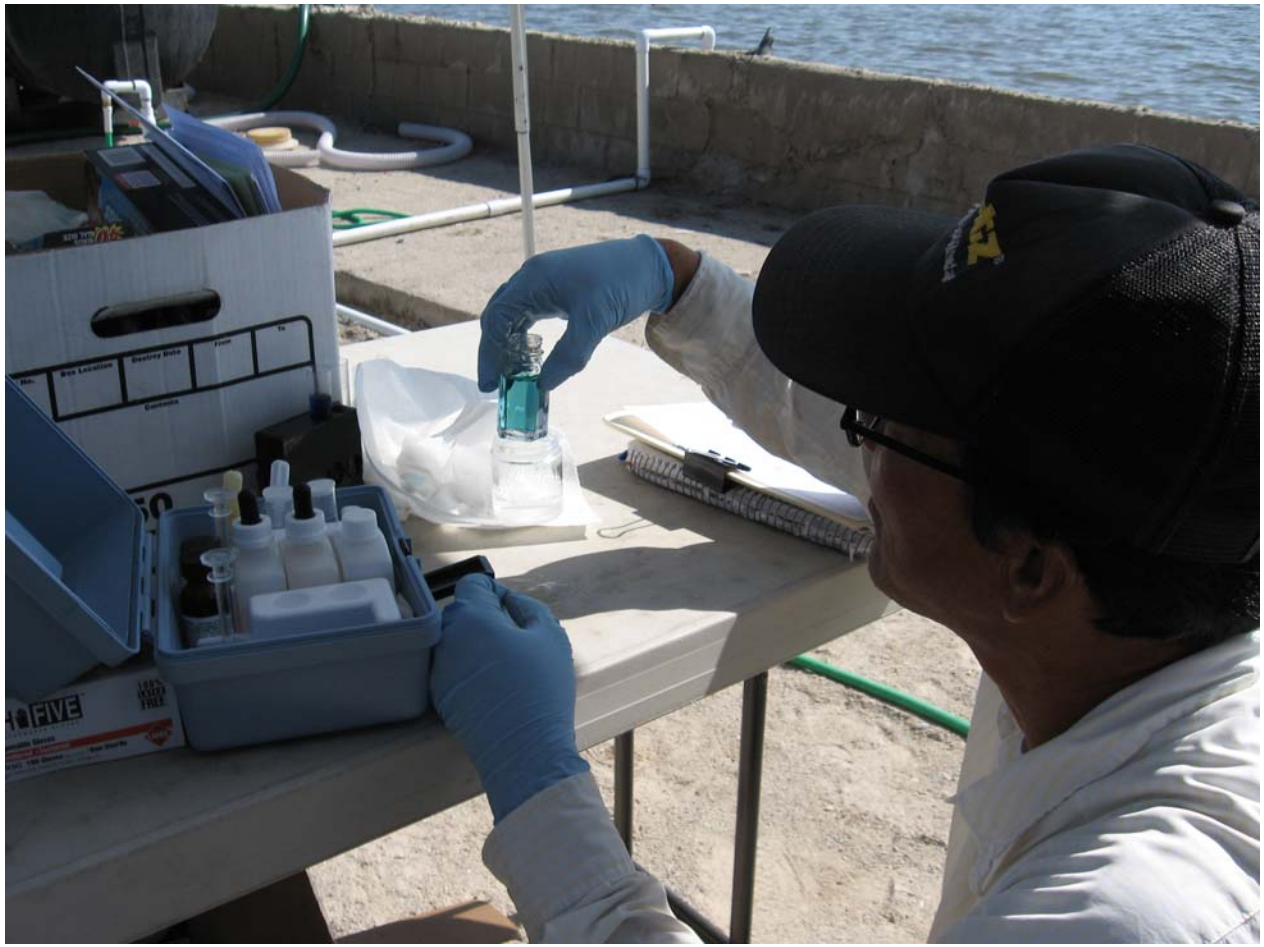

Photo 8 – Hach tests for dissolved sulfide and residual ozone were used in the field to select operation parameters.

Attachments B, C & D are provided in the electronic version of this report.

Task 4: Ozonation Treatment Plant—Planning Level Cost Estimate

Prepared by:

TETRA TECH

1. Background

During the warm summer months of July and August, the Salton Sea experiences water quality problems caused by low oxygen transfer into the hypolimnetic area of the lake, especially when wind conditions limit mixing at the surface. The combination of limited lake mixing, low oxygen transfer, high temperatures, and high concentrations of nutrients and organic material fosters the production of hydrogen sulfide in the hypolimnetic zone of the lake.

Hydrogen sulfide is toxic to wildlife at low concentrations and causes odor problems that adversely impact the recreational use of the land and neighboring communities adjacent to the Salton Sea. To address the potential release of hydrogen sulfide to areas surrounding the sea, the Salton Sea Revitalization and Restoration Plan proposes the use of advanced oxidation treatment of withdrawn hypolimnetic water. The treatment can oxidize hydrogen sulfide in the water prior to its release into the canals. Figure 1-1 illustrates a simplified version of the Authority's Plan and identifies the location of the proposed ozonation treatment plant. Sludge from the plant is proposed to be disposed in the South Lake.

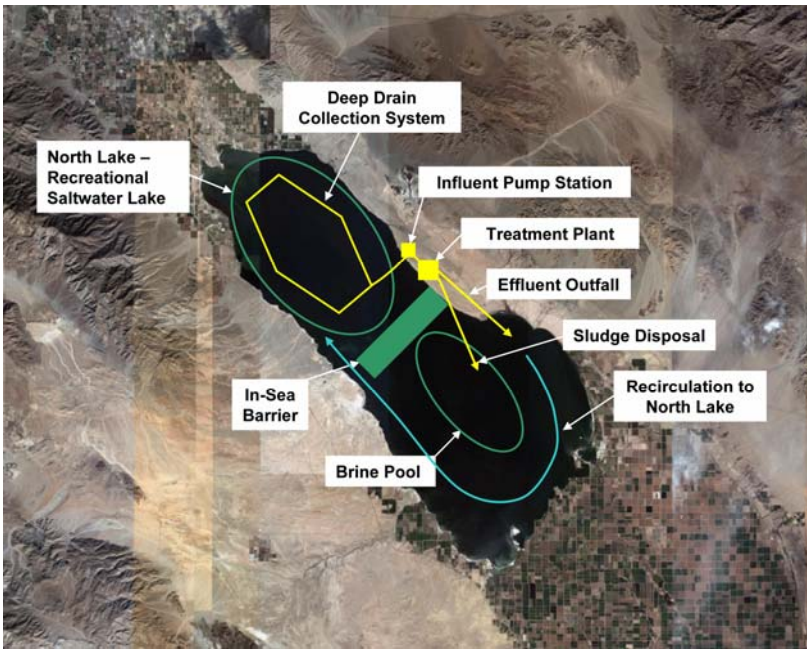

Figure 1-1. Salton Sea Revitalization and Restoration Plan Hypolimnetic Treatment System

2. Pilot Test

A pilot test was conducted at the Salton Sea from October 12 through November 15, 2006. The pilot unit consisted of a HiPOx advanced oxidation and filtration system designed to chemically oxidize the hydrogen sulfide contained in the hypolimnetic water from the Salton Sea. Water samples were collected to assess the hydrogen sulfide removal efficiency of the advanced oxidation system and to evaluate other aesthetic components of the Salton Sea water after processing.

The advanced oxidation system selected for this project consisted of a skid mounted HiPOx unit capable of dosing ozone (O_3) or ozone/peroxide into a plug flow reactor. During operation of the pilot plant, the system was operated at varying ozone and ozone/peroxide doses to evaluate the oxidation requirements for treating the hypolimnetic water of the Salton Sea.

Most samples were artificially spiked with sodium sulfide to create artificially elevated sulfide concentrations of up to 25 milligrams per liter (mg/L). Elevated sulfide concentrations in water in this range have been observed during the hot summer months typically June through September when the Sea is stratified. Sulfide is produced as a result of oxygen demand in the sediments and hypolimnetic waters, as well as low oxygen transfer from upper layers. Sulfide concentrations decrease when the lake destratifies and the water column is oxygenated. Because of the wind-driven mixing in the Sea, sulfide concentrations are reported to be highly variable even during the summer months.

The operation flow of the pilot test system was set at 10 gpm to test for adequate operation of the filters, oxidation systems, and system control. A VFD feed pump was used to pump water from the feed tank to the dual media (i.e. sand and anthracite) filter and then into the HiPOx system. The filter provided 2.5 square feet of surface and was hydraulically loaded at approximately 4 gpm/ft^2. After processing, the water was transferred into a holding tank prior to discharge into the Salton Sea. The water in the holding tank was designed to supply the VFD pump with backwash water for the multimedia filter or to prevent a discharge of water during startup and low ozone concentrations. Backwash water was filtered with a 10 micron bag filter unit prior to discharge into the Sea. The sand filter was backwashed once after processing approximately 35,700 gallons of Salton Sea water.

Based on the results of analysis of samples collected during the pilot testing the following results were obtained:

- The most significant reduction in TSS, TOC, and COD was achieved by the multimedia filter.
- The oxidation of dissolved sulfide and total sulfide was demonstrated with the addition of ozone and ozone/peroxide.
- The results indicate ozone dosages ranged from approximately 2 to 4 mg ozone per mg sulfide destroyed over the range of sulfide concentrations tested (approximately 4 mg/L to 29 mg/L) The average dosage was approximately 3.76 mg/l of ozone to oxidize 1 mg/L of total sulfide. Lower concentrations of sulfide required higher dosage levels of ozone. The ozone demand is expected to be associated with the level of ozone required to oxidize total sulfide and other compounds in the Salton Sea water that can be oxidized by ozone.

- A reduction of COD was not consistently observed at increased ozone dosages in samples analyzed by Calscience and the University of California, Riverside. This may have resulted from the interference inorganic compounds in the matrix of the Salton Sea samples or the required dilution which may have increased the error.

- During the multimedia filter backwash operation, it was determined that filtration alone will not offer sufficient treatment to process backwash wastewater water. A chemical treatment (i.e., flocculation or coagulation with filtration) may be required to treat backwash wastewater.

3. Design Criteria

The following design criteria were developed by Tetra Tech for the cost estimation on the ozonation treatment system, based on preliminary results from the pilot studies and modeling efforts:

- Plant Capacity = 450 MGD
- Sulfide Concentrations = 2 mg/l
- Operating Duration = 6 months per year
- Total Suspended Solids = 20 mg/l

4. Treatment System Processes

The proposed hypolimnetic treatment plant will consist of a deep drain hypolimnetic water collection system, an influent pump station, a plant influent screening system, a filtration system to reduce TSS, an ozone treatment system to chemically oxidize the dissolved sulfide concentrations, and an treatment effluent discharge pipeline and outfall into the south lake. General design criteria for each unit process of the treatment plant are presented in Table 4-1. A schematic process flow diagram is illustrated in Figure 4-1. A preliminary hydraulic profile for the hypolimnetic water extraction, treatment and recycle system is illustrated on Figure 4-2. A conceptual layout of the major process facilities is presented on Figure 4-3.

Table 4-1
Design criteria for hypolimnetic water extraction, treatment and discharge system

Flow and Load Basis of Design	Value	Units
Design flow - average	450	Mgd
Dissolved sulfides concentration	2	mg/L
Dissolved sulfides loading	7506	Ppd
Total suspended solids concentration	20	mg/L
Total suspended solids loading	75060	Ppd
Total recycled solids loading	22518	Ppd
Influent Pump Station		
Capacity	450	Mgd
Head	31	Ft
Efficiency	68%	
Required bhp	3598	Bhp
Number of duty pumps	6	Ea
Standby pumps	1	Ea
Individual pump capacity	52083	Gpm
Individual pump bhp	600	Bhp
Total energy consumption	64368	kWh/d
Headworks/Fine Screen		
Capacity	450	mgd
Screen size - perforated plate	0.125	in
Power requirement	4	mgd/hp
Power requirement for screen and compactor	112.5	bhp
total energy consumption	2012	kWh/d
Rapid Mix Tanks		
Detention Time	30	sec
Number of Filters served per Rapid Mix Tank	2	
Number of Rapid mix tanks	24	
Flow per Rapid mix tank	14822.5	gpm
Volume of Rapid Mix Tank	7411.25	gallons
Depth = 1.2*W	22	ft
Length	18	ft
Width	18	ft
Power required for each rapid mix tank	24.8	bhp/rapid mix tank
Total power required for rapid mixing	594	bhp
Total energy consumption	10629	kWh/d

Table 4-1 (cont'd)
Design criteria for hypolimnetic water extraction, treatment and discharge system

Filters	Value	Units
Gravity filter hydraulic loading rate	5	gpm/sf
Filter surface area required	65972	sf
Filter cell width	38.5	ft
Filter cell length	38.5	ft
Number of filter cells required for through put	45	ea
Number of filters backwashed simultaneously	3	max
Total number of filter cells	48	ea
Filter backwash pumps	4	ea
Duty pumps	2	ea
Backwash system loading rate	20	gpm/sf
Backwash water pump capacity	29645	gpm/filter
Backwash water pump head	15	ft
Pump efficiency	70%	
Surface wash system	2	gpm/sf
SW system head requirement	60	ft
Estimated filter run time	12	hrs
Backwash period	15	minutes
Surface wash system operation time	15	minutes
Filter to waste flow time	10	minutes
Filter production efficiency	94.7%	
Suspended solids removal efficiency	90.0%	
power requirement for filter backwash pump	160	bhp
Total backwash pump operating time per day	24	hrs
total energy required for backwashing per day	2868.3	kWh/d
Filter Backwash Water Treatment System		
Total Backwash water and drain water produced	27036240	gpd
number of clarifiers	4	
Flow per clarifier	6759060	gpd
Clarifier surface loading rate	800	gpd/sf
Clarifier surface area required	8449	sf
Diameter of clarifier	104	ft
Suspended solids captured by filtration	87820	ppd
Suspended solids capture efficiency by clarifier	70%	
Sludge concentration	1.0%	
Sludge flow to sludge lagoons	737100	gpd
Number of sludge pumps	4	
Duty cycle	20%	
Sludge pump capacity	640	gpm
Pump efficiency	45.0%	
Head	50	ft
Sludge pump driver size	18	bhp
Energy requirement per day	257	kWh/d

Table 4-1 (cont'd)
Design criteria for hypolimnetic water extraction, treatment and discharge system

Chemical Dose	VALUE	Units
Anionic polymer dose	0.5	mg/L
Mass of neat polymer	1900	ppd
Total Neat Polymer usage rate (*p*=9 lbs/gal)	211	gpd
Polymer application concentration	0.5%	
Polymer solution dose	29	gpm
Polymer solution pump discharge head	50	ft
Polymer solution pump efficiency	50.0%	
Polymer pump driver size	3.0	Bhp
Polymer make down system	5.0	Bhp
Energy requirement per day	143.04	kWh/d
Sludge from Suspended Solids and Chemical Addition		
Polymer	1900	Ppd
Solids from TSS influent	75060	Ppd
Total solids production - as dry solids	38	tons/d
Sludge volume at 1% solids	922782	gpd
Sludge volume at 6% solids	153797	gpd
Area required for drying beds	28.71	acres
Return sludge supernatant	534	gpm
Polymer pump discharge head	25	ft
Pump efficiency	60.0%	
Polymer pump driver size	17.0	bhp
Energy requirement per day	303.96	kWh/d
Ozone Generation		
Ozone dose	4	mgO_3/mgS^{-2}
Ozone production requirement	30024	ppd
Ozone production capacity per unit	3753	ppd
Ozone generator high voltage inverter	22118	kWh/d
Ozone primary cooling water requirement	815	gpm
Primary cooling water head requirement	104	ft
Driver efficiency	75%	
Primary cooling water pump size	29	bhp
Closed loop cooling water pump	715	gpm
Closed loop cooling water head requirement	58	ft
Driver efficiency	75%	
Closed loop cooling water pump size	14	bhp
Oxygen plant power requirement	59904	kWh/d
Total energy consumption for ozone generation	210168	kWh/d

Table 4-1 (continued)
Design criteria for hypolimnetic water extraction, treatment and discharge system

Ozone Injection and Contact System		
Number of contact chambers	8	ea
Design capacity per contact chamber	56.25	mgd
Ozone contact time	15	minutes
Volume per Contact Chamber	0.5859375	mgal
Depth of ozone contact chamber	18	ft
Width of ozone contact tank	30	ft
Length of ozone contact tank	148	ft
Ozone eductor pumps	16	ea
Ozone eductor pumps capacity	1600	gpm
Ozone eductor pump head	57.75	
Pump efficiency	70%	
Ozone eductor pump drive requirement	33	bhp
Total connected eductor pump horsepower	533	bhp
Total energy consumption for ozone application	9574	kWh/d

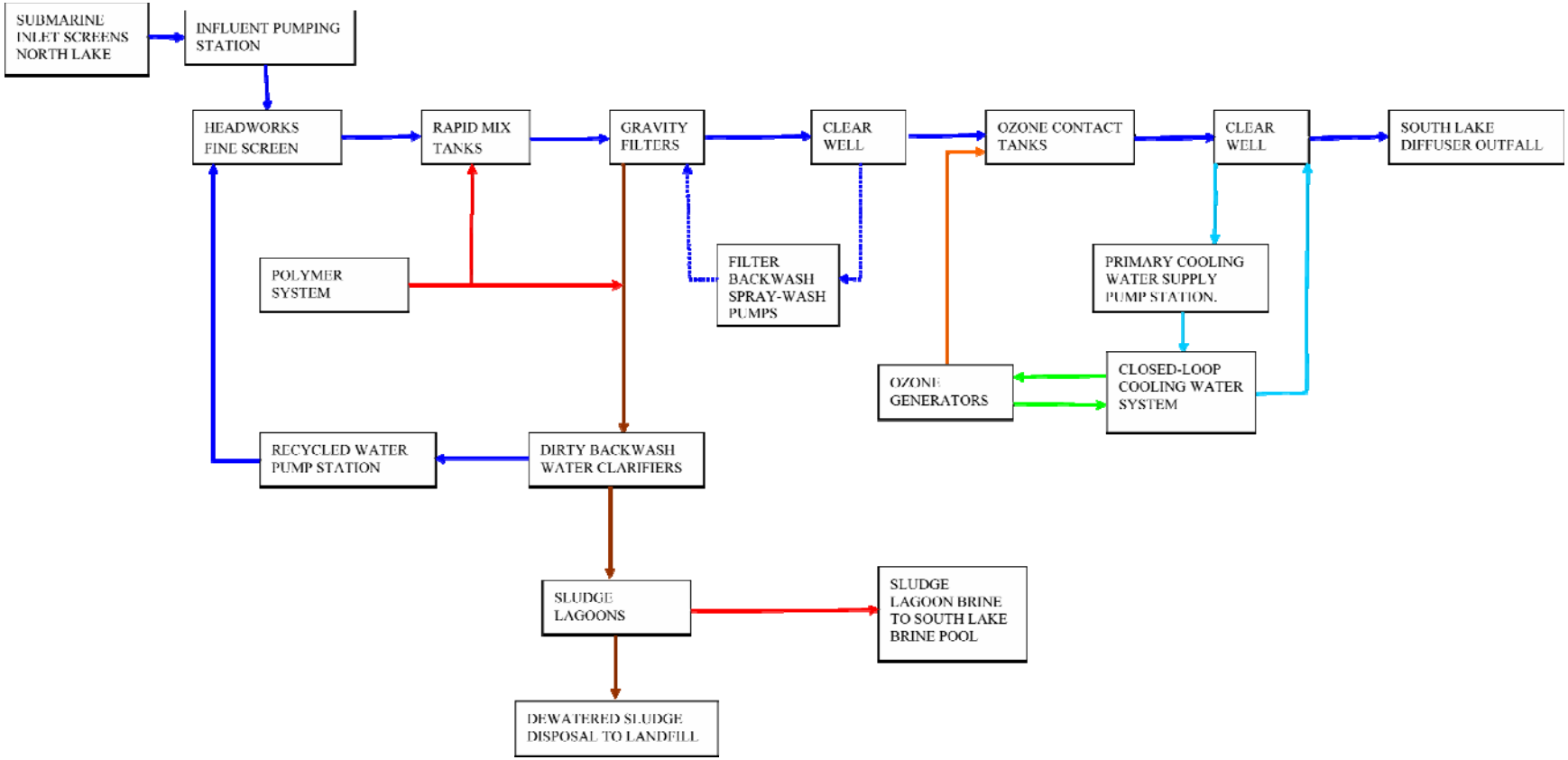

Figure 4-1. Schematic process flow diagram for Salton Sea hypolimnetic water treatment system

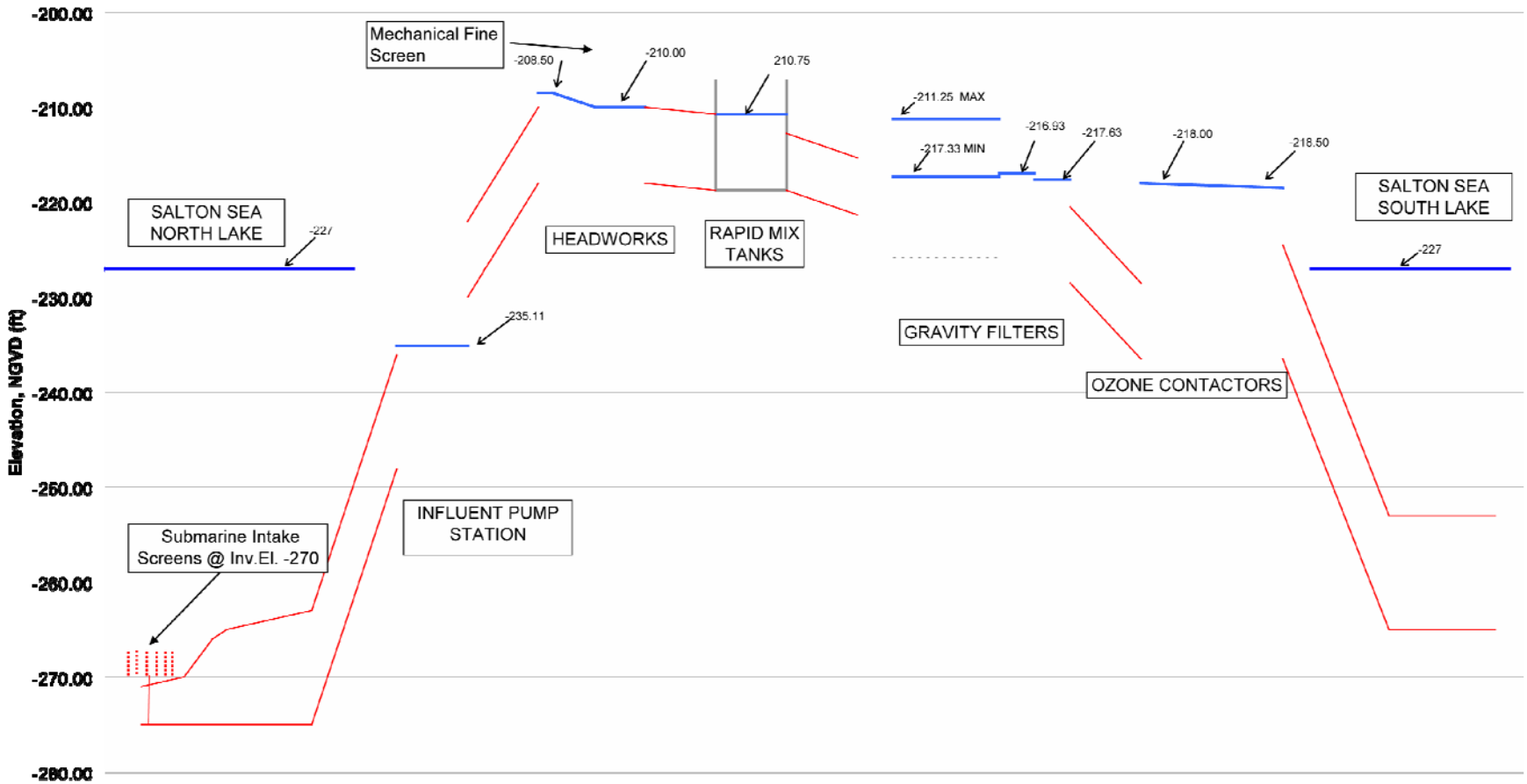

Figure 4-2. Salton Sea hypolimnetic water treatment plant - hydraulic profile at 450 mgd

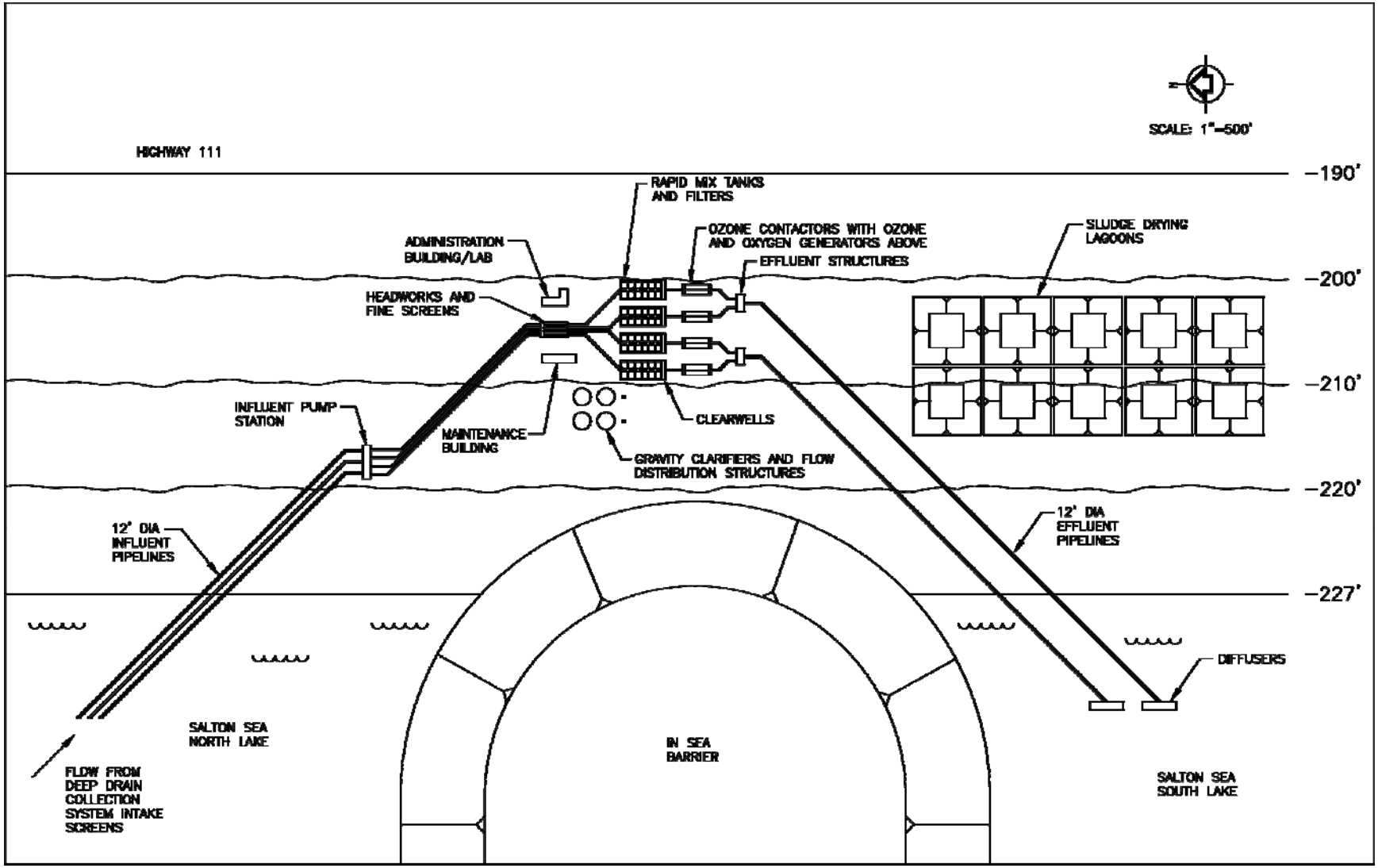

Figure 4-3. Salton Sea hypolimnetic treatment plant – conceptual plant layout

4.1. Deep Drain Collection System

The deep drain collection system will consist of a multi-point extraction system. Because of the shallow nature of the north lake a single point of extraction is not likely to provide adequate hydraulic control of the hypolimnion. For the purposes of this analysis the concept of using a series of 18 intake ports equally distributed near the lake bottom defined at approximately -275 ft was developed. Each of the hypolimnetic water intake ports would be outfitted intake screens engineered to withstand the conditions of the Salton Sea, and the particular problem of encrustation with barnacles. For the purpose of cost estimation, it is assumed that T-type wedge wire intake screens similar to those manufactured by Johnson Screens will be utilized. Screens would be manufactured from 316L stainless steel; however materials of construction should be confirmed by further analysis. Each screen would provide for intake of approximately 25 mgd. The entrance velocity at the face of the screen would not exceed 0.5 fps.

The intake screens will require periodic cleaning. This would be accomplished by back flushing the screen with a large volume burst of compressed air. Due the remote distance and the number of screens involved, application of the compressed air would likely be delivered from a properly outfitted barge mounted compressor and receiver. An umbilical hose connected to a buoy would allow connection of the barge mounted compressed air supply sparging system to flushing connection on the screen. By releasing a large volume of compressed air inside the screen is reported to effectively dislodge and remove debris and fouling organisms from the face of screen surface. This type of arrangement is reported to be used successfully in existing seawater intake screen applications.

The piping systems for transport of the hypolimnetic water to the treatment plant will need to be resistant to the highly corrosive water. Pipe fabricated from non-metallic materials of construction would be the most appropriate materials of construction. Reinforced concrete pipe might provide adequate service if fabricated using type V sulfate resistant cement. PVC and HDPE piping is not manufactured in the diameters required for this project. Spirally wound fiberglass reinforced plastic pipe is considered the most appropriate material for conveyance piping and was therefore used as the material for construction presented in this cost estimate. A schematic of the piping network required for extraction of the hypolimnetic water is presented in Figure 4-3. Approximately 29 miles of fiberglass pipe would need to be constructed and installed. The concept developed consists of 19 miles of 12 inch diameter and approximately 1.9 miles each of 4, 6, 8, 10 and 11 foot diameter pipe, respectively. Due to the large diameter and quantity of the required FRP piping, the pipe would be most cost effectively manufactured on-site. The deep drain collection system needs to be capable of collecting and conveying 450 MGD from the North Recreational Saltwater.

The cost to construct the hypolimnetic water collection piping and submarine screening system including engineering, construction management, permitting and a 30 percent contingency allowance is estimated to be approximately $477 million. The estimated cost for operation and maintenance of the collection system is anticipated to consist of annual inspection screens and pipelines and cleaning of the influent screens. Operation and maintenance labor was estimated to 3,000 hours per year.

4.2. Influent Pump Station

The influent pump station will draw hypolimnetic water into the wet well through the collection system then convey it to the treatment plant headworks. The approximate location of the influent pump station is schematically shown on Figure 4-3. The concept for the

influent pump station consists of a land based reinforced concrete structure featuring a wet well where the hypolimnetic water extracted from the lake will be conveyed and then subsequently lifted to the headworks of the treatment plant. The influent pump station would provide the primary energy to withdraw the hypolimnetic water from the lake and provide sufficient lift to allow gravity conveyance though the entire treatment plant with sufficient residual head to afford gravity conveyance of the treated water through the south lake outfall. The influent pump station would feature six – 75 mgd low head (32 feet) axial flow pumps, driven by 600 horsepower motors. Motors would operate on 4160 volt AC power. Pumps would be fabricated from high chromium stainless steel conforming to ASTM 990 Grade 5 and UNS 32750 or 32760, due to the corrosive nature of the water. The wet well of the pump station structure would be constructed of reinforced concrete prepared with Type V cement.

The wet well of the pump station would need to ventilated to eliminate the buildup and hydrogen sulfide gas in the pump house and the emission of fugitive odor from the wet well. The ventilation air from the pump station wet well will likely contain significant hydrogen sulfide and therefore should be scrubbed prior to discharge to the ambient atmosphere. The odor control treatment system would use treated oxygenated water as the collector for the odor control packed tower wet scrubber. The estimated capacity of the odor scrubber was estimated to be 10,000 scfm.

The cost to construct the hypolimnetic water influent pump station system including engineering, construction management, permitting and a 30 percent contingency allowance is estimated to be approximately $64.4 million. Operation and maintenance labor for this process is estimated to require 7,727 hours per year.

5. Treatment Plant

5.1. Plant Headworks and Fine Screening System

Hypolimnetic water from the north lake will be pumped by the influent pump station to the headwork. Although intake port for the hypolimnetic water collection system will be outfitted with fine screens it is likely that fouling organisms could likely develop on the interior of the collection pipe walls and therefore mechanical fine screening equipment is considered necessary to prevent fouling of gravity filters. Fine screen of the perforated plate or step screen design would be appropriate with a maximum opening of 0.25 inch. Screens would be fabricated from 316 stainless steel. The headworks channels would be covered and the headspace between the water surface in the channels and the channel covers would be withdrawn and conveyed to a foul air treatment system since there would likely be significant potential for off-gassing of hydrogen sulfide when the facility is in operation.

The cost to construct the treatment plant headwork and fine screening system including engineering, construction management, permitting and a 30 percent contingency allowance is estimated to be approximately $48.3 million. The estimated cost for operation and maintenance of the collection system is anticipated to consist of annual inspection and cleaning of the influent screen. Operation and maintenance labor was estimated to 4,000 hours per year.

5.2. Filtration System

The filtration system consists of a dual media gravity filters. Filter media will be anthracite and sand. Hypolimnetic water will be conveyed by gravity to rapid mix tank where a polymer solution will be injected in to the water to flocculate the particulates in the water prior to filtration. Filter runtimes are estimated to be at least 12 hours been backwash cycles based on the data collected during the pilot test. The filtration rate will be 5 gpm/ft^2. A total of 48 filters will be required. Filters will be arranged in four process trains. The filtered effluent will be collected in a clearwell located at the end of each filter process train. Adequate retention storage volume would be provided in the clear well to assure an adequate supply of filtered water for backwashing. Backwash water supply pumps will be capable of conveying flow up to 20 gpm/ft^2 to ensure adequate fluidization of the filter media and upflow velocity to carry the filtered solids out of the filter. The dirty backwash water will be conveyed to gravity clarifiers for removal of the settleable solids. A total of four 100 ft diameter clarifiers will be provided to concentrate the solids collected by filtration. Provisions will be made to allow addition of polymer or other flocculent aid to enhance the settleability of the solids. Effluent from the gravity clarifier will be pumped back to the headworks by the in-plant return water pump station. Sludge from the gravity clarifier will be disposed of in sludge lagoons outfitted with manual descant and gravity drainage systems. The supernatant off the sludge lagoons will be pumped to the South Lake Brine Pool.

The cost to construct the hypolimnetic water gravity filtration facilities (rapid mix, gravity filters filter backwash system, polymer systems, backwash water treatment system, sludge lagoons, and return water pump station) including engineering, construction management, permitting and a 30 percent contingency allowance is estimated to be approximately $276.3 million. Operation and maintenance labor for this process is estimated to require 48,000 hours per year.

5.3. Ozone Treatment System

The ozone treatment system consists of an on-site oxygen plant, ozone generators, and ozone contact tanks. To treat 450 mgd of hypolimnetic water with 2 mg/l of sulfide approximately 1300 pounds per hour of ozone is required. In order to generate this amount of ozone, approximately 150 tons per day of oxygen will be required to feed the ozone generators. Since it is not feasible to transport this volume of liquid oxygen to the treatment plant site, an on-site oxygen plant is required.

The on-site oxygen plant proposed two vacuum pressure swing absorption (VPSA) trains with each train having a capacity of 1000 scfm. Each train will provide approximately 66% of the maximum oxygen demand rate of the maximum capacity of the ozone generators. This is a non-cryogenic oxygen plant uses air as its source to generate oxygen at a purity of 90% to 92%. This plant will have a footprint of approximately 70 feet by 110 feet and will include molecular sieve adsorption columns, surge tanks, control systems and two 400 hp compressors, to increase the effluent pressure from 2 psig to 35 psig. The power required to run the plant is 620 kVa at 480 volts, and 2500 kVa at 4160 volts. No water source is required, but the plant will need to dispose of approximately 15 gpd of condensate which would be discharged into the plant recycle. Tetra Tech/KCM received 2 estimates, ranging from $5 million to $18 million in capital costs. One of the vendors typically owns and operates their plants and would charge a monthly fee of $95,000 for all 12 months of the year, even if the plant is only generating oxygen 6 months of the year. This would be a 10 year agreement and the monthly costs do not include power or other utilities, but it does include the capital costs and O&M.

Eight separate ozone generators will be required to generate the total mass of ozone required, 1300 pounds of ozone per hour. The ozone generator system consists of the ozone generators, power supply units, controls, field instruments and monitors, field valves, diffusion system and destruct units. These generators each have a footprint of approximately 18 feet by 8 feet and a power demand of 4.6 kWh per pound. The power supply units have an approximate footprint of 22 feet by 8 feet, and the residual ozone destruction units have an approximate footprint of 10 feet by 6 feet. One power supply unit is required for each ozone generator. A good quality water source is required for the cooling system at a quantity of 7.5 MGD.

The ozone contact tanks will provide 15 minutes of hydraulic contact time between the ozone and the filtered water to be treated. Therefore, this site would require four tanks, each measuring about 30 feet wide by 148 feet long by 18 feet deep. Tanks will be arranged in groups of two parallel contact tanks sharing a common center wall as illustrated on the drawings. The ozone contact tanks would be constructed of reinforced concrete as previously described for other structure and would be constructed with internal baffles to reduce short circuiting. The ozone would be applied to the contact tanks through a venturi eductor system to provide high efficiency mass transfer of the ozone gas into the water. Approximately 8 percent of the flow of filtered water conveyed to each respective ozone contact tank will be pumped to provide the motive force to drive the ozone injectors. The off-gas from the ozone contact tanks will be collected and pumped through a catalytic ozone destruction unit prior to discharge to the ambient. The ozone generation equipment would be housed in a building built above the ozone contact tanks.

The cost to construct the ozone treatment process facilities (oxygen plant, ozone generators, ozone contact tanks, residual ozone destruction systems, and associated ozone generator cooling water systems) including engineering, construction management, permitting and a 30

percent contingency allowance is estimated to be approximately $284.8 million. Operation and maintenance labor for this process is estimated to require 25,000 hours per year.

5.4. Treated Effluent Recycle

Although the Authority's plan identified an effluent pump station, the hydraulic analysis conducted for this study indicates that an effluent pump station is not required and that the treated effluent may be discharged to the south lake by gravity conveyance utilizing the residual head from the treatment plant. The treated water will be recycled to the south lake through two parallel 12 ft diameter FRP pipelines. The terminal end of each of the effluent pipelines will be outfitted with a multiport diffuser. The constructed value of the treated effluent conveyance pipelines and multi-port outfall diffusers is estimated to be approximately $173 million. The estimated cost for operation and maintenance of the treated water discharge piping and diffuser outfall is anticipated to consist of annual inspection of pipelines and cleaning of outfall diffusers. Operation and maintenance labor was estimated to 500 hours per year. The costs for accomplishing effluent monitoring and chemical and biological analyses on the treated effluent and receiving water are not defined and therefore have not been included in the annual operating costs.

6. Operation and Maintenance cost

Operation and maintenance costs were estimated based on the assumption that the processing facilities would be operated 7 months per year. Annual operations and maintenance costs are summarized in Table 9-1. Labor requirements for operation, maintenance and administration of the facility were estimated on a unit process basis in accordance with the methodologies and data presented in EPA 1979 and Langlais et al. 1991. Where specific data were not available, values were estimated using best professional judgment (BPJ). A summary of operations and maintenance labor requirements by unit process is presented in Table 9-2. A total of 52 full time employees will be necessary to operate and maintain the hypolimnetic water extraction, treatment and discharge system including administrative and analytical laboratory personnel. The total annual cost for operation and maintenance including labor, materials and utilities for the hypolimnetic water extraction, treatment and discharge system is estimated to be approximately $33 million.

7. Comparison with Cost Estimates of Phosphorus Removal Plant for Inflows

One element of the restoration plant that has been proposed by the SSA is the use of a chemical treatment plant sited on the Alamo River that would remove sediments, salts, and nutrients from the New and Alamo Rivers. The primary basis for the planning, design and construction of a conventional physical-chemical water treatment plant is to significantly reduce the phosphorus concentrations in the New and Alamo Rivers immediately before the waters flow into the Salton Sea. Phosphorus loads provide the fuel that causes eutrophication that in turn leads to oxygen depletion and hydrogen sulfide production in the hypolimnion of the Sea. Over the long term, phosphorus load reduction is a way to attack the problem of hydrogen sulfide production, independent of ozonation. Estimated costs for a water treatment plant of appropriate scale are presented here for comparison with the ozonation plant. This cost estimation was originally developed as part of a prior study for the SSA (Tetra Tech, 2007).

The physical-chemical treatment technology conventionally used for phosphorus removal involves precipitation of the phosphorus using metal ions of aluminum, calcium, or iron as collectors. In general, alum, a hydrated aluminum sulfate, has proven to be the most cost-effective and efficient chemical for precipitation of orthophosphates and collection of organic and inorganic phosphorus. The practical lower limit for total phosphorus removal using only gravity sedimentation has been reported to be approximately 0.5 mg/L. If conventional rapid filtration or membrane filtration is employed subsequent to gravity sedimentation, then the total phosphorus concentration can be consistently reduced so that the residual total phosphorus concentration is in the range of 0.020 to 0.040 mg/L. For the purposes of the analysis presented below, it is assumed that the total phosphorus concentration can be reduced to achieve treated water with total phosphorus concentration of approximately 0.025 mg/L. An alum dose equal to a mole ratio of 2 moles of aluminum per mole of phosphorus was assumed based on experience and data reported in the literature for other water similar in nature that required treatment to achieve this low residual phosphorus concentration.

The treatment facility would start with a fine screen headworks to remove all debris greater than 0.125 inches. The resulting debris from the screening system would be washed, compacted, and then disposed of as green waste. After screening, liquid alum would be blended into the water to precipitate the dissolved phosphorus and to stimulate the coagulation of the suspended and colloidal solids in the water. The resulting coagulated water would be conveyed to flocculating type circular clarifiers outfitted with a sludge thickening and collection mechanism. Sludge would be pumped from each of the clarifiers at a solids concentration of approximately 1% solids and conveyed to solar sludge drying beds or lagoons. Based on the climatic conditions in the area, non-mechanical sludge dewatering of the sludge might be the most cost-effective means for dewatering the solids. The amount of land required for sludge drying beds or lagoons would range between 350 to 700 acres.

7.1. Capital Costs for Treating Inflows

Three scenarios were developed to evaluate costs for a range of treatment levels. Scenario A is the most aggressive approach. It is designed to reduce the phosphorus loading to the Salton Sea from 1.23 million kg/yr to approximately 0.1 million kg/yr, which is a reduction of 92 percent. This corresponds to an average concentration of approximately 0.08 mg/L total phosphorus for the combined average flow for both rivers. To accomplish this level of phosphorus reduction, approximately 84 percent of the flow of the New River and 100 percent of the flow of the Alamo River would be intercepted and pumped to the physical-

chemical treatment facility. It is assumed that the water from each of the respective rivers would be intercepted and pumped to a common treatment facility. Scenario 2 is designed for a 79 percent reduction, or loading of 0.26 million kg/yr. Approximately 48 percent of the New River flow and 100 percent of the Alamo River flow would be intercepted and pumped to the physical-chemical treatment facility. Scenario 3 is designed for a 49 percent reduction, or loading of 0.63 million kg/yr. Approximately 50 percent of the New River flow and 50 percent of the Alamo River flow would be intercepted. Table 9-3 presents a generalized basis for design for the three scenarios.

Construction costs were principally estimated using the cost models generated by the United States Environmental Protection Agency (EPA, 2001) and then adjusted to current costs using the Engineering News Record Construction Cost Indexes for the years that the cost models were generated. The respective cost indices are shown on the cost estimate data sheets for each respective treatment scenario. Costs for engineering design, construction management, permitting and project contingency were developed using percentages of the estimated construction costs that are characteristically applied to project of this magnitude and complexity. Table 9-3 presents the cost results for total capital investment.

Table 9-3 also presents the costs for treatment for the same scenarios, except the cost for filtration has been excluded. Although most studies report that filtration is required after sedimentation to reliably reduce total phosphorus below 0.050 mg/L, pilot testing accomplished for the South Florida Water Management District (2000) indicated that total phosphorus concentrations of 0.010 mg/L could be achieved through coagulation/precipitation with alum followed by flocculation and sedimentation alone without the need for filtration. As shown in the cost tables herein, the project costs for both capital facility investment and operation and maintenance requirements would be significantly lower if filtration was not required. Site pilot testing would be recommended to determine if the low levels of total phosphorus can be achieved in treating the New and Alamo River water without the need to include filtration as part of the treatment process.

7.2. Operations and Maintenance Costs for Plant Treating Inflows

The analysis also addresses long-term costs associated with operation and maintenance of the treatment plant. Operations and maintenance labor costs were generated based on best professional judgment. Annual maintenance of mechanical equipment and facilities was estimated at 2 percent of the estimated construction cost. Alum, polymer, electrical power, and sludge haul costs based on the estimated usage rates shown and best professional judgment.

Table 9-3 presents the cost results for total capital investment, and annual operation and maintenance costs. Present worth of the pumping and treatment systems for each scenario are also presented based on a 50-year facility life cycle including both capital costs and operation and maintenance costs. The estimate annual cost to construct and operate the facilities for 50 years is presented as well as a cost for treatment with respect to the mass of phosphorus removed.

8. Summary

A conceptual design and cost estimate was developed for a large (450 mgd) plant for extraction of anoxic, sulfide rich hypolimnetic water and ozonation. Both capital and operating and maintenance costs were estimated. The total capital investment is estimated to be $1.28 billion, of which about 40% is associated with the construction of the system of

pipes for hypolimnetic extraction. The total annual cost for operation and maintenance including labor, materials and utilities for the hypolimnetic water extraction, treatment and discharge system is estimated to be approximately $33 million. Amortized over a thirty-year period at an interest rate of 3.5%, the annualized capital cost is $69.5 million. The total annual costs are $102.3 million. In contrast to the hypolimnetic extraction and ozonation, a plant for the treatment of inflows is somewhat less expensive. Capital costs range from $208 million to $620 million, depending on the volumes of flow treated and whether filtration is used. The annualized capital and O&M costs range from $28 million to $50 million.

9. Supporting Documentation

Supporting cost documentation utilized for preparing this estimate is presented Appendices A, B, and C.

Table 9-1
Salton Sea Hypolimnetic Treatment Plant

Cost Indexes							
1978 ENR construction cost index			2694.00	Mar-78			
January 1999 ENR construction cost index			5999.63	Jan-99			
January 2001 ENR construction cost index			6280.00	Jan-01			
January 2003 ENR construction cost index			6580.00	Jan-03			
Current ENR construction cost index			7856.27	Mar-07			
Major Process Facilities							**notes**
Submarine intake screens				450	mgd	$34,044,600	(1)
Air sparging system for intake screens				1	ea	$500,000	BPJ
48" Intake conveyance piping				8,800	ft	$6,044,074	(2)
60" Intake conveyance piping				8,800	ft	$7,335,526	(2)
84" Intake conveyance piping				8,800	ft	$7,935,836	(2)
108" Intake conveyance piping				8,800	ft	$11,315,467	(2)
120" Intake conveyance piping				8,800	ft	$12,935,002	BPJ
132" Intake conveyance piping				8,800	ft	$15,607,797	(2)
144" Intake conveyance piping				75,648	ft	$157,576,310	(2)
Influent pump station				450	mgd	$39,522,600	(2)
Treatment plant headworks and fine screens				450	mgd	$29,601,000	(3)
Gravity Filters				450	mgd	$127,770,000	(4)
Polymer Feed and Rapid Mix				450	mgd	$3,809,000	(3)
Ozone Contact Facilities				9.375	mgal	$35,580,485	(5)
Ozone Generators				30,024	lbs/d	$121,169,343	(5)
Oxygen Generators				115	tons/day	$18,000,000	(6)
Effluent pipeline				52,800	feet	$106,705,000	(1)
Backwash water pumping system				43	mgd	$8,671,000	(2)
Backwash water treatment clarifiers				43	mgd	$6,908,200	(2)
Plant return water pump station				50	mgd	$9,600,500	(2)
Sludge lagoons with decanting facilities				450	mgd	$11,600,000	(3)
Sludge lagoon supernatant pump station				1	mgd	$1,128,000	(7)
Administration building and laboratory				10,000	sf	$2,500,000	BPJ
Emergency Power				1000	kilowatts	$558,288	(3)
Maintenance building				10,000	sf	$1,500,000	BPJ
Supervisory control and data acquisition system				450	mgd	$6,115,000	(3)
Site improvements and general utilities				10%		$78,403,303	(8)
				Estimated Construction Cost		$784,033,029	
Engineering Design				15%		$117,604,954	BPJ
Construction Management				15%		$117,604,954	BPJ
Permitting				3%		$23,520,991	BPJ
Contingencies				30%		$235,209,909	BPJ
				ESTIMATED TOTAL CAPITAL INVESTMENT		**$1,277,970,000**	
Operations and Maintenance							
Labor							
	Personnel	52	persons	50,000	per person	$2,593,208	(5)(8)(9)
Materials							
	Anionic polymer	404,542	lbs/yr	$3.00	per lbs	$1,213,625	(8)
	Mechanical equipment maintenance			3%	CC	$23,520,991	(5)(8)(9)
Services							
	Sludge load and haul	40,965	wet tons/yr	$5	per ton@20%	$204,826	BPJ
Utilities							
	Buildings & Site Electricity	2,102,400	kWh/yr	$0.08	kWh	$168,192	(8)
	Process Electricity	63,943,846	kWh/yr	$0.08	kWh	$5,115,508	
				ESTIMATED TOTAL ANNUAL OPERATION AND MANTENANCE		**$32,820,000**	
Present worth	3.5%		50 years			**$2,400,000,000**	
CC-APMT	3.5%		30years			$69,480,000	
AO&M						$32,820,000	
				ESTIMATED TOTAL ANNUAL COST		**$102,300,000**	

Notes

(1) EPA 2003 & escalated 15% based on materials
(2) EPA 2003 & escalated 30% based on materials
(3) EPA 2003
(4) EPA 2003 & escalated 25% based on materials
(5) Langlais et.al. 1991 + vendor estimate
(6) Vendor Estimates refer to Appendix C
(7) EPA 2003 & escalated 100% based on materials and fluid
(8) EPA 1979
(9) Peters and Timmerhaus 1980
BPJ Best professional judgment

Table 9-2
Operations and Maintenance Labor Estimate By Process

Process Area	Labor - hr/yr
Submarine intake screens	1000
Intake conveyance piping	2000
Influent pump station	7727
Treatment plant headworks and fine screens	4000
Gravity Filters	39253
Polymer Feed and Rapid Mix	968
Ozone Facilities	25049
Effluent pipeline	500
Backwash water pumping system	414
Backwash water treatment clarifiers and sludge pumps	5080
Plant return water pump station	1622
Sludge lagoons	656
Admin & Maintenance Bldgs Laboratory & site	15460

Table 9-3
Estimated Cost Data for Chemical Treatment Plant[1]

	Scenario A	Scenario B	Scenario C	Scenario A - Without Filtration2	Scenario B - Without Filtration2	Scenario C - Without Filtration2
Design Criteria						
Average Operating Rate (mgd)	883	739	473	883	739	473
Annual Treatment Volume (AF/yr)	989,000	828,000	530,000	989,000	828,000	530,000
Percentage of Alamo River to be Treated (%)	100	100	50	100	100	50
Percentage of New River to be Treated (%)	84	48	50	84	48	50
Total Phosphorus Reduction (%)	92	79	49	92	79	49
Total Phosphorus Load to Salton Sea After Treatment (kg/yr)	1,129,343	969,739	599,927	1,129,343	969,739	599,927
Phosphorus Concentration to Salton Sea After Treatment (mg/L)	0.08	0.20	0.48	0.08	0.20	0.48
Capital Cost (in millions)	**$M**	**$M**	**$M**	**$M**	**$M**	**$M**
Treatment Plant[3]	$329	$275	$198	$141	$122	$94
Pump Station and Intake/Diversion Structure	$52	$44	$34	$52	$44	$34
Engineering Design (15%)	$57	$48	$35	$29	$25	$19
Construction Management (15%)	$57	$48	$35	$29	$25	$19
Permitting (3%)	$11	$10	$7	$6	$5	$4
Contingencies (30%)	$114	$96	$70	$58	$50	$38
TOTAL CAPITAL COSTS	**$620**	**$520**	**$378**	**$314**	**$270**	**$208**
Operating & Maintenance (O&M) Cost (in millions)	**$M/year**	**$M/year**	**$M/year**	**$M/year**	**$M/year**	**$M/year**
Labor & Supervision	$1	$1	$1	$1	$1	$1
Maintenance & Materials	$16	$13	$12	$12	$10	$10
Residuals Management	$5	$5	$5	$5	$5	$5
Utilities	$1	$1	$1	$1	$1	$1
TOTAL ANNUAL O&M COSTS	**$24**	**$21**	**$19**	**$20**	**$18**	**$17**
Total Capitalized Present Worth (3.5% interest, 50 years)	**$1,175**	**$1,154**	**$990**	**$781**	**$763**	**$713**
Total Annual Cost	**$50**	**$49**	**$38**	**$32**	**$33**	**$28**
Cost per Kilogram of Phosphorus Removed	**$9**	**$10**	**$13**	**$6**	**$7**	**$10**

Notes:

1. Reproduced from Tetra Tech, 2007.
2. Most studies report that filtration is required after sedimentation to reliably reduce total phosphorus below 0.050 mg/L. Pilot testing performed for the South Florida Water Management District (2000) indicated that total phosphorus concentrations of 0.010 mg/L could be achieved through coagulation/precipitation with alum followed by flocculation and sedimentation alone, without the need for filtration. Site pilot testing would be needed to determine if the low levels of total phosphorus can be achieved without filtration.
3. Treatment plant includes headworks and fine screen, flocculation and clarification, filters, chemical storage tanks, chemical feed system, sludge handling, administration building and laboratory, emergency power, and supervisory control and data acquisition system.

10. References

EPA. 2001. 1999 Drinking Water Infrastructure Needs Survey, Modeling the Cost of Infrastructure. EPA 816-R-01-005. February 2001.

EPA. 2003. Drinking Water Infrastructure Needs Survey, Modeling the Cost of Infrastructure. EPA 816-R-06-007, June 2006.

EPA. 1979. Estimating Water Treatment Costs, Volume 2 Cost Curves Applicable to 1 to 200 mgd Treatment Plants EPA 600/2-79-162b.

Langlais, Bruno, Reckhow, David A., and Brink, Debrorah R. 1991. Ozone in Water Treatment: Application and Engineering. 569p. American Water Works Association Research Foundation and Lewis Publishers. ISBN 0-87371-474-1.

Peters, Max S. and Timmerhaus, Klaus D. 1980. Plant Design and Economics for Chemical Engineers. McGraw Hill Publishers. ISBN 0-07-049582-3.

Sanks, Robert L. 1978. Water Treatment Plant Design for the Practicing Engineer. Ann Arbor Science Publishers, Inc. ISBN 0-250-401183-5.

South Florida Water Management District, 2000. Chemical Treatment Followed by Solids Separations Advanced Technology Demonstation Project; Contract No. C-E10650. prepared by HAS Engineers and Scientists, Milian, Swain & Associates, and Lockhart AG Technologies.

Tetra Tech. 2007. New and Alamo River Wetlands Master Plan, prepared for the Salton Sea Authority and the Wildlife Conservation Board. With support from Wetlands Management Services, Chelsea, Michigan.

Williams, Robert W. and Culp, Gordon L., 1986. Handbook of Public Water Systems, 1113 p. Van Rostrand Reinhold Company Inc. ISBN 0-442-21597-5.

Appendix A

PROPOSAL

April 13, 2007

Tetra Tech/KCM
1420 Fifth Avenue, Suite 600
Seattle, WA 98101

ERSHIGS
A Denali company
The Leader in FRP Systems

Attention: Ann Bryant

Subject: **Ershigs' Budget Proposal No. 710104**
FRP Circulating Water Pipe for the Salton Sea Intake Pipe

Ershigs is pleased to offer the following budget proposal for the design and manufacture of Fiberglass Reinforced Plastic (FRP) Buried Circulating Water Piping for the subject project.

Ershigs has been supplying quality products and dependable service to our customers since 1921. Our 40 years of experience as the leader in the FRP Industry provides our customers with the knowledge that Ershigs has successfully addressed almost every type of design and manufacturing challenge faced in the corrosion resistant FRP market. Given the opportunity, we are prepared to demonstrate our capabilities.

Ershigs is part of the largest custom FRP design, manufacturing and specialty Contractor Company in the U.S., the Denali Company. Our combined resources include FRP manufacturing operations in Bellingham, WA, Sarnia, Ontario and Grand Bay, AL.

ADVANTAGES OF FIBERGLASS REINFORCED PLASTIC PIPING:

- Smoother interior: FRP has a Hazen and Williams roughness coefficient of 150. This can equate to smaller diameter for FRP Pipe or a decrease in pump size in comparison to concrete or steel.
- FRP ranges from 1/10 to 1/20 the weight of reinforced concrete pressure pipe and about 1/3 the weight of steel pipe depending on diameters. In addition, the FRP can be supplied in 60' lay lengths. This equates to a cost and schedule savings with an FRP system due to a lesser number of spools to offload and set, lighter lifting equipment and a greater amount of pipe that can be shipped on a freight load.
- The longer FRP pipe lengths equate to fewer field joints thus minimizing the potential for leaks and providing a cost savings in joint testing.
- FRP requires no secondary grouting or cathodic protection.
- FRP provides corrosion resistance throughout the matrix of the pipe. In many cases, reinforced concrete or coated carbon steel is attacked from the outside of the pipe due to aggressive external conditions.

SCOPE OF WORK
Ershigs Inc. will:

Design the subject FRP piping system in accordance with AWWA-C950, AWWA M45, and Ershigs proven engineering practices for composite material.

Produce and submit manufacturing drawings to customer for review and approval. Ershigs standard CAD drafting procedures are proposed. Please note that Ershigs' drawings will depict FRP equipment only or equipment supplied by Ershigs.

Manufacture one lot of 120" ID FRP Circulating Water Piping.

Test and inspect the proposed piping in accordance with our established QA/QC procedures.

Prepare and load completed piping on trucks for shipment to your jobsite. Preparation for shipment will include cleaning of the pipe, stenciling spool mark numbers on outside of pipe spools and setting on wood chocks.

ITEMS AND SERVICES NOT INCLUDED IN ERSHIGS' SCOPE

Unloading and Installation.

Spare parts and special tools.

Fasteners and gaskets except for manways and o-rings.

Valves and instrumentation.

Shop or field hydrostatic test.

Taxes and freight.

MATERIALS AND MANUFACTURING DETAILS

Resin will be an isophthalic polyester system throughout.

The corrosion barrier will consist of one (1) layer of C-glass and one (1) layer of 1½ oz/ft^2 chopped strand for a 50-mil structural thickness.

Exterior wall on the pipe will consist of filament wound continuous strand fiberglass reinforcement. Fittings and joints will consist of alternating layers of chopped strand and woven roving to the designed wall thickness.

Exterior surface will receive a paraffinated surface coat with UV inhibitors. Standard colors are gray or white. Custom colors can be provided at an additional price.

Pipe spools will be shipped in maximum 60' lengths.

Elbows will be three-piece, two-miter filament wound construction.

Flanges will be flat face with dimensions per ANSI B16.5 with 125# drilling dimensions.

Field joints for underwater piping will be Ershigs standard double O-ring bell and spigot restrained joints, complete with O-rings, test ports and stainless steel restraints (where required).

Above ground field joints to be our standard butt and wrap type joint. Field joint materials are included in our offering for all above ground joints.

ENGINEERING AND DESIGN DETAILS
Ershigs' proposal for the pipe is designed in accordance with AWWA C950 and AWWA M45 based on the following assumed conditions.

Design Temperature:	Ambient 110° to –15°F
Design Pressure:	50 psig
Vacuum:	None assumed
Truck Loading:	Yes
Water Level:	50' (max)

BUDGET PRICING (+/- 15%)
To manufacture one (1) lot of 120" ID Circ. Water Piping: **$116,160,000.00**

TERMS
F.O.B. our plant near the Salton Sea. Freight to prepaid and added.

Pricing above excludes all sales and use taxes.

This offering is based on Ershigs standard terms and conditions, ES-801.1 attached.

SCHEDULE
Drawings and calculations typically require five to six weeks after receipt of order and clarification of all details.

Shipments can commence three to four months after customer release. Total manufacture will require approximately two years to complete.

Schedules are based on current backlog and are subject to prior commitments. Please confirm schedules at time of order placement.

We trust you will find our proposal satisfactory. If you have any questions or require additional information on our quality FRP products, please do not hesitate to contact Glenn Haley at (360) 887-1824 or our V-P of Sales and Marketing, Chaun Trenary at (480) 926-5782.

Sincerely,

ERSHIGS, INC.

Thomas L. Rhone
Regional Sales Manager

cc: G. Haley
C. Trenary
J. Konkle

(710104p1r)

Appendix B

Johnson screens™
A Weatherford Company
JOHNSON SCREENS, INC.
1950 OLD HWY 8 NW
NEW BRIGHTON MN 55112
UNITED STATES

QUOTATION

Quote Number:	**145818 SQ**
Order Date:	**MAY 31 2007**
Customer Reference:	**Salton Sea, CA**
Location:	**13001 NEW BRIGHTON**
Phone No.:	**800.833-9473**
Fax No.:	**651.638-3177**
Sales Person:	**LON D MCMILLIN**

TERMS	QUOTE VALIDITY	ENTERED BY
Net 30 days		COOK, LINDA S

SHIPPING TERMS	SHIPPING INSTRUCTIONS
EXW Ex Works	EXW-FACTORY PREPAID IN USA

LINE NO.	ITEM NUMBER DESCRIPTION	UOM	QTY SHIPPED	UNIT PRICE	EXTENDED PRICE
	. . *Attn: Ann Bryant* *Tetra Tech* *Seattle, WA* *Ph: 206-883-9330* *e-mail: ann.bryant@tetratech.com* . . *Quote valid to 7/31/07* . .				
1.000	Johnson T-84HCE Intake Screen... . . *T-84 High Capacity Extended Intake Screen* *Wire: #93* *Slot: .250"* *Material: 316L stainless steel* *Air Backwash Connection: None* *Flow: 75 MGD/ Screen has under* *. .5 ft/sec max thru slot velocity* *Depth: 50 FT* *Outlet: Flange pattern to match AWWA C-207* *. class D 60" PS with pipe connect* *End Connections: Dished Head X Dished Head* . . *Johnson Intake Screens are covered by one or more of the following patents - #6,051,131; #6,712,959; and other patents pending.* . . *DELIVERY ON INTAKES:* *2-3 Wks for drawing submittals* *10-12 Wks after drawing approval, subject to manufacturing capacity*	EA	6.00	110,000.0000	660,000.00

CONTINUED

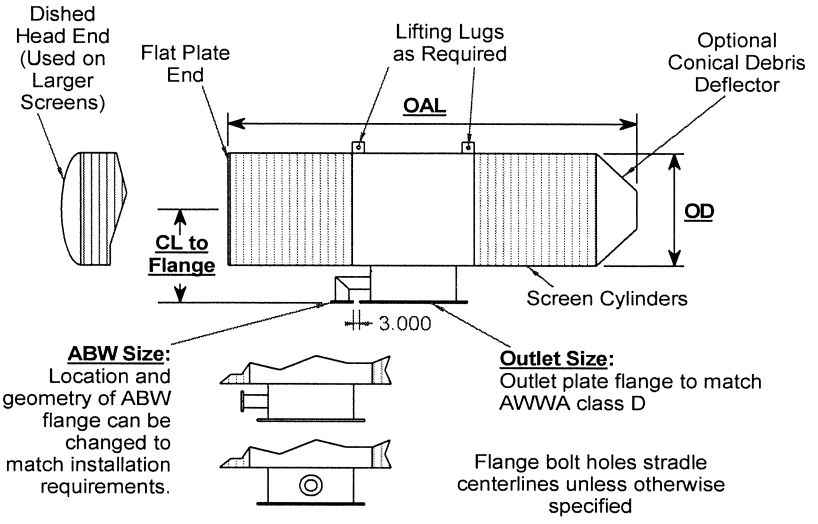

Dimension/Sizes	Value	Unit	Comments
Model	T84HCE		
OD	84.00	in	Nominal See note 1
OAL	322.00	in	Nominal See note 1
CL to Flange	46.00	in	Nominal See note 1
Outlet Connection Size	60PS		See note 2
ABW Connection Size	None		See note 2
Weight	12000	lbs	
Left End Closure	dish		
Right End Closure	dish		

Screen Specifications			
Slot Opening	0.25	in	
Open Area Percentage	73.75%		
Wire Type	93		

Design:			
Depth	50	Ft	Hydrostatic Load
Collapse Rating	21.68	psi	
Material	316L		SS or Z-Alloy

Flow Capacities:			
Flow/Screen	75	MGD	See note 3
Maximum Slot Velocity	0.50	fps	See note 3
Average Slot Velocity	0.43	fps	See note 3
Estimated DP/Screen	0.0034	psi	Thru clean screen surface only-See note 4
Estimated DP/Assy	0.4173	psi	Through entire clean assembly - See note 4

Notes:

1 Dimensions shown are nominal. All screens are made to order, and can be adapted to a wide variety of installation requirements.

2 These is based on the size of the connecting and abw pipe and may vary from the values listed in the technical brochure.

3 Capacities based on use of patented Johnson flow modifier design.

4 Pressure drops below .1 psi should be considered an order of magnitude only, as testing date for these low values is not available.

The concepts and assemblies shown should be considered proprietary and should not be copied, redistributed without the permission of Johnson Screens. All dimensions are preliminary, changes may be made and can effect final price and configuration. All rights reserved.

Johnson Screens
1950 Old Hwy. 8, New Brighton, MN 55112
(651)-638-3110 (Phone), (651)-638-3177 (Fax)

Model T84HCE
Preliminary Intake Screen Specification
Salton Sea, CA

Date:
5/31/2007

Appendix C

Bryant, Ann -- Tetra Tech

From: Bak Srikanth [bsrikanth@aptwater.com]
Sent: Tuesday, April 17, 2007 4:24 PM
To: Bryant, Ann
Cc: Bryant, Ann; Markus, John; Douglas Gustafson; Douglas Liddie; Keel Robinson; Shawn Ferron
Subject: RE: P1821 Tetra Tech Salton Sea project

Ann,
We've had some internal discussions regarding your request for a 450 MGD HiPOx system for the Salton Sea. Here's our super-ballpark / super-preliminary estimate of the cost:
As you and I discussed, it wouldn't be one single HiPOx unit but multiple. Conceptually, it'd be Qty. 10 (ten) HiPOx units. The ozone dose is based on your specified total ozone dose of about 1,300 pph.
Total Installed Price: $150 million. This price would include the ozone generators, HiPOx reactors/injectors, control systems and installation.
Space/Dims: We don't have any estimate on the footprint or space at this time.

A Friendly Word of Caution:
Ann, as you can imagine, the above is only a preliminary estimate at best. As this opportunity moves along and matures into a potential project (whenever that is), then we'll re-visit and make a more informed estimate.
Pilot Test: Such an estimate would have to be preceded by an on-site pilot test with say, a 22.5 or 45 MGD pilot system intended to provide a more accurate info/data with respect to scalability.

Thanks Ann. Please call with any questions.

Best Regards,
Bak Srikanth
Regional Director of Customer Solutions
Applied Process Technology, Inc.
P.O. Box 221811
Santa Clarita, California 91322-1811
Cell: (661) 747-6668
E-mail: bsrikanth@aptwater.com
www.aptwater.com

From: Bryant, Ann [mailto:Ann.Epler@tetratech.com]
Sent: Tuesday, April 17, 2007 12:08 PM
To: Bak Srikanth
Cc: ann.bryant@tetratech.com; Markus, John
Subject: RE: P1821 Tetra Tech Salton Sea project

Bak –
Thank you for calling back this morning. I understand that you are meeting this afternoon to talk about this project and will get back to us tomorrow morning with a ballpark cost estimate. We know that the flow through the plant will be approximately 450 MGD and that the required ozone dosage is about 1300 lbs/hour. Along with the ballpark cost estimate, please include the approximate size of the equipment and what the cost estimate includes (i.e. ozone generator, diffusers, etc).
If you have any questions, I will be in the office all afternoon.
Thank you,
Ann

Ann Bryant, PE | Civil Engineer
Direct: 206.883.9330 | Main: 206.883.9300 | Fax: 206.883.9301
ann.bryant@tetratech.com

Tetra Tech/KCM | Seattle

1420 Fifth Avenue, Suite 600 | Seattle, Washington 98101 | www.tetratech.com

PLEASE NOTE: This message, including any attachments, may include privileged, confidential and/or inside information. Any distribution or use of this communication by anyone other than the intended recipient is strictly prohibited and may be unlawful. If you are not the intended recipient, please notify the sender by replying to this message and then delete it from your system.

From: Bak Srikanth [mailto:bsrikanth@aptwater.com]
Sent: Monday, April 16, 2007 4:28 PM
To: Bryant, Ann
Subject: RE: P1821 Tetra Tech Salton Sea project

Ann,
Got your voice-mail message. Sorry for the delay on our part. I understand you don't have all the info to fill out the HiPOx form. Whatever info you could provide would be much appreciated.

Also, can you define the scope of work as far as our (Applied's role) in this project? That would greatly help. Thanks Ann.

From: Bak Srikanth
Sent: Friday, March 30, 2007 3:27 PM
To: Ann Bryant (Ann.Bryant@TetraTech.com)
Subject: P1821 Tetra Tech Salton Sea project

Ann,
Nice talking to you this afternoon. Thanks for the call. Here's the HiPOx process request form. Please fill it out and return with available water quality and other info. Thanks Ann. I look forward to hearing from you. Have a good weekend.

MITSUBISHI ELECTRIC POWER PRODUCTS, INC.
. . . The Power of Commitment

MITSUBISHI ELECTRIC POWER PRODUCTS, INC.
530 Keystone Drive
Warrendale, PA 15086-7538
Phone (724) 778-5111 Fax (724) 778-5149
Home page: www.meppi.com

SALTON SEA

OZONE EQUIPMENT TECHNICAL INFORMATION AND SCOPE DOCUMENT for an

OXYGEN FED OZONE SYSTEM

MEPPI PROJECT REFERENCE RZ0192

July 2007

Mitsubishi Electric Power Products, Inc.
Ozone & Industrial Systems Division
Thorn Hill Industrial Park
530 Keystone Drive
Warrendale, PA 15086-7538
Telephone: (724) 778-5111
Fax: (724) 778-5149

Home Page: **www.meppi.com**

This document is the property of Mitsubishi Electric Power Products, Inc. and contains proprietary and confidential information, which must not be duplicated, used or disclosed other than as expressly authorized by Mitsubishi Electric Power Products. Inc.

Preliminary Budgetary Bid

TABLE OF CONTENTS

PROPOSAL LETTER

SECTION 1 BUDGET COMMERCIAL OFFER 1-1

1.1 OZONE GENERATION SYSTEM 1-1
1.1.1 Scope Oxygen system ..... ***Error! Bookmark not defined.***
1.1.2 Scope Ozone System ..... ***Error! Bookmark not defined.***
1.1.3 Oxygen Storage System. ..... ***Error! Bookmark not defined.***
1.2 TERMS AND CONDITIONS 1-1
1.3 DELIVERY 1-1

SECTION 2 EQUIPMENT SPECIFICATION 2-1

2.1.1 LOX Quality Requirements *2-1*
2.2 NITROGEN BOOST SYSTEM 2-2
2.3 PRESSURE REGULATING AND GASEOUS OXYGEN FILTER SYSTEM 2-2
2.4 OZONE COOLING WATER SYSTEM 2-3
2.5 OZONE GENERATION AND POWER SUPPLY 2-3
2.5.1 Ozone Generator Cell Specification *2-3*
2.5.2 PSU Parameters *2-4*
2.5.3 HV Inverter Unit Parameters *2-5*
2.6 OZONE GENERATOR CONTROL SYSTEM 2-5
2.7 HIGH CONCENTRATION OZONE MONITORING 2-5
2.8 AMBIENT OZONE MONITORING 2-5
2.9 INJECTOR SYSTEM 2-6
2.10 SKID MOUNTED OZONE OFF-GAS DESTRUCTION UNITS 2-6
2.10.1 Pre Heater Unit *2-6*
2.10.2 Catalytic Destructor *2-7*
2.11 ANCILLARY EQUIPMENT 2-8
2.12 PIPE WORK AND VALVES 2-8
2.13 SPECIAL TOOLS ..... **ERROR! BOOKMARK NOT DEFINED.**
2.14 SPARE PARTS ..... **ERROR! BOOKMARK NOT DEFINED.**

SECTION 3 AUTOMATIC CONTROL - OPERATION OF THE CONTROL PANEL 3-1

3.1 GENERAL 3-1
3.2 CONTROL 3-1
3.3 EQUIPMENT ALARMS 3-1
3.4 AMBIENT OZONE ALARMS 3-1

SECTION 4 SCOPE OF SUPPLY & SERVICES 4-1

4.1 EQUIPMENT SUPPLY 5-2
4.2 SERVICES OFFERED 5-2

SECTION 5 PRODUCT DESIGN SUBMITTALS 6-1

SECTION 6 FACTORY TESTS 7-1

6.1 FUNCTIONAL TESTING 7-1

SECTION 7 EQUIPMENT LAYOUT DRAWINGS ..... ERROR! BOOKMARK NOT DEFINED.

SECTION 8 P&ID DIAGRAMS ..... ERROR! BOOKMARK NOT DEFINED.

Preliminary Budgetary Bid

TABLE OF CONTENTS

SECTION 9 MEPPI STANDARD TERMS AND CONDITIONS.....8-1

Preliminary Budgetary Bid

MITSUBISHI ELECTRIC POWER PRODUCTS, INC.
. . . The Power of Commitment

MITSUBISHI ELECTRIC POWER PRODUCTS, INC.
530 Keystone Drive
Warrendale, PA 15086-7538
Phone (724) 778-5111 Fax (724) 778-5149

July 2, 2007

Attn Ann Bryant, PE

Tetra Tech/KCM
1420 Fifth Avenue,
Suite 600
Seattle,
Washington 98101

Dear Ms Bryant,

Mitsubishi Electric Power Products, Inc. (MEPPI) is pleased to provide a budget bid and technical specification for the Slaton Sea project This document has been prepared in response to information provided in an e-mail from our Manufacturers Representatively Jon Anderson from Selg and Associates.
We understand that you are looking at treating 450 mgd from the Salton Sea in California to remove the H2S.

This proposal includes the following items

- VPSA system
- Pressure Regulating and Filtration System
- Nitrogen Boost System
- Ozone Generation System
- Side stream Injection system
- Destructor System

Mitsubishi Electric has extensive experience and expertise in the research, development, design, manufacture, installation, testing and commissioning of Ozone Generation Systems world wide, and are looking forward to the opportunity of working with on this project.

Should you require any further information or would like to schedule a meeting please let us know. In the interim, should you have any questions please do not hesitate to contact Jon.

Preliminary Budgetary Bid

Section 1 BUDGET COMMERCIAL OFFER

Mitsubishi Electric Power Products, Inc. is pleased to provide a budgetary estimate for the Salton Sea ozone generation systems.

1.1 Salton Sea Ozone Generation System

The scope of work included in this proposal includes all labor, materials, and equipment necessary to design, fabricate, and test the ozone system, excluding electrical and mechanical installation. This budget offer includes: two VPSA systems, oxygen filtration and pressure regulation equipment, the nitrogen boost system, the HV power supply unit, ozone generator cell and dielectric system, feed gas monitors, ambient ozone monitors, dewpoint monitor, residual ozone monitoring system, injection system and ozone destruction systems, power supply and instrumentation and control systems, as detailed this document. Corresponding functional and performance testing, installation support, and training with supporting operation & maintenance manuals are also included as specified.

The proposal allows for eight inverter type generators each rated for 3960 ppd at 16% concentration by weight. The generators will operate in duty/assist /standby mode.

1.2 Ozone Generating System

Complete ozone generation and dissolution system as detailed in this document..

For the sum of $ 34,680,000.00 USD

(Thirty Four Million Six Hundred Thousand US Dollars)

1.3 Terms and Conditions

This offer is provided in accordance with Mitsubishi Electric Power Products, Inc. (MEPPI) standard terms and conditions, which are provided in Section 8.

However, should there be any conflict between the MEPPI terms and conditions and specific customer requirements, MEPPI is open to negotiation to achieve mutual agreement.

1.4 Delivery

The lead-time for the major items of plant is in the region of 12 months. Actual delivery dates will be tailored to meet specific contract requirements.

Preliminary Budgetary Bid

Section 2 EQUIPMENT SPECIFICATION

2.1 VPSA equipment

2.1.1 General

We have included for installing two 1000 scfm VPSA systems. Each system will be able to supply 66% of the necessary oxygen. The equipment includes the compressor, O2 generator, surge tanks and air preparation syatems.

2.1.2 VPSA Specification

The Air Separation Technology used shall be Vacuum Pressure Swing Adsorption (VPSA) utilizing a two bed system with both Pressure Equalization and Gas Purging to enhance system efficiency.
The Sieve beds of the Oxygen Generator shall be designed, built, tested, inspected and stamped ('U'- stamp) in accordance with the American Society of Mechanical Engineers' (ASME) Boiler Code, Section 8, Division 1.
The electrical and pneumatic controls for the Oxygen Generator shall be located inside an electrical enclosure box. This box shall conform with the National Electrical Manufacturers Association (NEMA) Standard for Type 12 boxes (rated by the International Electrical Commission, IEC as IP 55). Which are general industrial enclosures and provide a degree of protection against dust, falling dirt and non-corrosive liquids.
An electrical enclosure box rated as NEMA 4X shall be optionally available. Which will provide a degree of protection against corrosion, windblown dust and rain, and splashing or hose-directed water.
The operation of the Oxygen Generator shall be controlled by a Programmable Logic Controller (PLC) which meets Conformite European (CE) guidelines for Noise Immunity and Radio Frequency Interference (RFI).
The PLC shall have at least one RS-232 data communication port.
The wiring connections inside the enclosure box shall be made to valves, switches and power distribution terminals through DIN- rated electrical connectors. The entire system shall be rated 'Touch-Safe' and Compliant with CE Machinery Safety Regulations.
The DIN electrical connectors to the process control valves shall have internal lights to indicate when each valve is energized.
The electrical power consumption of the Oxygen Generator shall be less than 0.5 KW. The power supply shall be from a single phase source of 115 VAC at 50/60 Hz. The process control valves shall be mounted in a horizontal and upright orientation to minimize valve wear and facilitate easy maintenance.
The Oxygen Generator shall have both lifting lugs, to move it via connection to an overhead crane and forklift slots, for carriage by forklift.
3. Instrumentation and Controls:
The Oxygen Generator shall have a single, internally-lighted, three position control switch. The three positions of the switch shall allow the operator to select the mode of operation (Off, Continuous Cycling, or Automatic Operation).
The Oxygen Generator shall have a non-adjustable Digital Hours meter that records running hours.

Preliminary Budgetary Bid

The Oxygen Generator shall have an internal pressure switch which will turn the Generator on and off based on the Oxygen Storage Tank pressure. This switch will only be affective while the 'Automatic' mode of operation is selected on the Control Switch. The pressure switch set points shall be factory set, but be adjustable for modification.
The Oxygen Generator shall have a dial gauge to indicate the Regulated Feed Air Pressure as feed air enters the Oxygen Generator.
The Oxygen Generator shall have a dial gauge to indicate the Oxygen Discharge Pressure as it departs the Oxygen Generator.
The Oxygen Generator shall have a manual push button to vent accumulated condensate in the filter bowl housings.
The PLC controlling the Oxygen Generator shall have indicating lights which indicate the point in the separation process the Generator is at while it cycles.

2.1.3 Power Requirements

Each VPSA unit will require 400 HP compressor set operating on 480V 60 Hz

2.1.4 LOX Quality Requirements

The table below shows the minimum GOX requirements:

Item	Analysis	Required
1	Oxygen	93% minimum
2	Nitrogen	0.02% min., 0.05% max. (200 ppm min., 500 ppm max.)
3	Argon	less than 0.5% (5,000 ppm)
4	Hydrocarbons	Less than 0.0020% (20 ppm)
5	Halogenated Hydrocarbons	Less than 0.0001% (1 ppm)
6	Nitrogen Oxides	Less than 0.0001% (1 ppm)
7	Carbon Monoxide	Less than 0.0005% (5 ppm)
8	Carbon Dioxide	Less than 0.0005% (5 ppm)
9	Dewpoint	-80.0 ^{o}F max at standard atmospheric pressure

2.2 Nitrogen Boost System

None required

2.3 Pressure Regulating and Gaseous Oxygen Filter System

The GOX pressure regulating station will be comprised of two systems, one duty one standby, both mounted on a rack. The change over would be a manual operation Each system will be comprised of a pressure regulation valve and filtration system with all necessary instrumentation, pressure relief and isolation valves as detailed in the P&ID.

Preliminary Budgetary Bid

The filters consist of sub-micronic filter assemblies with cartridge type filters, pressure differential indictors and monitors.

The filters would be sized for the design flow of 1500 scfm oxygen.

The pressure regulating valves will be pilot operated capable of reducing the downstream pressure to 15 psi from the VPSA system pressure between 100 and 60 psi.

A dewpoint instrument monitors the gas for dryness and if the dewpoint reaches less than –60°F the plant will shut down.

2.4 Ozone Cooling Water System

The cooling water system included in our budget offer will be an open loop/closed loop system consisting a closed loop heat exchanger mounted on a separate skid complete with all necessary valves instruments and secondary pumps. Primary pumps have not been included in this offer.

We assume that the primary cooling water pumps would be fed from then process water system using treated potable water. The heat exchanger will be manufactured from titanium to prevent corrosion problems.

Primary cooling water flow required 815 gpm at 45 PSIG.

The closed loop systems will be mounted on the ozone generator skid. Each skid will contain the following items:

- Heat Exchanger
- Closed loop circulation pump 715 gpm at 25 psig
- Expansion tank
- Make up tank
- Chemical feed tank
- Strainer (on inlet from open loop tanks)

The plant general arrangement drawings show heat exchangers mounted on the generator skid which considerably reduces the space requirement when compared to a separate closed loop cooling water skid.

2.5 Ozone Generation and Power Supply

We have included for 8 generators at 12% concentration at a maximum cooling water temperature of 85°F generators will be provided, two duty/assist and one standby. Each generator skid will be complete with all necessary inlet and outlet valves as detailed on the PID. Generators installed will provide a maximum dose of 4 mg/l in to 48 mgd.

2.5.1 Ozone Generator Cell Specification

See **Error! Reference source not found.** for full details.

Preliminary Budgetary Bid

Ozone Generation System

- Type — Cylindrical, multi-tube, silent discharge
- Model — OS-A75000
- Duty — Continuous
- Ozone Production Design Capacity — 3960ppd each unit, at 16% concentration
- Maximum Ozone Concentration — 16% by weight at rated Capacity
- Ozonized Oxygen Volume — 194scfm scfm @ 16 %
- Generator Cell Voltage — 7.43kV at 1900 Hz to 2200 Hz
- Cell Supply Frequency — 1900 - 2200 Hertz
- Material — 316L Stainless Steel
- Optimum Inlet Air Operating Pressure — 0.83 bar
- Pressure Drop Across Cell — Less than 0.7 bar at 88.7 scfm
- Cooling flow PSU — 715 gpm water at 85 °F.
- Number of tubes — 3659
- Cooling Method — Open/closed integral to generator
- Cooling Water Inlet Temperature — Maximum 85°F
- Maximum Cell Cooling Water Flow Rate — 670 gpm at 85 °F
- Cell Weight net — 17100 lbs
- Cell Size — 133 inch(W) x 92 inch(D) x 111inch(H)
- PSU weight net — 20,200 lbs
- PSU weight operational — PSU: 600 inch(W) x 50 inch(D) x 87 inch(H)
-

2.5.2 PSU Parameters

- Type — Packaged
- Input — 480 Volts, 60 Hertz, 3 Phase
- Ancillaries — Power factor better than 0.95 lead/lag
- Rating — 1152 kVA
- Harmonic Mitigation — Main element is a 12 pulse Inverter used with a 12-pulse isolation transformer. Primary voltage 480V Delta winding. Secondary voltage 800V Star winding and 800 V Delta winding.

Preliminary Budgetary Bid

2.5.3 HV Inverter Unit Parameters

- Inverter Type — Water cooled/air cooled, constant current type
- Input — 800 Volts, 60 Hertz, 3 Phase isolation transformer
- Output — 1 x 940 Volts, 1900-2600 Hertz, 1 Phase
- Pulse Number — 12 pulse
- Installed KVA — 1152kVA
- HV Reactor Rating — 1900-2600 Hertz, 1 Phase
- Maximum Cell Voltage — 5700 kVrms

2.6 Ozone Generator Control System

The generator cell is skid mounted and is comprised of the all valves and instrumentation necessary to provide a fully operational plant.

2.7 High Concentration Ozone Monitoring

A high concentration UV type ozone in oxygen monitor will be installed on each ozone generator skid.

- UV absorption type
- NEMA 4X Enclosure
- Calibrated for 0 –15% w/w
- Pressure, temperature and molecular weight compensated
- 4-20 mA isolated outputs for control
- Alarm relays (two: one high, one low)
- Auto Zero
- Fitted with ozone destruct unit

The outlet from the instrument will be connected to a waste oxygen manifold to vent the gas out of the building.

2.8 Ambient Ozone Monitoring

Four ambient ozone monitors will be installed, two in the ozone generation building adjacent to each of the generators and two located in the destructor skid area.

- NEMA 4X Enclosure
- Calibrated for 0 –1% w/w
- 4-20 mA isolated outputs for control
- Alarm relays (two: one high, one low)
- Auto Zero

Two factory set alarm points one at 0.1 ppm and one at 0.3 ppm are used to control the safety alarms, ventilation and ozone generator shutdown.

Preliminary Budgetary Bid

On receipt of a 0.1 ppm signal an enter with caution alarm is raised and the extract fan is started. On receipt of a 0.3 ppm alarm the ozone generator is shut down and do not enter lights will be illuminated along with a high db audible alarm sounding within the ozone production area.

2.9 Injector System

The injection system will consist of eight skid mounted systems each will have 2 injectors, 2 pumps and 2 degas separators.

Technical details are shown below.

2 Venturi Injection System:
Consisting of two high efficiency Stainless Steel injector with specifications as follows:

Water flow rate:	1600 gpm
Water Inlet Pressure:	25 psi
Water Outlet Pressure:	10 psi

2 Gas Check Valve Assembly

2 Two Centrifugal Pumps
Materials: 316 SS
Motor, 1,750 RPM, TEFC
Power: 600 V/3 PH/60 HZ 40 Hp

2 Skid Mounting Items
-Includes NEMA 3 R Pump Panel w/disconnect and H-O-A Switch

8 Nozzles
Material: Kynar
Connection: 3” Raised faced flange
Gas mixing velocity: 22.9 ft/Second

The system would provide a mass transfer of greater than 95%.

2.10 Skid Mounted Ozone Off-Gas Destruction Units

Two destructors would be installed as depicted on the PID.

2.10.1 Pre Heater Unit

Preliminary Budgetary Bid

The pre heater will be an inline unit constructed of Type 316 stainless steel with non-asbestos synthetic gaskets, to resist the inlet moist ozone-in-oxygen off-gas. Each heater will have the design capacity to increase the temperature of the incoming off-gas over the design flow and temperature range, as specified, to a minimum of 30°F above the inlet off-gas temperature. The unit will be specifically designed for use with moist ozone-in-oxygen off-gas.

A temperature-sensing element would function to monitor and transmit a signal to the heater single loop controller to maintain an off-gas outlet temperature between 70°F and 100 °F.

A high temperature alarm, selectable between 120 and 150 °F will be installed.

2.10.2 Catalytic Destructor

Destruction units will be designed and installed to prevent any off-gas from bypassing the catalyst bed. The catalyst containment vessel, piping and other metallic components will be of Type 316L stainless steel. The catalyst will be non-hazardous manganese dioxide (Carulite^{R}) based material suitable for catalytic ozone destruction. Gaskets and seals will be ozone and heat resistant. The containment vessels will be designed and fabricated to withstand the maximum internal pressure and vacuum to which they may be exposed under any operating condition. The vessel will be designed for easy inspection and change out of the catalyst, by incorporating catalyst trays and removable access panels.

The motor will be variable speed drive, which will modulate to maintain a –2” water vacuum in the headspace of the contact tanks.

General

The electric resistance heater, chamber, piping and all other components will be arranged upon the skid to provide accessibility for ease of maintenance as detailed on the drawing. The heater, catalyst chamber, all interconnecting piping, and any other heated components will be insulated, as required, to ensure that surface temperatures will not exceed 110°F. Insulation will include aluminum jacketing.

Each off-gas destructor skid will be equipped with a blower. Each blower will be designed to maintain a minimum negative pressure of minus 3” water column at the top of the ozone contact tanks over the full range of off-gas flows.

All components of the blower exposed to off-gas will be Type 316L stainless steel. The destruct unit would be connected direct to the degas separator units, no additional blower would be required.

An equipment control panel will be provided for each unit and will be integrally mounted on its skid. The control panel will include all control and protective devices and functions for a complete and operational ozone off-gas destruction unit. Ozone Destruct System Details

- Off-Gas Flow Rate 600 scfm scfm each unit

Preliminary Budgetary Bid

• Off-Gas Humidity	100% RH
Off-Gas Inlet Temperature (Max./Min.)	50 – 90 ^{o}F
• Off-Gas Inlet Concentration	2% ozone by weight maximum
• Off-Gas Outlet Concentration	0.9% by weight maximum
• Preheating Unit Outlet Temperature	30 F° above inlet temperature
• Catalyst Chamber Face Velocity	2.0 fps [0.610 m/sec]
• Catalyst Chamber Empty Bed Contact Time (Min.)	1.00 second

2.11 Ancillary Equipment

Control Panel

A control panel will be installed to provide overall control and monitoring of the ozone system complete with touch screen man machine interface to monitor the plant and accept instructions.

All control and monitoring signals for standard dose control have been included. Hard-wired alarms are required for shutdown of the ozone generators on ozone leak detection and fire alarm and have been included. The control panel will be enclosed in a NEMA 12 enclosure and will meet all the requirements of the National Electrical Code.

The control panel will contain the all-necessary equipment to control the operation of the ozonation system.

2.12 Pipe Work and Valves

Skid mounted equipment interconnecting pipe work has not been included in this offer.

Preliminary Budgetary Bid

Section 3 AUTOMATIC CONTROL - OPERATION OF THE CONTROL PANEL

3.1 General

Initially the PLC will control and monitor the following plant items:

- LOX storage and evaporation system or PSA system
- Nitrogen booster system
- Ozone generator
- Ozone generator cooling system
- Ozone injection system
- Ozone destruct unit
- Ambient ozone monitors

3.2 Control

Two forms of control will be available to the operator, selectable from the man machine interface (MMI) mounted on the door of the control panel.

The forms of control are:

1 Feed forward flow pace control.
2 Dissolved ozone control

Set points for all forms of control will be input into the system from the MMI. The PLC in the control panel will carry out all of the calculations to allow the plant to operate in an efficient and safe way. In addition, it will monitor all plant items for failure and will automatically start standby equipment on duty equipment failure.

A functional design specification will be prepared and issued for approval prior to any software production. The software will be prepared and will be fully tested by simulation prior to the FAT, where it will control the ozone generator during the tests.

3.3 Equipment Alarms

The control panel will monitor all instruments and equipment for alarms. An alarm page will be programmed into the MMI and will record events and failures for historic information.

All alarms will be included and made available in a contiguous block for SCADA monitoring.

3.4 Ambient Ozone Alarms

There are four ambient monitors. The signals from these will be received at the control panel and should a high level alarm be received (above 0.3 ppm) ozone generation will be shutdown.

Preliminary Budgetary Bid

Visual and audible alarms sound if a 0.1 ppm of ozone is detected.

Preliminary Budgetary Bid

Section 4 ELECTRICAL LOADING AND WATER USAGE

Equipment	Loading each	Quantity
VPSA Compressors	400Hp	2
Ozone generators	1152 kVA	8
Side stream pumps	40Hp	16
Generator cooling water flow	815 gpm (primary flow)	8

Preliminary Budgetary Bid

Section 5 SCOPE OF SUPPLY & SERVICES

This proposal covers the supply of equipment and services relating to the ozone generation system.

5.1 Equipment Supply

Summary of equipment to be supplied, and included in this offer, is as follows:

- 2 VPSA System
- 8 Ozone Generators and Power Supply Units
- 3 Off Gas Ozone Destruction System
- 8 Ozone Injection System
- Valves and Appurtenances
- Instrumentation and Control Systems
- Ozone and Oxygen Analyzer
- Additional Minor Appurtenances
- O&M Manuals

5.2 Services Offered

The services offered will be tailored to comply with the requirements of the specification, but would normally consist of the following, as a minimum:

Prepare Submittals
Conduct Shop Testing
Prepare Operation and Maintenance Manuals
Factory Tests
Installation Supervision
Installation Inspection
Commissioning
Site Support

Preliminary Budgetary Bid

Section 6 PRODUCT DESIGN SUBMITTALS

The table below gives a typical submittal schedule; however, this would be modified to suit the actual project requirements.

The key dates are as follows.

Table 6-1 Document Submittal Schedule

Submittal Item	Calendar Days	Event	
Purchase Order Acceptance	7	After	Receipt of P.O.
Insurance Certificates	7	After	Date of P.O. Acceptance
Engineering Schedule	7	After	Date of P.O. Acceptance
Engineering Submittals	90	After	Date of P.O. Acceptance
Manufacture	50 Weeks	After	Approval of shop drawings
Preliminary O&M Manuals	120	After	Approval of shop drawings
Shop Inspection Notice	14	Before	Inspection
Test Reports	ASAP	After	Inspection
Shipping Notice	1	Before	Shipment
Final O&M Manual	7	Before	Shipment

Preliminary Budgetary Bid

Section 7 FACTORY TESTS

All equipment will be fully factory tested prior to dispatch to site. Factory testing will be carried out at our Warrendale facility and will include full production tests. Additional testing may be carried out in accordance with our standard test format to comply with ISO 9000 quality requirements.

7.1 Functional Testing

Functional Testing will be carried out on the following equipment:

- All Control Panels
- Ozone Generator Power Supplies
- Destruct Units
- Nitrogen Boost Units
- Supplemental Air System Control
- Ozone Leak Shutdown Control System

All plant items will carry a test certificate. The certificates will state what tests have been performed as well as additional information as required by the specification, including cleaned for oxygen service information and certified performance curves (as applicable). The certificates will be submitted in accordance with the specification.

Preliminary Budgetary Bid

Section 8 MEPPI STANDARD TERMS AND CONDITIONS

Preliminary Budgetary Bid

August 9, 2004

TERMS AND CONDITIONS

These Terms and Conditions ("T&C") shall govern the sale of all products (the "Products") from and the provision of all services (the "Services") by Mitsubishi Electric Power Products, Inc. ("MEPPI") to Purchaser. Any different or additional terms and conditions submitted by Purchaser, whether in any order, contract or other document, are hereby rejected and shall have no force or effect. The sale of the Products and the provision of the Services are expressly conditioned upon Purchaser's assent to these T&C. Purchaser shall be deemed to have expressly accepted these T&C if Purchaser so agrees in writing or receives the Products or accepts performance of the Services subsequent to receipt of these T&C.

Except as expressly agreed in writing by a duly authorized representative of MEPPI, these T&C supersede any prior or contemporaneous understandings, agreements or correspondence between the parties and shall govern any order or contract (each, an "order") for the Products or the Services.

1.0 VALIDITY
Each quotation or offer is valid for 30 days from its date unless otherwise stated therein.

2.0 TAXES
Prices do not include any applicable sales, use or other taxes, and the amount of any such taxes which MEPPI may be required to pay or collect shall be added to each invoice or separately invoiced by MEPPI to Purchaser, and Purchaser shall promptly pay all such invoices.

3.0 TERMS OF PAYMENT
A. Terms of Payment
Prices for the Products and the Services shall be as specified in MEPPI's quotation or offer. An invoice will be issued upon Product shipment or completion of the Services. Except as otherwise provided in these T&C, all payments by Purchaser shall be made net 30 days from date of MEPPI's invoice.

B. Overdue Payments
MEPPI's past due invoices shall bear interest at the rate of 1.5% per month, but not in excess of the maximum lawful rate, from the due date thereof until paid in full.

C. Advance Payments
If, MEPPI reasonably believes the financial condition of Purchaser is impaired or otherwise has a reasonable basis for insecurity as to Purchaser's ability or intention to comply with these T&C, MEPPI may require full or partial payment in advance as a condition to its further performance.

D. Purchaser's Insolvency
Should Purchaser become insolvent, make a general assignment for the benefit of creditors, institute or have instituted against it any bankruptcy or reorganization proceeding or if a receiver of any property of Purchaser shall be appointed in any action, suit or proceeding by or against Purchaser and such filing or appointment shall not be dismissed, vacated or annulled, as the case may be, within sixty (60) days, MEPPI shall, if permitted by applicable state and/or federal law, have the right at its election to cancel any or all pending orders and to recover its proper cancellation charges pursuant to Section 10.0 from Purchaser or Purchaser's estate.

E. Collection Costs
Purchaser shall be responsible for all costs and expenses incurred by MEPPI, including attorneys' fees and costs, in connection with collection of amounts due from Purchaser and enforcement of any provision of these T&C.

4.0 DELIVERY
A. Freight Prepaid
All prices include shipping charges to the accessible US common carrier point nearest to the final destination.

B. Cartage
Transportation charges and any storage charges incurred from the nearest accessible common carrier point to final destination or to shipside (in case of shipment to U.S. Possessions) are the responsibility of Purchaser.

C. Origin, Method of Shipment and Routing
Unless otherwise requested by Purchaser, MEPPI will select the method of transportation and the routing of shipment. If Purchaser requests shipment by a method or routing other than that determined by MEPPI, Purchaser shall be responsible for any excess or premium in transportation charges. In no event will MEPPI be responsible for demurrage or detention charges. Any charges for special services, including but not limited to special train, lighterage, construction or repair of transportation facilities shall be paid or reimbursed by Purchaser.

D. Shipment Damage
Except in the event of FOB destination shipments, MEPPI will not participate in any settlement of claims for concealed or other shipment damage. When shipment has been made on an FOB destination basis, Purchaser shall unpack the Products immediately and, if damage is discovered, shall:

1. Not move the Products from the point of examination.
2. Retain all shipping containers and packing materials.
3. Notify the carrier of any apparent damage in writing on carrier's delivery receipt and request the carrier to make an inspection.
4. Notify MEPPI within 72 hours of delivery.
5. Send MEPPI a copy of the carrier's inspection report.

MEPPI shall have no responsibility for any damage on FOB destination shipments unless Purchaser complies with the foregoing obligations.

Preliminary Budgetary Only

5.0 FORCE MAJEURE

Shipping dates are approximate and are based on receipt of complete information with each order. If drawing approval is required, Purchaser shall be required to return drawings on schedule to maintain shipping dates.

MEPPI shall not be liable to Purchaser for failure to perform or for delay in performance due to any cause beyond its reasonable control, including, without limitation, fire, flood, strike or other labor difficulty, act of God, act of governmental authority, act of Purchaser, riot, embargo, fuel or energy shortage, failure of or delay in transportation or delay in obtaining or inability to obtain necessary labor, materials or manufacturing facilities from usual sources. In the event of such delay, the date of delivery or time for completion shall be extended by a period of time reasonably necessary to overcome the effect of such delay.

6.0 TRANSFER

In the event of a transfer to a third party of any Product or interest therein, Purchaser shall either (A) obtain for MEPPI written assurance from the transferee, in form and content acceptable to MEPPI, that MEPPI and its subcontractors' and suppliers' protection against liability following the transfer is limited to that provided by these T&C, or (B) be obligated to indemnify, defend and hold harmless MEPPI and its subcontractors and suppliers against any liability they may incur or that may be claimed against them in excess of that which they would have incurred had Purchaser obtained such assurance from the transferee.

7.0 PATENT INDEMNITY

Subject to the provisions of this section, MEPPI shall, at its own expense, defend or, at its option, settle any claim, suit or proceeding brought against Purchaser, and/or any of Purchaser's customers alleging that any Products or any part thereof furnished by MEPPI to Purchaser infringes any US patent. This obligation shall be effective only if Purchaser shall have made all payments due MEPPI and Purchaser gives MEPPI prompt notice and full authority, information and assistance for the defense of such claim, suit or proceeding. MEPPI shall pay all damages and costs awarded in such suit or proceedings in accordance with these T&C. If a Product or any part thereof becomes the subject of such claim, suit or proceeding MEPPI may at any time thereafter at, its option and expense, either:

1. Procure for Purchaser the right to continue use of such Product or part thereof;

2. Replace such Product with a non-infringing product or part;

3. Modify such Product so it becomes non-infringing; or

4. Remove such Product and refund a depreciated portion of the purchase price, including the transportation and installation costs thereof, determined on the basis of a 20-year useful life.

The foregoing indemnity does not apply to the following:

v. Patented processes performed by the Product, or another product produced thereby.

x. Products supplied according to a design other than that of MEPPI and which is required by Purchaser.

y. Combinations of the Product with another product not furnished by MEPPI except to the extent MEPPI is a contributory infringer.

z. Any settlement of a suit or proceeding made by Purchaser or Purchaser's customer.

The foregoing states the entire liability of MEPPI and the exclusive remedy of Purchaser with respect to alleged patent infringement by any Product or any part thereof.

Purchaser shall indemnify MEPPI in the manner and to the extent MEPPI agrees to indemnify Purchaser in the first paragraph of this section insofar as the terms thereof are appropriate with respect to any claim, suit or proceeding against MEPPI based on any activity enumerated in clause v, x, y or z hereof.

8.0 TITLE - RISK OF LOSS

Risk of loss to the Products, or any part thereof, shall pass to Purchaser upon delivery of the Products or parts to the US common carrier, unless otherwise specified in the order. MEPPI shall retain title to all Products and parts sold to Purchaser until fully paid for by Purchaser. In furtherance of the foregoing, Purchaser hereby grants to MEPPI a security interest in the Products and parts purchased by Purchaser from MEPPI and all proceeds thereof to secure the performance of all obligations of whatever kind or nature due by Purchaser to MEPPI under these T&C. Purchaser authorizes MEPPI to file such financing statement(s), including any necessary or required amendments thereto, describing the Products and parts as MEPPI shall deem necessary to confirm, perfect and maintain its retained ownership thereof or the security interest granted under these T&C.

9.0 INDEMNIFICATION

MEPPI shall indemnify, defend and hold harmless Purchaser from and against liabilities to third parties for property damage, personal injury or death arising as a result of the negligence or willful misconduct of MEPPI, its affiliates or their officers, directors, employees, agents, servants and assigns. The foregoing obligation shall be effective only if Purchaser shall have made all payments due MEPPI and if Purchaser gives MEPPI prompt notice and full authority, information and assistance for the defense of any claim or action which might give rise to any such liability. MEPPI's obligation to indemnify Purchaser shall not apply to any liabilities or damages arising from the negligence, willful misconduct or other legal fault of Purchaser, its affiliates, any third party and their respective

Preliminary Budgetary Bid

officers, directors, employees, agents, servants and assigns.

10.0 TERMINATION

A. By Purchaser

Any order may be terminated by Purchaser only by notice to MEPPI and upon payment to MEPPI of reasonable and proper termination charges, including, but not limited to, all costs identified to the order which have been incurred up to the date of notice of termination. All additional costs resulting from the termination and 10% of the final net price shall be included in the termination charges to compensate MEPPI for disruptions in scheduling, planned production, and other direct costs.

B. By MEPPI

MEPPI shall have the right to terminate any order at any time by notice to Purchaser in the event:

1. Purchaser breaches the order or these T&C and fails to remedy such breach within 30 days after notice thereof;

2. Purchaser fails to make any payment on the due date or refuses to accept delivery of any shipment;

3. MEPPI has reasonable basis for insecurity with respect to Purchaser's performance of its obligations to MEPPI, and Purchaser fails to provide to MEPPI adequate assurance of Purchaser's performance within 30 days of MEPPI's demand for such assurances.

Upon termination by MEPPI pursuant to this section all amounts due and to become due to MEPPI shall be immediately payable by Purchaser.

11.0 HELD ORDERS

Any order held, delayed or rescheduled at the request of Purchaser shall be subject to the prices and conditions of sale in effect at the time of the release of the hold, end of the delay or the reschedule. Any such order, held, delayed or rescheduled beyond a reasonable period of time may be treated by MEPPI as a Purchaser termination. When final assembly of the Products has commenced, the Products are ready for shipment or the Services are ready to be performed and delivery or performance is not be made because of Purchaser's hold, delay or rescheduling, MEPPI may invoice Purchaser for such Products and Services, which invoice shall be payable upon receipt thereof, and may, upon written notice to Purchaser, store such Products at Purchaser's expense and delay performance of the Services. In such event the following conditions shall apply:

Risk of loss to the Products shall pass to Purchaser upon moving such Products to storage. All expenses incurred by MEPPI in connection with the storage of Products, including demurrage, the cost of preparation for storage, storage charges, insurance if placed, and handling charges and with the delay of performance of the Services shall be payable by the Purchaser upon submission of invoices by MEPPI.

12.0 MINIMUM BILLING

The minimum order charge shall be $250.

13.0 DRAWING APPROVAL

If, at drawing approval, MEPPI has failed to design the Product in accordance with the Specifications, MEPPI will make the appropriate changes at no charge to Purchaser. Where the Specifications are not definitive, MEPPI reserves the right to design the Product according to MEPPI's judgment and good commercial practices. If, at drawing approval, Purchaser makes changes outside of the design as covered in the Specifications, Purchaser shall be responsible for and shall pay, upon invoicing, additional charges determined by MEPPI, and there shall be a commensurate delay in shipping date based on the changes involved.

14.0 PRODUCT NOTICES

Purchaser shall provide the user (including its employees) of the Products with all MEPPI-supplied product notices, warnings, instructions, recommendations and similar materials.

15.0 NUCLEAR APPLICATION

In the event that Purchaser or third parties use the Services, Products or any part thereof in connection with any activity or process involving nuclear fission or fusion or any use or handling of any source, special nuclear or by-product material, as those materials are defined in the U.S. Atomic Energy Act of 1954 (as amended), such items shall be sold pursuant to MEPPI's Conditions of Sale - Form B, which are in addition to these T&C. Purchaser shall immediately notify MEPPI of such nuclear application so that nuclear regulations and insurance provisions contained in those terms and conditions can be satisfied.

16.0 WARRANTY

A. Standard Warranty

MEPPI warrants that the Products supplied to Purchaser will be of the kind and quality described in the Specifications and will be free of defects in workmanship and material and that the Services shall be performed in a good and workmanlike manner.

Remedy: In the event any Product or Service fails to comply with this warranty and MEPPI is so notified promptly upon discovery of the failure, in writing, within one year from the Shipment Date, MEPPI shall correct such nonconformity by repair or, at its option, replacement of the defective Product, part or parts FOB its factory or repair facility; provided the Products have been stored, installed, operated and maintained in accordance with MEPPI's manuals, instruction books, recommendations and industry standard practices. However, if MEPPI has installed the Products, the warranty period shall terminate one year after the completion of installation or 18 months after the Shipment Date, whichever occurs earliest. In no event shall MEPPI be responsible for gaining access to the Product(s), disassembly, reassembly or transportation of the Products or any parts thereof from and to the place of installation.

Preliminary Budgetary Price

Products supplied by MEPPI, but manufactured by third parties, are warranted only to the extent of the manufacturer's warranty.

Certain Product warranties are dependent upon the presence of MEPPI personnel at specified critical phases during installation. Such requirements are specified in the quote or offer relating to the Products. If MEPPI personnel are not present at such specified times, this standard warranty is void.

B. Optional Warranties

Option 1 - Extended Warranty

If requested by Purchaser and specifically accepted in writing by MEPPI, the Standard Warranty shall be extended for two years from the Shipment Date for a price addition of 2% of the Product purchase price.

Option 2 - Special Warranty

If requested by Purchaser and specifically accepted in writing by MEPPI, the Standard Warranty shall be extended, for a price addition of 2% of the Product purchase price, to cover the direct costs of:

1. Disassembling the Products or parts and loading on adjacent rail car or line-haul truck.

2. Transporting the Products or parts to and from the factory or repair facility.

3. Off-loading from rail car or line-haul truck adjacent to installation and re-installing the Products or parts.

The total liability of MEPPI under clauses (1), (2) and (3), hereof shall be limited to 50% of the purchase price of the particular Product being repaired. Such liability excludes all costs associated with:

x. Removing adjacent equipment, structures or walls.

y. Loading, off-loading and local transportation when rail car or line-haul truck cannot be placed adjacent to installation.

z. Special services, including but not limited to, special trains or trucks, premium transportation, lighterage and construction or repair of transportation facilities.

C. Title Warranty

MEPPI warrants that the Products will be delivered free of any and all rightful claims, demands, liens or encumbrances. In the event of a breach of this warranty, Purchaser shall give MEPPI prompt notice, and MEPPI, at its expense, shall defend the title to any affected product or part, and, if unsuccessful, shall promptly provide to Purchaser at no cost a replacement products or part which complies with this warranty.

D. Warranty Disclaimer and Limitation of Remedies

The foregoing warranties are exclusive and meppi makes no other warranties of any kind whatsoever to Purchaser or any third parties with respect to the Products and/or Services and hereby expressly disclaims all warranties, express or implied, including the implied warranties of merchantability and fitness for particular purpose and all warranties arising from course of dealing or usage of trade.

The remedies provided for in these T&C are Purchaser's sole remedies for any failure of MEPPI to comply with its obligations. Correction of any non-conformity in the manner and for the period of time provided for in these T&C shall constitute complete fulfillment of all the liabilities of MEPPI, whether the claims of Purchaser are based in contract, in tort (including negligence or strict liability) or otherwise, with respect to or arising out of the applicable product or service.

17.0 LIMITATION OF LIABILITY

Neither MEPPI nor any of its contractors and suppliers of any tier shall be liable in contract, in tort (including negligence or strict liability) or otherwise for damage or loss of other property or equipment, loss of profits or revenue, loss of use of equipment or power system, cost of capital, cost of purchased or replacement power or temporary equipment (including additional expenses incurred in using existing facilities), claims of customers of Purchaser, or for any special, indirect, incidental or consequential damages of any kind or nature whatsoever.

The remedies of Purchaser set forth in these T&C are exclusive, and the total cumulative liability of MEPPI with respect to any order or anything done in connection therewith such as the performance or breach thereof, or from the manufacture, sale, delivery, resale, or use of any Product, whether in contract, in tort (including negligence or strict liability) or otherwise shall in no event exceed the price of the Product or part or for the Services on which such liability is based.

18.0 CONFIDENTIALITY

"Confidential Information" shall mean information disclosed by a party ("Discloser") to the other or its affiliates (collectively, "Recipient") which information is marked "Confidential", "Proprietary" or with a similar legend. If Confidential Information is orally disclosed, it shall be identified as such at the time of disclosure and a brief written description and confirmation of the confidential nature of the information shall be sent to the Recipient within 30 days after the disclosure. Confidential Information, however, shall not include any information which: (1) is known to the Recipient at the time of its disclosure to the Recipient; (2) is or becomes publicly known through no wrongful act of the Recipient; (3) is received from a third party without a restriction on its disclosure; (4) is independently developed by the Recipient or any of its affiliated companies; (5) is furnished to any third party by the Discloser without a similar restriction on such third party's rights; or (6) is approved for release by the prior written consent of the Discloser.

Preliminary Budgetary Bid

The Recipient shall maintain the Confidential Information in strict confidence and shall not disclose, disseminate, copy, divulge, recreate, or otherwise use Confidential Information (other than disclosure to personnel of the Recipient, its affiliates, customer or suppliers with a need to know and who receive such information subject to an obligation of confidentiality) without the prior written consent of the Discloser or in a manner not expressly permitted under this Agreement, unless the Confidential Information is required to be disclosed by law or an order of any court or other governmental authority with proper jurisdiction (and provided the Recipient promptly notifies the Discloser before disclosing such information so as to permit the Discloser reasonable time to seek an appropriate protective order). Recipient agrees to use protective measures no less stringent than the Recipient uses within its own business to protect its own most valuable information, which protective measures shall under all circumstances be at least reasonable measures to ensure the continued confidentiality of the Confidential Information. The parties acknowledge and agree that the Confidential Information is and shall remain the property of the Discloser and that any unauthorized use, disclosure, dissemination, or other release of the Confidential Information will substantially injure the Discloser.

19.0 NO ASSIGNMENT
Purchaser may not assign any rights, interests or benefits under any order or these T&C to any other party without the express prior written consent of MEPPI.

20.0 HEADINGS
The headings contained in these T&C are for convenience of reference and shall have no effect in the interpretation or instruction of the language contained therein.

21.0 GOVERNING LAW
These T&C shall be governed by and construed according to the laws of the Commonwealth of Pennsylvania.

22.0 ARBITRATION
All disputes or controversies arising out of or in any manner relating to any order or these T&C which the parties do not resolve in good faith within ten days after either party notifies the other of its desire to arbitrate such disputes or controversies shall be settled by arbitration by a single arbitrator in accordance with the then standard prevailing commercial rules, as modified or supplemented by this section, of the American Arbitration Association ("AAA"). The arbitration shall be held in Allegheny County, PA. The arbitration award shall be in writing and shall specify the factual and legal bases of such award. The arbitration award shall be final and binding, and a judgment consistent therewith may be entered by any court of competent jurisdiction. The parties agree that the arbitration award shall be treated as Confidential Information. The arbitrator shall not have the power to render an award of punitive damages. To the extent of any conflict, this section shall supersede and control AAA rules.

23.0 NOTICES
All notices and demands with respect to these T&C or any order shall be in writing and shall be sent by certified or registered mail, return receipt requested, in the case of MEPPI, at the address appearing in these T&C and to the attention of its President and, in the case of Purchaser, to the address set forth in its order or otherwise made known to MEPPI.

Preliminary Budgetary Bid

Bryant, Ann -- Tetra Tech

From: William.NEZGOD@ozonia.com
Sent: Tuesday, April 24, 2007 8:20 AM
To: Bryant, Ann
Cc: Markus, John
Subject: Fw: Salton Sea - Lake treatment system

Attachments: 5 x 6360_Salton Sea CA_4-24-07.pdf

5 x 6360_Salton Sea CA_4-24-07...

Ann,

Sorry for the delay in getting back to you. End of last week became very hectic.

With reference to your request, the ozone system budget cost estimate is based on the design criteria given below:

Design Criteria
Water Flow Rate: 450 MGD
Ozone Dosage: 8.5 mg/l at rated flow
No. of O3 Generators: 5
Oxygen Source VPSA (on-site) oxygen generation (By others)

Budgetary Price: See attached

2. Footprint Information (major equipment)
Ozone Generators (5) 210" L x 96" W x 130" H
Power Supply Units (5) 272" L x 96" W x 96" H
Ozone Destruct Units (5) 120" L x 78" W x 110" H

3. Operating Costs
Power Consumption: Ozone Generator/PSU 4.6 Kwh/lb (includes destruct equipment)
VPSA Oxygen Gen. 1.7 Kwh/lb (estimated)

Oxygen Required 160 tons/day oxygen
Cooling Water Reqd Approx. 7.5 MGD - good quality water (closed loop system not included in budget estimate)

Please let me know if you have any questions or require additional information. Please keep in mind the information provided is "very, very preliminary" in nature.

(See attached file: 5 x 6360_Salton Sea CA_4-24-07.pdf)

Regards,

William Nezgod
Sales Manager - Large Systems
Degremont Technologies - Ozonia

P 201-794-3100 Ext. 230
F 201-794-3358
E-mail william.nezgod@ozonia.com

This message and all attachments are confidential and intended solely for the addressees. Any use not in accord with its purpose, any dissemination or disclosure, either in whole or partially, is prohibited except upon formal approval.

If you receive this message in error, please delete it and immediately notify the sender.

Neither Ozonia nor any of its subsidiaries or affiliates shall be liable for the message if altered, changed or falsified.

Salton Sea - Lake water treatment system
Plant Size: 450 MGD - 31,800 lbs/day O3 Capacity

Capital System Cost Estimate

Estimate based on 31,800 lbs/day at 10% concentration with a system consisting of five (5) ozone generators, each rated for 6360 ppd

Plant Item	Number of Units	Budget Price $
Ozone Generators - OF 320 AT	5	$ 12,600,000
Power Supply Units - NPS-16-2250-WE12	5	
(Includes local valves and instruments		
shipped loose)		
Controls	1	Incl. above
Field Instrumentation and Monitors	1 lot	Incl. above
Field Valves	1 lot	Incl. above
Diffusion System	4 Systems	Incl. above
Destruct Units - Model VOD-XX-XXXX-XX	5	Incl. above
Miscellaneous Items, e.g.:	(see note 1)	Incl. above
N2 System, Freight, Start-up, Training,		
Testing, Warranty, etc.		
Total Budget Capital Cost		**$ 12,600,000**

Other Major Equipment Required: 2 x 80 tons/day on-site VPSA Oxygen Generation Plants
2 x VSA Oxygen Plants ~ $ 18,000,000 By Industrial Gas Co.

NOTES:

1. Typical Allowance - at this time, detailed scope of supply unspecified